STUDIES ON THE MOLECULAR REGULATIONS OF STRUCTURE AND FUNCTION IN OXYGEN BINDING HEMOPROTEINS(Dissertation_全文)

AUTHOR(S):

Ishimori, Koichiro

STUDIES ON THE MOLECULAR REGULATIONS OF STRUCTURE AND FUNCTION IN OXYGEN BINDING HEMOPROTEINS

KOICHIRO ISHIMORI

Division of Molecular Engineering
Graduate School of Engineering
Kyoto University

1989

STUDIES ON THE MOLECULAR REGULATIONS OF STRUCTURE AND FUNCTION IN OXYGEN BINDING HEMOPROTEINS

KOICHIRO ISHIMORI

Division of Molecular Engineering
Graduate School of Engineering
Kyoto University

1989

are also discussed. To study the possibility of the application of hemoproteins to chemical reaction, photoreaction of porphyrin-substituted hemoproteins were examined and effective production of singlet oxygen is pointed out (Part VI). Finally, summary and general discussions of the present work are presented at the end of this thesis (Part VII).

ACKNOWLEDGMENTS

The present thesis is the summary of the author's study from 1984 to 1989 at the Division of Molecular Engineering of Graduate School of Engineering of Kyoto University. The author is indeed happy to express his sincere acknowledge to Professor Teijiro Yonezawa for his warm encouragement, Professor Ken-ichi Honda for his continuing interest, and Associate Professor Isao Morishima for his continuous guidance and discussion through the course of this study.

It should be emphasized that the works involved in this thesis have required the thoroughgoing cooperation with many groups of investigators, each with its own expertise. Grateful acknowledgment is made to Associate Professor Hideki Morimoto, Associate Professor Kiyohiro Imai, Dr. Gentaro Miyazaki and Mr. Antonio Shigetsune for their helpful discussion and valuable instructions when he carried out some works in Osaka University. The author is wishes to express sincere thanks to Professor Teizo Kitagawa and Dr. Takashi Ogura for their resonance Raman measurements. It is also his great pleasure to thank Dr. Shosuke Kawanishi for valuable instruction when the author started some experiment about porphyrin-substituted hemoproteins. He is grateful to Professor Shinya Yoshikawa for his helpful suggestion and criticism. Messrs. Mitsunobu Hara, Takashi Inoue and Miss Reiko Azumi participated in some of the work presented here as part of postgraduate research projects; their generous collaborations and discussions are appreciated. He is greatly indebted to Drs. Toshiro Inubushi, Saburo Neya, Yoshitsugu Shiro, Takashi Funahashi and Motoru Takeda and Messrs. Masuo Kurono, Yasuhiko Takamuki, Masahiro Aoki, Tomoyuki Wakino, Keizo Nakajima, Yotaro Yano, Kikuo Takatera, Hiroshi Fujii, Shin-ichi Adachi, Taku Kamikawa, Masashi Unno and Yukinobu Ohta for their helpful suggestions. The author is also grateful to Mr. Haruyuki Harada for assistance in the operation of NMR instruments and the maintenance of the machine.

Finally, he express his sincere gratitude to his parents for their unfailing understanding and affectionate encouragement.

January, 1989
Kyoto

Koichiro Ishimori

LIST OF PUBLICATIONS

PART II

CHAPTER 1. Ruthenium-Iron Hybrid Hemoglobins as a Model for Partially Liganded Hemoglobin: NMR Studies of Their Tertiary and Quaternary Structures
Ishimori, K., & Morishima, I. (1988) *Biochemistry 27*, 4060-4066.

CHAPTER 2. Ruthenium-Iron Hybrid Hemoglobins as a Model for Partially Liganded Hemoglobin: Their Sulfhydryl Reactivity of β93 Cys
Ishimori, K., Azumi, R., & Morishima, I. submitted for publication (*J. Biol. Chem.*)

CHAPTER 3. Ruthenium-Iron Hybrid Hemoglobins as a Model for Partially Liganded Hemoglobin: Their Oxygen Equilibrium Curve and Raman Spectra
Ishimori, K., Morishima, I., Tsuneshige, A., & Imai, K. submitted for publication (*Biochemistry*)

PART III

CHAPTER 1. Interaction of Fully Liganded Valency Hybrid Hemoglobin with Inositol Hexaphosphate. Implication of the IHP-Induced T State of Human Adult Methemoglobin in the Low-Spin State
Morishima, I., Hara, M., & Ishimori, K. (1986) *Biochemistry 25*, 7243-7250.

PART V

CHAPTER 1. NMR Study of Hybrid Hemoglobins Containing Unnatural Heme: Effect of Heme Modification on Their Tertiary and Quaternary Structures
Ishimori, K., & Morishima, I. (1986) *Biochemistry 25*, 4892-4898.

CHAPTER 2. Study of the Specific Heme Orientation in Reconstituted Hemoglobins
Ishimori, K., & Morishima, I. (1988) *Biochemistry 27*, 4747-4753.

Other publications not included in this thesis.

Decreased Intracellular Free Magnesium in Erythrocytes of Spontaneously Hypertensive Rats

Matsuura, T., Kohno, M., Kanayama, Y., Yasunari, K., Murakawa, K., Takeda, T., Ishimori, K., Morishima, I., & Yonezawa, T. (1987) *Biochem. Biophys. Res. Commun. 143*, 1012-1017.

CONTENTS

PART I.

GENERAL INTRODUCTION

The globins are heme-containing oxygen-binding proteins. As a class they are ancient and widely distributed throughout the animal kingdom; a few examples are known from plants. The "Atlas of Protein Sequence and Structure[1]" lists sequence information for nearly a hundred different globins. The three-dimensional structures of globins from man,[2] horse,[3-5] whale,[6,7] seal,[8] tuna,[9] lamprey,[10,11] midge,[12] and bloodworm[11] have been determined by X-ray diffraction (Figure 1.). The structures are remarkably similar despite the fact that erythrocruorin from the midge *Chironomas thummi* differs from human globin chains in more than 80 % of its amino sequence.[12] The heme iron is normally ferrous and is bound to the globin *via* the imidazole side chain of a histidine residue. A gaseous ligand (O_2, CO, or NO) can be only bound at the ferrous form, not the ferric form (called met) by oxidizing agents such as ferricyanide or on standing in air. In the met state, the sixth coordination position of the iron can be occupied by water, OH^-, CN^-, N_3^-, F^-, and similar ionic ligands but not by gaseous ligands. Free ferrous heme is very unstable in water and rapidly oxidizes to the ferric form. The protein is therefore essential to the oxygen binding function.

Despite a number of extensive studies, the molecular mechanism of the structural and functional regulation in such oxygen binding protein is not yet fully understood. The most challenging task in this field is to establish the relationship between structure and function from the aspect of molecular science. It will provide valuable knowledge to find out general rule of regulation mechanism in proteins and enzymes. In this thesis, the author intended to find out the structural regulation to function of oxygen binding hemoprotein by use of physico-chemical and physiological approaches.

In many oxygen binding hemoproteins, hemoglobin has long served as a paradigm for cooperative ligand binding in protein.[13,14] In order to elucidate the detailed control mechanism of cooperative ligand binding, the key tasks in current hemoglobin research are (1) to describe the structural and functional changes induced at each oxygenation step by characterizing the properties of the intermediate ligated species, namely, hemoglobin A with one, two, and three ligand molecule bound within a tetramer ($\alpha_2\beta_2$), (2) to elucidate a propagation mechanism of the structural and functional changes between the subunits and (3) to describe the regulation mechanism of allosteric effect of hemoglobin.

Because at any given fractional oxygen saturation between the fully deoxy and fully oxy state, various molecular species with binding of zero to four

ligand molecule coexist as a statistical mixture, it is not feasible to isolate a stable intermediate ligation states by using hemoglobin A. To gain an insight into structural and functional characterizations of such a intermediate species, the half-liganded hemoglobin models have been studied by utilizing metal hybrid hemoglobins.[15-18] In the present thesis, the structure and function of an unique metal hybrid hemoglobin containing ruthenium-porphyrin which can be served as a model for stable oxygenated heme were discussed and a mechanism of the structural and functional regulation in oxygenation was proposed.

In order to clarify the propagation mechanism of structural and functional changes, it is critical what and how amino acid residue controls the structure and function. To this end, some extensive efforts by use of natural mutant hemoglobins having a point mutation of amino acid residue have been made.[19,20] In spite of their elegant studies, the information has been rather limited because researchers had to wait the opportunity that they encounter a new natural mutant and the number of the natural mutants are limited. And quality and quantity of the natural mutant hemoglobins also involves difficulty, their unstability and limited amount. One of, probably only one, methods to overcome above problems is artificial mutant hemoglobins synthesized in *Escherichia coli* by use of the site-directed mutagenesis. In this thesis, the mutation was introduced at the specific hydrogen bonded residue at which the natural mutation has not been reported. Their structural and functional characterization was carried out to discuss the propagation mechanism of structural and functional changes from one subunit to another subunit.

One of the interesting points in the mechanism of allostericity in hemoglobin is an effect of allosteric effector on structure and function. Out of a number of such effectors, IHP (inositol hexakisphosphate) is a powerful effector to decrease the oxygen affinity of hemoglobin and binds between interface of the β subunits. It has been controversial point whether the binding IHP accompanies quaternary structural changes in the low spin hemoglobin in which heme iron fixed "in plain" of porphyrin. The author investigated the IHP effect on the structure of the low spin hemoglobin by use of NMR spectroscopy and compared the results with the "trigger model" proposed by Perutz which indicates that the quaternary structural changes in hemoglobin originated the movement of heme iron, "in plain" or "out of plain" of heme iron.

On other hand, extensive X-ray diffraction studies have revealed detailed

three-dimensional structure of some oxygen carriers.[2-12] Their structural data allows globins to be served as models to discuss the general properties of proteins and enzymes such as mechanism of substrate specificity or allostericity. Many specific functions of enzymes seem to be concerned with non-bonding interactions, however, the detailed mechanism has not been understood yet probably due to the lack of the knowledge about their structure and function of enzymes. To discuss nature of non-bonding interaction, hemoglobin and myoglobin were utilized as model in this thesis. As shown in the following parts, it became clear that globin senses the steric difference of the substiuents of the porphyrin through the non-bonding interactions or the conformational and functional changes also propagated by non-bonding interactions. These properties can be thought to be typical regulation mechanisms to the substrate specificity or allostericity of proteins through weak interactions.

It should be also noted that these proteins involve the possibility of application to the specific chemical reactions due to the formation of local environment by protein molecule. In order to investigate this point, the photo-reaction of porphyrin-substituted hemoproteins are discussed. Previous studies reported that photo-hypersensitivity was observed in erythropoietic protoporphyria, which is one of the hereditary diseases having a default in heme biosysthesis, and porphyrin is incorporated to hemoglobin instead of protoheme (iron-porphyrin complex) in the patient's red cell.[21] Although photo-hypersensitivity seems to arise from the formation of singlet molecular oxygen by photoreaction of porphyrin, free porphyrin in aqueous solution *in vitro* poorly produced the singlet oxygen. However, the red cell of the patient generates singlet oxygen with high efficiency. Therefore, it is suggested that porphyrin-hemoglobin which is observed for the patients is the active species for the formation of the singlet oxygen. To clarify this point, porphyrin-substituted hemoprotein is synthesized and the efficiency of the production of singlet oxygen is determined. The possibility of the porphyrin-hemoprotein as a high efficiency singlet oxygen generation system is discussed.

In summary, the following three points are focused on in this thesis:
(1) How does hemoglobin regulate its structure and function and what is the molecular mechanism of cooperativity?
(2) What interaction exerts between globin and heme or subunit and subunit?
(3) What is induced from these interaction as general nature of protein or enzyme and is it possible that hemoprotein can be applied to some chemical

reactions?

In Part II, III and IV, the molecular mechanism of oxygen binding of hemoglobin (1) are discussed and Part V and VI illustrates the discussion point (2) and (3).

REFERENCES

1. Dayhoff, M. O. ed., (1972) *Atlas of Protein Sequence and Structure*, Vol. 5 Natl. Biomed. Res. Found., Silver Spring, Maryland.
2. Muirhead, H., & Geer, J. (1970) *Nature (London) 228*, 516
3. Perutz, M. F., Muirhead, H., Cox, J. M., Goaman, L. C. G., Mathews, F. S., McGandy, E. L., & Webb, L. E. (1968) *Nature (London) 219*, 29.
4. Peritz, M. F., Muirhead, H., Cox, J. M., & Goaman, L. C. G. (1968) *Nature (London) 219*, 131.
5. Bolton, W., & Perutz, M. F. (1970) *Nature (London) 228*, 551.
6. Kendrew, J. C., Dickerson, R. E., Strandberg, B. E., Hart, D. R. G., Davis, D. R., Phillips, D. C., & Shore, V. C. (1960) *Nature (London) 185*, 422.
7. Kendrew, J. C., Watson, H. C., Strandberg, B. E., Dickerson, R. E., Phillips, D. C., & Shore, V. C. (1961) *Nature (London) 190*,666.
8. Scouloudi, H. (1969) *J. Mol. Biol., 40*, 353.
9. Lattman, E. E., Mockolds, C. E., Kretsinger, R. H., & Love, W. E. (1971) *J. Mol. Biol., 60*, 271.
10. Hendrickson, W. A., & Love, W. E. (1970) *Nature (London), New Biol. 232*, 197.
11. Love, W. E., Klock, P. A., Lattman, E. E., Padlan, E. A., Ward, K. B. Jr., & Hendrickson, W. A. (1970) *Cold Spring Harbor Symp. Quant. Biol., 36*, 349.
12. Huber, R., Epp, O., Steigemann, & Forkmanek, H. (1971) *Eur. J. Biochem., 19*, 42.
13. Antonini, E., & Burunori, M. (1971) *Hemoglobin and Myoglobin in Their Reactions with Ligands*, North-Holland, London.
14. Dickerson, R. E., & Geis, I. (1983) *Hemoglobin: Structure, Function, Elution and Pathology*, Benjamin/Cummings, New York.
15. Inubushi, T., Ikeda-Saito, M., & Yonetani, T. (1983) *Biochemistry 22*, 2904.
16. Simolo, K., Stucky, G., Chen, S., Bacley, M., Scholes, C., & Mclendon, G. (1985) *J. Am. Chem. Soc., 107*, 2865.

17. Arnone, A., Rogers, P., Blough, N. V., McGourty, J. L., & Hoffman, B. M. (1986) *J. Mol. Biol., 188*, 693.
18. Shibayama, N., Inubushi, T., Morimoto, H., & Yonetani, T. (1987) *Biochemistry 26*, 2194.
19. Fung, L. W. -M., & Ho, C. (1975) *Biochemistry 14*, 2526-2535.
20. Takahashi, S., Lin, A. K. -L. C., & Ho, S. (1980) *Biochemistry 19*, 5196-5202.
21. Magnus, J. A., Jarrett, A., Prankert, T. A. J., and Rimington, C. (1961) *Lancet. 2*, 448-451.

FIGURE LEGENDS

Figure 1.

Schematic representations of protoporphyrin (A), myoglobin (B) and Hemoglobin (C).

Fe-Protoporphyrin-IX
Protoheme
Fe
N
N
N
N
O
O⁻
⁻O
O
(A)
Myoglobin
(B)
Hemoglobin
α1
α2
β2
β1
(C)

Figure. 1

PART II.

STRUCTURES AND FUNCTIONS OF PARTIALLY OXYGENATED HEMOGLOBINS

CHAPTER 1.

Ruthenium-Iron Hybrid Hemoglobins As a Model for Partially Liganded Hemoglobin:

NMR Studies of Their Tertiary and Quaternary Structures.

ABSTRACT: Diruthenium-substituted Ru-Fe hybrid hemoglobins (Hb) were synthesized by heme substitution from protoheme to ruthenium(II) carbonyldeuteroporphyrin in the α or β subunits. As the carbonmonoxide coordinated to ruthenium(II) is not released under physiological conditions, deoxygenated Ru-Fe hybrid derivatives, [$\alpha(Fe)_2\beta(Ru\text{-}CO)_2$ and $\alpha(Ru\text{-}CO)_2\beta(Fe)_2$], can serve as models for half-liganded Hbs. On the basis of proton NMR spectra of hyperfine-shifted proton resonances, these Ru-Fe hybrid Hbs have only small structural changes in the heme environment of the partner subunits at low pH. The proton NMR spectra of the intersubunit hydrogen-bonded protons also showed that the quaternary structures of the two complementary hybrids both remain in the "T-like-state" at low pH, suggesting that the T to R structural conversion is induced by ligation of the third ligand molecule. Marked conformational changes in the heme vicinity are observed at high pH only for $\alpha(Ru\text{-}CO)_2\beta(Fe)_2$ and its quaternary structure is converted into the "R-state"; the $\alpha(Fe)_2\beta(Ru\text{-}CO)_2$ hybrid does not undergo this change. This implies that the free energy difference between the two quaternary states is smaller in the β-liganded hybrid than in the α-liganded one.

Hemoglobin (Hb) has long served as a paradigm for cooperative ligand binding in proteins (Antonini at al., 1971; Edelstein, 1975; Dickerson & Geis, 1983). On the basis of numerous experimental studies, particularly X-ray crystallography (Perutz, 1976, 1979) and nuclear magnetic resonance (NMR) spectroscopy (Ho et al., 1975; Shulman et al., 1975), a number of specific mechanisms to account for the cooperativity have been proposed (Monod et al., 1965; Koshland et al., 1965; Gelin & Karplus, 1977; Warshel, 1977; Perutz, 1976). However, detailed understanding of the control mechanism of ligand affinity in Hb may well be achieved only by analyzing the tertiary and quaternary structures and functional properties of the protein as a function of the degree of ligation. Therefore, the most uncompromising problem that we encounter in studying the quaternary and tertiary structural change induced by ligation is physical and chemical characterizations of Hb species at the intermediate state of ligation, which have been very elusive owing to the difficulty in isolating such species.

To gain an insight into structural characterizations of the partially liganded Hb, the half-liganded Hbs have been studied by utilizing valency hybrid Hb (Ogawa & Schulman, 1972), metal hybrid Hb (Inubushi et al., 1983, 1986; Blough et al., 1980, 1982; Simolo et al., 1985; Shibayama et al., 1987) and intersubunit cross-linked Hb (Miura & Ho, 1982, 1984). However, there has not been an ideal model which is stable enough to study the structure of partially liganded Hb in detail, which would be requisite in characterizing the effect of partial ligation on the properties of individual subunits and the tetrameric Hb molecule as well. Ogawa & Shulman (1972) used Fe(III)-CN^- heme as a structural model for a oxy heme, but it was very difficult to deoxygenate the Fe(III)-Fe(II) hybrids due to auto-oxidation. In this sense, iron-ruthenium symmetric hybrid Hbs in which α or β subunit contains Ru(II)-CO porphyrin, with the other subunit having deoxygenated Fe(II) porphyrin, could be an ideal models for testing the properties of the intermediate ligand binding state. Ru(II)-CO porphyrin has the following unique properties. (1) Carbonmonoxyporphyrin ruthenium(II) is virtually isoelectronic with low-spin iron(II) porphyrins involved in oxy-Hb or carbonmonoxy-Hb. Furthermore, since Ru(II)-CO bonding is very stable, Ru(II) does not readily react with exogenous ligands nor release the sixth ligand. (2) Deoxygenated Ru-Fe hybrid Hb such as $\alpha(\text{Ru-CO})_2\beta(\text{Fe})_2$ and $\alpha(\text{Fe})_2\beta(\text{Ru-CO})_2$ can bind two molecular oxygens to the iron-containing subunits. This implies that the oxygen binding property of Ru-Fe hybrids can be compared directly with that of native Hb. Because of the diamagnetic

property of Ru(II) in half-liganded Ru-Fe hybrid Hbs, the paramagnetic ^1H NMR resonances from deoxygenated Fe(II) subunits can be observed separately. (3) Half-liganded Ru(CO)-deoxy Fe(II) hybrids can be prepared easily from $\alpha(Ru\text{-}CO)_2\beta(Fe\text{-}O_2)_2$ and $\alpha(Fe\text{-}O_2)_2\beta(Ru\text{-}CO)_2$ by flushing with Ar gas and adding of dithionite. The Ru(II)CO-containing subunit is therefore expected to be in a "fixed" oxy-like tertiary and quaternary structure and Ru-Fe hybrid Hbs can serve as models for the intermediate species in the half-liganded state and deserve to be characterized structurally by physical and chemical methods.

^1H NMR is a powerful tool in studies of the tertiary and quaternary structural changes induced by ligand binding to the Hb molecule (Ho & Russu, 1981). NMR studies of Ru-Fe hybrid Hbs may offer an opportunity to monitor these structural alterations in Hb by the use of following characteristic NMR features: (1) the hyperfine-shifted resonance of the imidazole N_1H proton of the proximal histidine (His F8) coordinated to the paramagnetic heme iron and the resonances of the methyl groups which are attached to the porphyrin skeleton and (2) the exchangeable proton resonances due to inter- and intrasubunit hydrogen bonds associated with the tertiary and quaternary structural changes of the Hb molecule. The hyperfine-shifted proximal histidine N_1H and the heme methyl resonances have been assigned to the Fe-containing subunits (La Mar et al., 1977; Takahashi et al., 1980). Proton resonances in the protein hydrogen-bonded region are associated with the T to R quaternary transition in Hb (Ogawa et al., 1972). The "T-" and "R-state" marker have been assigned to specific hydrogen bonds in the inter- and intrasubunit interface (Fung & Ho, 1975; Viggiano et al., 1978), and they have been used to monitor the T to R transition in a variety of Hb species (Ho & Russu, 1981). In this chapter, we report some unique structural features of these Ru-Fe hybrid Hbs as revealed by ^1H NMR spectroscopy in relation to the tertiary and quaternary structural changes induced by the ligand binding to either α or β subunits. We also discuss some implications for the allosteric mechanism of Hb.

MATERIALS AND METHODS

Ruthenium(II) carbonyldeuteroporphyrin[1] (Ru-DPIXCO) was prepared by a variant of the previous method (Tsutsui et al., 1971; Morishima et al.,

[1]Unfortunately, the syntheses of ruthenium(II) carbonylprotoporphyrin (Ru-PPIXCO) was not successful because the vinyl groups of protoporphyrin were modified during the incorporation reaction of ruthenium(II) into porphyrin.

1986).

Hemolysate was prepared in the usual manner from fresh whole blood obtained from the local blood bank. Hb A and its isolated chains were prepared in carbonmonoxide forms as described by Kilmartin et al. and Gerai et al.(Kilmartin & Rossi-Bernadi, 1971; Kilmartin et al., 1973; Gerai et al., 1969). Heme-free chain globins were prepared from isolated α and β chains by the method of Shibayama et al.(1987). The reconstitution of Ru-DPIXCO containing chains to form the tetrameric hybrid Hb were performed as reported by Shibayama et al.(1987). Apo α chain (500 mg) was dissolved in 300 ml of 20 mM borate/NaOH buffer (pH 12). The spectrophotometric titration of apoglobin with Ru-DPIXCO at 400 nm gave a well-defined inflection point, from which a molecular stoichiometry of 1 : 1 was estimated. The solution of apo α chain was mixed with a slight excess of Ru-DPIXCO, which was dissolved in a minimal amount of DMF. The mixture was gently stirred over night in the dark, and then concentrated by ultrafilteration and passed through a Sephadex G25 (Pharmacia) column of 20 mM borate/NaOH buffer, pH 10.5. The concentration of the α(Ru-CO) chain was determined from the absorption of the soret band. An equimolar amount of β(Fe-O_2) chains was treated with 32 mM-DL-dithiothreitol, added to α(Ru-CO) chains and left at 0 °C for 2 h. The α(Ru-CO)$_2$β(Fe-O_2)$_2$ solution thus obtained was passed through a Sephadex G25 column using a 20 mM Tris-HCl buffer, pH 7.2, then applied to a DE-23 cellulose (Whatman) column followed by a CM-23 cellulose (Whatman) column, both of which were equilibrated with the same 20 mM Tris-HCl buffer. The fraction that passed through both DE-23 and CM-23 cellulose columns was collected, concentrated by ultrafilteration and stored in liquid nitrogen.

Preparation of α(Fe-O_2)$_2$β(Ru-CO)$_2$ was carried out by the procedure described above, using appropriate constituents, Ru-DPIXCO, apo β chain, and α(Fe-O_2) chain.

For the preparation of Ru-HbCO, we used apo-Hb which had been made from native Hb A by the same procedure mentioned above. The apo-Hb was combined with a slight excess of Ru-DPIXCO, and the reconstituted Ru-HbCO was isolated by the purification procedure described above. The purity of all the samples was checked by isoelectric-focusing electrophoresis (Ampholine pH 6.5 to 9).

Millimolar extinction coefficients were calculated on the basis of the Ru concentration determined with AA-780 flameless atom absorption spectrometer.

Half-liganded samples were prepared by the addition of a minimal amount of sodium dithionite ($Na_2S_2O_4$) under an argon atmosphere. All samples were approximately at 1 mM/tetramer in 50 mM Bis-Tris or 50 mM Tris-HCl buffer containing 0.1 M Cl^-.

^1H NMR spectra at 300 MHz were recorded on a Nicolet NT-300 spectrometer equipped with a 1280 computer system. Hyperfine-shifted NMR spectra were obtained with 8K data transform of ±36-kHz and a 6.5-μs 90° pulse after the strong solvent resonance in H_2O solution was supressed by a 500-μs low power pulse. We used a Redfield 2-1-X pulse sequence with a 29.5-μs pulse and 8K data points over a 6-kHz spectral width for recording the exchangeable proton resonances in the subunit interface of Hb. The probe temperature was determined to ±0.5 °C by the temperature control unit of the spectrometer. The volume of the NMR sample was 0.3 mL. Proton shifts were referenced with respect to the water signal, which is 4.8 ppm downfield from the proton resonance of 4,4-dimethyl-4-silapentane-1-sulfonate (DSS) at 23 °C.

RESULTS

UV-vis Spectra of Ru-substituted Hb. Figure 1 shows UV-vis spectra of some of the Ru-substituted Hbs, Ru-HbCO (A), $\alpha(Ru\text{-}CO)_2\beta(Fe\text{-}O_2)_2$ (B) and $\alpha(Ru\text{-}CO)_2\beta(Fe)_2$ (C). The absorption spectra of Ru-HbCO indicated that there was a distinctively larger and sharper Soret peak at 396 nm compared with that of native Hb-CO. The millimolar extinction coefficients of Ru-HbCO which was determined on the basis of the atomic absorption spectra are summarized in Table I. In the oxygenated Ru-Fe hybrid Hb (B), the peaks at 396 and 517 nm are assigned to the α subunits which contained Ru(CO) and the shoulder around 415 nm and a peak at the 576 nm are assigned to $Fe(O_2)$ subunits. Deoxygenated Ru-Fe hybrid Hb shows the well resolved peaks at 396 and 430 nm, arising from α(Ru-CO) subunits and deoxy β(Fe) subunits, respectively. All of these spectral data are compiled in Table I.

Tertiary and Quaternary Structure of Ru-HbCO. Figure 2 shows the ^1H NMR spectra of native HbCO, $[\alpha(Fe\text{-}CO)_2\beta(Fe\text{-}CO)_2]$ and Ru-HbCO $[\alpha(Ru\text{-}CO)_2\beta(Ru\text{-}CO)_2]$ in 50 mM Bis-Tris buffer, pH 7.0. For native Hb, the ring-current-shifted proton peak at - 6.6 ppm has been assigned (Lindstrom et al., 1972) to the γ_1-methyl resonance of α and β E11 Val. The corresponding signal for Ru-HbCO was observed at 6.7 ppm with a

small shoulder at a downfield side probably due to the heme isomerism[2]. In the downfield region, the resonances at 8.2 ppm and 7.4 ppm, which were assigned to the exchangeable protons associated with the $\alpha_1\beta_1$ interface, hydrogen bond between β135 (C1) Tyr and α129 (F9) Asp (Asakura et al., 1976), and hydrogen bond between α103 (G10) His and β108 (G10) Asn (Russu et al., 1987) respectively, remains almost unchanged upon the heme substitution from the native heme to Ru-CO heme. A 5.9 ppm resonance, which has been utilized as an indicator for the oxy-like quaternary structure (Fung & Ho, 1975), is also insensitive to heme substitution.

Hyperfine-Shifted Proton Resonances. Figures 3A, 3B, 4A and 4B show the ^{1}H NMR spectra of deoxygenated Ru-Fe hybrid Hbs and native deoxy Hb A which correspond to the half-liganded and unliganded states, respectively. The hyperfine-shifted resonances at 72.1 and 59.5 ppm of the proximal His N_1H have been assigned respectively to β and α subunit, of native Hb A (Takahashi et al., 1980). The hyperfine-shifted proton resonances of the heme methyl groups were observed in the 5 to 20 ppm region . The signal at 18.6 ppm was assigned to β subunits and the resonances at 12.6 and 7.6 ppm were assigned to α subunits (Takahashi et al., 1980). In the spectrum of $\alpha(Ru\text{-}CO)_2\beta(Fe)_2$, the hyperfine-shifted resonance at 59.5 ppm for the deoxy α subunit disappeared from this region due to the diamagnetic nature of the porphyrin ruthenium(II) in the α subunits. The N_1H resonance of the β(Fe) subunits which is located at almost the same position as that of native Hb A is slightly shifted downfield with raising pH from 6.2 to 8.7. The resonance of the heme methyl group in β(Fe) subunits was also insensitive to the heme substitution of the partner subunits in the low pH region, while this signal exhibited a marked pH dependence. As pH is raised, the new signal arising from the heme methyl group appeared at 14.3 ppm and concomitantly the peak at 18.6 ppm decreased its intensity.

As Figure 4 shows, the resonance at 58.7 ppm for the counterpart symmetric hybrid Hb, $\alpha(Fe)_2\beta(Ru\text{-}CO)_2$, is readily assigned to the proximal His N_1H proton and those at 12.6 and 7.6 ppm to the heme methyl groups of the α(Fe) subunits by comparison with deoxy native Hb A. Their signal positions are almost identical to those of deoxy native Hb A and exhibit little

[2]For the Ru(CO) heme containing subunit, there are heme orientation isomers as visuarized by the splitting of the Val E11 methyl proton resonance. Either of these isomers is not converted to the other in time, because Ru-bound CO is strongly fixed at the heme coordination site. However, it was shown in our previous paper (Ishimori & Morishima, 1986) that the heme disorder in one subunit does not affect the quaternary structure of the complementary subunit and the quaternary structure as well.

pH dependence in the range 5.7 to 8.2. This observation suggests that the ligation of the β subunits does not affect the heme environmental structure of the α subunits. The positions of the hyperfine-shifted resonances are assembled in Table II.

Intra- and Intersubunit Hydrogen-Bonded Proton Resonances. Upon heme substitution in an α subunit from protoheme to Ru-DPIXCO, the "T-state"[3] signals at 9.2 and 6.1 ppm are observed at almost full intensity at low pH (Figure 3C). The former signal is observed at 9.4 ppm for deoxy native Hb A and has been assigned to the $\alpha_1\beta_2$ intersubunit hydrogen bond between tyrosine-α42(C7) and aspartic acid- β99(G1) (Fung & Ho, 1975) and the latter at 6.3 ppm for native Hb A has been assigned to the intrasubunit hydrogen bond between valine-β98(FG5) and tyrosine-β145(HC2) (Viggiano et al., 1978). As the pH is raised, these T-marker signals decrease in intensity and at pH 8.7, a small new resonance is detected at 5.9 ppm, which was also observed for the fully-liganded hybrid, $\alpha(Ru\text{-}CO)_2\beta(Fe\text{-}O_2)_2$, and may be assigned to the "R-state" marker signal (Fung & Ho 1975).

Different features in the spectra of the intersubunit hydrogen bonded protons are noticed for $\alpha(Fe)_2\beta(Ru\text{-}CO)_2$. The substitution of the native heme by Ru-DPIXCO in the β subunits reduced the intensity of the "T-state" marker substantially at 9.7 ppm but the signal was observed at pH 8.5 (Figure 4C). Another "T-state" marker, which is observed as a single peak at 6.4 ppm for deoxy native Hb (Figure 4C) and 6.1 ppm for the other hybrid (Figure 3C), experienced a similar tendency. The "R-state" marker at 5.9 ppm for the oxy spectrum (Figure 4C) at 5.9 ppm is absent in the spectra of the half-liganded species at various pH values. All the resonance positions of the hydrogen-bonded protons are summarized in Table II.

DISCUSSION

Ru-HbCO and Native HbCO. Inspection of Figure 2 and Table II shows that there is essentially no difference between native HbCO and Ru-HbCO in their ^1H NMR spectra (5 ~ 10 ppm) of intra- and intersubunit hydrogen bonded protons. The ring-current-shifted resonance at -5 to -7 ppm is also similar between native HbCO and Ru-HbCO. These results indicate that the

---

[3]We defined the deoxy structure as "T" and the oxy structure as "R" as frequently used in the literatures. In this paper we used the "T-like" and "R-like" structures when the quaternary structure of Ru-Fe hybrid Hb is close to the deoxy and oxy structures, respectively.

quaternary structure, which is manifested by hydrogen-bonded protons located in the $\alpha_1\beta_2$ and $\alpha_2\beta_1$ subunit interfaces, and the tertiary structure, visualized by the ValE11 methyl resonances, are essentially identical in Ru-HbCO and native HbCO. Keeping in mind that the porphyrin substitution from protoporphyrin to deuteroporphyrin induces only localized conformational changes (Seybert & Moffat, 1976; Ishimori & Morishima, 1986), it is likely that the Ru-HbCO can serve as a model for the "fixed" oxy-like state and the Ru-Fe hybrid Hbs used here could work as the models for the partially liganded Hb.

Ligation Effect on the Tertiary and Quaternary Structure of Ru-Fe Hybrid Hbs. We have demonstrated that the heme substitution from native heme to Ru-DPIXCO for one subunit induces slight changes in the hydrogen-bonded and hyperfine-shifted proton resonances as shown Table II. The "T-state" marker at approximately 9 ppm was observed for both hybrids (9.4 ppm for native Hb, 9.0 ppm for α-liganded hybrid and 9.5-9.8 ppm for β-liganded hybrid). Another T state marker around 6 ppm appeared in the β(Fe)-containing hybrid with decreased intensity in the complementary hybrid, whereas the "R-state" marker is only observed at high pH in $\alpha(\text{Ru-CO})_2\beta(\text{Fe})_2$. Since these T-marker signals are slightly shifted from those of native Hb A, we can conclude that the quaternary structures of the two hybrids at low pH are in the "T-like-state" which is defined as a quaternary structure somewhat different from the usual "T-state", as also found for the fully liganded valency hybrid in the presence of IHP (Morishima et al., 1986), cross-linked valency hybrid Hbs (Miura & Ho, 1984) and asymmetric Fe-Co hybrid Hbs (Inubushi et al., 1986). The resonances of the proximal N_1H and the heme methyl group also appeared at almost the same position as native deoxy Hb at low pH, and is consistent with the features of the hydrogen-bonded proton resonances. This implies that the tertiary structure of the two hybrids remains in the deoxy-like structure.

It thus follows that the "R state" is not induced by the binding of two ligands at low and neutral pH. The crystal structure study of the half-liganded hybrid Hb, $\alpha(\text{Fe-CO})_2\beta(\text{Mn})_2$ (Arnone et al., 1986), also revealed that its quaternary and tertiary structure is almost identical to that of native deoxy Hb. On the basis of the MWC model analysis of the oxygen equilibrium curve, a switch-over point, i_s, which expresses the degree of oxygenation at which the populations of the "R-" and "T-state" are equal, was determined in the range 2 ~ 3 (Imai 1983), suggesting that the R-T transition is induced by the binding of the third oxygen. These results appear to be

consistent with our present finding that the doubly liganded Hb is still in the "T-like-state". However, Simolo et al. (1985) reported that the $\alpha(Fe\text{-}CO)_2\beta(Zn)_2$ hybrid Hb exhibits the "R-state" marker signal. The "R-state" marker was also observed for iron-cobalt symmetric hybrid hemoglobins (Yonetani personal communication). These results suggest that ligation of the two ligands induces quaternary structural transition from the T- to "R-state", which is contrary to our results. Such a difference may arise from the different state of the heme iron in the hybrid Hbs and/or the different properties of the substituted heme-metal. Our Ru-Fe hybrid Hbs have deoxygenated iron, whereas the heme iron in Co-Fe and Zn-Fe hybrid Hbs is liganded. These substituted metals also have different ionic radii, bond lengths to the axial ligands and other properties. In other words, the difference in the quaternary structures of these half-liganded hybrid Hbs reflects these structural differences.

Difference of the Tertiary and Quaternary Structures of Two Complementary Ru-Fe Hybrid Hemoglobins. In order to characterize the tertiary and quaternary structure of diliganded Ru-Fe hybrid Hbs, we examined the pH dependence of their NMR spectra.

In the hydrogen-bonded region of the ^1H NMR spectra of these two symmetric Fe-Ru hybrid Hbs, we demonstrated that the heme substitution induces some different structural alterations between these two complementary hybrids. In the liganded subunit hybrid, $[\alpha(Ru\text{-}CO)_2\beta(Fe)_2]$, the "T-state" markers at approximately 6 and 9 ppm almost maintained their signal intensities at low pH. As pH is raised, the "T-state" marker signals decreased their intensities and a small "R-state" marker signal appeared as illustrated in Figure 3 and Table II, implying that the quaternary structure is converted from the "T-like-state" into the "R-like state" at high pH. In the hyperfine-shifted spectral region, a new heme methyl resonance appeared concomitantly to the decrease of the signal intensity of the peak around 18 ppm, which has been assigned to the deoxygenated β(Fe) subunits. Since such a pH dependence of the heme methyl resonances is associated with the quaternary structural change, the pH-induced quaternary structural changes of the α(Ru-CO) hybrid are accompanied by the tertiary structural alterations in the heme environments.

These results may show that the small free energy difference between two quaternary structures (ΔG_2^{trans}) for the α liganded hybrid is enough to change its quaternary structure by varying pH. Such a small free energy was also estimated on the basis of the oxygen equilibrium curve for native Hb

A. Imai (1979) reported the ΔG_2^{trans} is approximately +9 x 10^3 J at pH 6.5 and -3 x 10^3 J at pH 9.1, showing that the "T-state" is more favored at low pH. This appears to be consistent with our present results.

The complementary hybrid, [$\alpha(Fe)_2\beta(Ru\text{-}CO)_2$], exhibited a pH dependence which is quite different from $\alpha(Ru\text{-}CO)_2\beta(Fe)_2$. At low pH, two "T-state" markers, which are shifted slightly from those for native protein and exhibit the reduced intensities, are observed, showing that the β-liganded hybrid also maintains its quaternary structure in the "T-like state". At pH 8.5 where the quaternary structure of the α-liganded hybrid is converted into the "R-state", the spectrum of the β-liganded hybrid is essentially the same as that at low pH. The hyperfine-shifted resonances were also insensitive to varying pH as shown in Table II. This implies that the quaternary and tertiary structure of the β-liganded hybrid is still in the "T-like-state" at high pH, but not in the equilibrium between "R-" and "T-like state" as found for the α-liganded hybrid. This observation also suggests that the free energy difference (ΔG_2^{trans}) for the β-liganded hybrid is positive at high pH and its pH dependence is different from that of native Hb and the complementary hybrid. From above discussion it is concluded that the β-liganded hybrid exhibits more "T-state" character than α-liganded one at high pH, which suggests that the ligation for α subunits affects more substantially the quaternary and tertiary structures of the partner subunits than does the ligation for β subunits.

Such a different behavior between two complementary hybrids has also been encountered for several metal hybrid Hbs (Inubushi et al., 1983, 1986; Simolo et al., 1985; Shibayama et al., 1987). In Co-Fe hybrid Hbs (Inubushi et al., 1983, 1986), the ligation for the β subunits induced larger conformational changes in its quaternary structure, whereas Zn-Fe (Simolo et al., 1985), Ni-Fe (Shibayama et al., 1987) hybrids exhibited preferential structural changes by the ligand binding of α subunits. $\alpha(Ru\text{-}CO)_2\beta(Fe)_2$ shows marked pH dependence for the hydrogen-bonded proton resonances, but $\alpha(Fe\text{-}CO)_2\beta(Ni)_2$ experiences no significant pH-dependent spectral changes in the same region and the spectrum of the complementary hybrid [$\alpha(Ni)_2\beta(Fe\text{-}CO)_2$] depends on pH as found for $\alpha(Ru\text{-}CO)_2\beta(Fe)_2$. Since many controversial points still remain open to further studies about the relationship between the partial ligand binding in one subunit and the quaternary structure, it is premature to conclude that there is an equivocal correlation between the ligand binding and the quaternary structure in the complementary pairs of hybrids. It may be safer to say that the quaternary

structure of the half-liganded hybrids is not determined uniquely and is easily perturbed by the physical properties of the substituted metals or the specific structural changes of the subunits.

In summary, the present NMR results have revealed the structures of the half-liganded Fe-Ru hybrid Hbs which may serve as a model for the intermediate species in oxygenation of native Hb. The partial ligation of one subunit does not give rise to the drastic quaternary and heme environmental structural changes in the partner subunits at low pH. In other words, the half-liganded Ru-Fe hybrid Hbs maintains their quaternary structure in the "T-like-state" and the T to R structural transition can be induced by binding of three ligand molecules. However, the substantial structural changes accompanied by the quaternary structural transition which are induced at high pH for the α-ligand hybrid, suggest that the energy difference between two quaternary structures of the α-liganded hybrid Hb is small. More detailed studies on the properties of the half-liganded Fe-Ru hybrid Hbs such as oxygen binding affinity are now under way.

REFERENCES

Antonini,E., & Brunori, M. (1971) *Hemoglobin and Myoglobin in Their Reactions with Ligands*, North-Holland, London.

Arnone, A., Rogers, P., Blough, N. V., McGourty, J. L., & Hoffman, B. M. (1986) *J. Mol. Biol. 188*, 693-706.

Asakura, T., Adachi, K., Wiley, J. S., Fung, L. W. -M., Ho, C., Kilmartin, J. V., & Perutz, M. F. (1976) *J. Mol. Biol. 104*, 185-195.

Blough, N. V., Zemel, H. & Hoffman, B. M. (1980) *J. Am. Chem. Soc. 102*, 5683-5685.

Blough, N. V., & Hoffman, B. M. (1982) *J. Am. Chem. Soc. 104*, 4247-4250.

Dickerson, R. E., & Geis, I. (1983) *Hemoglobin: Structure, Function, Elution and Pathology*, Benjamin/Cummings Publishing Co., New York.

Edelstein, S. J. (1975) *Annu. Rev. Biochem. 44*, 209-232.

Fung, L. W. -M., & Ho, C. (1975) *Biochemistry 14*, 2526-2535.

Gelin, B. R., & Karplus, M. (1977) *Proc. Natl. Acad. Sci. U. S. A. 74*, 801-805.

Gerai, G., Parkhurst, L. J., & Gibson, Q. H. (1969) *J. Biol. Chem. 244*, 4664-4667.

Ho, C., Fung, L. W. -M., Weichelman, K. J., Pifat, G., Johnson, M. E. In *Erythrocyte Structure and Function*, Brewer, G. J., Ed., Liss, New York, 1975, pp 43-64.
Ho, C., & Russu, I. M. (1981) *Method Enzymol. 76*, 275.
Huang, T. -H. (1979) *J. Biol. Chem. 254*, 11467-11474.
Imai (1979) *J. Mol. Biol. 133*, 233-247.
Imai (1983) *J. Mol. Biol. 167*, 741-749.
Inubushi, T., Ikeda-Saito, M., & Yonetani, T. (1983) *Biochemistry 22*, 2904-2907
Inubushi, T., D'Ambrosio, C., Ikeda-Saito, M., & Yonetani, T. (1986) *J. Am. Chem. Soc. 108*, 3799-3803.
Ishimori, K. & Morishima, I. (1986) *Biochemistry 25*, 4892-4898.
KilMartin, J. V., & Rossi-Bernardi, L (1971) *Biochem. J. 124*, 31-45.
Kilmartin, J. V., Fogg, J., Luzzana, M., & Rossi-Bernardi, L. (1973) *J. Biol. Chem. 248*, 7039-7043.
Koshland, D. E., Nemethy, G., & Filmer, D. (1965) *Biochemistry 5*, 365-385.
La Mar, G. N., Budd, D. L., & Goff, H. (1977) *Biochem. Biophys. Res. Commun. 77*, 104-110.
Lindstrom, T. R., Noren, I. B. E., Charache, S., Lehmann, H., & Ho, C. (1972) *Biochemistry 11*, 1677-1681.
Miura, S., & Ho, C. (1982) *Biochemistry*, 21, 6280-6287.
Miura, S., & Ho. C. (1984) *Biochemistry*, 23, 2492-2499.
Monod, J., Wyman, J., & Changeux, J. P. (1965) *J. Mol. Biol. 12*, 88-118.
Morishima, I., Shiro, Y., & Nakajima, K. (1986) *Biochemistry 25*, 3576-3584.
Morishima, I., Hara, M., & Ishimori, K. (1986) *Biochemistry 25*, 7243-7250.
Ogawa, S., & Schulman, R. G, (1972) *J. Mol. Biol.*, 70, 315-336.
Ogawa, S., Mayer, A., & Schulman, R. G. (1972) *Biochem. Biophys. Res. Commun. 49*, 1485-1491.
Perutz, M. F. (1976) *Br. Med. Bull. 32*, 195-208.
Perutz, M. F. (1979) *Annu. Rev. Biochem. 48*, 327-336.
Russu, I. M., Ho, N. T., & Ho, C. (1987) *Biochim. Biophys. Acta. 914*, 40-48.
Schulman, R. G., Hopfield, J. J., & Ogawa, S. (1975) *Q. Rev. Biophys. 8*, 325-420.
Serbert, D. & Moffat, K. (1976) *J. Mol. Biol. 106*, 895-902.

Shibayama, N., Inubushi, T., Morimoto, H., & Yonetani, T. (1987) *Biochemistry 26*, 2194-2201.

Simolo, K., Stucky, G., Chen, S., Bacley, M., Scholes, C., & Mclendon, G. (1985) *J. Am. Chem. Soc. 107*, 2865-2872.

Takahashi, S., Lin, A. K. -A. C., & Ho, C. (1980) *Biochemistry 19*, 5196-5202.

Tsutsui, M., Ostfeld, D., & Hoffman, L. M. (1971) *J. Am. Chem. Soc. 93*, 1820-1823.

Viggiano, G., Wiechelman, K. J., Cherverick, P. A., & Ho, C. (1978) *Biochemistry 17*, 795-799.

Warshel, A. (1977) *Proc. Natl. Acad. Sci. U. S. A. 74*, 1789-1793.

FIGURE LEGENDS

Figure 1.

Absorption spectra of Ru-HbCO (A), $\alpha(Ru\text{-}CO)_2\beta(Fe\text{-}O_2)_2$ (B) and $\alpha(Ru\text{-}CO)_2\beta(Fe)_2$ (C) in 50 mM Bis-Tris buffer with 0.1 M chloride pH 7.0 at 25 °C. ε (mM) is a millimolar extinction coefficient of Hb (heme).

Figure 2.

Proton NMR spectra (300MHz) for native Hb CO (A) and Ru-HbCO (B) in 50 mM Bis-Tris with 0.1 M chloride pH 7.0 at 23 °C.

Figure 3.

Proton NMR spectra (300 MHz) of deoxy native Hb (pH 7.0) (lowest spectrum), $\alpha(Ru\text{-}CO)_2\beta(Fe)_2$ and $\alpha(Ru\text{-}CO)_2\beta(Fe\text{-}O_2)_2$ (pH 7.0) (top spectrum in C) in 50 mM Bis-Tris or Tris buffer with 0.1 M chloride at 23 °C: hyperfine-shifted proton resonances of proximal His N_1H (A) and heme methyl group (B); hydrogen-bonded proton resonances (C). "T" and "R" show the "T-state" marker and "R-state" marker, respectively.

Figure 4.

Proton NMR spectra (300 MHz) of deoxy native Hb (pH 7.0) (lowest spectrum), $\alpha(Fe)_2\beta(Ru\text{-}CO)_2$ and $\alpha(Fe\text{-}O_2)_2\beta(Ru\text{-}CO)$ (pH 7.0) (top spectrum in C) in 50 mM Bis-Tris or Tris buffer with 0.1 M chloride at 23 °C: hyperfine-shifted proton resonances of proximal His N_1H (A) and heme methyl group (B); hydrogen-bonded proton resonances (C). "T" and "R" show the "T-state" marker and "R-state" marker, respectively.

Table I
Spectrophotometric properties of Ru-substituted Hbs

A. Ru-HbCO					
nm	395	517	548		
ε (mM / tetramer)	888	54.4	58.0		
B. $\alpha(Ru\text{-}CO)_2\beta(Fe\text{-}O_2)_2$					
nm	395	415	519	546	576
ε (mM / tetramer)	536	301	39.4	52.2	31.2
C. $\alpha(Ru\text{-}CO)_2\beta(Fe)_2$					
nm	395	427	518	550	
ε (mM / tetramer)	499	253	41.5	51.8	
D. $\alpha(Fe\text{-}O_2)_2\beta(Ru\text{-}CO)_2$					
nm	395	415	520	545	575
ε (mM / tetramer)	545	310	38.1	50.0	30.0
E. $\alpha(Fe)_2\beta(Ru\text{-}CO)_2$					
nm	396	428	517	548	
ε (mM / tetramer)	498	256	39.4	48.5	

Table II
Resonance Positions of Native Hb, Ru-HbCO and Ru-Fe Hybrid Hbs

Hb	Proximal N_1H			Heme Methyl		Hydrogen Bond			
	β	α				T		T	R
Native oxy Hb							8.2 7.4		5.9
$\alpha(Ru\text{-}CO)_2$ $\beta(Ru\text{-}CO)_2$							8.2 7.4		6.(
$\alpha(Ru\text{-}CO)_2$ $\beta(Fe\text{-}O_2)_2$							8.1 7.4		5.9
$\alpha(Ru\text{-}CO)_2$ $\beta(Fe)_2$									
pH 8.7	72.9		17.0	11.8			8.2 7.4		5.9
pH 7.6	72.2		17.4	11.5			8.2 7.4		
pH 6.5	71.7		18.5			9.0	8.2 7.4	6.1	
pH 6.2	71.3		18.5			9.0	8.2 7.4	6.1	
$\alpha(Fe\text{-}O_2)_2$ $\beta(Ru\text{-}CO)_2$							8.2 7.4		5.9
$\alpha(Fe)_2$ $\beta(Ru\text{-}CO)_2$									
pH 8.5		58.7		12.8	7.8	9.5	8.2 7.4	6.4	
pH 6.9		58.7		12.8	7.7	9.6	8.1 7.4	6.4	
pH 6.5		58.7		13.0	7.5	9.7	8.1 7.4	6.4	
pH 5.7		58.6		13.0	7.6	9.8	8.1 7.5	6.4	
Native deoxy Hb	72.1	59.5	18.3	12.6	7.6	9.4	8.3 7.6	6.4	

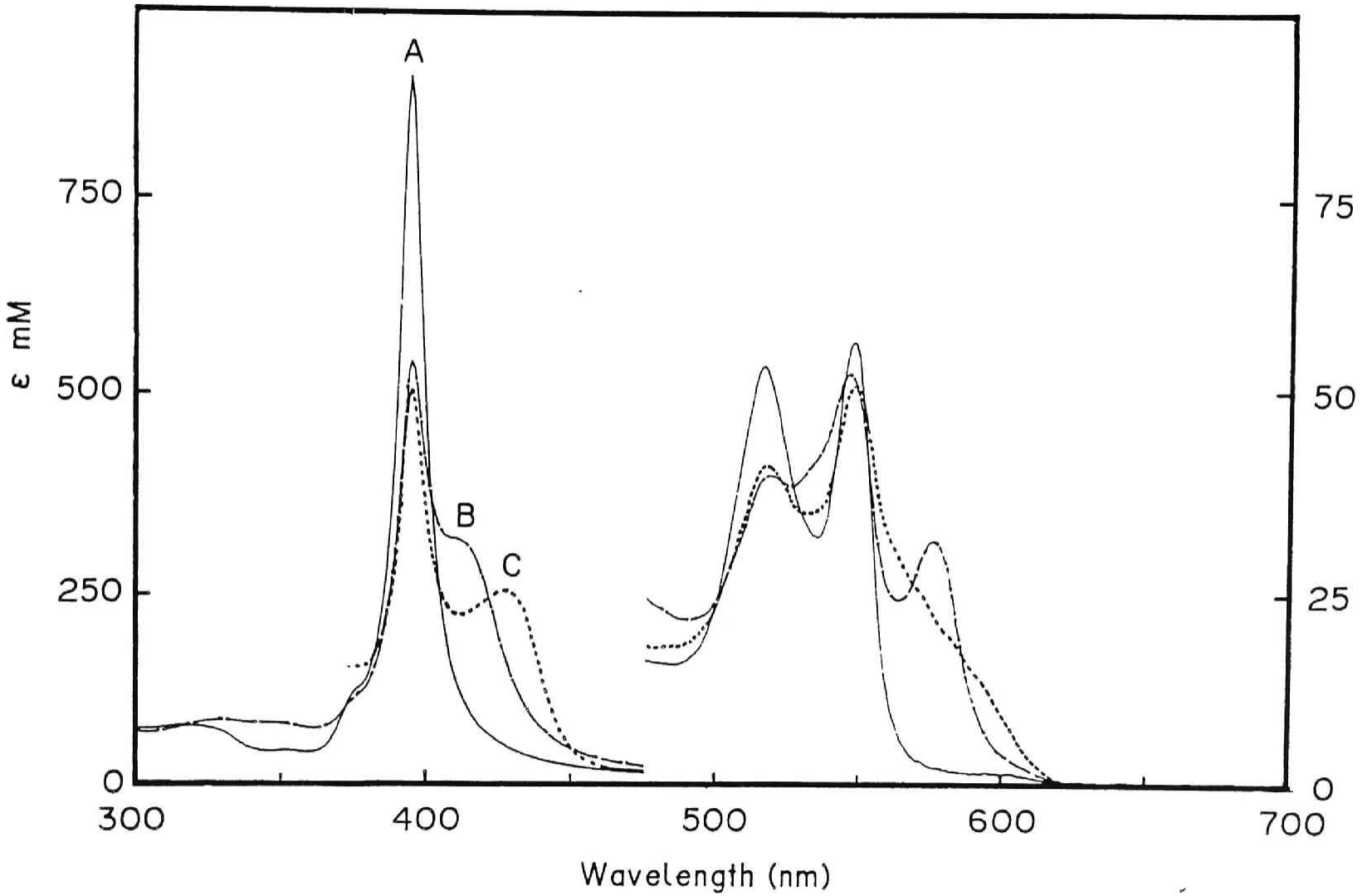
A
B
C
750
500
250
0
75
50
25
0
300
400
500
600
700
Wavelength (nm)
ε mM

Figure. 1

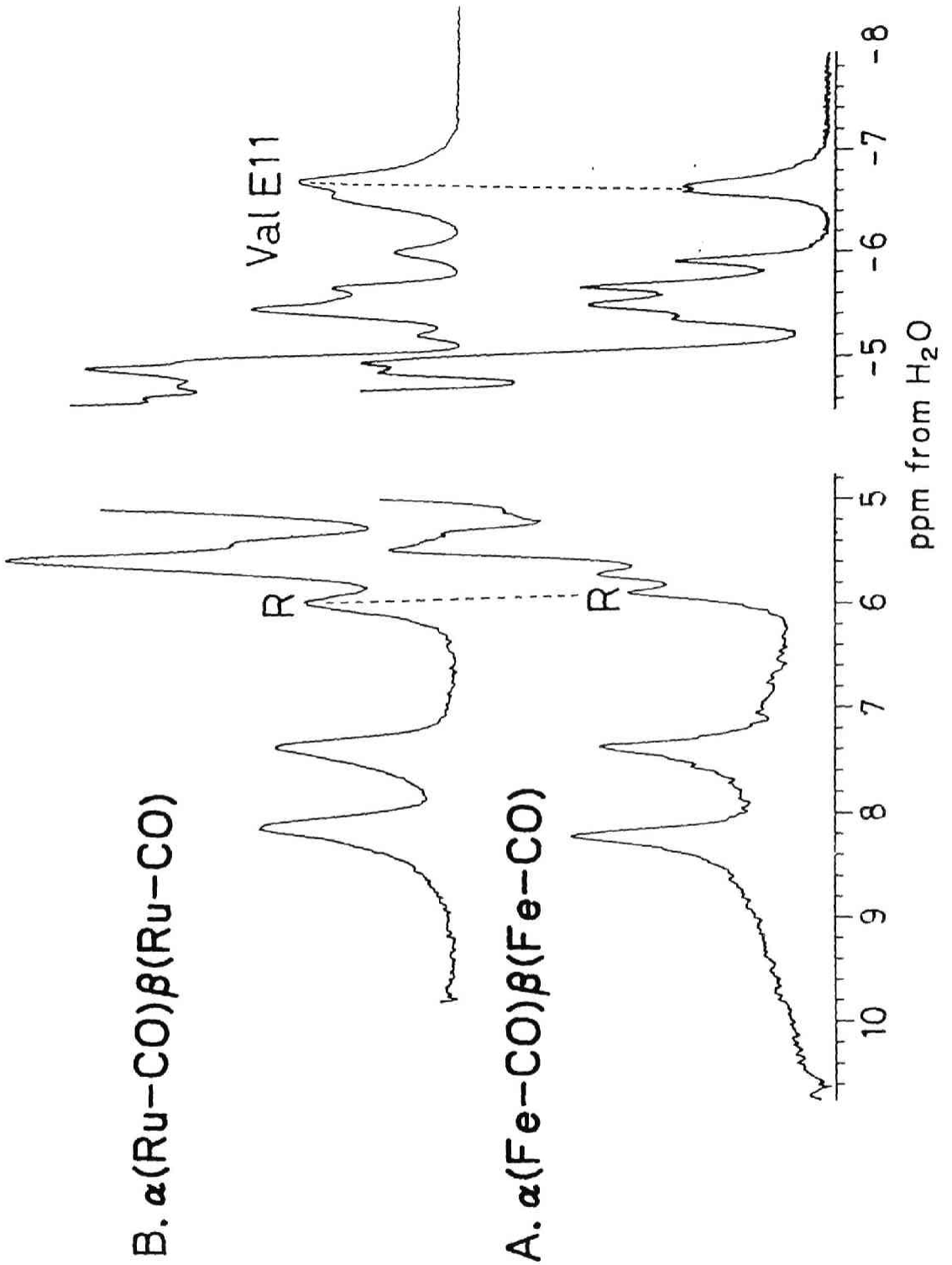
B. α(Ru−CO)β(Ru−CO)
A. α(Fe−CO)β(Fe−CO)
R
R
Val E11
10
9
8
7
6
5
-5
-6
-7
-8
ppm from H_2O

Figure. 2

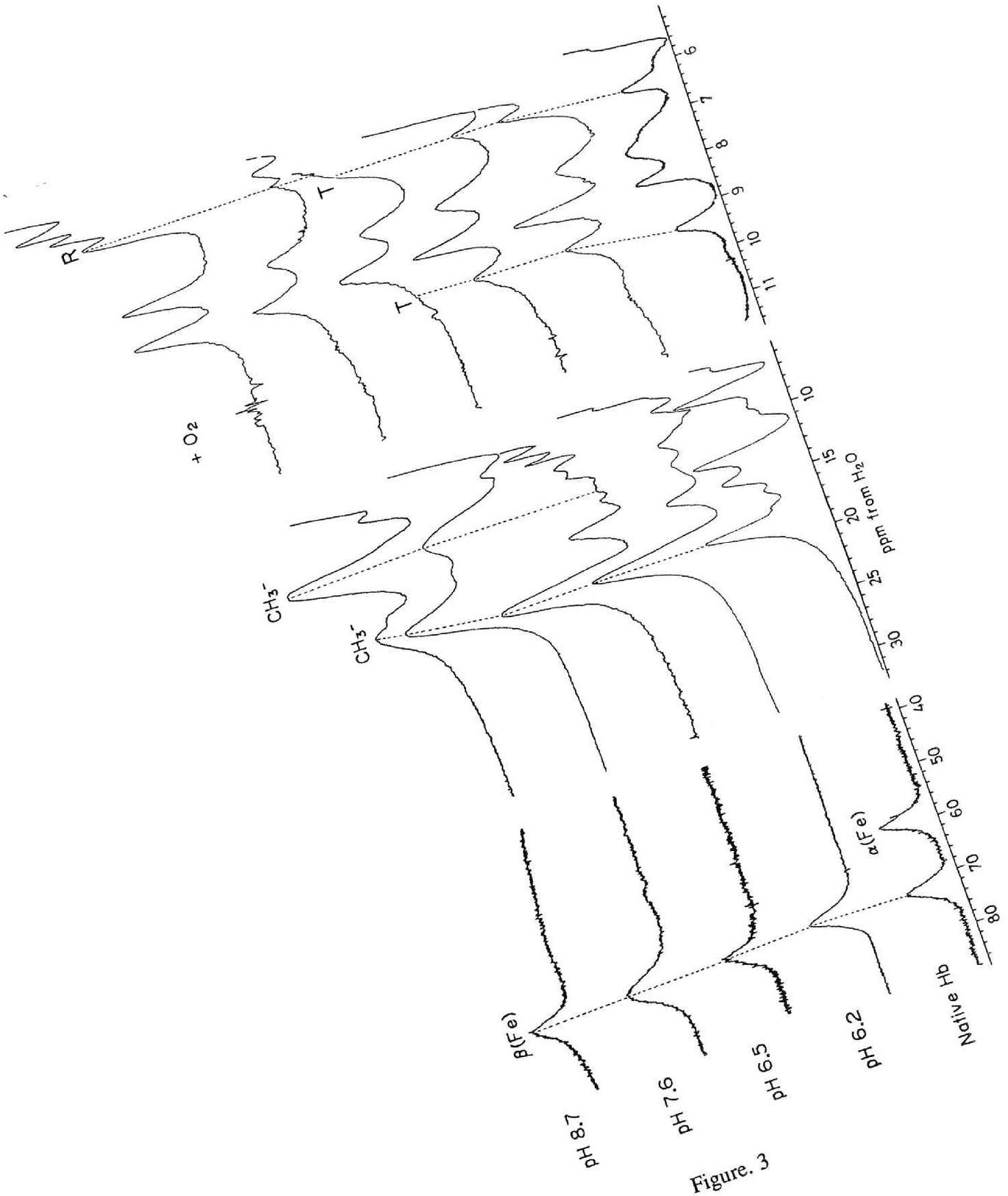
R
T
T
T
+ O2
CH3-
CH3-
ppm from H2O
α(Fe)
β(Fe)
pH 8.7
pH 7.6
pH 6.5
pH 6.2
Native Hb

Figure. 3

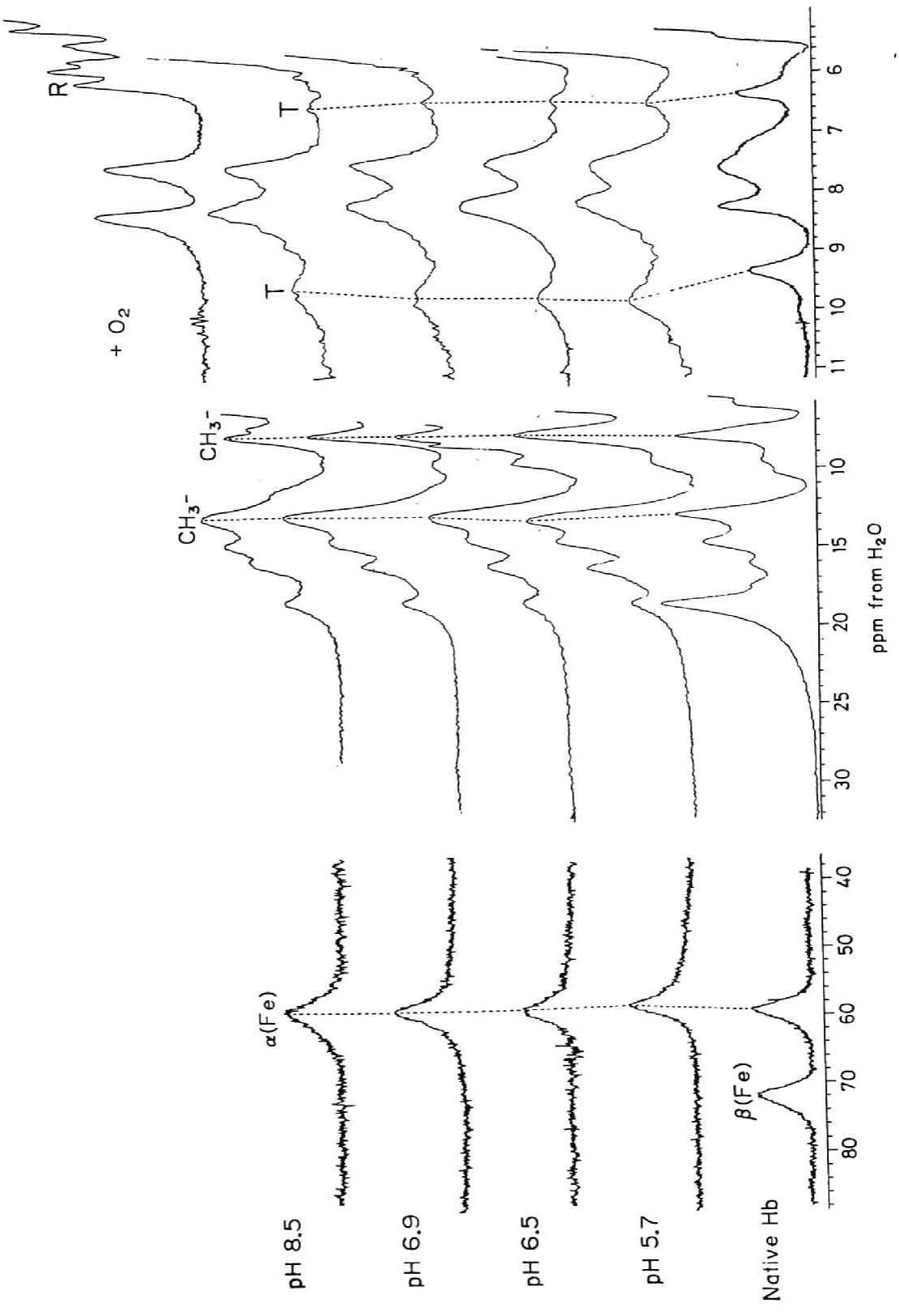
R
+ O2
T
T
CH3-
CH3-
ppm from H2O
α(Fe)
β(Fe)
pH 8.5
pH 6.9
pH 6.5
pH 5.7
Native Hb

Figure. 4

CHAPTER 2.

Ruthenium-Iron Hybrid Hemoglobins as a Model for Partially Liganded Hemoglobin:

Sulfhydryl Activity of β93 Cys.

ABSTRACT: The reaction of 4,4'-dithiodipyridine (4-PDS) with the SH groups of β93 Cys of Ru-Fe hybrid hemoglobins in which one subunit contains Ru(II) porphyrin while the other subunit contains native Fe(II) porphyrin has been studied to investigate the structure of the intermediate species in the oxygenation step. The pseudo-first rate constants for the reaction were plotted as function of pH. It is found, on the basis the rate data for native hemoglobin A and hybrid hemoglobin, that the reactivity of the β93 Cys is preferentially dependent on the ligation of the α subunit and the ligation of the neighbouring β subunit has smaller effect on the sulfhydryl reactivity than that of α the subunit. Thus, we can conclude that in order to cut the salt bridge completely, α40 Lys - β146 His - β94 Asp which is screening the SH group of β93 Cys and interfering the approach of the SH reagents, requires the rotation or deviation of the α C helix around α 40 Lys which is governed by the ligation of the a subunit, whereas the rotation of the β F helix, which is induced by the ligation of the β subunit, causes some structural changes around the salt bridge and is not sufficient for the complete cleavage of the salt bridge. Moreover, the comparison of other conformational and functional probes, such as NMR spectra and preliminary oxygen equilibrium curve, indicates that the drastic changes of the sulfhydryl reactivity precedes the other conformational and functional changes accompanied with the oxygenation and the salt bridge plays a key role for propagating structural changes from one subunit to other subunit.

Despite many elegant studies, the basis for cooperative ligand binding in Hb remains incompletely understood (1,2). One central question is "how does the structure of Hb change with sequential addition of one, two, three, or four ligands ?". To answer this question, stable Hb derivatives are needed to model intermediate ligation states. To this end, a number of studies have appeared over the past decades of "mix-valence" Hbs in which the heme in one type of subunit is oxidized to produce a six-coordinate Fe(III), while the heme in the other type subunit remains reduced and can be deoxygenated to produce a five-coordinate Fe(II) (3-10). More recently, mixed metal hybrids have been investigated as model for partially ligated Hbs (11-20). These systems have an added advantage in that the properties of the added metal can be tailored to provide specific probes of reactivity and structure that are not available for Fe(II) or Fe(III).

Among several metal substituted porphyrins, Ru(II) provides a particularly valuable probe, since six-coordinate ruthenium(II) CO porphyrins are virtually isostructural with six-coordinate, low spin iron(II) porphyrins as found in oxy- and carbonmonoxy Hb. In previous paper (20), we investigated the tertiary and quaternary structure of Ru(II)-Fe(II) hybrid Hbs in which one subunit contains Ru(II) while the other subunit contains Fe(II) by utilizing of ^{1}H NMR measurements. The NMR resonances of the proximal histidine N_1H and the hydrogen bonds located at the subunit interface show that the quaternary and tertiary structure of the half-liganded Ru-Fe hybrid Hbs is similar to that of native deoxy Hb and suggest a large quaternary structural transition (R-T transition) requires the binding of more than three molecule of oxygen.

However, the number of the NMR signals which have unambiguous assignment is limited (21-24) and it seems to be impossible to monitor the whole structural changes accompanied with the oxy- and deoxygenation only by NMR measurements. Therefore, in order to clarify the structure of the partially oxygenated Hb at the different conformational aspect, we tried to look at the changes of the sulfhydryl reactivity of the cysteine at the 93 position of the β subunit, which has been served as the sensitive probe for tertiary and quaternary structure alteration (25-31).

X-ray studies have revealed two different stereochemical effects that can alter the reactivity of β93 Cys. The first kind is exemplified by the transition from carbonmonoxy- to met Hb which is accompanied by an increase in the second-order rate constant of the reaction with *p*-HgBzO by a factor of two. Perutz and co-workers pointed out (28) that this is due to

small changes in tertiary structure in the immediate vicinity of the heme which include a slight rotation of helix F of the β subunits. The second, more drastic, effect on the sulfhydryl reactivity is linked to the change to the quaternary deoxy structure. This is due to the screening of the sulfhydryl group in the quaternary T structure by β146 HC3 His which is jointed by salt bridges to β94 FG1 Asp and to α40 C6 Lys (35).

We here performed extensive study of the sulfhydryl reactivity for Ru-Fe hybrid Hbs and, in particular, tried to access the ligation effect of each subunit on the structure of the salt bridge located at the $\alpha_1\beta_2$ interface. Moreover, by comparing of the other structural and functional probes, we discuss the mechanism of the structural propagation from the ligated subunit to the un-liganded subunit for the oxygenation step.

MATERIALS AND METHODS

Materials Ru-Fe hybrid Hb, Ru-HbCO and stripped Hb A were prepared as previously reported (20). 4-PDS was a specially prepared grade from Wako Pure Chemical, Ltd. (Osaka, Japan).

Kinetic Measurements The reaction between 4-PDS and Hb samples was measured with UV/vis spectrometer, Hitachi-330 (Hitachi Co. Ltd., Hitachi, Japan) equipped with a data processor, PC-9800 personal computer (NEC Co. Ltd., Tokyo, Japan). In order to obtain the half-liganded Ru-Fe hybrid Hbs, 2 ml of Hb sample solution (25 μM in tetramer) and 2 ml of 4-PDS solution (3 mM) were put respectively into each compartment of a forked flask which is jointed to a cuvette. This flask was then evacuated with gentle shaking on ice. The deoxygenation was checked by the absorption spectrum. After the complete deoxygenation (usually after 1 hour), the flask was turned upside-down, and the Hb solution and 4-PDS solution were mixed and then transferred into the cuvette. The absorbance change due to the formation of 4-thiopyridine was followed at 324 nm. All experiments were carried out at 25 °C, in 50 mM Bis-Tris or 50 mM Tris buffer containing 0.1M Cl^-.

Initial rate of the reaction between 4-PDS and Hb derivatives were estimated by Guggenheim plot of the optical density over time as described in RESULTS AND DISCUSSION.

RESULTS AND DISCUSSION

Sulfhydryl Reactivity of Cys β93 in Ru-HbCO Figure 1 shows initial stages of the reaction between 4-PDS and deoxy Hb A, Hb A CO and Ru-

HbCO at pH 7.1. The initial rates were estimated by Guggenheim plot method, as shown in Figure 2. The plot is linear at the initial stage in each reaction, implying that the reaction at the initial stage can be interpreted as the pseudo-first order reaction. The rate constants (k_{app}) of deoxy Hb A, carbonmonoxy Hb A and Ru-HbCO *versus* pH were plotted in Figure 3 and summarized in Table I.

Our previous paper reported that the tertiary and quaternary structure of Ru-HbCO, which is manifested by the NMR signals of the hydrogen bonded protons and the methyl groups of Val E11, is almost the same as that of native Hb A CO and is in the typical "R-state" (20). Thus, although Ru-HbCO exhibits a slight higher reactivity than native Hb A CO as shown in Figure 3 and Table I, it is likely that this difference arises from the localized structural changes around SH group probably due to the heme substitution from protoporphyrin (native heme) to deuteroporphyrin (Ru-porphyrin). Since such high reactivity implies that the salt bridge, α40 Lys-β146 His-β94 Asp, which interferes the approach of SH reagents is broken and the conformation around β93 of Ru-HbCO Cys is in the "R-state", we can conclude that Ru-HbCO can be also served as a good model for carbonmonoxy Hb A in the aspect of the reactivity of its sulfhydryl group.

Sulfhydryl Reactivity of Ru-Fe Hybrid Hemoglobins In Figure 4, the initial rates of α-Ru-porphyrin substituted hybrid Hb with 4-PDS were plotted as a function of pH from 6 to 8. As clearly shown in the figure, in spite of the different ligation state of the β subunits, both of $\alpha(Ru\text{-}CO)_2\beta(Fe)_2$ and $\alpha(Ru\text{-}CO)_2\beta(Fe\text{-}CO)_2$ exhibit almost the same sulfhydryl reactivity and their rates are as fast as that of native Hb A CO (_._). This observation shows that the ligation of the α subunit is sufficient to break the salt bridge and enhance the reactivity of the sulfhydryl group of β93 Cys, in other words, the sulfhydryl reactivity of β93 Cys does not depend on whether the β subunits are ligated or not when the α subunit is ligated.

On the other hand, the profile of the rate constants under various pH conditions for $\alpha(Fe)_2\beta(Ru\text{-}CO)_2$ and $\alpha(Fe\text{-}CO)_2\beta(Ru\text{-}CO)_2$ are quite different from the complementary hybrid. As illustrated in Figure 5, the rates of β-ligated form, $\alpha(Fe)_2\beta(Ru\text{-}CO)_2$, are intermediate between that of deoxy- and carbonmonoxy Hb A. Although the heme substitution from protoheme to deuteroheme tends to slightly accelerate the reaction between SH group of Cys and 4-PDS as found for Ru-HbCO (Figure 3), the reaction rates of $\alpha(Fe)_2\beta(Ru\text{-}CO)_2$ clearly indicate that the structure around the salt bridge and β Cys 93 for $\alpha(Fe)_2\beta(Ru\text{-}CO)_2$ can be assignable to the

intermediate state between "T-" and "R-state". By binding carbonmonoxide to the α subunits, the increase of the rate constant was observed and the pH dependence of $\alpha(Fe\text{-}CO)_2\beta(Ru\text{-}CO)_2$ corresponds to that of native Hb CO. This shows that the structure around β Cys 93 for the fully-liganded Hb, $\alpha(Fe\text{-}CO)_2\beta(Ru\text{-}CO)_2$, is similar to that of native Hb A CO and the salt bridge is completely broken to accelerate the reaction between SH group and 4-PDS. Therefore, the preferentially ligand binding to the β subunit induces only a partial cleavage of the salt bridge such as a deviation of the amino acid residue around the salt bridge, and the complete cleavage as found for the native "R state" Hbs requires the conformational changes at the α subunit side, that is, the ligation of the α subunit.

Above observation can be also interpreted as following in term of the propagation of conformational changes. By the ligation of the α subunits, the rotation or deviation of the α C helix around α40 Lys is induced and this conformational change is propagated to the β subunit side. And then the conformational changes around β C-terminal (β146 His) and β FG helix (β 94 Asp) break the salt bridge, resulting in high sulfhydryl reactivity of β Cys 93. On the other hand, in the case for the ligation of the β subunits, the structural changes around the salt bridge at the β subunit side are localized and cannot be propagated to the α subunit side, α40 Lys and α C helix. Since the salt bridge is not completely broken, the sulfhydryl reactivity is not so much increased as that of the α-liganded hybrid.

Perutz and co-workers (28) pointed out that the reactivity of the sulfhydryl group also depends on the rotation of β F helix which is governed by the displacement of the heme-linked histidine from the plane of the porphyrin ring in the β subunit. In the present study, it is so somewhat surprising that the ligation of the β subunit which affects drastic changes around heme-linked histidine and F helix has no effect on the sulfhydryl reactivity of $\alpha(Ru\text{-}CO)_2\beta(Fe)_2$ as mentioned above. This suggests that, for the α-liganded hybrid, $\alpha(Ru\text{-}CO)_2\beta(Fe)_2$, the conformation around β F helix and proximal histidine of the β subunit already has some "R-state" character by the ligation of α subunit. Previous NMR study also reported that the structure of $\alpha(Ru\text{-}CO)_2\beta(Fe)_2$ exhibits more "R-state" character than the complementary hybrid (20). Thus, we can conclude that the ligation of the α subunits affects more substantially the conformation of the neighbouring β subunits than that of β subunit. Such preferential conformational propagations were also reported by the measurements of the sulfhydryl reactivity of the half-methemoglobin (36).

Although no detailed studies of the sulfhydryl reactivity of the metal hybrid Hbs have been reported, there have been several papers about the sulfhydryl reactivity of mix-valence hybrid Hbs. Antonini and Brunori (33,34) suggested that the rate of the reaction of PMB with β Cys 93 SH groups of Hb was dependent exclusively on the presence of ligation on the β chains and was independent of the state of the α chains by use of the artificial half-cyanomet Hbs. However, the basis of the kinetic data of half-methemoglobins, Maeda and Ohnishi (36) reported that the reactivity is primarily dependent on ligation of the β subunit but also depends on that of the neighbouring α subunit. Present results strongly indicate that the ligation of the α subunits is more essential to break the salt bridge and enhance the sulfhydryl reactivity of the β 93 Cys. Examination of these various results, which look some contradictory, leads to the following suggestion: the ligation effect of the α subunits on the sulfhydryl reactivity of β 93 Cys depends on the state of hemoglobin chains. Maeda & Ohnishi suggests that the cyanomet β chains are more rigid and restrict the propagation and the aquomet β chains are more flexible and allow the propagation. Therefore, it is likely that Ru-CO-porphyrin substituted β subunits may be as flexible as the aquomet β subunits and its tertiary structure is easily influenced by the structural changes of the α subunit side.

Comparison with Other Conformational Probes for Ru-Fe Hybrid Hbs

Previous NMR study of Ru-Fe hybrid Hbs reported that, by utilizing the characteristic "T state" marker NMR signal arising from the hydrogen bond between α42 C7 Tyr and β99 G1 Asp and the "R state" marker between α98 G1 Asp and β102 G4 Asp, the quaternary structures of two Ru-Fe hybrid Hbs remain in the "T-like" state at low pH and at high pH (pH > 8.5) only for $\alpha(Ru\text{-}CO)_2\beta(Fe)_2$ the quaternary structure can be converted into the "R state" (20). This observation suggests that the conformational rearrangement in the $\alpha_1\beta_2$ subunit interface has not completed yet at the half-liganded stage in the oxygenation. However, the reactivity of the $\alpha(Ru\text{-}CO)_2\beta(Fe)_2$ is completely recovered to that of native Hb A CO which is in the typical "R-state". For another hybrid, the sulfhydryl group also reacts more rapidly than that for the typical "T-state". Therefore, the conformational transition from "T state" to "R state" around the salt bridge connecting α C helix, β C-terminal and β FG corner precedes the rearrangement of the hydrogen bonds involving the cleavage of the "T state" marker hydrogen bond between α C helix and β G helix and formation of the "R state" maker hydrogen bond between α G helix and β G helix. Makino and Sugita (32)

also pointed out that the increase of the sulfhydryl reactivity precedes the oxygenation by the kinetic measurements for partially saturated Hbs.

Although, the NMR spectra of the half-liganded Ru-Fe hybrid Hbs exhibit characteristic hydrogen bond named "T-state" marker, preliminary measurements of oxygen equilibrium curve show that the two Ru-Fe hybrid Hbs have high oxygen affinities as found for isolated chains and lower cooperativity (n=1.2 ~ 1.3) than native Hb A. Because the two hybrid exhibits small but significant cooperativity, the functional properties of the two hybrids are assignable to the "R-like state", not the typical "R-state". Thus, it is likely that the this salt bridge is one of the way of propagating structural changes from one subunit to other subunit, not but the characteristic two hydrogen bond, "T-" and "R-state" marker. And this structural changes affect the conformation of the heme vicinity in the complementary subunit to raise its oxygen affinity. The transition to the complete "R-state" accompanying the rearrangement of the two hydrogen bonds may occur at the binding of third oxygen as mentioned previously (20). The two hydrogen bonds, "T-" and "R-state" marker, contribute the stability of the "T" and "R" quaternary structure, respectively, but they have small effect on the propagation of structure changes at subunit interface.

In summary, the reactivity of β Cys 93 primarily depends on the deviation of rotation of the α C helix around α Lys 40 in Ru-Fe hybrid Hbs as model for the intermediate species of native Hb A. And it become also clear that the structural changes by ligation can be propagated from α to β subunit through the salt bridge, where as the ligation of the β subunits has small effect on the structure of the subunit interface. Such a conformational propagation through the salt bridge can regulate the oxygen affinity of the neighbouring subunits. A detailed investigations by oxygen equilibrium curve and resonance Raman spectra for Ru-Fe hybrid Hbs now go on. We will be able to further discuss the relationship between structure and function in the oxygenation of native Hb A by use of Ru-Fe hybrid Hbs.

REFERENCES

1. Antonini, E., & Brunori, M. (1971) *Hemoglobin and Myoglobin Their Reactions with Ligands*, North-Holland Publishing C, London.
2. Dickerson, R. E., & Geis, I. (1983) *Hemoglobin: Structure, Function, Elution and Pathology*, Benjamin/Cummings, New York.
3. Brunori, M., Amiconi, G., Antonini, E., Wyman, J., & Winterhalter, K.

H. (1970) *J. Mol. Biol. 49*, 461-471.
4. Cassoly, R., & Gibson, Q. H. (1972) *J. Biol. Chem. 247*, 7332-7341.
5. Ogawa, S., & Shulman, R. G. (1971) *Biochem. Biophys. Res. Commun. 42*, 9-15.
6. Cassoly, R., Gibson, Q. H., Ogawa, S., & Shulman, R. G. (1971) *Biochem. Biophys. Res. Commun. 44*, 1015-1021.
7. Ogawa, S., Shulman, R. G., & Yamane, T. (1972) *J. Mol. Biol. 708*, 291-300.
8. Ogawa, S., Shulman, R. G., Fujiwara, M., & Yamane, T. (1972) *J. Mol. Biol. 708*, 301-314.
9. Ogawa, S., & Shulman, R. G. (1972) *J. Mol. Biol. 708*, 315-336.
10. Nagai, K., & Kitagawa, T. (1980) *Proc. Natl. Acad. Sci. U.S.A. 77*, 2033-2037.
11. Hoffman, B. M. (1979) in *The Porphyrins*, Dolphin, D., Ed Academic Press, New York, Vol. 7, pp 435-437.
12. Hoffamn, B. M. (1975) *J. Am Chem. Soc. 97*, 1688-1694.
13. Fiechtner, M. D., McLendon, G., & Bailey, M. W. (1980) *Biochem. Biophys. Res. Commun. 92*, 277-284.
14. Fiechtner, M. D., McLendon, G., & Bailey, M. W. (1980) *Biochem. Biophys. Res. Commun. 96*, 618-625.
15. Ikeda-Saito, M., Yamamoto, H., & Yonetani, T. (1977) *J. Biol. Chem. 252*, 8639-8644.
16. Inubushi, T., Ikeda-Saito, M., & Yonetani, T. (1983) *Biochemistry 22*, 2904-2907.
17. Simolo, K., Stucky, G., Chen, S., Bailey, M., Scholes, C., & McLendon, G. (1985) *J. Am. Chem. Soc. 107*, 2865-2872.
18. Inubushi, T., D'Ambrosio, C., Ikeda-Saito, M., & Yonetani, T. (1986) *J. Am. Chem. Soc. 108*, 3799-3803.
19. Shibayama, N., Morimoto, H., & Miyazaki, G. (1986a) *J. Mol. Biol. 192*, 323-329.
20. Ishimori, K., & Morishima, I. (1988) *Biochemistry 27*, 4060-4066.
21. Fung. L. W. -M., & Ho, C. (1975) *Biochemistry 14*, 2526-2535.
22. Viggiano, G., Wiechelman, K. J., Cherverick, P. A., & Ho, C. (1978) *Biochemistry 17*, 795-799.
23. Takahashi, S., Lin, A. K. -A. C., & Ho, C. (1980) *Biochemistry 19*, 5196-5202.
24. Russu, I. m., Ho, N. T., & Ho, C. (1987) *Biochim. Biophys. Acta. 914*, 40-48.

25. Riggs, A. (1961) *J. Biol. Chem. 236*, 1948-1954.
26. Benesch,R. E., & Benesch, R. (1962) *Biochemistry 1*, 735-738.
27. Guidotti, G. (1965) *J. Biol. Chem. 240*, 3924-3927.
28. Perutz, M. F., Fersht, A. R., Simon, S. R., & Roberts, C. K. (1974) *Biochemistry 13*, 2174-2186.
29. Kilmartin, J. V., Hewitt, J. A., & Woodtton, J. F. (1975) *J. Mol. Biol. 93*, 203-218.
30. Antonini, E., & Brunori, M. (1969) *J. Biol. Chem. 244*,3909-3912.
31. Gibson, Q. H. (1973) *J. Biol. Chem. 248*,1281-1284.
32. Makino, N., & Sugita, Y. (1982) *J. Biol. Chem. 257*, 163-168.
33. Antonini, E., & Brunori, M. (1969) *J. Biol. Chem. 244*, 3909-.
34. Brunori, M., Amiconi, G., Antonini, E., Wyman, J., & Winterhalter, K. H. (1970) *J. Mol. Biol. 49*, 461-.
35. Perutz, M. F. (1970)*Nature (London) 228*, 726-739.
36. Maeda, T., & Ohnishi, S. (1971) *Biochemistry 10*, 1177-1180.

FIGURE LEGENDS

Figure 1.

Examples of sulfhydryl reactivity of native oxy Hb A, deoxy Hb A and Ru-HbCO. Hb concentration, about 25 μM as tetramer. In 50 mM Tris-0.1 M Cl^- buffer, pH 7.1, at 25 °C. Wavelength of observation, 324 nm.

Figure 2.

Guggenheim plots of the reaction of 4-PDS with native carbonmonoxy Hb A (--), deoxy Hb A (-) and Ru-HbCO (_._). Hb concentration, about 25 μM as tetramer. In 50 mM Tris-0.1 M Cl^- buffer, pH 7.1, at 25 °C. Wavelength of observation, 324 nm.

Figure. 3.

pH dependence of the kinetics constants for sulfhydryl reactivity of native oxy Hb A, deoxy Hb A and Ru-HbCO. Hb concentration, about 25 μM as tetramer. In 50 mM Tris-0.1 M Cl^- or 50 mM Bis-Tris-0.1 M Cl^- buffer, at 25 °C. Wavelength of observation, 324 nm.

Figure 4.

pH dependence of the kinetics constants for sulfhydryl reactivity of $\alpha(Ru\text{-}CO)_2\beta(Fe)_2$ and $\alpha(Ru\text{-}CO)_2\beta(Fe\text{-}CO)_2$. Hb concentration, about 25 μM as tetramer. In 50 mM Tris-0.1 M Cl^- or 50 mM Bis-Tris-0.1 M Cl^- buffer, at 25 °C. Wavelength of observation, 324 nm.

Figure 5.

pH dependence of the kinetics constants for sulfhydryl reactivity of $\alpha(Fe)_2\beta(Ru\text{-}CO)_2$ and $\alpha(Fe\text{-}CO)_2\beta(Ru\text{-}CO)_2$. Hb concentration, about 25 μM as tetramer. In 50 mM Tris-0.1 M Cl^- or 50 mM Bis-Tris-0.1 M Cl^- buffer, at 25 °C. Wavelength of observation, 324 nm.

Table I

Kinetics constant for sulfhydryl reactivity of deoxy Hb, carbonmonoxy Hb and RuCO Hb Hb concentration, about 25 μM as tetramer. In 50 mM Bis-Tris-0.1 M Cl^- buffer, pH 7.1 at 25 °C. Wavelength of observation, 324 nm.

	rate constant (x $10^{-2}sec^{-1}$)
deoxy Hb	0.17
carbonmonoxy Hb	3.3
RuCO Hb	4.8

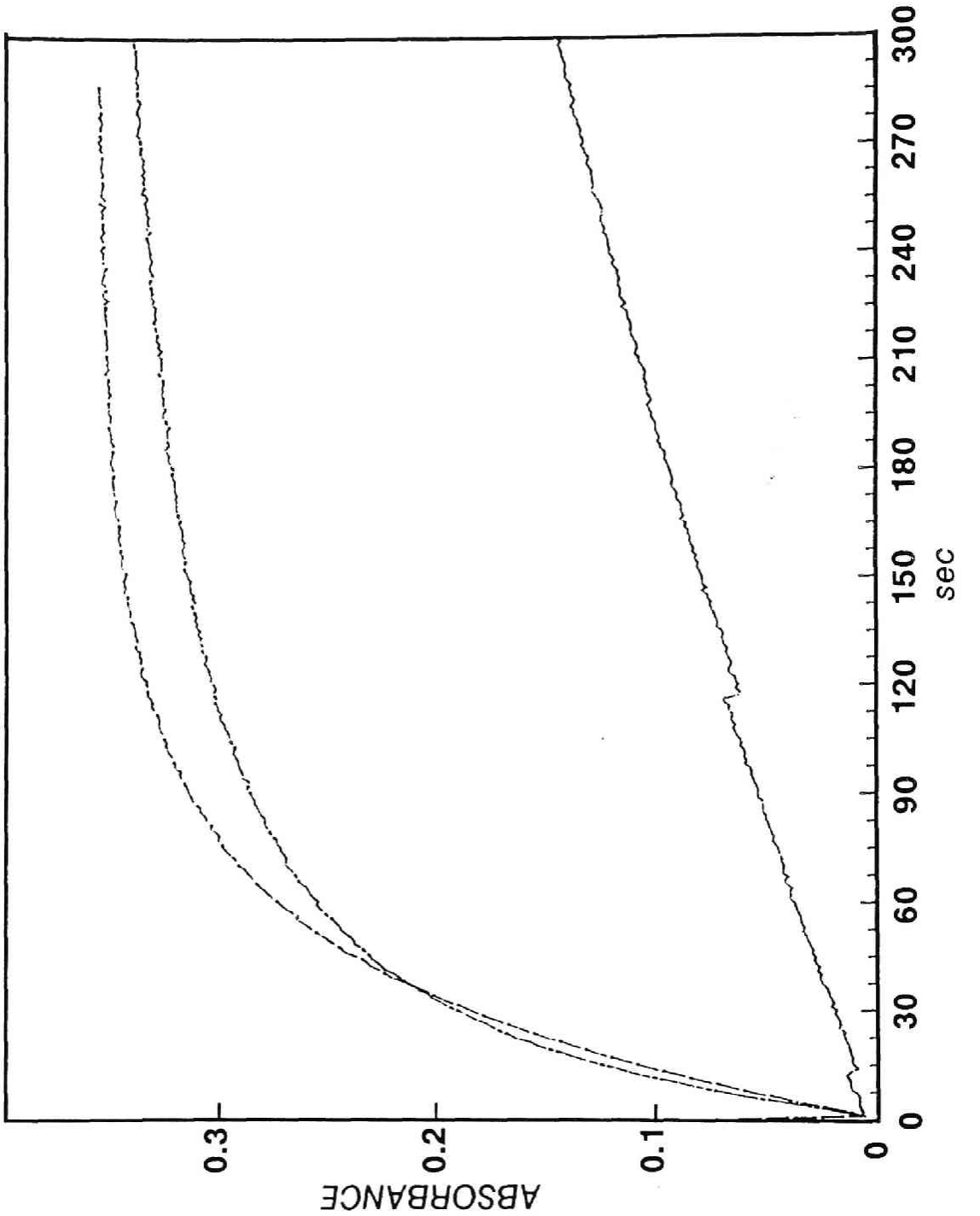

Figure. 1

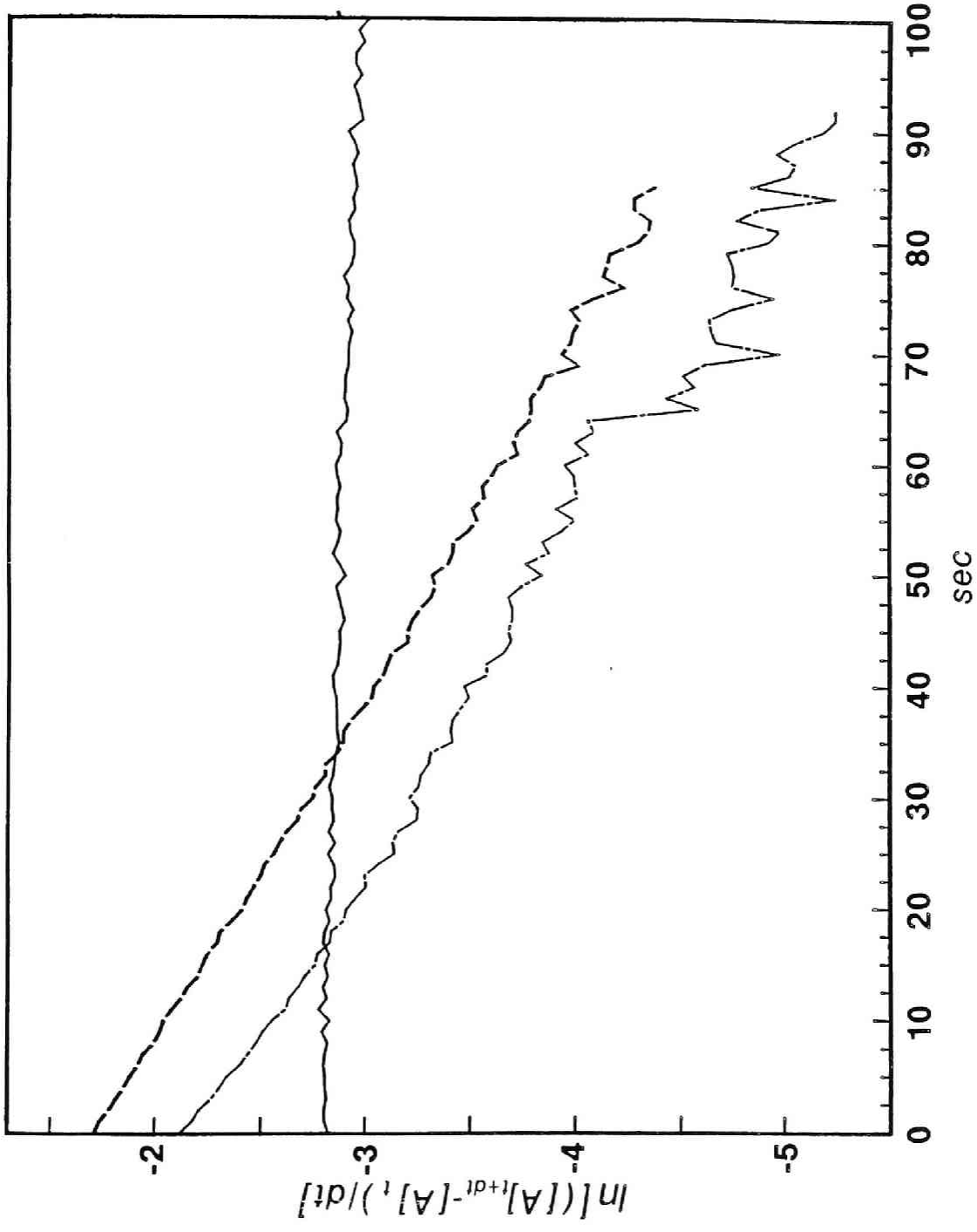

Figure. 2

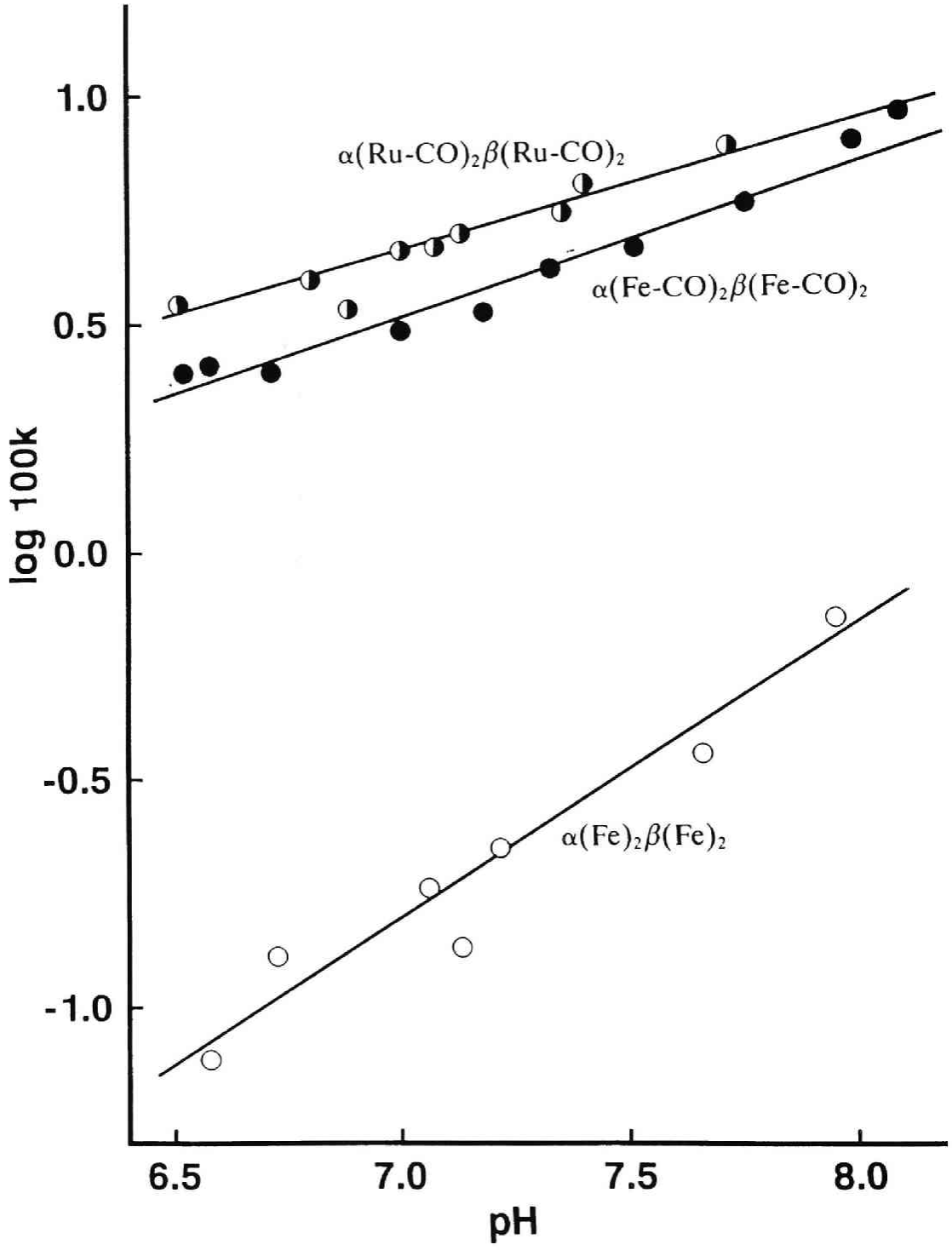
1.0
0.5
0.0
-0.5
-1.0
log 100k
α(Ru-CO)2β(Ru-CO)2
α(Fe-CO)2β(Fe-CO)2
α(Fe)2β(Fe)2
6.5
7.0
7.5
8.0
pH

Figure. 3

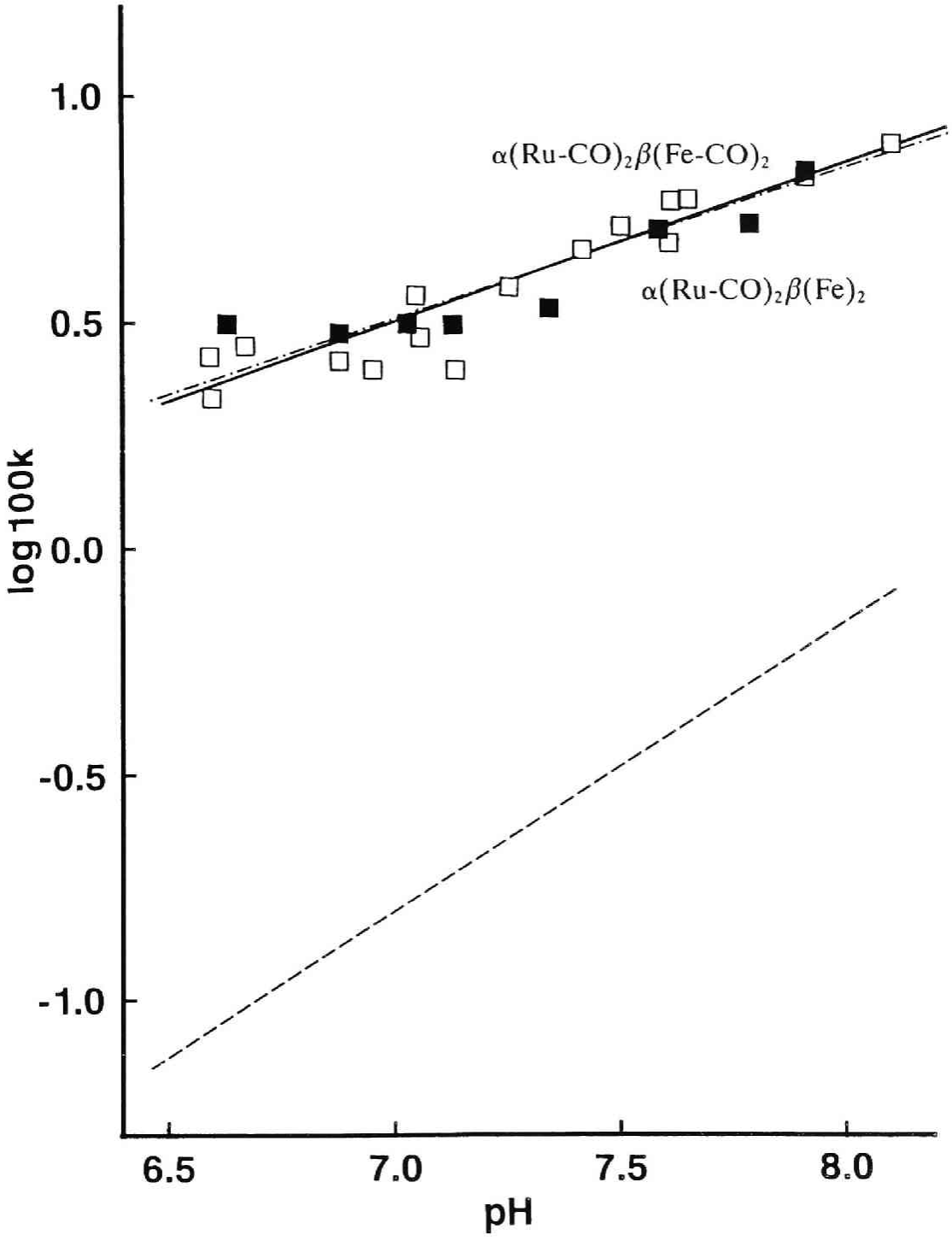

Figure. 4

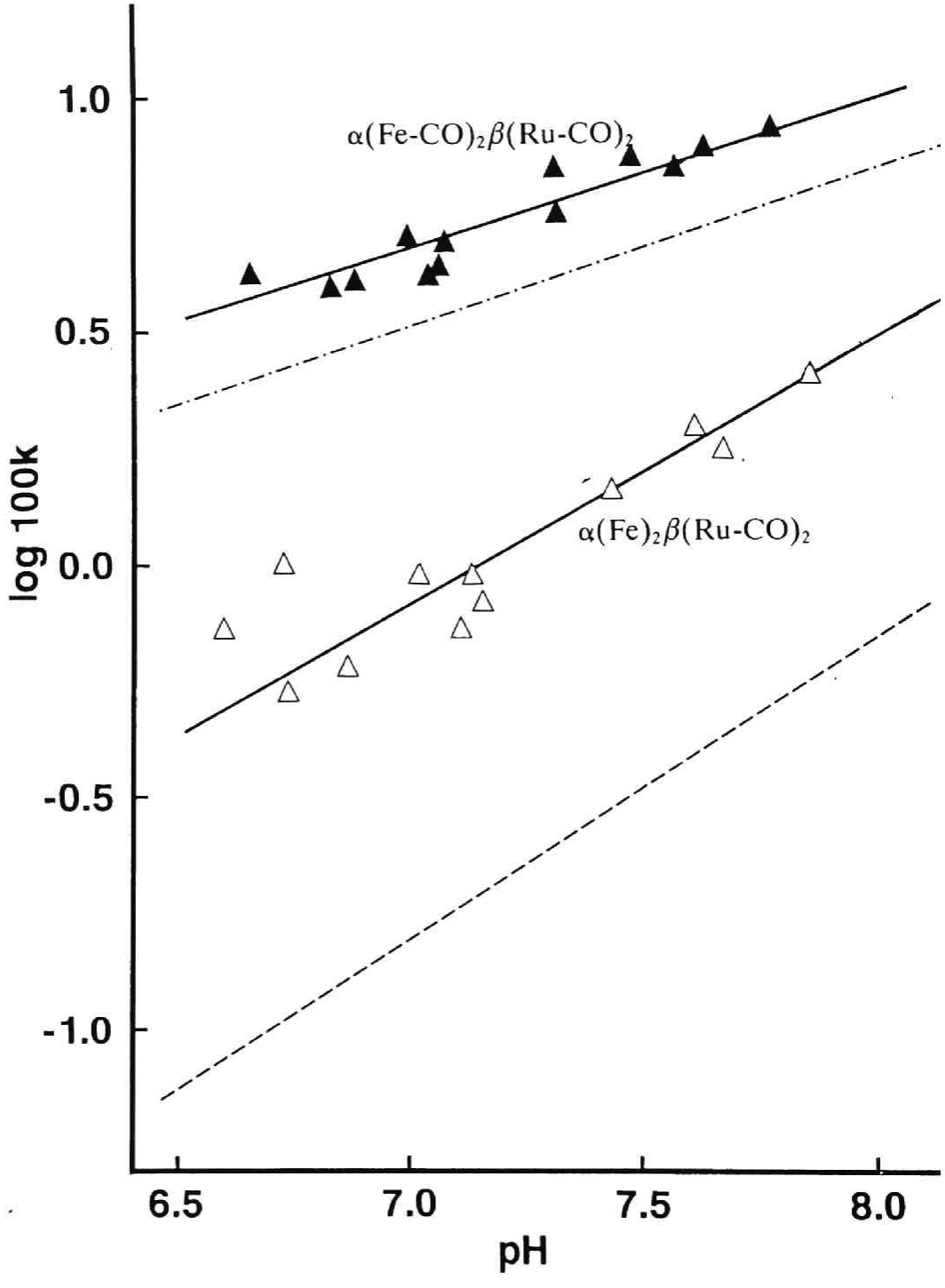

Figure. 5

CHAPTER 3.

Ruthenium-Iron Hybrid Hemoglobins as a Model for Partially Liganded Hemoglobin:

Oxygen Equilibrium Curves and Resonance Raman Spectra.

ABSTRACT: The structure and function of iron(II)-ruthenium(II) hybrid hemoglobins, $\alpha(Ru\text{-}CO)_2\beta(Fe)_2$ and $\alpha(Fe)_2\beta(Ru\text{-}CO)_2$, which can be served as models for the intermediate species of oxygenation step in native human adult hemoglobin was investigated by measuring oxygen equilibrium curves and the Fe(II)-N_ε (His F8) stretching resonance Raman lines. The oxygen equilibrium properties indicated that iron-ruthenium hybrid hemoglobins are good models for the half-liganded hemoglobin. The pH dependence of the oxygen binding properties and the resonance Raman line revealed that the quaternary and tertiary structural transition was induced by varying pH. By lowering pH, two iron-ruthenium hybrid hemoglobins show that the relatively higher cooperativity and the typical "deoxy-like" Raman line, indicating that its structure is shifted to the "T-like-state". However, the oxygen affinity of $\alpha(Fe)_2\beta(Ru\text{-}CO)_2$ was lower than that of $\alpha(Ru\text{-}CO)_2\beta(Fe)_2$ and the transition to the "deoxy-like" Fe-N_ε stretching Raman line of $\alpha(Fe)_2\beta(Ru\text{-}CO)_2$ was completed at pH 7.4, while that of the complementary counterpart still remained in the "oxy-like-state" at the same condition. These observation clearly indicated that the β-liganded hybrid has more "T-state" character than α-liganded hybrid. In other words, the ligation to the α subunit induced more profound changes in the structure and function in Hb than the binding to the β subunit. Such functional and structural characterizations corresponds to the previous structural results obtained by NMR and sulfhydryl reactivity. On the basis of the structural and functional characterization, we tried to discuss the molecular mechanism of the oxygenation step in native human adult hemoglobin.

In spite of the large amount of research during the last several decades, the molecular mechanism of cooperative oxygen binding by hemoglobin (Hb)[4] is not yet fully understood. The cooperativity arises from the reversible transition between fully ligated and fully deoxy forms of human normal adult hemoglobin (Hb A), whose structures have been determined by X-ray crystallography [for example, see Baldwin (1980), Shaanan (1983), and Fermi et al. (1984)]. One of the most challenging tasks in current Hb research is to describe the structural change induced at each oxygenation step by characterizing the properties of the intermediate ligated species, namely, Hb A with one, two, and three ligand molecules bound within a tetramer, and comparing them with the properties of the fully deoxy and ligated species, and thus to be able to interpret alterations in functional properties in terms of molecular structural changes. Because at any given fractional saturation between the fully deoxy and fully oxy states, various molecular species with binding of zero to four ligand molecules coexist as a statistical mixture, it is not feasible to isolate a stable intermediate ligation state by using Hb A. (This difficulty in studying the intermediate ligation states is not due to the Hb A itself but rather to the use of O_2 as the ligand.) The cooperative nature of oxygen binding further reduces the relative populations of intermediate ligated states to a small fraction in comparison with those of fully deoxy and ligated forms. Thus, the majority of the information available about properties of the Hb molecule has been unfortunately limited to either the fully ligated or the fully deoxy form of Hb A, and the functional properties of Hb have been interpreted on the basis of the information on deoxy and oxy structures.

Some efforts have been made to study the intermediate states of ligation, mainly focused on symmetrically ligated hybrid intermediate Hb molecules. Three types of symmetric hybrid Hbs have been extensively studied: (i) cyanomet valency hybrid Hbs, which contain two ferric hemes with cyanide at the α or β subunits (Brunori et al., 1970; Maeda et al., 1972; Bannerjee & Cassoly, 1969; Ogawa & Shulman, 1972; Cassoly & Gibson, 1972); (ii) the M type of Hbs, such as Hb M Milwaukee (Fung et al., 1976,1977); and (iii) metal hybrid Hbs, such as iron-cobalt hybrid (Ikeda-Saito et al., 1977; Ikeda-Saito &Yonetani,1980; Inubushi, et al., 1983; Hofrichter et al., 1985), iron-zinc hybrid (Simolo et al., 1985), iron-manganese hybrid (Arnone et al.,

[4]Abbreviations: Hb A, human adult hemoglobin; NMR, nuclear Magnetic resonance; Bis-Tris, [bis(2-hydroxyethyl)amino]tris(hydroxymethyl)methane; Tris, tris(hydroxymethly)aminomethane

1986) and iron-nickel hybrid (Shibayama et al., 1987).

Among these models, metal hybrid Hb has some advantages in that they are relatively stable molecules and can be much prepared enough to investigate their physicochemical and physiological properties. However, there has not been a good and stable model for the oxy heme in the metal-substituted porphyrins. Recently, ruthenium carbonylporphyrin is used as a model for the oxy heme (Ishimori & Morishima, 1988) and the structures of iron-ruthenium hybrid Hbs in which the α or β subunit contains ruthenium substituted porphyrin with the other subunit having a deoxygenated iron porphyrin were investigated. Previous our studies (Ishimori & Morishima, 1988; Ishimori et al., 1988) showed the ruthenium carbonylporphyrin is a novel structural model for the oxy heme and a mechanism of the structural propagation in the oxygenation step was proposed. In this chapter, to get further insight of the structural and functional properties of the intermediate species in the oxygenation, oxygen equilibrium curves and resonance Raman spectra of iron-ruthenium hybrid Hbs are measured. On the basis of these structural and functional properties of the iron-ruthenium hybrid Hbs, we try to describe the detailed mechanism of the R-T transition.

MATERIALS AND METHODS

Preparation of Iron-Ruthenium Hybrid Hbs. Hemolysate was prepared in the usual manner from fresh whole blood obtained from the local blood bank. Hb A and its isolated chains were prepared in carbonmonoxide forms as described by Kilmartin et al. and Gerai et al. (Kilmartin & Rossi-Bernadi, 1971; Kilmartin et al., 1973; Gerai, et al., 1969). Iron-ruthenium hybrid Hbs were prepared by the method of the previous paper (Ishimori & Morishima, 1988).

Measurement of the O_2 Equilibrium Curves. Oxygen equilibrium curves were determined with an automatic recording oxygenation apparatus (Imai et al., 1970) equipped with an aerobic cell with variable light-path length (Imai & Yonetani, 1977) set at 6 mm. The spectrophotometer used was a Cary model 118C. The wavelength of detection light was 620 nm. The temperature of Hb sample was maintained constant within ± 0.05 °C. The concentration of Hb sample was 60 μM as heme. The pH condition used in this study are listed in Table I. The buffers were 0.05M Bis-Tris for pH 7.4, 6.9 and 6.4, and 0.05M Tris for pH 7.9. The buffers containing 0.1M Cl^- were prepared from 0.05M bis-Tris or 0.05M Tris solutions containing 0.1M HCl adjusted pH with conc NaOH solution at the same temperature as

for the oxygen equilibrium measurements.

The oxygen equilibrium curves of iron-ruthenium hybrid Hbs were analyzed according to the two-step oxygenation scheme (Nagai et al., 1986). In this case, the K_3 and K_4 are expressed as

$$K_3K_4=1/P_{50}^2 \qquad (1)$$

$$K_3/K_4=[n_{max}/(2-n_{max})]^2$$

where P_{50} is the partial oxygen pressure at the 50% saturation and n_{max} is Hill's constant.

Measurements of the Resonance Raman Spectra. Raman scattering was excited by the 441.6 nm line of a He-Cd laser (Kinmon CDR 80 SG, Tokyo, Japan) and was recorded on a JEOL-400D Raman spectrometer. In order to avoid the photoreaction of ruthenium substituted porphyrin, we used a spinning cell (1800 rpm) equipped with a system for evacuation. Sample volume is ~300 μl and the concentration is 50 μM. Measurements were carried out at 20°C in the same buffer as used for the measurement of oxygen equilibrium curves. The frequency calibration of the spectrometer was performed with CCl_4 as a standard.

RESULTS

Oxygen Equilibrium Curves of Iron-Ruthenium Hybrid Hbs. Figure 1 shows the oxygenation curves (A) and the Hill plot of the oxygen equilibrium curves at pH 7.4 of Hb A and iron-ruthenium hybrid Hbs, $\alpha(Ru\text{-}CO)_2\beta(Fe)_2$ and $\alpha(Fe)_2\beta(Ru\text{-}CO)_2$, in which one subunit contains ruthenium-substituted porphyrin and the other subunit has native iron heme. Table I lists the oxygen affinity (P_{50}), Hill's constant (n_{max}) and the estimated K_3 and K_4 values by using eq (1). The O_2 equilibrium curves of the iron-ruthenium hybrid Hbs converge at a high saturation range, while the lower asymptotes diverge from that of native Hb A. The O_2 binding curve of $\alpha(Ru\text{-}CO)_2\beta(Fe)_2$ shows low cooperativity with a Hill coefficient value of 1.22. The estimated K_3 and K_4 value are plotted against pH as shown in Figure 2A (closed circle and triangle, respectively). K_4 of $\alpha(Ru\text{-}CO)_2\beta(Fe)_2$ is observed to be less pH dependent than K_3. Its value is similar to that of Hb A, which is essentially pH independent. The K_3 value of $\alpha(Ru\text{-}CO)_2\beta(Fe)_2$ shows a pH dependence similar to that of K_3 of native Hb A, but some small difference was observed in acidic region. log P_{50} of $\alpha(Ru\text{-}CO)_2\beta(Fe)_2$ is plotted as a function of pH as shown in Figure 2B (closed circle). The oxygen affinity of $\alpha(Ru\text{-}CO)_2\beta(Fe)_2$ is very high but significant lower than that of isolated α or β subunit. The slope of the curves of log P_{50} are about

0.3 for $\alpha(Ru\text{-}CO)_2\beta(Fe)_2$ at pH 7.4, indicating that about 0.15 proton per native β subunit of $\alpha(Ru\text{-}CO)_2\beta(Fe)_2$ are released upon oxygenation.

The oxygen equilibrium curves of $\alpha(Fe)_2\beta(Ru\text{-}CO)_2$ at various pH values are shown in Figure 1A (open square). Introducing two ruthenium substituted porphyrin at the β subunits also causes the oxygen affinity to increase as found for the complementary hybrid Hb. However, the O_2 affinity of this hybrid Hb was considerably lower than that of $\alpha(Ru\text{-}CO)_2\beta(Fe)_2$. The curve shows more cooperativity and gives an *n* value of 1.3 at pH 7.4 and 1.5 at pH 6.4 (1.2 at pH 7.4 and 1.3 at pH 6.4 for $\alpha(Ru\text{-}CO)_2\beta(Fe)_2$.) The pH dependence of the estimated O_2 binding constants was essentially the same as those of Hb A and the complementary hybrid Hb. A larger Bohr effect was remained in this hybrid Hb than in $\alpha(Ru\text{-}CO)_2\beta(Fe)_2$. On the basis of the slope of the P_{50}, 0.5 proton was released with the oxygenation of the two α subunits, which is almost the same number of protons as Bohr effect from native Hb A, are released from $\alpha(Fe)_2\beta(Ru\text{-}CO)_2$ during oxygenation.

Resonance Raman Spectra of Iron-Ruthenium Hybrid Hbs. The excitation of Raman scattering at 441.6 nm selectively enhanced the Raman lines of the Fe subunits within iron-ruthenium hybrid Hbs. In Figure 3, the resonance Raman spectra of $\alpha(Ru\text{-}CO)_2\beta(Fe)_2$ at various pH are shown. At pH 7.4 with IHP, the resonance Raman line of the Fe-N_ε stretching in the β subunit was observed at 219 cm^{-1},which is assignable to that of the typical "deoxy-like" state as found for $\alpha(Fe^{III}\text{-}CN^-)_2\beta(Fe)_2$ in the presence of IHP (Nagai & Kitagawa, 1980). With raising pH, the Fe-N_ε stretching Raman line exhibited a frequency shift from 220 cm^{-1} to 223 cm^{-1}. Nagai & Kitagawa (1980) reported the Fe-N_ε stretching Raman line at 223 cm^{-1} corresponds to the "oxy-like" structure.

Figure 4 illustrates the resonance Raman spectra of the complementary counterpart, $\alpha(Fe)_2\beta(Ru\text{-}CO)_2$ at various pH. For the deoxygenated α subunit, the Raman line of the Fe-N_ε stretching was observed at the lower wave number region and in the presence of IHP at pH 7.4, $\alpha(Fe)_2\beta(Ru\text{-}CO)_2$ showed the Raman line at 206 cm^{-1}, corresponding to the structure of the "deoxy-like" α subunit (Nagai & Kitagawa, 1980; Ondrias et al., 1982). Contrary to $\alpha(Ru\text{-}CO)_2\beta(Fe)_2$, the Raman line of the α subunits in the absence of IHP were broad and showed sometimes a flattened peak. No significant frequency shift was observed from pH 6.4 to 7.9. At pH 8.4, the Raman line become slightly sharp and asymmetrical, resulting higher wave number shift to 217 cm^{-1}. Similar behaviour was reported in the case of

iron-nickel hybrid Hbs (Shibayama et al., 1986). Such resonance Raman spectra can be interpreted in two ways, one assuming a single line at an intermediate frequency and the other assuming a composite of two lines at 206 cm^{-1} and 220 cm^{-1} which corresponds to the "deoxy-like" and "oxy-like" structure in α subunit, respectively. The observed peak wave numbers of the Fe-N_ε stretching resonance Raman line are plotted against pH in Figure 5.

DISCUSSION

pH Dependence of Oxygen Binding Properties and Structure of Iron-Ruthenium Hybrid Hbs. This study indicates that K_3 and K_4 values of the two iron-ruthenium and their pH dependence are almost similar to those of native Hb A, indicating that Ru-DPIX is a good model for a permanent oxy heme. Thus, we can conclude that iron-ruthenium hybrid Hbs imitate half-liganded Hb well when they bind the first and second oxygen molecule.

Although the two hybrid Hbs show very high oxygen affinity comparable to isolated chains, significant cooperativity (n_{max}=1.2~1.5) is observed. These observation implies that the functional properties of the two iron-ruthenium hybrid Hbs can be assigned to the "R-like-state" which differs from the typical "R-state" and has some "T-state" character. In acidic region, relatively higher n values (1.3 for $\alpha(Ru\text{-}CO)_2\beta(Fe)_2$ and 1.5 for $\alpha(Fe)_2\beta(Ru\text{-}CO)_2$) were observed. The increase of the n value suggests that lowering pH causes some changes of the quaternary and tertiary structure of the iron-ruthenium hybrid Hbs, resulting the increase of the "T-state" character by lowering pH. In other words, it can be said that the functional properties of the hybrids are shifted from the "R-like state" to the "T-like state" by lowering pH. To discuss the tertiary structural changes, the frequency of the Fe-N_ε stretching resonance Raman line can be served as a good probe. Figure 5 clearly shows that the frequency of the Raman line is shifted to lower wave number as pH is lowered, indicating that the strain of the Fe-N_ε bond was increased as found for the transition from the "R-state" to the "T-state" (Nagai & Kitagawa, 1980). Therefore, it is concluded that the structural changes induced by lowering pH affects the Fe-N_ε bond to increase the oxygen binding affinity of the hybrids.

It should be also noted that oxygen binding properties of $\alpha(Fe)_2\beta(Ru\text{-}CO)_2$ show more dependent on pH than those of the complementary hybrid and the oxygen affinity of $\alpha(Fe)_2\beta(Ru\text{-}CO)_2$ is lower than that of $\alpha(Ru\text{-}CO)_2\beta(Fe)_2$. Previous paper (Ishimori & Morishima, 1988) found out the

pH dependent quaternary structural changes in NMR pattern for hydrogen-bonded proton region of $\alpha(Ru\text{-}CO)_2\beta(Fe)_2$. In the NMR of this hybrid, the resonance from the hydrogen bond between α42 Tyr and β99 Asp, which is one of the "T-state" markers (Fung & Ho, 1975) lost its signal intensity and the "R-state" marker, which is the hydrogen bond between α98 Asp and β102 Asp (Takahashi, et al., 1980) appeared. We concluded that the quaternary structural transition from the "T-like state" to the "R-like state" occurred by raising pH. On the other hand, the complementary hybrid Hb, $\alpha(Fe)_2\beta(Ru\text{-}CO)_2$, exhibited only small changes in the same region and its NMR pattern indicated that its quaternary structure is fixed at "T-like-state" in the basic condition. Larger *n* values of $\alpha(Fe)_2\beta(Ru\text{-}CO)_2$ also correspond to "T-state" character in this hybrid. Therefore, the oxygenation in $\alpha(Fe)_2\beta(Ru\text{-}CO)_2$ accompanies more drastic structural changes as found for native Hb than that of $\alpha(Ru\text{-}CO)_2\beta(Fe)_2$. Since the Bohr effect clearly appeared in native Hb A and is not observed for the isolated chains, it is likely that the larger pH dependence of the β-liganded hybrid, $\alpha(Fe)_2\beta(Ru\text{-}CO)_2$, arises from its "T-state" character. On the other hand, the functional and structural properties of the α-liganded hybrid Hb has less "T-state" character and more similar to the isolated chains than that of the α-liganded hybrid, the functional properties are more resistant to the pH perturbation like the isolated chains.

Such a non-equivalence between the two hybrids also reflects their pH dependence of the Fe-N_ε stretching resonance Raman line. The wave number of the Raman line of $\alpha(Ru\text{-}CO)_2\beta(Fe)_2$ was shifted from that of the "deoxy-like" state to the "oxy-like" state at pH 6.9, whereas in $\alpha(Fe)_2\beta(Ru\text{-}CO)_2$ the transition of the Raman line began at more basic pH. This implies that the "T-like state" in $\alpha(Fe)_2\beta(Ru\text{-}CO)_2$ is more stable than that of $\alpha(Ru\text{-}CO)_2\beta(Fe)_2$. Therefore, on the basis of the Fe-N_ε stretching resonance Raman line of the iron-ruthenium hybrid Hbs, one can also conclude that the β-liganded hybrid has more "T-state" character while the α-liganded one has more "R-state" character.

These different structural and functional pH dependences between complementary hybrid Hbs are also encountered at the iron-nickel hybrid Hbs (Shibayama et al., 1987). Shibayama et al., reported that the $\alpha(Fe\text{-}CO)_2\beta(Ni)_2$ exhibited only slight NMR spectral changes by lowering pH, while the NMR spectra of $\alpha(Ni)_2\beta(Fe\text{-}CO)_2$ show a drastic change involving the rearrangement of the hydrogen bonds at the basic region due to the changes of the coordination state of the nickel-substituted porphyrin in the α

subunit. The NMR pattern of $\alpha(Fe\text{-}CO)_2\beta(Ni)_2$ identified to that of the "R-state" and the complementary hybrid exhibited the characteristic "T-state" markers in its NMR spectrum at the acidic condition. In this case, the "R-state" is also more stable in the α-liganded hybrid. Moreover, iron-zinc hybrid Hbs indicated same tendency (Simolo et al., 1985). Thus, the binding to the α subunit causes more drastic conformational and functional change for Hb.

However, in the two monoliganded asymmetric Fe-Co hybrids, a comparison of the signal intensity of the "T-state" markers indicated that the quaternary structure of $[\alpha(Fe\text{-}CO)\beta(Co)]_A[\alpha(Co)\beta(Co)]_CXL$ had more "T-state" character than its complementary counterpart, $[\alpha(Co)\beta(Fe\text{-}CO)]_A[\alpha(Co)\beta(Co)]_CXL$ (Inubushi et al., 1986). They concluded that the binding of the first ligand to the β subunit induced more profound changes in the quaternary structure of Hb than the binding to the α subunit. It is likely that such discrepancy arises from the different modification of Hb, however, more detailed investigation will be needed to determine which model is best model for native Hb A.

The Mechanism of the Conformational Propagation in the Oxygenation. Previous papers (Ishimori & Morishima, 1988, Ishimori et al., 1988) revealed the quaternary and tertiary structure of iron-ruthenium hybrid Hbs by utilizing their NMR spectra and sulfhydryl reactivity. The results obtained by these studies are summarized in Table II. As shown in this table, different spectroscopic techniques provide different assignment of the conformation of iron-ruthenium hybrid Hbs. Some probes suggest a "T" structure by comparison with deoxy Hb while other probes suggest a "R" structure. As the interpretation of the result, it is clear that the structure of the intermediate species in the oxygenation cannot be described as the "two-state" model and the structural changes at various parts in Hb at the oxygenation is not concerted. Table II indicates that the transition from the "T-state" to the "R-state" around the salt bridge at the $\alpha_1\beta_2$ interface, α_1C5 Lys-β_2HC3 His-β_2FG1 Asp, precedes to those of the hydrogen bonds at the $\alpha_1\beta_2$ interface and the Fe-N_ε stretching. The Fe-N_ε stretching could be converted from "T" state to "R" state by raising pH, while the NMR spectra of the hydrogen bonds suggested the large arrangements of the hydrogen bonds requires at the binding of the third oxygen molecule.

These findings allow us to propose a mechanism for the conformational propagation in the oxygenation as schematically shown in Figure 6. When the two α subunits are ligated, the structural change around the heme iron

affects the structure of α C helix and induces the conformational change at α C5 Lys residue. This conformatinal change breaks the salt bridge to βFG1 Asp *via* βHC3 His and the ligation effect is propagated to the complementary subunit. Then, the high oxygen affinity of the two hybrid and the high wave number shift of the the Fe-N_ε stretching resonance Raman line indicate that t heme moiety structure of the β subunit is converted to the high oxygen affinity form, that is, the reduction of the strain at the Fe-N_ε bond. At this moment, the rearrangement of the hydrogen bonds at the subunit interface involving the cleavage of the "T-state" marker and the formation of the "R-state" marker is not completed. The complete transition from the "T-state" to the "R-state" occurs by binding of the third oxygen molecules to Hb. In the case for the ligation to the β subunit, the salt bridge was not broken completely (Ishimori et al., 1988) and the structural changes from the liganded β subunit to the unliganded α subunit was propagated partially. Thus, the unliganded α subunit had more "T-state" character. Present studies show that the salt bridge is assignable to one of the structural propagation ways from the liganded subunit to the unliganded subunit and the characteristic hydrogen bonds play a key role for the stabilization of the high or low oxygen affinity from in Hb rather than the structural propagation.

In summary, a series of studies on the iron-ruthenium hybrid Hbs clarified the structural and functional properties of the half-liganded Hbs, intermediate species in the oxygenation, and on the basis of these results, a mechanism of the structural propagation accompanying the functional changes in oxygenation was proposed. To get further insight of the mechanism, we try to prepare asymmetric hybrid Hbs containing ruthenium substituted porphyrin. The more detailed investigation will be reported in future publications.

REFERENCES

Arnone, A., Rogers, P., Blough, N. V., McGourty, J. L., & Hoffman, B. M. (1986) *J. Mol. Biol. 188*, 639-706.

Baldwin, J. M. (1980) *J. Mol. Biol. 136*, 103-128.

Banerjee, R., & Cassoly, R. (1969) *J. Mol. Biol. 42*, 351-361.

Brunori, M., Amiconi, G., Antonini, E., Wyman, J., & Winterhalter, K. H. (1970) *J. Mol. Biol. 49*, 461-471.

Cassoly, R., & Gibson, Q. H. (1972) *J. Biol. Chem. 247*, 7332-7341.

Fermi, G., Perutz, M. F., Shaanan, B., & Fourme, R. (1984) *J. Mol. Biol. 175*, 159-174.

Fung , L. W. -M., & Ho, C. (1975) *Biochemistry 14*, 2526-2535.

Fung, L. W. -M., Minton, A. P., & Ho, C. (1976) *Proc. Natl. Acad. Sci. U.S.A. 73*, 1581-1585.

Fung, L. W. -M., Minton, A. P., Lindstrom, T. R., Pisciotta, A. V., & Ho, C. (1977) *Biochemistry 16*, 1452-1462.

Gerai, G., Parkhurst, L. J., & Gibson, Q. H., (1969) *J. Biol. Chem. 244*, 4664-4667.

Ikeda-Saito, M., & Yonetani, T. (1980) *J. Mol. Biol. 138*, 845-858.

Ikeda-Saito, M., Yamamoto, H. & Yonetani, T. (1977) *J. Biol. Chem. 252*, 8639-8644.

Imai, K., Morimoto, H., Kotani, M., Watari, H., Hirata, W., & Kuroda, M. (1970) *Biochem. Biophys. Acta, 200,* 189-196.

Imai, K., & Yonetani, T. (1977) Biochem. Biophys. Acta, 490, 164-170.

Inubushi, T., Ikeda-Saito, M., & Yonetani, T. (1982) *Biochemistry 22*, 2904-2907.

Inubushi, T., D'Ambrosio, C., Ikeda-Saito, M., & Yonetani, T. (1986) *J. Am. Chem. Soc. 108*, 3799-3803.

Ishimori, K., & Morishima, I. (1988) *Biochemistry 27*, 4060-4066.

Ishimori, K., Azumi, R., & Morishima, I. (1988) to be published.

Kilmartin, J. V., & Rossi-Bernardi, L. (1971) *Biochem. J. 124*, 31-45.

Kilmartin, J. V., Fogg, J., Luzzana, M., & Rossi-Bernardi, L. (1973) *J. Biol. Chem. 248*, 7039-7043.

Maeda, T., Imai, K., & Tyuma, I. (1972) *Biochemistry 11*, 3685-3689.

Nagai, K., & Kitagawa, T. (1980) *Proc. Natl. Sci. U.S.A. 77*, 2033-2037.

Ogawa, S., & Shulman, R. G. (1972) *J. Mol. Biol. 70*, 315-336.

Ondrias, M. R., Rousseau, D. L., Kitagawa, T., Ikeda-Saito, M., Inubushi, T., & Yonetani, T. (1982) *J. Biol. Chem. 257*, 8766-8770.

Shaanan, B. (1983) *J. Mol. Biol. 171*, 31-59.

Shibayama, N., Morimoto, H., Kitagawa, T. (1986) *J. Mol. Biol. 192*, 331-336.

Shibayama, N., Inubushi, T., Morimoto, H., & Yonetani, T. (1987) *Biochemistry 26*, 2194-2201.

Simolo, K., Stucky, G., Chen, S., Bacley, M., Scholes, C., Mclendon, G. (1985) *J. Am. Chem. Soc. 107,* 2865-2872.

Takahashi, S., Lin, A. K. -A. C., & Ho, C. (1980) *Biochemistry 19*, 5196-

5202.

FIGURE LEGENDS

Figure 1.

Oxygen equilibrium Curves (A) and Hill plots (B) of native Hb A, α(Ru-CO)$_2\beta$(Fe)$_2$ and α(Fe)$_2\beta$(Ru-CO)$_2$. *Y* is fractional oxygen saturation of ferrous subunits; P is partial pressure of oxygen in mmHg in 50 mM Bis-Tris with 100 mM-chloride at pH 7.4; measurement temperature is 25°C; heme concentration, 60 μM; the wavelength of detection light was 620 mm.

Figure 2.

pH dependence of the equilibrium constant for first (K_3) and second (K_4) oxygen to bind to iron-ruthenium hybrid Hbs, and third and fourth oxygen to bind to Hb A. Conditions for hybrid Hbs and native Hb A are described in the experimental section.

Figure 3.

Resonance Raman spectra of α(Ru-CO)$_2\beta$(Fe)$_2$ in 50 mM Tris or Bis-Tris with 100 mM-chloride at various pH in the absence of IHP and at pH 7.4 in the presence of IHP. Measurements were carried out at 20°C, excited at 441.6 nm.

Figure 4.

Resonance Raman spectra of α(Fe)$_2\beta$(Ru-CO)$_2$ in 50 mM Tris or Bis-Tris with 100 mM-chloride at various pH in the absence of IHP and at pH 7.4 in the presence of IHP. Measurements were carried out at 20°C, excited at 441.6 nm.

Figure 5.

The plots of the peak wave number of Fe-N_ε stretching resonance Raman lines against pH for the two iron-ruthenium hybrid Hbs. (○) β(Fe) subunit of α(Ru-CO)$_2\beta$(Fe)$_2$, (□) α(Fe) subunit of α(Fe)$_2\beta$(Ru-CO)$_2$. Conditions for measurements were as described for Figures 3 and 4. Filled symbols indicate the presence of IHP (5 mM).

Figure 6.

Schematic representation of the mechanism of the structural propagation in oxygenation (see text).

Table I

Oxygenation parameters of iron-ruthenium hybrid Hbs

	$\alpha(Ru\text{-}CO)_2\beta(Fe)_2$				$\alpha(Fe)_2\beta(Ru\text{-}CO)_2$			
pH	P_{50}	n	K_3	K_4	P_{50}	n	K_3	K_4
6.4	1.54	1.32	0.33	1.26	3.30	1.51	0.098	0.93
6.9	1.02	1.22	0.63	1.53	1.50	1.33	0.34	1.32
7.4	0.604	1.22	1.06	2.59	0.845	1.31	0.62	2.25
7.9	0.457	1.16	1.58	3.02	0.461	1.22	1.39	3.39

The oxygen pressure (mmHg) at half saturation (1 mmHg ~ 133.3 Pa).
The equilibrium constant for the first (K_3) and second (K_4) oxygen molecule to bind to Hb (mmHg)

Table II
Summary of apparent quaternary structure of iron-ruthenium hybrid Hbs using different structural probes

	$\alpha(Ru\text{-}CO)_2\beta(Fe)_2$		$\alpha(Fe)_2\beta(Ru\text{-}CO)_2$		
	pH 7.4	pH 8.4	pH 7.4	pH 8.4	ref
α_1G1 Asp-β_2G4 Asn exchangeable proton	T	R (pH 8.7)	T	T	a
α_1C7 Tyr-β_2G1 Asp exchangeable proton	R	R	T	T	a
α_1C5 Lys-β_2HC3 His-β_2FG1 Asp salt bridge	R	R	intermediate	intermediate	b
Fe-N_ε stretching	R	R	T	R	this work
P_{50} (mmHg)	0.604	0.457 (pH 7.9)	0.845	0.461 (pH 7.9)	this work

[a]Ishimori & Morishima, 1988; [b]Ishimori et al., 1988

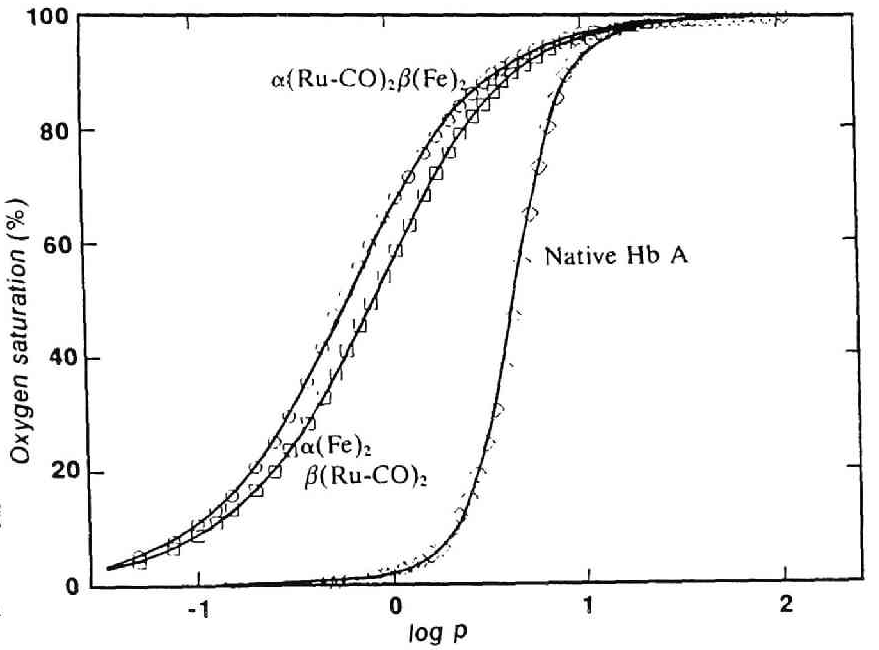
100
80
60
40
20
0
Oxygen saturation (%)
α(Ru-CO)₂β(Fe)₂
Native Hb A
α(Fe)₂
β(Ru-CO)₂
-1
0
1
2
log p

(A)

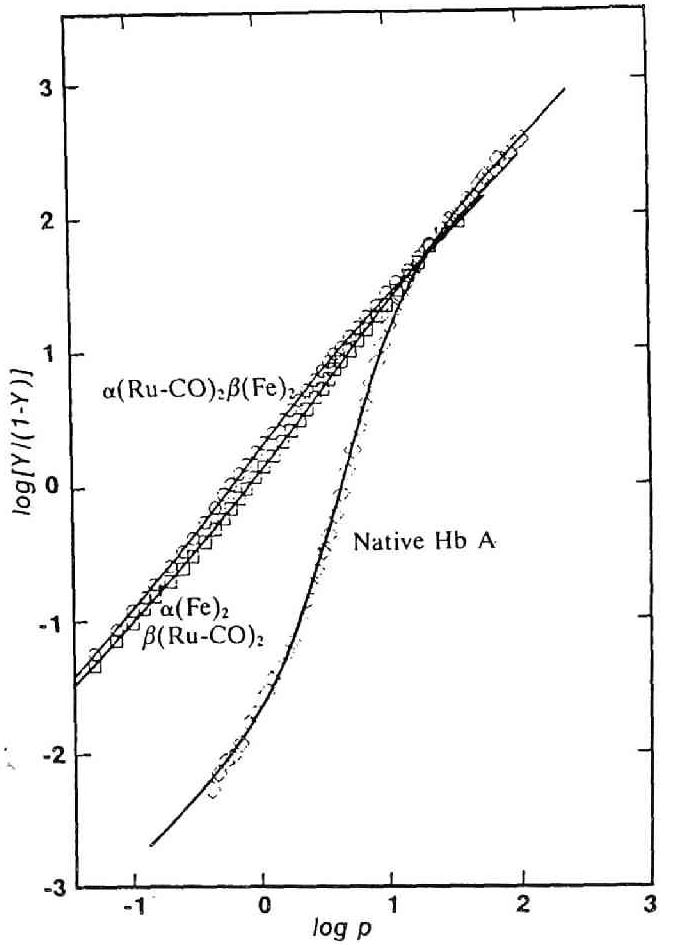
3
2
1
0
-1
-2
-3
log[Y/(1-Y)]
α(Ru-CO)₂β(Fe)₂
Native Hb A
α(Fe)₂
β(Ru-CO)₂
-1
0
1
2
3
log p

(B)

Figure. 1

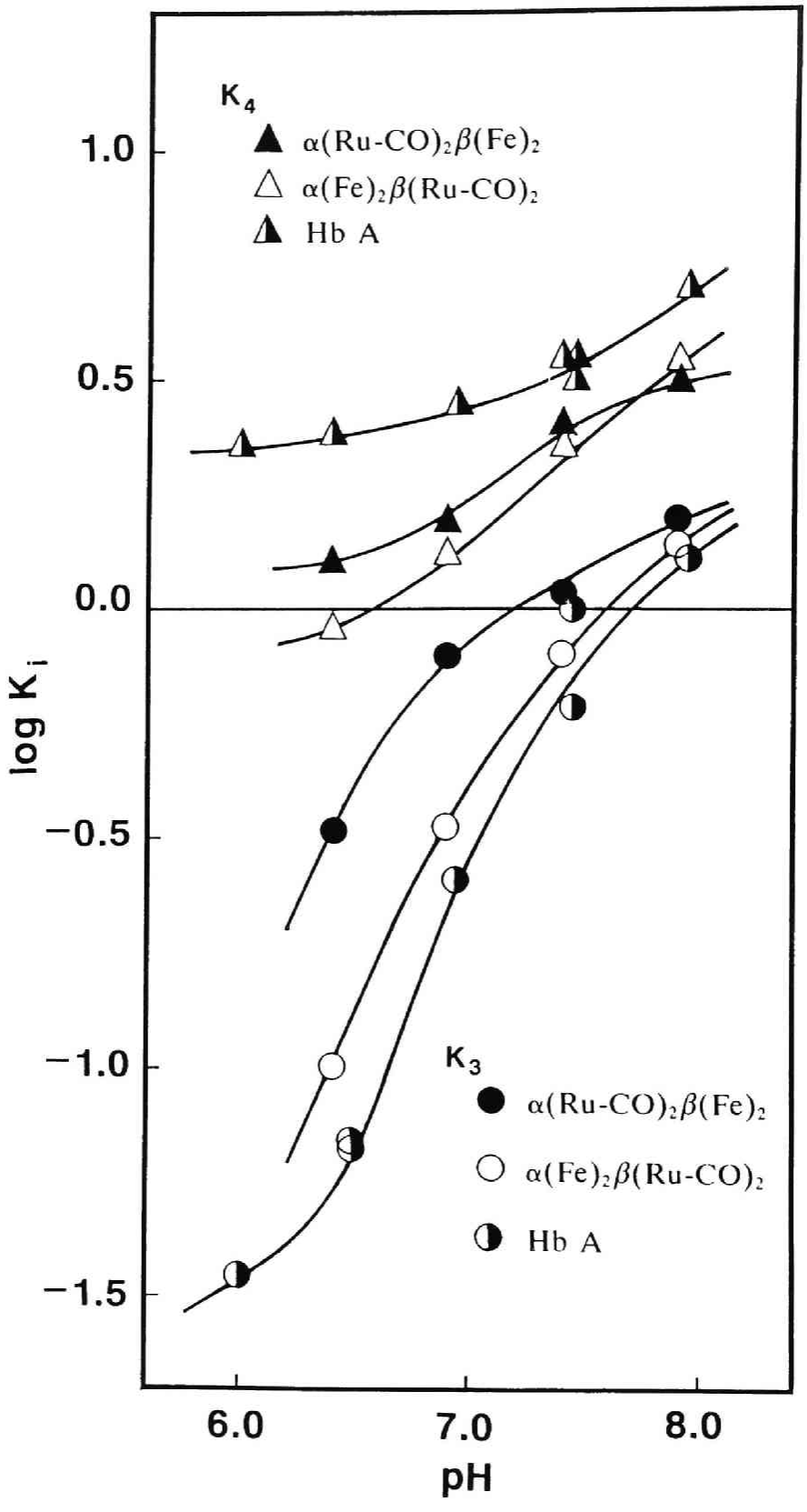
K4
α(Ru-CO)2β(Fe)2
α(Fe)2β(Ru-CO)2
Hb A
1.0
0.5
0.0
−0.5
−1.0
−1.5
log Ki
K3
α(Ru-CO)2β(Fe)2
α(Fe)2β(Ru-CO)2
Hb A
6.0
7.0
8.0
pH

Figure. 2

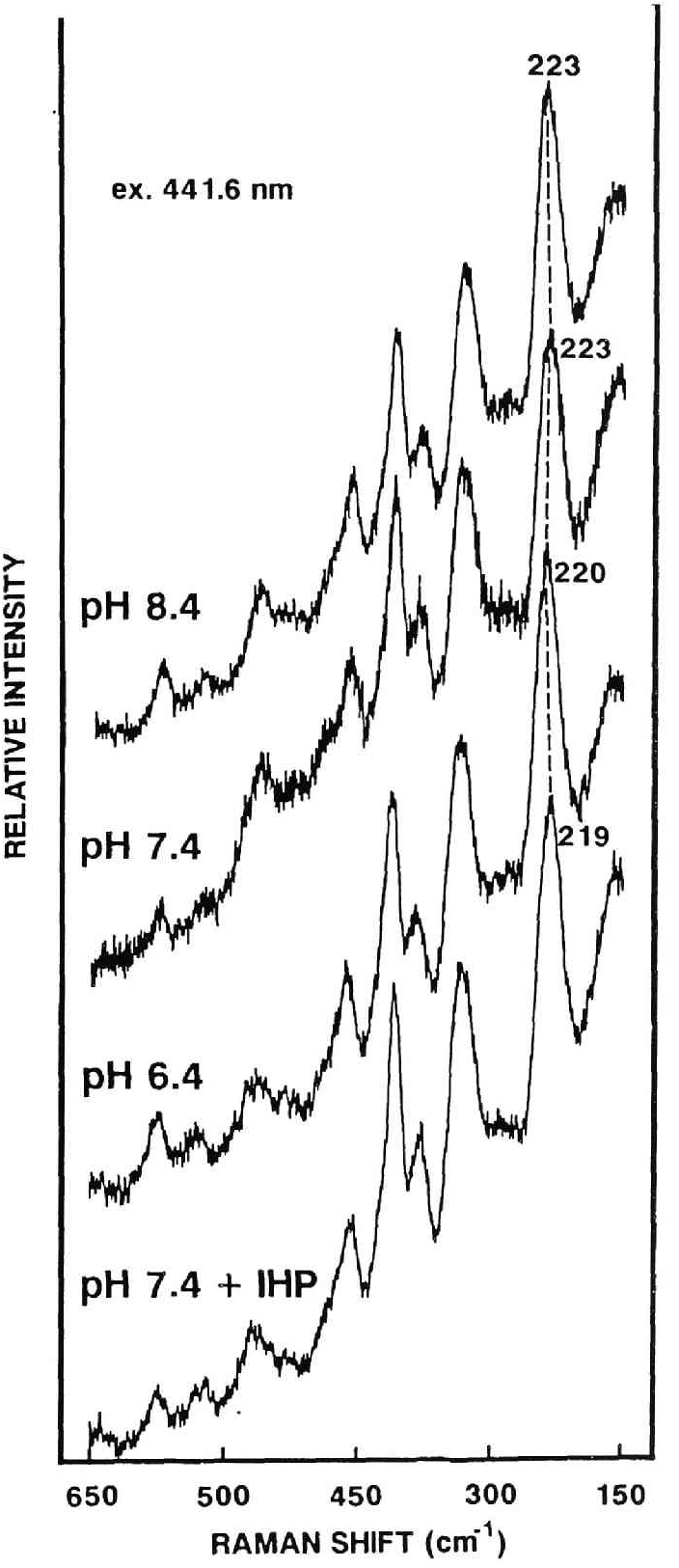
223
ex. 441.6 nm
223
220
pH 8.4
pH 7.4
219
pH 6.4
pH 7.4 + IHP
RELATIVE INTENSITY
650
500
450
300
150
RAMAN SHIFT (cm-1)

Figure. 3

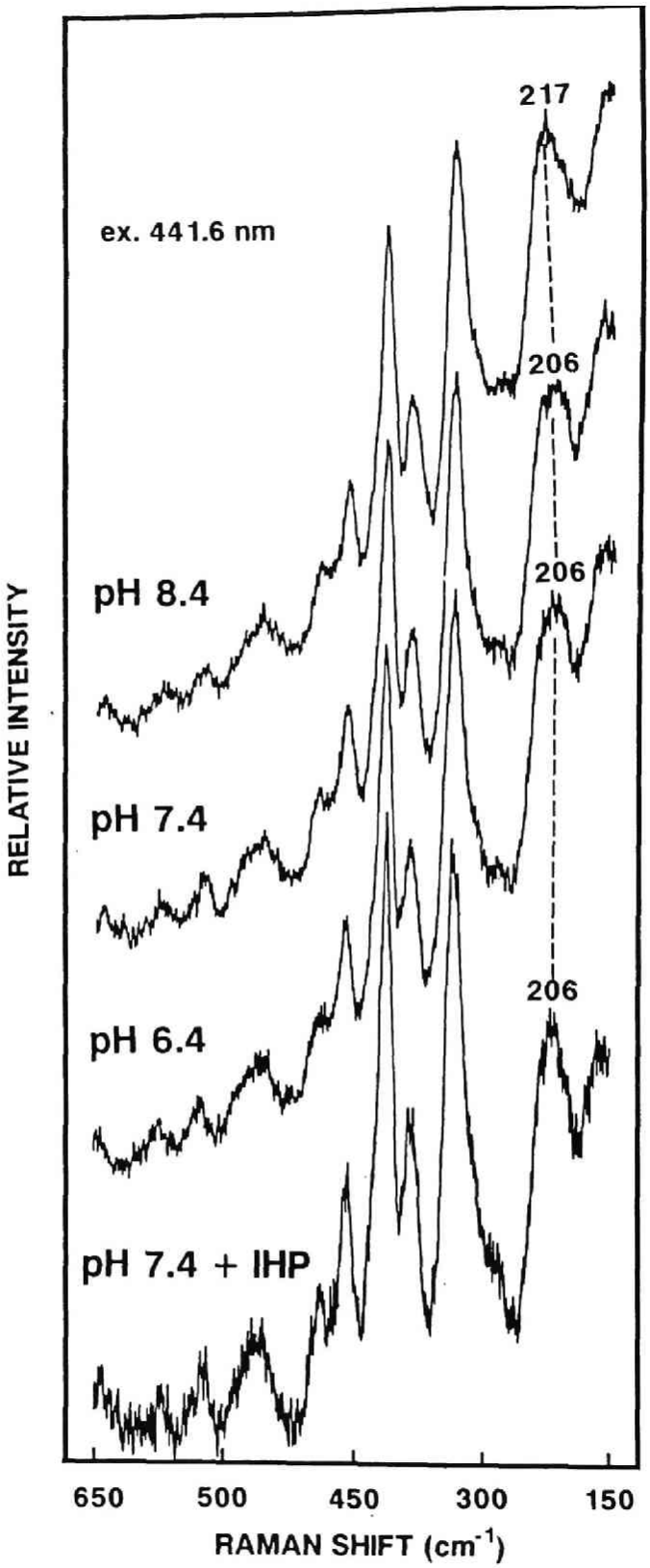
217
ex. 441.6 nm
206
206
pH 8.4
pH 7.4
206
pH 6.4
pH 7.4 + IHP
RELATIVE INTENSITY
650
500
450
300
150
RAMAN SHIFT (cm-1)

Figure. 4

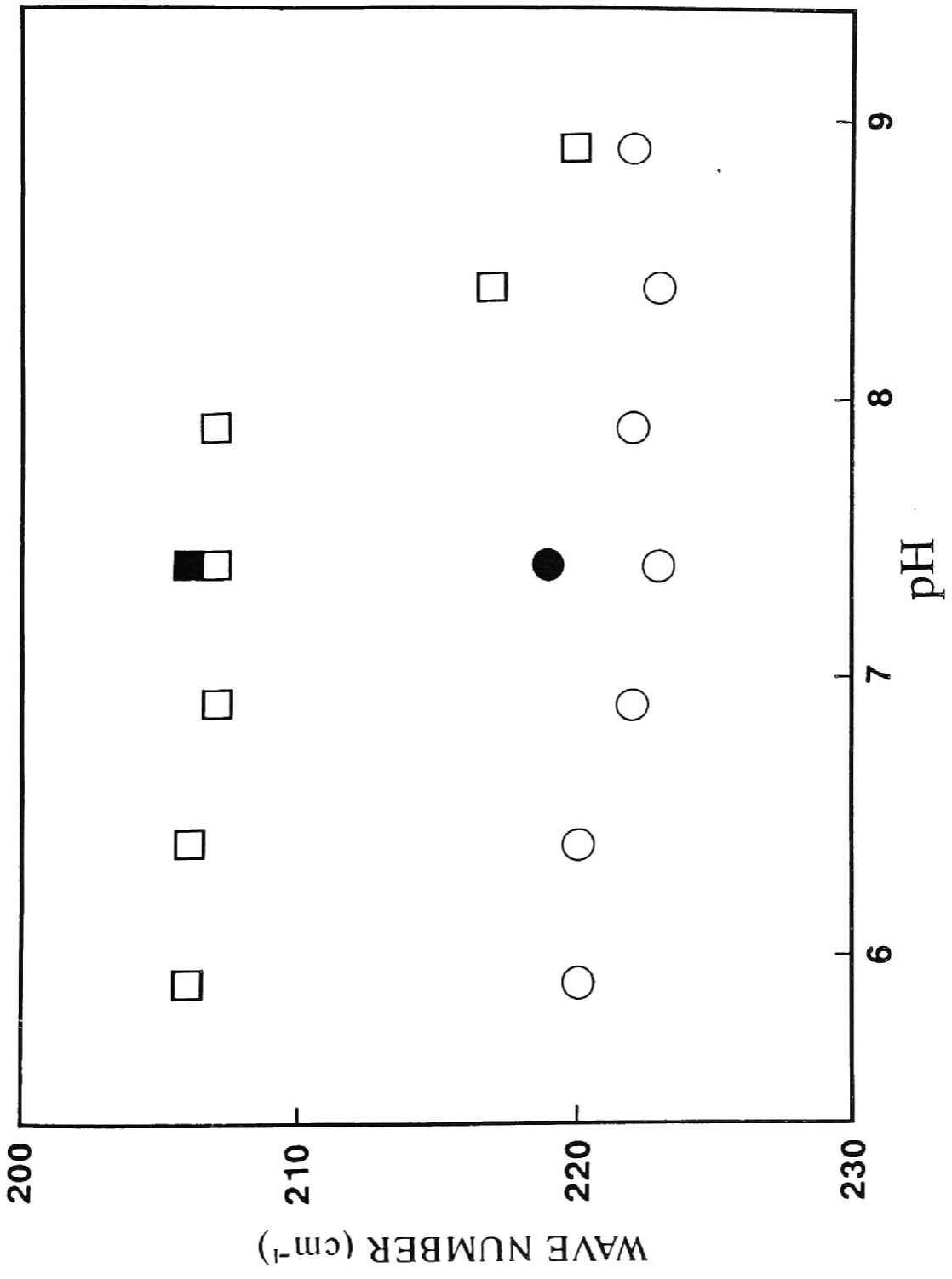

Figure. 5

Figure. 6

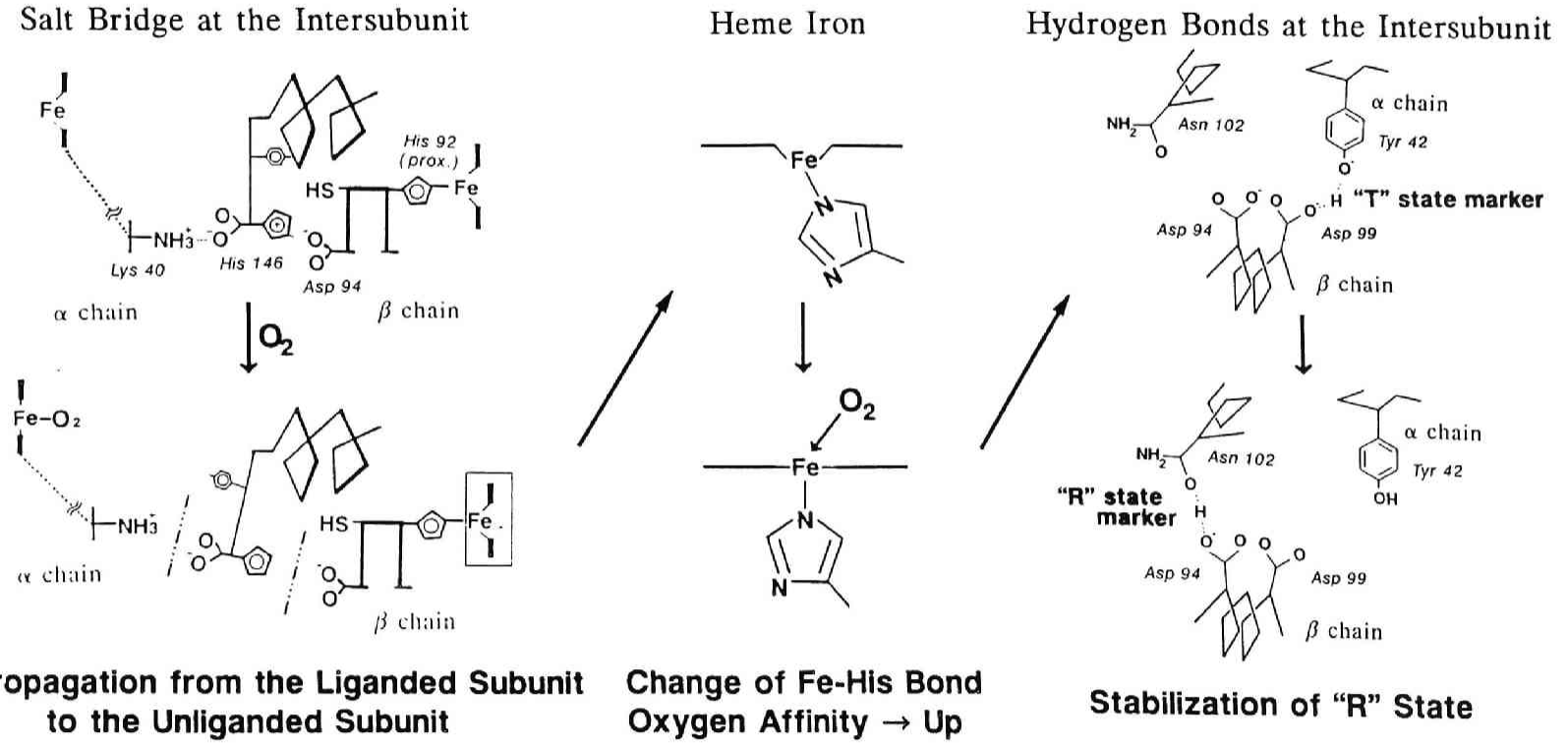
Salt Bridge at the Intersubunit
Heme Iron
Hydrogen Bonds at the Intersubunit
Fe
NH3
Lys 40
His 146
His 92 (prox.)
HS
Fe
Asp 94
α chain
β chain
O2
Fe-O2
Asn 102
Tyr 42
"T" state marker
Asp 94
Asp 99
"R" state marker
OH
Propagation from the Liganded Subunit to the Unliganded Subunit
Change of Fe-His Bond Oxygen Affinity → Up
Stabilization of "R" State

PART III.

ALLOSTERIC TRANSITION IN FERRIC AND FERROUS LOW SPIN HEMOGLOBINS

CHAPTER 1.

Interaction of Fully Liganded Valency Hybrid Hemoglobin with Inositol Hexaphosphate:

Implication of the IHP-induced T state of human adult methemoglobin in the low spin state.

ABSTRACT: To gain further insight into the quaternary structures of methemoglobin derivatives in the low spin state, the interaction of fully liganded valency hybrid human hemoglobins with IHP was studied here by proton NMR spectroscopy. Upon addition of IHP to $(\alpha_{CO}\beta^{+}_{N_3^-})_2$, the same resonances as the previously reported IHP-induced NMR peaks for azidomethemoglobin $(\alpha^{+}_{N_3^-}\beta^{+}_{N_3^-})_2$ appeared, whereas the binding of IHP did not significantly affect the NMR spectra for $(\alpha^{+}_{N_3^-}\beta_{CO})_2$. The binding of IHP also brought about more pronounced spectral changes for $(\alpha_{CO}\beta^{+}_{Im})_2$ and $(\alpha_{CO}\beta^{+}_{H_2O})_2$ than for $(\alpha^{+}_{Im}\beta_{CO})2$ and $(\alpha^{+}_{H_2O}\beta_{CO})_2$. Therefore, the IHP-induced NMR peaks for azidomethemoglobin are attributed to the β heme methyl group. Such IHP-induced β heme methyl resonances were also observed for $(\alpha_{NO}\beta^{+}_{N_3^-})2$, which undergoes quaternary structural change, analogously to the R-T transition by the binding of IHP. From above results, it was suggested that the IHP-induced β heme methyl resonances for azidomethemoglobin and $(\alpha_{CO}\beta^{+}_{N_3^-})_2$ may also be associated with the quaternary structure of these Hbs, implying the presence of the IHP-induced "T-like" state in low spin metHb A.

A variety of physico-chemical properties of hemoglobin tetramer have been often understood on the basis of two quaternary conformational states: The T and R states, normally associated with deoxy and oxy hemoglobin structures and also characterized by low and high oxygen ligand binding affinity, respectively (Monod et al.,1965). These two quaternary states have been defined in terms of some detailed protein and heme environmental structures (Shulman et al.,1975; Baldwin,1975). The X-ray structural analysis revealed that the iron is out of the heme plane in deoxyhemoglobin (Fermi,1975), but planar in oxyhemoglobin (Shaanan,1982). On the basis of these structural differences, Perutz(1970) has proposed that this movement of iron displacement into or out of the heme plane, linked to the spin state of heme iron, exerts an influence on the globin structures of the protein which promotes the T to R structural transition upon ligand binding. In support of such relationship between the quaternary structural change and the spin state of the heme iron, Perutz and his co-worker(Perutz et al.,1974a,b,c) extended their spectral studies to high and low spin derivatives of methemoglobin and found that the allosteric effector IHP[5], which binds preferentially to the T state, converts the high spin methemoglobin derivatives with the iron located out of the heme plane from the R to T state (Perutz et al.,1974a,b; Massana et al.,1978; Fermi & Perutz,1977; Hensley et al.,1975 a,b; Edelstein & Gibson,1975). For low spin methemoglobin derivatives, however, Perutz et al.(1974b,c) showed that the IHP binding does not change their quaternary structures, although their tertiary structure is perturbed.

We have previously studied the effect of IHP on the tertiary and quaternary structures of methemoglobin derivatives by the use of proton NMR spectroscopy and found that the IHP-induced hyperfine-shifted proton peaks which are distinguishable from those observed in the absence of IHP appeared for the azide and imidazole complexes in the low spin state where the heme iron is in the heme plane (Neya & Morishima,1980,1981). These IHP-induced NMR peaks for the low spin azidomethemoglobin (HbN_3^-) were not observed when azide was titrated to stripped aquomethemoglobin, indicating that IHP-induced peaks are not due to the dissociation of azide. Azide titration to aquomethemoglobin in the presence of IHP further revealed that the IHP-induced peaks are not due to the localized structural change but rather to the presence of an IHP-induced new conformer (Neya &

[5]Abbreviation: IHP, inositol hexakis(phosphate); DPG, 2,3-diphosphoglycerate; Bis-Tris, [bis(2-hydroxyethyl)amino]tris(hydroxymethyl)methane.

Morishima,1981). The pD dependence of the intensities of these peaks was found to be closely similar to that of the exchangeable proton NMR peak which has been used as a marker of the T quaternary conformation (Perutz et al.,1978; Huang,1979). It was further suggested that the IHP-induced quaternary structural transition is accompanied by the tertiary structural alterations in both of the α and β subunits (Neya & Morishima,1981). Above previous finding of the IHP-induced NMR peaks for those low spin methemoglobin derivatives led us to suggest that the low spin methemoglobin can switch from the R to T quaternary structure by the binding of IHP. Although these IHP-induced NMR peaks were attributed to a new conformer in low spin methemoglobin, an unequivocal support for the presence of the T quaternary structure was incomplete, because these IHP-induced heme methyl resonances have not so far been observed in the hemoglobin derivative that is definitely known to be in the T quaternary state.

In order to complement the results obtained previously and to give more confirmative evidence for the IHP-induced quaternary structural changes in the ferric low spin methemoglobin, we examined here the effect of IHP binding on the NMR spectra of human adult fully liganded valency hybrid Hbs, which may serve to assign the IHP-induced NMR peaks to α and/or β subunits and also to delineate their quaternary structures in the presence or absence of IHP.

MATERIALS AND METHODS

Human adult hemoglobin was prepared from whole blood as reported previously (Morishima & Hara,1983). The isolated α and β chains were prepared using the method of Ikeda-Saito et al. (Ikeda-Saito et al.,1981).

The azide-carboxy hybrids were prepared by addition of the metazide derivatives of one chain with the carboxy form of the other with a slight excess of the β chain. Then the mixture is passed through sephadex G-25 equilibrated with 10 mM phosphate buffer pH 6.5 and applied to CM-52 (whatman) equilibrated with the same buffer. The excess β chain was washed off by the same buffer and the hybrid hemoglobin tetramer was eluted with 0.1M phosphate buffer pH 7.0.

The azide-nitrosyl hybrids were obtained following the procedure described by Henry & Banerjee (1973) with a slight modification. The oxygenated chain in 0.1 M phosphate buffer, pH 7.0 was deoxygenated by flushing the dry nitrogen gas. Nitric oxide was then allow to react by the

successive addition of sodium nitrite and dithionite. Excess NO and dithionite were removed by filtering rapidly in a sephadex G-25 column equilibrated with 0.05 M deoxygenated Bis-Tris buffer pH 6.5, under completely anaerobic conditions. Then, an equivalent amount of metazide chain was mixed immediately.

The aquomet-carboxy hybrids were prepared as follows; the oxygenated chain in 0.1 M phosphate buffer, pH 7.0 was oxidized by adding a 1.2 equivalent ferricyanide. Excess ferri- and ferrocyanide were removed by passing through a sephadex G-25 equilibrated with the same buffer and then the carboxy chains injected immediately with a slight excess of β chain. The hybrids thus obtained were purified according to the same procedures as described for azide-carboxy hybrids. The purity of the samples was checked by calculating the fraction of carboxyl ferroheme (Banerjee & Cassoly,1969).

The imidazole-carboxy hybrids were prepared by adding the imidazole to aquomet-carboxy hybrids. All of the operations were carried out at 4 °C.

Proton NMR spectra at 300 MHz were recorded on a Nicolet NT-300 spectrometer equipped with a 1280 computer system. Typical NMR spectra consisted of 5000 pulses and hyperfine shifted NMR spectra were obtained by a 4K data transform of 30-kHz (high spin complexes) and 12-kHz (low spin complexes) spectral width and 5.5-μs 90° pulse after the strong solvent resonance in H_2O solution was suppressed by 500-μs low power pulse. We used Redfield 2-1-X pulse sequence with 22.9-μs pulse and 8K data points over a 8-kHz spectral width for recording the exchangeable proton resonances in the subunit interface of Hb. Probe temperature was determined by the temperature control unit of the spectrometer, accurate to ±0.5 °C. The volume of the NMR sample was 0.3 mL, and heme concentration was about 2 mM. Proton shifts were referenced with respect to the water proton signal, which is 4.8 ppm downfield from the proton resonance of 4,4-dimethyl-4-silapentane-1-sulfonate (DSS) at 23 °C.

RESULTS

IHP-induced Tertiary Structural Changes for Valency Hybrid Hemoglobins. The hyperfine-shifted proton NMR spectra of HbN_3^- in the presence and absence of IHP have been described before(Neya & Morishima,1980,1981). In the absence of IHP at pH 6.5 and 23 °C, the α heme methyl resonances were observed at 23.0 17.1 and 9.8 ppm and β heme methyl resonances at 21.8, 16.1 and 9.0 ppm(Davis et al.,1969). Upon

addition of IHP, new peaks appeared at 26.3, 20.0 and 15.4 ppm. The contributions of the α and β subunits to these IHP-induced resonances in HbN_3^- could be evaluated by studying the valency hybrids $(\alpha^+_{N_3}\beta_{CO})_2$ and $(\alpha_{CO}\beta^+_{N_3})_2$, where only the ferriazide chains give paramagnetically shifted resonances.

Figure 1 shows the proton NMR spectra of $(\alpha^+_{N_3}\beta_{CO})_2$ and $(\alpha_{CO}\beta^+_{N_3})_2$ in the presence and absence of IHP in 0.05 M Bis-Tris buffer at pH 6.5. Without IHP, the hyperfine-shifted α and β heme methyl resonances of HbN_3^- appear to be composite of those of valency hybrids, indicating that these fully liganded hemoglobins are more or less the same in their heme environmental conformations. The NMR spectra for $(\alpha^+_{N_3}\beta_{CO})_2$ are not changed by the addition of IHP except for the slight IHP-induced increase in the line width of three heme methyl resonances, while those for $(\alpha_{CO}\beta^+_{N_3})_2$ are much influenced by IHP. Upon addition of IHP to $(\alpha_{CO}\beta^+_{N_3})_2$, there appear new resonances at 26.4 and 20.0 ppm at 23 °C. The intensities of these resonances gradually increased with lowering the temperature from 23 °C to 4 °C. It is to be noted that those IHP-induced peaks for $(\alpha_{CO}\beta^+_{N_3})_2$ are identical with those for HbN_3^-. The IHP-induced NMR peaks for HbN_3^- could therefore be attributed to the β subunit.

The effect of IHP binding on the NMR spectra of $(\alpha^+_{N_3}\beta_{NO})_2$ and $(\alpha_{NO}\beta^+_{N_3})_2$ was also examined (Figure 2). The IHP-induced spectral changes for nitrosyl-azide valency hybrids are almost the same as those for carboxy-azide valency hybrids. Upon addition of IHP, the NMR spectrum of $(\alpha^+_{N_3}\beta_{NO})_2$ remains unchanged, while for $(\alpha_{NO}\beta^+_{N_3})_2$ the intensities of the heme methyl resonances around 23.0 and 17.0 ppm gradually decrease with a concomitant appearance of the characteristic resonances at 27.4, 22.4 and 15.7 ppm. The 23.0 and 17.0 ppm peaks, which are observed in the absence of IHP, completely disappear to give only a set of IHP-induced new peaks when a saturating amount of IHP is added. These IHP-induced resonances for $(\alpha_{NO}\beta^+_{N_3})_2$ are placed at slightly lower field by 1 ~ 2 ppm, compared with those for $(\alpha_{CO}\beta^+_{N_3})_2$ and HbN_3^-.

In Figure 3 is shown the proton NMR spectra of $(\alpha_{NO}\beta^+_{N_3})_2$ with and without IHP in 0.05 M Bis-Tris buffer at pH 6.5 and 23 °C. There appears a broad signal at 27.2 ppm in the absence of IHP. This peak could be attributed to the same resonance as the IHP-induced one since an appreciable increase in intensity is encountered upon addition of IHP. As shown in Figure 2, this broad signal is not observed in the absence of IHP at 4 °C, probably because it is too broadened to be detectable at this temperature. The appearance of

the same resonance as the IHP-induced one even in the absence of IHP indicates that the IHP-induced peaks for $(\alpha_{NO}\beta^{+}_{N_3^-})_2$ are not due to the IHP-induced localized structural change within $(\alpha_{NO}\beta^{+}_{N_3^-})_2$, but rather to the presence of the new conformer to which IHP preferentially binds and which could stabilize its conformation.

We also examined the effect of IHP binding on the NMR spectra of $(\alpha^{+}_{Im}\beta_{CO})_2$ and $(\alpha_{CO}\beta^{+}_{Im})_2$ at pH 6.5 and 4 °C in 0.05 M Bis-Tris buffer, as shown in Figure 4. For $(\alpha^{+}_{Im}\beta_{CO})_2$, the NMR spectrum in the presence of IHP is identical with that in the absence of IHP, while that of $(\alpha_{CO}\beta^{+}_{Im})_2$ exhibits a marked spectral change upon addition of IHP. This observation may also allow us to ascribe the IHP-induced NMR peaks for HbIm, which was previously reported (Neya & Morishima,1980,1981), to the β subunit. All the resonance positions of azide and imidazole derivatives are assembled in Table I.

The left side of Figure 5 illustrates the NMR spectra of $(\alpha^{+}_{H_2O}\beta_{CO})_2$ and $(\alpha_{CO}\beta^{+}_{H_2O})_2$ with and without IHP. The resonances that appear over the spectral region from 30 to 90 ppm come from the heme peripheral proton groups and/or the protons of the amino acid residues in the immediate surroundings of the heme group. These resonances for $(\alpha^{+}_{H_2O}\beta_{CO})_2$ exhibit minor spectral changes upon addition of IHP, as shown in Figure 5. The exchangeable resonance at 93.9 ppm, which is most probably assigned to the proximal histidyl (E7) NH proton in the ferric α subunit (La Mar & deRopp,1979), also remains unchanged. For $(\alpha_{CO}\beta^{+}_{H_2O})_2$, the more obvious spectral change was induced as shown in Figure 5. The binding of IHP produces more pronounced spectral changes for $(\alpha_{CO}\beta^{+}_{H_2O})_2$ over the region from 40 to 90 ppm, in contrast to $(\alpha^{+}_{H_2O}\beta_{CO})_2$ which experiences no significant spectral changes.

IHP-induced Quaternary Structural Changes for Valency Hybrid Hemoglobins. Figure 6 shows the exchangeable proton resonances for $(\alpha_{NO}\beta^{+}_{N_3^-})_2$ in the presence and absence of IHP at 4 °C. Of particular interest is the appearance of the exchangeable proton resonances at 9.3 and 6.2 ppm by addition of IHP. The former resonance has been assigned to the *inter*subunit hydrogen bond between tyrosine-α42(C7) and asparatic acid-β99(G1), characteristic of the deoxy quaternary structure (Fung & Ho,1975), and the latter to the *intra*subunit hydrogen bond between valine-β98(FG5) and tyrosine-β145(HC2), which is characteristic of the deoxy tertiary structure (Viggiano et al.,1978). It is also worthy to note that the intensity of the resonances at 9.3 and 6.2 ppm for $(\alpha_{NO}\beta^{+}_{N_3^-})_2$ with IHP

appears to bear half of the signal intensity of the 9.4 and 6.4 ppm peaks for deoxyhemoglobin (Perutz et al.,1974). This suggests that IHP can switch the quaternary structure for $(\alpha_{NO}\beta^{+}_{N_3^-})_2$, although the quaternary structure of the hybrid Hb in the presence of IHP is somewhat different from the usual T quaternary structure. An attempt to look for the exchangeable proton resonances associated with the hydrogen bond at the subunit interface in HbN_3^-, carboxy-azide hybrid Hbs and $(\alpha^{+}_{N_3^-}\beta_{NO})_2$ was not successful because of the spectral overlaps in this region with the paramagnetically shifted resonances.

In the right side of Figure 5, the exchangeable proton resonances of carboxy-aquomet hybrid hemoglobin with and without IHP are shown. Although Fung et al.(1976,1977) reported the NMR spectra of hemoglobin M Milwaukee, which contains the mutant aquomet β heme, the quaternary structures of the aquomet-carboxy hybrid Hbs have not been reported. In the spectrum of $(\alpha^{+}_{H_2O}\beta_{CO})_2$, a resonance at 6.0 ppm, which has been utilized as an indicator of the R quaternary structure (Fung & Ho,1975), loses its signal intensity and shifts to 5.9 ppm upon addition of IHP. The most obvious change is the appearance of the broad resonance at 10.1 ppm, which has been established as a reliable T state marker in aquomethemoglobin (Perutz et al.,1978; Huang,1979). $(\alpha_{CO}\beta^{+}_{H_2O})_2$ also exhibits the T marker signal at 10.1 ppm upon addition of IHP, indicating that IHP switches the quaternary structure of this hybrid Hb from the R to T state, although its paramagnetic resonances experience no significant changes as shown in Figure 5. These observations show that some of the hybrid Hb derivatives undergo the R to T quaternary structural transition by the binding of IHP. It is also noteworthy that the resonance at 6.5 ppm which has been assigned to the *intra*subunit hydrogen bond, characteristic of the tertiary structure within the T state, is observed for $(\alpha_{CO}\beta^{+}_{H_2O})_2$. Upon addition of IHP, a 6.5 ppm peak experienced a slight upfield shift to 5.9 ppm. All the resonance positions of the hydrogen bonded protons for the aquomet derivatives and $(\alpha_{NO}\beta^{+}_{N_3^-})_2$ are summarized in Table II.

DISCUSSION

Tertiary Structural Changes Induced by Addition of IHP for Low Spin Methemoglobin Derivatives. The present NMR results on carboxy-azide and nitrosyl-azide valency hybrids have served to identify the IHP-induced NMR peaks in the hyperfine-shifted region for HbN_3^- and give additional support for the presence of the new conformer which is induced by the

addition of IHP to low spin methemoglobin as was proposed in our previous report (Neya & Morishima, 1980, 1981).

In the NMR spectrum of HbN_3^- with IHP, contributions from the α and β subunits to IHP-induced NMR peaks are easily distinguished when the spectrum of $(\alpha^+_{N_3^-}\beta_{CO})_2$ or $(\alpha^+_{N_3^-}\beta_{NO})_2$ with IHP is compared with that of $(\alpha_{CO}\beta^+_{N_3^-})_2$ or $(\alpha_{NO}\beta^+_{N_3^-})_2$ without IHP. As shown in Table I, it is thus confirmed that the IHP-induced NMR peaks in HbN_3^- are originated from the β subunit. Accordingly, we now correct our previous suggestion that both α and β subunits for HbN_3^- are equally perturbed by the binding of IHP and the IHP-induced NMR peaks arise from the structural alteration in both subunits (Neya & Morishima,1981). In our previous report, we have performed the azide titration to IHP-bound aquomethemoglobin and found that the IHP-induced NMR peaks appeared first and then the α, β heme methyl groups grow up with increasing amount of azide. This observation could also be re-interpreted as follows; the heme methyl peaks characteristic of the IHP-induced conformer appeared first, then followed by the appearance of the native conformer peaks. This seems to be in good agreement with the result obtained by Olson (1976) that azide binding rate at the β subunit is 50-fold larger than at the α subunit in the presence of IHP.

Although the structural origin of the IHP-induced resonances for $(\alpha_{CO}\beta^+_{Im})_2$ is not certain at the present stage, IHP gives rise to more pronounced NMR spectral changes for $(\alpha_{CO}\beta^+_{Im})_2$ than for $(\alpha^+_{Im}\beta_{CO})_2$ as shown in Table I. In the case of aquomet-carboxy hybrids (Figure 5), the β heme moiety of $(\alpha_{CO}\beta^+_{H_2O})_2$ also undertakes more pronounced structural change than the α heme moiety of $(\alpha^+_{H_2O}\beta_{CO})_2$.

Such a different behaviour of responses toward organic phosphate between the complementary pairs of valency hybrids seems to be a general phenomenon. Cassoly & Gibson(1972) have shown that addition of IHP to $(\alpha_{deoxy}\beta^+_{CN^-})_2$ produces the marked absorption difference spectrum in the soret region, while the spectrum of $(\alpha^+_{CN^-}\beta_{deoxy})_2$ remains almost unchanged. They also studied the effect of DPG binding on the kinetics of carbon monoxide binding to cyanide-deoxy valency hybrids which exhibits a strong heterogeneous character in the absence of organic phosphate. Upon addition of DPG, only $(\alpha_{deoxy}\beta^+_{CN^-})_2$ showed a decrease in the fraction of fast phase component although DPG is more strongly bound to $(\alpha^+_{CN^-}\beta_{deoxy})_2$ than to $(\alpha_{deoxy}\beta^+_{CN^-})_2$. Perutz et al.(1976) have reported that addition of IHP to $(\alpha_{NO}\beta^+_{CN^-})_2$ causes a substantial changes of the absorption spectra in either the UV or visible region, but $(\alpha^+_{CN^-}\beta_{NO})_2$

experiences no significant spectral changes. This was also encountered for the ESR spectra(Rein et al.,1972; Henry & Banerjee,1973; Miura & Morimoto,1980; Nagai et al.,1978). The ESR spectra of $(\alpha_{NO}\beta^{+}_{CN^-})_2$, $(\alpha_{NO}\beta^{+}_{H_2O})_2$ and $(\alpha_{NO}\beta^{+}_{F^-})_2$ exhibited three distinct hyperfine structures upon addition of IHP, whereas those of their complementary hybrids were insensitive to the addition of IHP. We have no available data to show the difference in the affinity of IHP toward both complementary hybrids. However, it is unlikely that the apparent affinity of IHP to these hybrids can differ remarkably, since IHP is a strong allosteric effector which binds, for example, to oxy- and azidomethemoglobin with the large binding constant, $1.4 \times 10^4\ M^{-1}$ and $1.88 \times 10^4 M^{-1}$, respectively (Neya et al.,1983; Jonig et al.,1971). Therefore, we would rather like to suggest that the α and β subunits could have different sensitivity to organic phosphate.

Quaternary Structural Changes Induced by Addition of IHP --Evidence for the T-like Structure in Low Spin Methemoglobin. In the quaternary structural transition from the R to T state in hemoglobins, Perutz et al.(1974a,b) previously found the characteristic changes in ultraviolet absorption and circular dichroism. In ferric high spin methemoglobin, aquomet or fluoromethemoglobin, exactly the same changes as those for ferrous hemoglobin can be produced by the addition of IHP. NMR spectra (Perutz et al.,1978) also showed that the addition of IHP to human fluoro- and aquomethemoglobin leads to the slowly exchanging proton resonance at about 10 ppm diagnostic of the T structure. Thus, Perutz et al.(1978) concluded that IHP is capable of switching the quaternary structure of certain high-spin ferric hemoglobins from the R to T state. As to ferric low spin methemoglobin, however, Perutz et al.(1974a) also investigated azide and cyanide methemoglobin, and concluded that IHP appears to modify the structure of these low spin derivatives without changing their quaternary structure to the T state.

On the other hand, Neya & Morishima(1980,1981) found an IHP-induced new conformer in low spin azidomethemoglobin by utilizing NMR spectra, and suggested that human low spin methemoglobin can be switched into the T quaternary structure by the binding of IHP. Neya et al.(1983) also reported the UV-spectral evidence for the IHP-induced quaternary structural alteration in HbN_3^-; IHP induced the changes in the UV absorption spectra of Tyr-α42(C7) and Trp-β37(C3), corresponding to the perturbation of the subunit boundary structure.

The resonances of the hydrogen bonded proton located at the *inter-* and

*intra*subunit are expected to further clarify the quaternary structure of $(\alpha_{NO}\beta^{+}_{N_3^-})_2$. As shown in Table III, the quaternary structure of the new conformer is analogous to the T state structure in ferrous hemoglobin. Since the T marker signal at 9.4 ppm for native Hb is shifted to 9.3 ppm for $(\alpha_{NO}\beta^{+}_{N_3^-})_2$ and the intensity of the T marker for the hybrid hemoglobin is half of the one for deoxyhemoglobin, the quaternary structure of the new conformer could be described as the "T-like" state rather than the usual T state. The t marker signal at 6.4 ppm for native Hb is also shifted to 6.3 ppm for $(\alpha_{NO}\beta^{+}_{N_3^-})_2$. It is apparent from Figure 3 that the "T-like" structural marker signals are not only induced by addition of IHP, but also exists even in the absence of IHP. This may suggest that IHP changes the R-T conformational equilibrium inherent in $(\alpha_{NO}\beta^{+}_{N_3^-})_2$. Huang(1979) reported that stripped nitrosylhemoglobin is 70 % in the T state below pH 6.4 and is in the R state at pH above 6.4 and that IHP raises this transition point from pH 6.4 to 7.5. These findings indicate that the IHP can shift the equilibrium from the R to T quaternary state for $(\alpha_{NO}\beta^{+}_{N_3^-})_2$ and the nitrosylhemoglobin as well. It is thus likely that IHP induces the quaternary structural change of the valence hybrid hemoglobin containing ferric low spin iron, $(\alpha_{NO}\beta^{+}_{N_3^-})_2$, which is analogous to the R-T transition as was found for ferric high spin Hbs. Based on the close similarity of the IHP-induced heme methyl resonances among HbN_3^-, $(\alpha_{CO}\beta^{+}_{N_3^-})_2$ and $(\alpha_{NO}\beta^{+}_{N_3^-})_2$ as shown in Table I, the IHP-induced resonances for HbN_3^- and $(\alpha_{CO}\beta^{+}_{N_3^-})_2$ could also be attributed to the T-like conformer of these hemoglobins. Accordingly, we can conclude that IHP induces the quaternary structure not only in ferric high spin hemoglobins but also in low spin hemoglobins and the quaternary structural change by addition of IHP is similar to the R-T transition, although quaternary structure of ferric low spin hemoglobin with IHP is somewhat different from that of ferric high spin or ferrous hemoglobins.

Here one may ask why the NMR spectra of the complementary pairs $(\alpha^{+}\beta)_2$ are little affected by addition of IHP as shown in Figures 1, 2 and 4. It is also to be noted that Cassoly & Gibson(1972) and Perutz et al.(1976) suggested on the basis of no optical spectrum responses to the addition of organic phosphate that organic phosphate does not change the quaternary structure of valency hybrid hemoglobin containing ferric heme in the α subunit. Therefore, the energy to change the quaternary structure for $(\alpha\beta^{+})_2$ seems to be smaller than that for $(\alpha^{+}\beta)_2$, since the binding energy of IHP would suffice to change quaternary structure of the protein to the T-like

state for $(\alpha\beta^{+})_2$, but not for $(\alpha^{+}\beta)_2$. In other words, the T-like quaternary structure is more favoured in $(\alpha\beta^{+})_2$ compared with $(\alpha^{+}\beta)_2$. This is further confirmed by the present observation that there appears the t state marker signal at 6.5 ppm for stripped $(\alpha_{CO}\beta^{+}{}_{H_2O})_2$ but not for $(\alpha^{+}{}_{H_2O}\beta_{CO})_2$ as shown in Figure 5. The same result was also obtained here for carboxy-fluoride valency hybrids (the result is not shown). The higher oxygen affinity for $(\alpha^{+}{}_{N_3}\text{-}\beta_{deoxy})_2$, $(\alpha^{+}{}_{H_2O}\beta_{deoxy})_2$ and $(\alpha^{+}{}_{F}\text{-}\beta_{deoxy})_2$ than for their complementary hybrids (Banerjee & Cassoly,1969) may also be interpreted along these lines. However, Ogawa & Shulman(1972) and Ogawa et al.(1972) reported that oxy quaternary structure is much more favoured in $(\alpha_{deoxy}\beta^{+}{}_{CN}\text{-})_2$ than the deoxyhemoglobin-like structure because an extremely strong allosteric effector like IHP is required to switch its quaternary structure, whereas in $(\alpha^{+}{}_{CN}\text{-}\beta_{deoxy})_2$, the energy to change its quaternary structure is rather small and can be switched by DPG or inorganic phosphate. Therefore, it is premature to conclude that there is an unequivocal correlation between those different physico-chemical properties and quaternary conformations in the complementary pairs of hybrids. It may be more safe to say that the different spectral responses between the complementary pairs of valency hybrids to organic phosphate could be due to difference in their quaternary conformations. Possible presence of such many different quaternary structures also suggests that the two structural models are not always adequate to describe the quaternary structures of Hb, as mentioned for the case of the asymmetric hybrid Hbs(Miura & Ho,1982).

In summary, the present NMR results have served to elucidate the different sensitivities to IHP between α and β subunits and gave the additional support for the presence of the "T-like" state in ferric low spin methemoglobins, which means that the quaternary structure of hemoglobins does not always link to the movement of iron displacement into or out of the heme plane.

REFERENCES

Baldwin, J. M. (1975) *Prog. Biophys. Molec. Biol. 29*, 225-320.

Banerjee, R., & Cassoly, R. (1969) *J. Mol. Biol. 42*, 351-361.

Cassoly, R., & Gibson, Q. H. (1972) *J. Biol. Chem. 247*, 7332-7341.

Davis, Charache, S., & Ho. C. (1969) *Pro. Natl. Sci. U.S.A. 63*, 1403-1409.

Edelstein, S. J., & Gibson, Q. H. (1975) *J. Biol. Chem. 250*, 961-965.

Fermi, G. (1975) *J. Mol. Biol. 97*, 237-256.

Fermi, G., & Perutz, M. F. (1977) *J. Mol. Biol. 114*, 421-431.
Fung, L. W. -M., & Ho, C. (1975) *Biochemistry 14*, 2526-2535.
Fung, L. W. -M., Minton, A. P., & Ho, C. (1976) *Pro. Natl. Sci. U.S.A. 73*, 1581-1585
Fung, L. W. -M., Minton, A. P., Lindstrom, T. R., & Ho, C. (1977) *Biochemistry 16*, 1452-1461
Henry, Y., & Banerjee, R. (1973) *J. Mol. Biol. 73*, 469-482.
Hensley, P., Moffat, K., & Edelstein, S. J. (1975a) *J. Biol. Chem. 250*, 9391-9396.
Hensley, P., Edelstein, S. J., Wharton, D. C., & Gibson, Q. H. (1975b) *J. Biol. Chem. 250*, 952-960.
Huang, T. -H. (1979) *J. Biol. Chem. 254*, 11467-11474.
Ikeda-Saito, M., Inubushi, T., & Yonetani, T. (1981) *Methods. Enzymol. 76*, 113-121.
Jonig, G. R., Ruchpaul, K., & Jung, F. (1971) *FEBS Lett. 17*, 173-176
La Mar, G. N., & de Ropp, J. S. (1979) *Biochem. Biophys. Res. Commun. 90*, 36-41.
Massana, C., Cerdonio, M., Shenkin, P., Noble, R. W., Fermi, G., Perutz, R. N., & Perutz, M. F. (1978) *Biochemistry 17*, 3652-3662.
Miura, S., & Morimoto, H. (1980) *J. Mol. Biol. 143*, 213-221.
Miura, S., & Ho, C. (1982) *Biochemistry 24*, 6280-6287.
Monod, J., Wyman, J, & Changeux, J.-P. (1965) *J. Mol. Biol. 12*, 88-118.
Morishima, I., & Hara, M. (1983) *J. Biol. Chem. 258*, 14428-14432.
Nagai, K. (1977) *J. Mol. Biol. 111*, 41-53.
Nagai, K., Hori, H., Yoshida, S., Sakamoto, H., & Morimoto, H. (1978) *Biochim, Biophys. Acta 532*, 17-28.
Neya, S., & Morishima, I. (1980) *Biochem. Biophys. Res. Commun. 92*, 825-832.
Neya, S., & Morishima, I. (1981) *J. Biol. Chem. 256*, 793-798.
Neya, S., Hada, H., & Funasaki, N. (1983) *Biochemistry 22*, 258-264.
Ogawa, S., & Shulman, R. G. (1972) *J. Mol. Biol. 70*, 315-336.
Ogawa, S., Mayer, A., & Shulman, R. G. (1972) *Biochem. Biophys. Res. Commun. 49*, 1485-1491.
Olson, J. S. (1976) *J. Biol. Chem. 251*, 447-458
Perutz, M. F. (1970) *Nature(London) 228*, 726-739.
Perutz, M. F., Lander, J. E., Simon, S. R., & Ho, C. (1974a) *Biochemistry 13*, 2163-2173.
Perutz, M. F., Fersht, A. R., Simon, S. R., & Roberts, G. C. K. (1974b)

Biochemistry 13, 2174-2186.
Perutz, M. F., Heinder, E. J., Lander, J. E., Beetlestone, J. G., Ho, C., & Slade, E. F. (1974c) *Biochemistry 13*, 2187-2200.
Perutz, M. F., Kilmartin, J. V., Nagai, K., Szabo, A., & Simon, S. R. (1976) *Biochemistry 15*, 378-387.
Perutz, M. F., Sanders, J. K. M., Chenery, D. H., Noble, R. W., Pennelly, R. R., Fung, L. W.-M., Ho, C., Gianini, I., Porschke, D., & Winker, H. (1978) *Biochemistry 17*, 3640-3652.
Rein, H., Ristau, O., & Scheler, W. (1972) *FEBS Lett. 24*, 24-26.
Shaanan, B. (1982) *Nature(London) 296*, 683-684.
Shulman, R. G., Hopefield, J. J., & Ogawa, S. (1975) *Quart. Rev. Biophys. 8*, 325-420.
Szabo, A., & Perutz, M. F. (1976) *Biochemistry 15*, 4427-4428.
Viggiano, G., Wiechelman, K. J., Chervenich, P. A., & Ho, C. (1978) *Biochemistry 17*, 795-799.

FIGURE LEGENGS

Figure 1.

Proton NMR spectra of the azide-carboxy valency hybrids, with and without IHP, in 0.05M Bis-Tris at pH 6.5 and 4 °C and 23 °C. A 5 mol of IHP/mol of tetramer was added. Only ferriazide chain give the paramagnetically shifted resonances. Asterisks show the IHP-induced heme methyl resonances.

Figure 2.

Proton NMR spectra of azide-nitrosyl valency hybrids, with and without IHP, in 0.05 M Bis-Tris at pH 6.5 and 4 °C. A 5 mol of IHP/tetramer was added to $(\alpha^{+}_{N_3}\text{-}\beta_{NO})_2$. For $(\alpha_{NO}\beta^{+}_{N_3}\text{-})_2$, the IHP/tetramer ratio was included in figure. Asterisks show the IHP-induced heme methyl resonances.

Figure 3.

Proton NMR spectra of $(\alpha_{NO}\beta^{+}_{N_3}\text{-})_2$ with and without IHP, in 0.05 M Bis-Tris at pH 6.5 and 23 °C. One mol of IHP/tetramer was added. Asterisks show the IHP-induced heme methyl resonances.

Figure 4.

Proton NMR spectra of imidazole-carboxy valency hybrids, with and without IHP, in 0.05 M Bis-Tris at pH 6.5 and 4 °C. A 5 mol of IHP/tetramer was added. Asterisk shows the IHP-induced resonances.

Figure 5.

Hyperfine-shifted proton resonances(left side) and exchangeable resonances(right side) for aquomet-carboxy valency hybrids, with and without IHP, in 0.05 M Bis-Tris at pH 6.0 and 23 °C. A 5 mol of IHP/tetramer was added. Asterisks show the IHP-induced resonances.

Figure 6.

Exchangeable proton resonances of $(\alpha_{NO}\beta^{+}_{N_3}\text{-})_2$, with and without IHP, in 0.05 M Bis-Tris pH 6.5 and 4 °C. One mol of IHP/tetramer was added. Asterisks show the IHP-induced resonances

Table I Resonance Positions of Heme Methyl Groups for Azide and Imidazole Derivatives

Hemoglobins	Resonance Position (ppm)						
HbN_3[a] - IHP		23.0	21.8		17.1	16.1	
HbN_3[a] + IHP	26.3*[b]	23.0	21.8	20.0*	17.1	16.1	15.4*
$(\alpha^{+}_{N_3}\text{-}\beta_{CO})_2$[a] - IHP		23.2			17.4		
$(\alpha^{+}_{N_3}\text{-}\beta_{CO})_2$[a] + IHP		23.5			17.2		
$(\alpha_{CO}\beta^{+}_{N_3})_2$[a] - IHP			21.8			16.1	
$(\alpha_{CO}\beta^{+}_{N_3})_2$[a] + IHP	26.4*		22.0	20.0*		16.4	14.1*[c]
$(\alpha^{+}_{N_3}\text{-}\beta_{NO})_2$[c] - IHP		24.1			17.9		
$(\alpha^{+}_{N_3}\text{-}\beta_{NO})_2$[c] + IHP		24.1			17.7		
$(\alpha_{NO}\beta^{+}_{N_3})_2$[c] - IHP			23.0			17.0	
$(\alpha_{NO}\beta^{+}_{N_3})_2$[c] + IHP	27.4*			22.4*			15.7*
$HbIm$[c] - IHP		28.6	22.5	20.0			14.0
$HbIm$[c] + IHP	31.2*[b]	28.6	22.5	20.1			14.8
$(\alpha^{+}_{Im}\beta_{CO})_2$[c] - IHP		28.7	23.2				14.3
$(\alpha^{+}_{Im}\beta_{CO})_2$[c] + IHP		28.7	23.1				14.1
$(\alpha_{CO}\beta^{+}_{Im})_2$[c] - IHP		28.7		20.6			14.5
$(\alpha_{CO}\beta^{+}_{Im})_2$[c] + IHP	31.2*	28.8		21.0			15.2

[a]Measured at 23 °C. [b]Asterisks show the IHP-induced heme methyl resonances. [c]Measured at 4 °C.

Table II Resonance Positions of Hydrogen Bonded Protons for Valency Hybrid Hemoglobins[a]

Hemoglobins	Resonance Position (ppm)				
HbH_2O - IHP		8.1	7.4		
HbH_2O + IHP	10.1*[b]	8.1	7.4	6.4*	
$(\alpha^{+}_{H_2O}\beta_{CO})_2$ - IHP		8.4	7.5	6.0	
$(\alpha^{+}_{H_2O}\beta_{CO})_2$ + IHP	10.1*	8.2	7.5	5.9	
$(\alpha_{CO}\beta^{+}_{H_2O})_2$ - IHP		8.3	7.6	6.5	
$(\alpha_{CO}\beta^{+}_{H_2O})_2$ + IHP	10.2*	8.3	7.5	6.3	
$(\alpha_{NO}\beta^{+}_{N_3^-})_2$[c] - IHP		8.1	7.2		
$(\alpha_{NO}\beta^{+}_{N_3^-})_2$[c] + IHP	9.3*	8.0	7.4	6.3*	

[a]Measured at 23 °C. [b]Asterisks show the IHP-induced resonances. [c]Measured at 4 °C.

Table III Resonance Positions of Hydrogen Bonded Protons for Native and Hybrid Hemoglobins[a]

Hemoglobins	Resonance Position (ppm)				
oxy Hb		8.3	7.4		R state
deoxy Hb	9.4*	8.3	7.6	6.4*	T state
- IHP		8.1	7.4		R state
metHbH$_2$O					
+ IHP	10.1*	8.1	7.4	6.4*	T state
- IHP		8.1	7.2		R state
($\alpha_{NO}\beta^{+}{}_{N_3}{}^{-}$)$_2$					
+ IHP	9.3*	8.0	7.4	6.3*	T-like state

[a]Measured at 23 °C. [b]Asterisks show the IHP-induced resonances. [c]Measured at 4 °C.

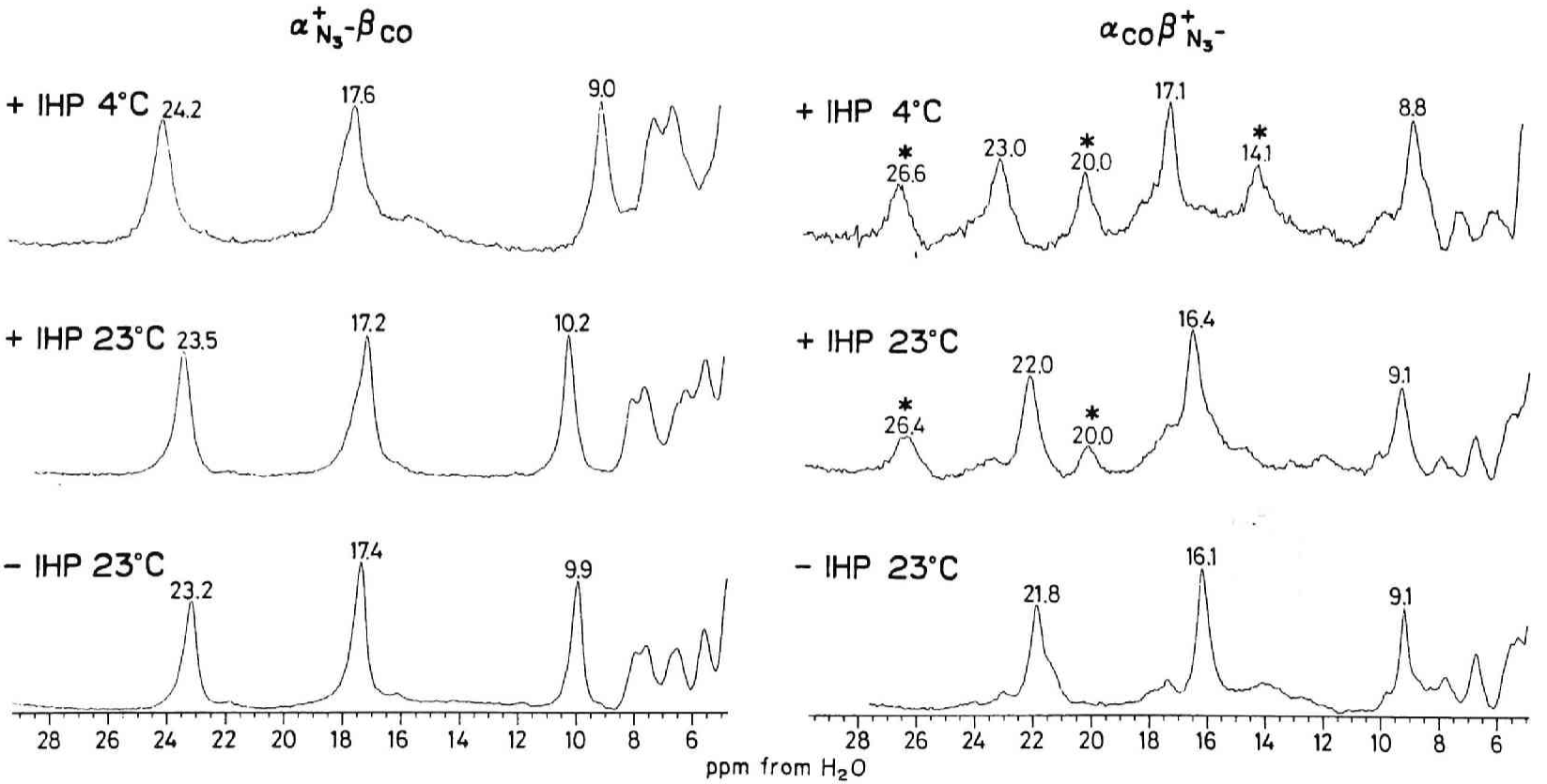
$\alpha^{+}_{N_3}$-β_{CO}
$\alpha_{CO}\beta^{+}_{N_3}$-
+ IHP 4°C
24.2
17.6
9.0
+ IHP 4°C
26.6
23.0
20.0
17.1
14.1
8.8
+ IHP 23°C
23.5
17.2
10.2
+ IHP 23°C
26.4
22.0
20.0
16.4
9.1
- IHP 23°C
23.2
17.4
9.9
- IHP 23°C
21.8
16.1
9.1
28 26 24 22 20 18 16 14 12 10 8 6
ppm from H_2O

Figure. 1

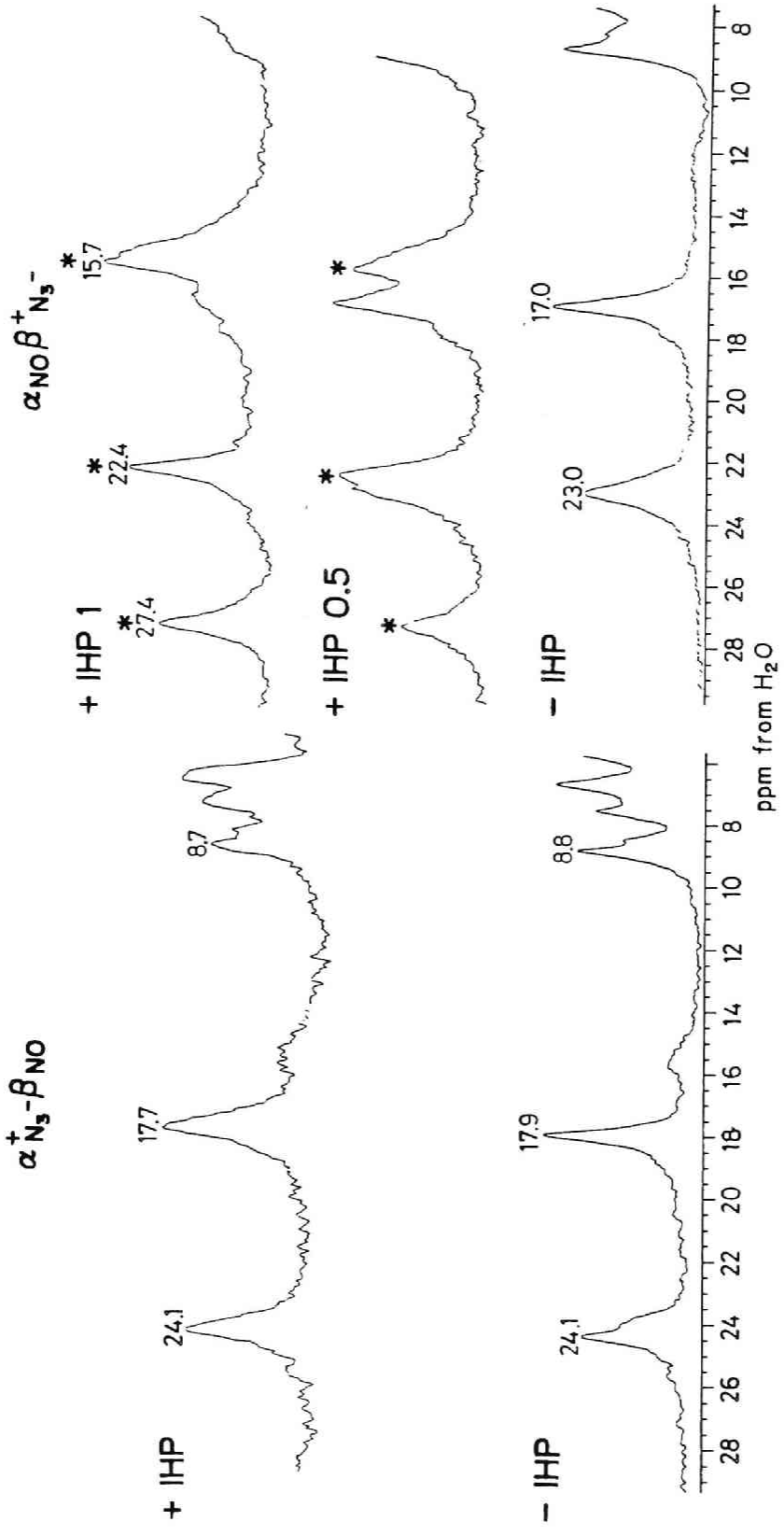
$\alpha^{+}_{N_3}$-β_{NO}
$\alpha_{NO}\beta^{+}_{N_3}$
+ IHP
+ IHP 1
+ IHP 0.5
− IHP
− IHP
24.1
17.7
8.7
27.4
22.4
15.7
24.1
17.9
8.8
23.0
17.0
ppm from H_2O

Figure. 2

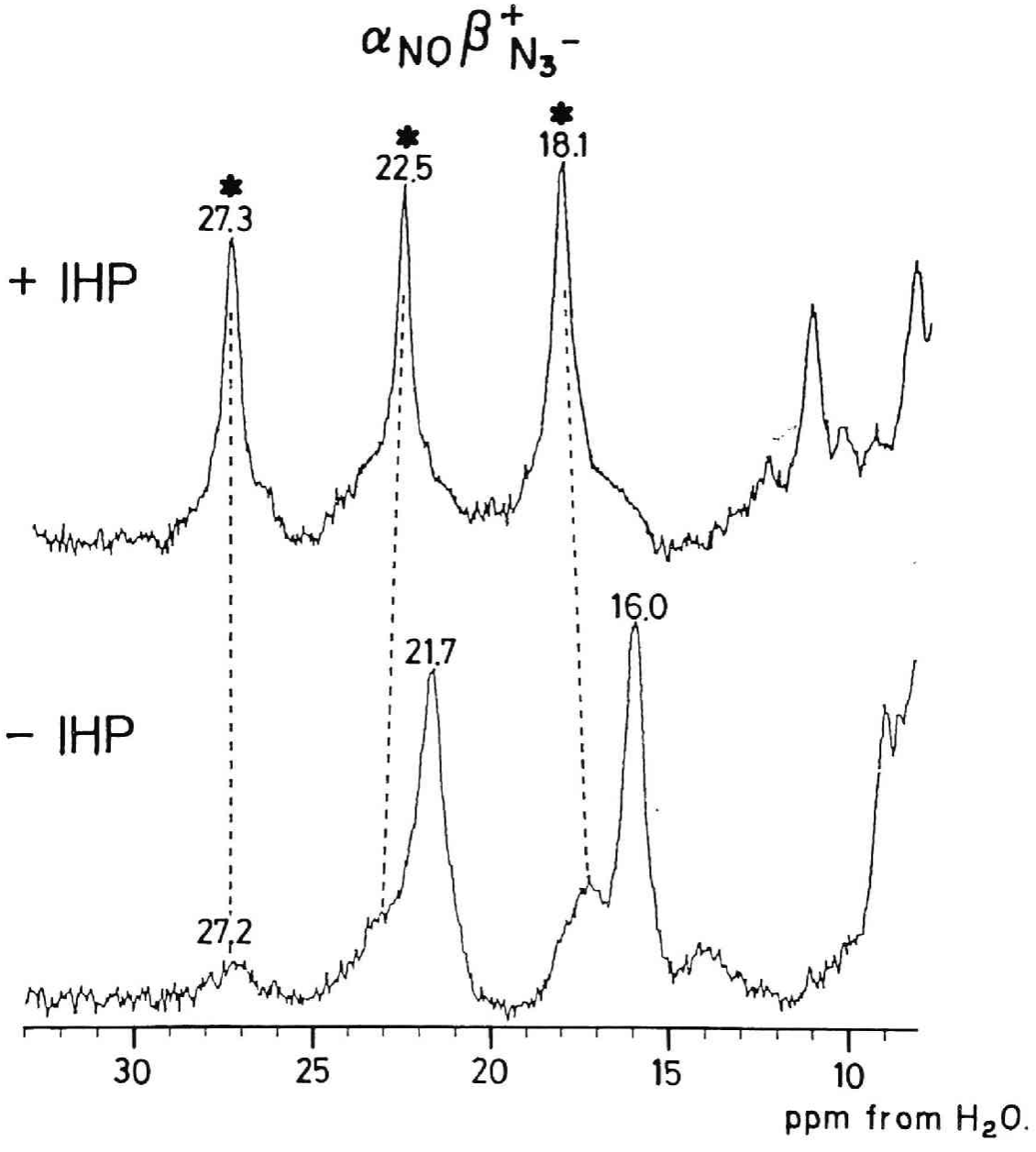
$\alpha_{NO}\beta^{+}_{N_3^-}$
+ IHP
27.3
22.5
18.1
- IHP
27.2
21.7
16.0
30
25
20
15
10
ppm from H_2O.

Figure. 3

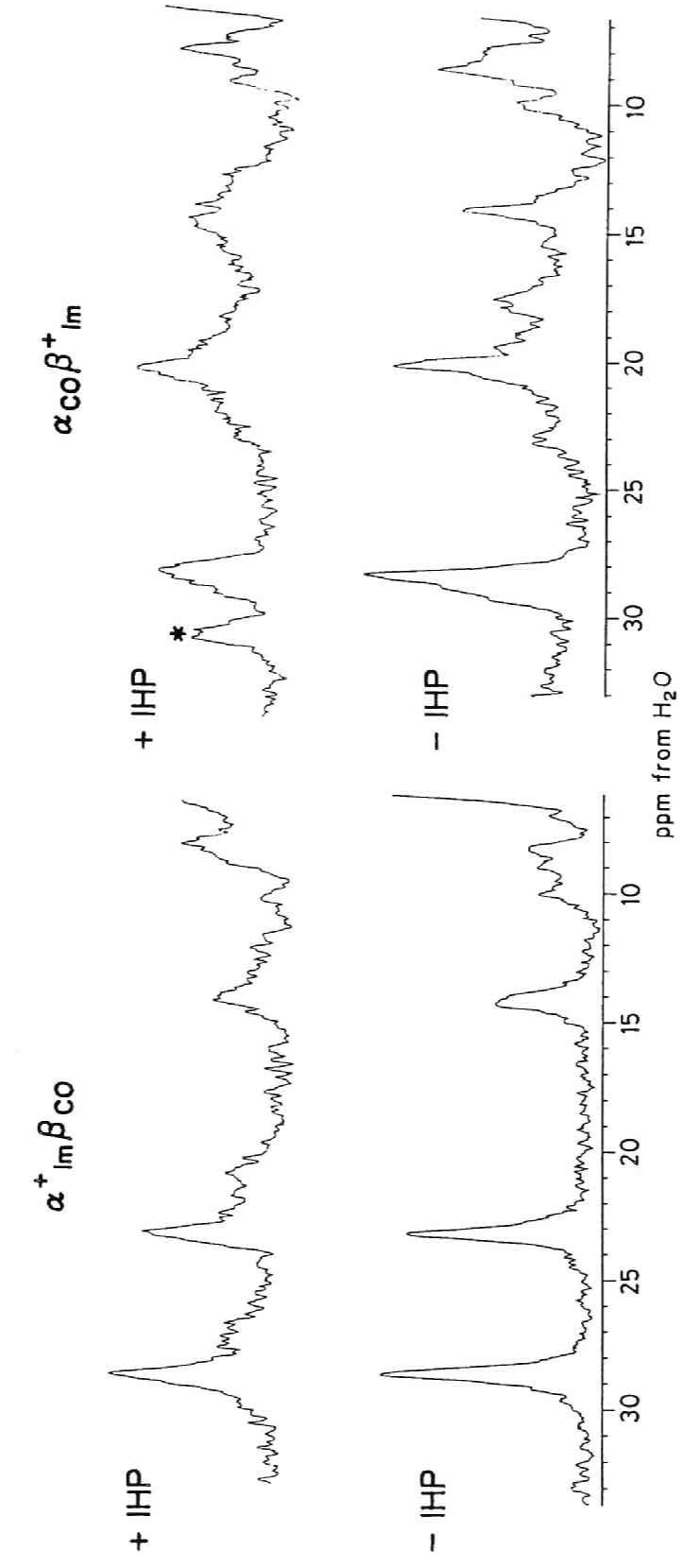
$\alpha^{+}_{Im}\beta_{CO}$
$\alpha_{CO}\beta^{+}_{Im}$
+ IHP
+ IHP
*
- IHP
- IHP
10
15
20
25
30
ppm from H_2O

Figure. 4

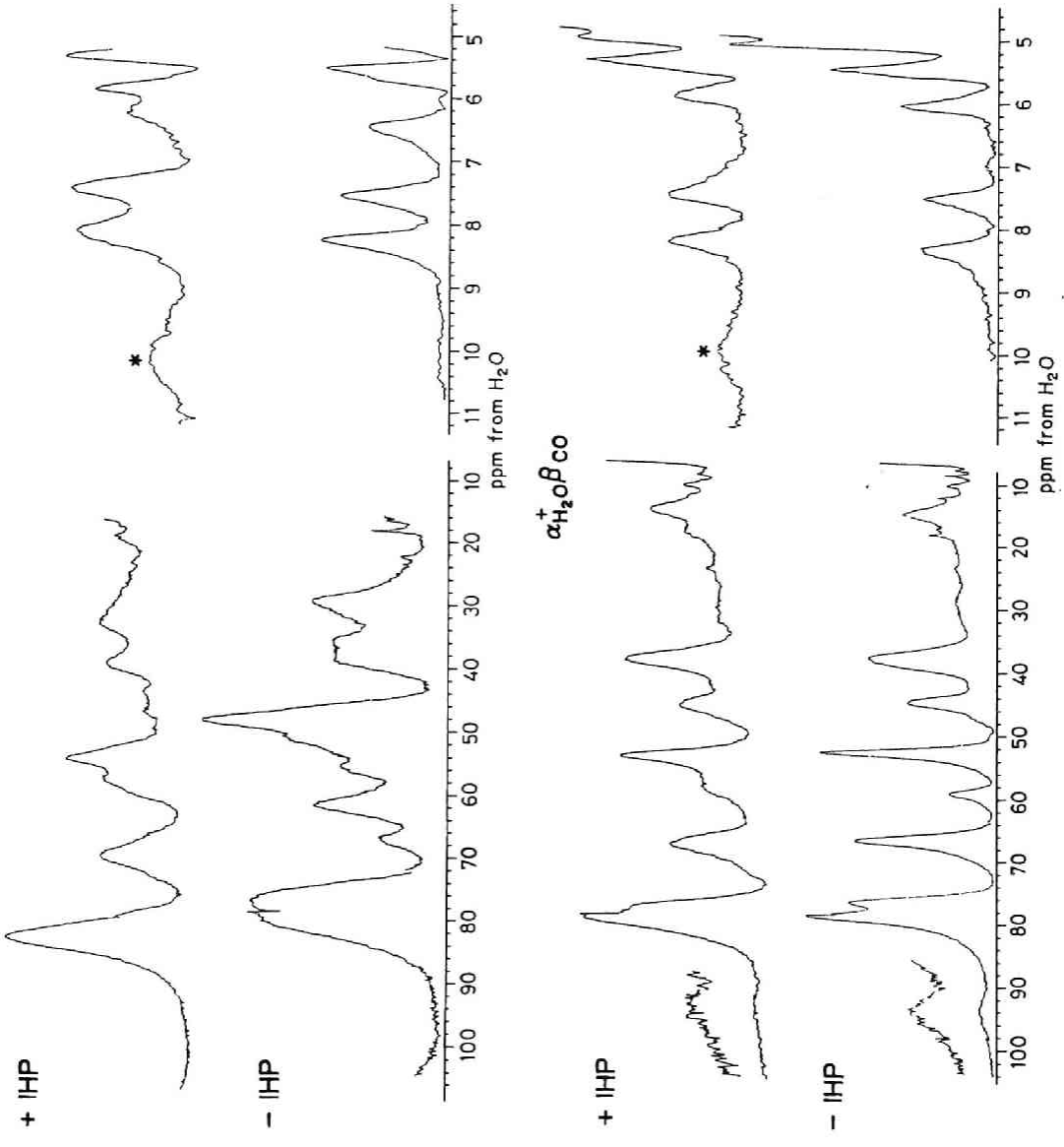

Figure. 5

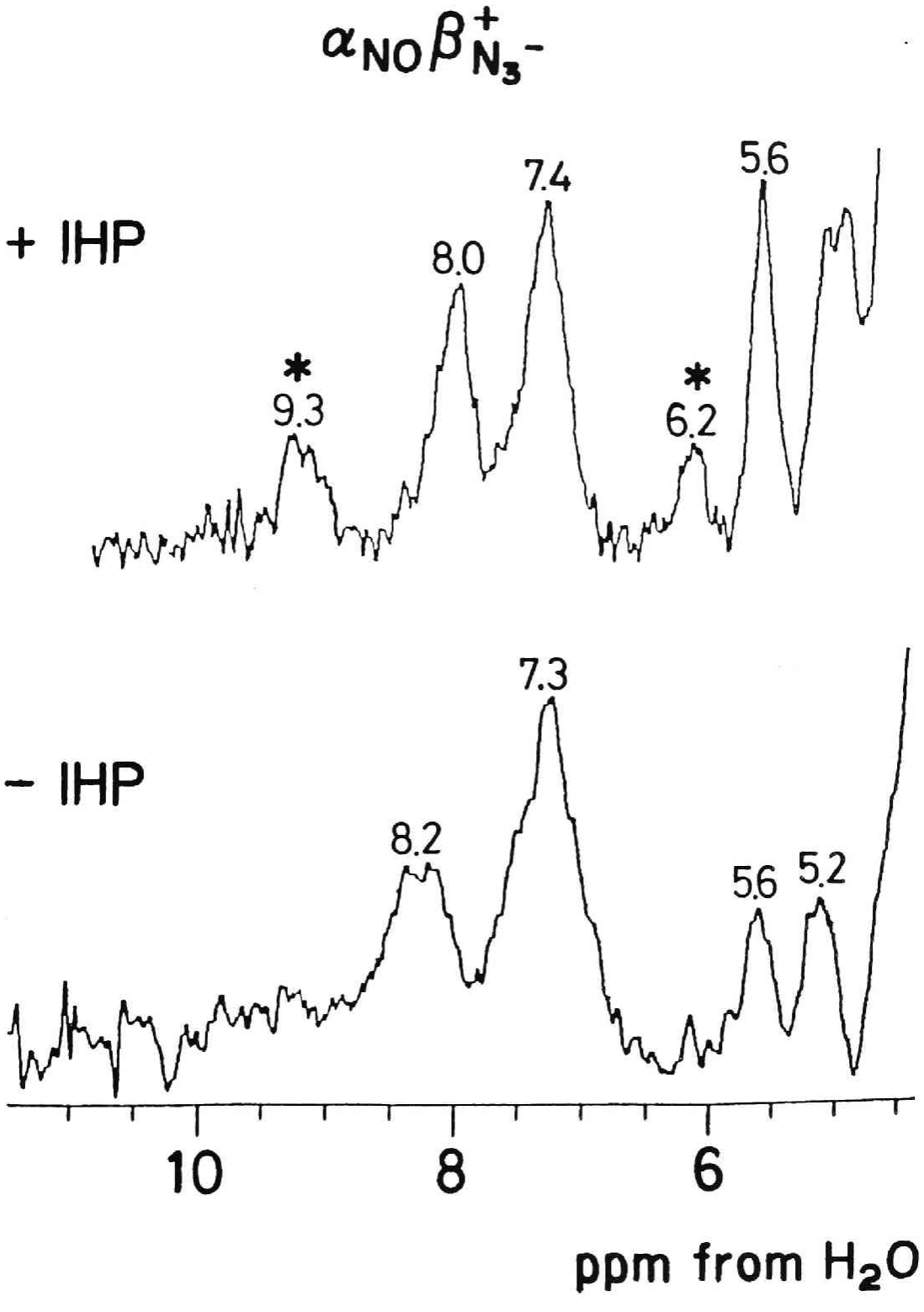
$\alpha_{NO}\beta^{+}_{N_3}$
+ IHP
9.3
8.0
7.4
6.2
5.6
- IHP
8.2
7.3
5.6
5.2
10
8
6
ppm from H_2O

Figure. 6

CHAPTER 2.

NMR Study on IHP Effect for Oxy- and Carbonmonoxy Hemoglobins:

An Evidence for a "Liganded T State".

ABSTRACT: Proton NMR spectra of oxy- and carbonmonoxy hemoglobin with and without IHP (inositol hexakisphosphate) in H_2O were studied with attention to the exchangeable proton resonances due to intra- and intersubunit hydrogen bonds. For oxyhemoglobin, the "R state" marker signal at 5.8 ppm gradually decreases its signal intensity with successive addition of IHP and concomitantly a new exchangeable proton peak grows up at 9.2 ppm, which may correspond to the "T state" marker signal observed at 9.4 ppm for deoxyhemoglobin. This is in accord with the well established result that binding of IHP to ferric high spin hemoglobins and nitrosylhemoglobin shift the R-T equilibrium toward the "T state". Similar tendency was observed for the carbonmonoxy derivative under 1 atm of CO. However, the "T state" maker signal at 6.4 ppm for deoxyhemoglobin which is characteristic of the deoxy tertiary structure did not appear and no significant differences were observed for the signal position of the methyl group of valine E11 in the presence of IHP. Therefore, it is concluded that there exists the R-T equilibrium not only in mutant or modified hemoglobins but also in native ferrous low spin hemoglobins, oxy- and carbonmonoxy hemoglobin, and the binding of IHP can shift the R-T equilibrium toward "T state" to form the "liganded T state" without dissociation of their ligands.

Various physical techniques have been employed to monitor the quaternary structure of Hb[6] derivatives (1-4). In general, the conclusions reached by these techniques are in good agreements. However, contradictory results have recently appeared concerning the quaternary structure of the low spin Hb in the presence of IHP. In ferric high spin Hbs such as aquomet and fluoromet Hb, Perutz and co-workers showed by the use of absorption, CD and NMR spectroscopies and crystallography (5) that the quaternary structure is converted from the "R state[7]" to the "T state" without dissociation of their ligands. Although it is also generally accepted that IHP induces some structural changes in the low spin derivatives, it is still controversial that binding of IHP changes their quaternary structures into the "liganded T state" as found for ferric high spin derivatives. On the basis of the absorption spectra of azide and cyanide met Hb, Perutz et al. (3,6) concluded that IHP alters the structure of the ferric low spin derivatives without changing their quaternary structure to the "T state" and that the "liganded T state" is obtained only for ferric high spin Hbs with the heme iron located out of the heme plane. Fung and Ho (7) also reported that no significant NMR spectral changes of oxy and carbonmonoxy Hb are induced by addition of IHP. However, Neya and Morishima (8,9), Neya et al. (10) and Morishima et al. (11) found by utilizing NMR and UV-visible spectra that the quaternary structure of an IHP-induced new conformer encountered in low spin azidomet Hb and azido-nitrosyl hybrid Hb is analogous to that of the deoxy "T state". They concluded that human low spin met Hbs and hybrid Hb containing ferric low spin hemes are in the R-T equilibrium and can be switched into the "liganded T state" by binding of IHP as the case for ferric high spin derivatives. More recently, Marden et al showed by the use of flash photolysis that all four hemes can bind oxygen or CO ligand in the "T" structure in the presence of IHP and/or Bzf (12).

In order to ascertain whether the structural changes induced by binding of IHP to low spin Hb are quaternary in nature and IHP can generally shift the R-T equilibrium to form the "liganded T state" in Hb, we have re-

---

[6]The abbreviations used are: Hb, hemoglobin; IHP, inositol hexakisphosphate; Bzf, bezafibrate, 2-[4-[2-[(4-chlorobenzoyl)amino]ethyl]phenoxy]-2-methylpropionic acid; Bis-Tris, [bis(2-hydroxymethyl)amino]tris(hydroxymethyl)methane; Tris, tris(hydroxyethyl)aminomethane

[7]As discuss in the later section of this paper, more than two quaternary structures may exist in the course of allosteric ligand binding to Hb. One must be careful in using the "T" and "R state" terminology. In this paper, the term "T state" is used to describe the quaternary structure of fully deoxy Hb A, and "R state" is used to describe the quaternary structure of fully oxy Hb A, respectively.

examined the IHP effect on the quaternary structure of ferrous low spin Hb, oxy and carbonmonoxy Hb, in the presence of IHP with attention to the exchangeable proton resonances arising from the intra- and intersubunit hydrogen bonds. It has been shown that the "T state" marker proton signal at 9.4 ppm in native Hb A arising from the hydrogen bond between α42 Tyr and β99 Asp located at the $\alpha_1\beta_2$ intersubunit plays an important role in the "T" quaternary structure formation. As to aquomet and fluoromet Hb in the presence of IHP, Perutz et al reported that the "T state" marker is observed at 10.1 ppm and concluded that their quaternary structures are in the "liganded T state" (5). On the other hand, some mutant Hbs which lack this hydrogen bond cannot be converted from "R state" to "T state" by deoxygenation (13-15). In this chapter, we wish to show that this "T state" marker is found in the NMR spectra of ferrous low spin Hbs in the presence of IHP and to discuss their quaternary structures.

MATERIALS AND METHODS

Hb A was prepared in the usual manner from fresh whole blood obtained from the local blood bank. After the injection of CO gas, Hb A_{II} and organic phosphates were removed by successive passage through a Sephadex G-25 and a CM-52 column equilibrated with 0.01 M Tris-HCl buffer at pH 7.2. After passage though a Sephadex G-25 equilibrated with 0.01 M Tris-HCl buffer at pH 8.0, Hb A was purified on a DEAE-Sephacel column from which the Hb was eluted with 50 mM Tris-HCl buffer, pH 7.2. Bound CO was removed by the method of Kilmartin & Rossi-Bernardi (16). Spectral measurements were carried out in 50 mM Bis-Tris buffer. All procedures were performed in a cold room (0-5 °C).

Proton NMR spectra at 300 MHz were recorded at 23 °C and 5 °C on a Nicolet NT-300 spectrometer equipped with a 1280 computer system. We used the Redfield 2-1-4 pulse sequence as reported previously (11).

RESULTS AND DISCUSSION

Figure 1 illustrates the exchangeable proton NMR traces of human oxy Hb at various degrees of IHP saturation. It is interesting to note that a signal around 9.2 ppm grows up with successive addition of IHP and that the peak concomitantly appeared at 5.8 ppm gradually decreases its signal intensity. The former signal corresponds to the "T state" marker signal which was previously assigned to the phenolic OH of Tyr-$\alpha_1$42 hydrogen bonded to Asp-$\beta_2$99 and is observed at 9.4 ppm for deoxy Hb (3,7). The latter signal

has been assigned to the "R state" marker signal arising from the intersubunit hydrogen-bonded proton between Asp-$\alpha_1$94 and Asn-$\beta_2$102 (7). In order to confirm the assignment of the peak at 9.2 ppm, nuclear Overhauser effect (NOE) measurement was performed here (result not shown). The NOE difference spectrum resulting from saturating the peak at 9.2 ppm showed that two NOE-enhanced resonances on the phenyl protons of Tyr-$\alpha_1$42 are observed in the aromatic region as found for deoxy Hb A (17).

These hydrogen bonds have been considered to play a key role in the quaternary structural transition. Some mutant Hbs which lack the "T state" marker at 9.4 ppm, such as Hb Yakima (β99 G1 Asp $\rightarrow$ His) (13), Hb Kempsey (β99 G1 Asp $\rightarrow$ Asn) (14), and Hb Radcliffe (β99 G1 Asp $\rightarrow$ Ala) (15), cannot take a "T state" and exhibit the low cooperativity. Hb Titusville (α94 G1 Asp "$\rightarrow$ Asn) (18) and Hb Kansas (β102 G4 Asn $\rightarrow$ Thr) (19), which lack the "R state" marker signal, indicate low oxygen affinity and their quaternary structures seem to be fixed to the "T state". Therefore, the appearance of the "T state" marker, accompanied by decrease of the signal intensity of the "R state" marker for oxy and carbonmonoxy Hb by addition of IHP, can be interpreted as resulting from the quaternary structural change from the "R state" to the "T state".

The "T state" marker for oxy and carbonmonoxy Hb in the presence of IHP is observed at 9.2 ppm, slightly upfield shifted compared with the one for deoxy Hb. Such a slightly upfield shifted T marker signal has also been observed for some deoxygenated globin-modified (4), valency hybrid (11) and reconstituted Hbs (20), implying that the T quaternary structure (the "liganded T state") of oxy- and carbonmonoxy Hb is not exactly the same as the "T state" for native deoxy Hb.

Another "T state" marker at 6.4 ppm for deoxy Hb A was not observed for oxy and carbonmonoxy Hb as shown in Figure 1. This "T state" marker has been assigned to the intrasubunit hydrogen bond (β98 FG5 Val - β145 HC2 Tyr) in the β subunit and is characteristic of the deoxy tertiary structure (21). Therefore, this signal directly represents the structural changes of the $\alpha_1\beta_2$ interface and the lack of the signal at 6.4 ppm suggests that the "T state" structure in the liganded Hb is somewhat different from native deoxy Hb.

Imai (22) reported that the binding of IHP greatly decreases the oxygen affinity and induces the dissociation of oxygen molecule from Hb in the acidic region. Then, the question may arise whether or not the "T state" marker signal results from the partial dissociation of ligand molecule. In order to further confirm the "liganded T state", we also examined the IHP

effect on carbonmonoxy Hb at 1 atm of CO (Figure 2). Under such condition, the IHP-induced dissociation of CO did not occur as confirmed by no UV/vis spectral changes (result not shown). As shown in Figure 2, the "T state" marker appeared at 9.2 ppm as found for oxy Hb. This shows that IHP induces the "liganded T state" in carbonmonoxy Hb and the signal at 9.2 ppm arises from Hb A CO, but not from deoxy Hb A.

Another interesting observation is that the intensity of the "T state" marker increases upon lowering temperature. Previous studies showed that temperature can perturb the equilibrium of the quaternary structures of trout Hb which can be converted to the "T state" in oxygenated form by the Root effect (23), the "T state" being more populated at lower temperature. This observation also lend credence to the result that the "T state" marker at 9.2 ppm corresponds to the "T" quaternary structure.

Lowering temperature causes the Hill plot to shift left (22) and eventually oxygen affinity to enhance. If the "T state" marker at 9.2 ppm arises from the deoxy Hb which is formed by dissociation of ligands upon the binding of IHP to the liganded Hbs, the intensity of the "T state" marker should decrease. This was not the case. It is, therefore, evident that the "T state" marker at 9.2 ppm does not arise from deoxy Hb A.

Since the signal around 6 ppm and the paramagnetic resonances characteristic of deoxy Hb A,(21,24), did not appear for carbonmonoxy Hb in the presence of IHP, we can conclude that the "T state" marker signal at 9.2 ppm arises from the liganded Hb, not from deoxy Hb. Above observation appears to be inconsistent with the previous finding (7) that no NMR spectral changes were induced by binding of IHP to oxy and carbonmonoxy Hb at pH 6.6, which is a bit higher pH than we examined here (pH 6.2). We have carefully reexamined the pH dependence of the 9.2 ppm signal. The intensity of the "T state" marker signal at 9.2 ppm was dependent on pH and this marker signal completely disappeared at pH 7.4. The signal intensity of the "T state" marker was, in fact, substantially reduced at lower pH. Such pH dependence of the "T state" marker signals was also encountered for nitrosyl Hb. Huang (25) found that the T-marker resonances at 9.6 and 6.6 ppm for nitrosyl Hb decrease gradually their intensities as pH is raised. This pH dependence may be associated with that of the IHP effect on the oxygen affinity. Imai (22) reported that the overall free energy of cooperative oxygenation (ΔG_{14}) is little affected by binding of IHP at pH 7.4 (3000 cal/mol to 3080 cal/mol), while at pH 6.5 ΔG_{14} is substantially reduced from 2750 cal/mol to 1260 cal/mol. It should be also

noted that the build-up of the 9.2 ppm resonance was not completed by the equimolar addition of IHP, whereas for human aquo or fluoromet Hb, addition of one mole of IHP per tetramer caused substantial changes in their UV-visible absorption, CD and NMR spectra (26,27). This is attributable to the low affinity of IHP to oxy Hb. In fact, the binding constant of IHP for deoxy Hb and oxy Hb are 2.4×10^7 and 2×10^3, respectively, as reported by et al. (28).

The structural changes in the heme vicinity induced by the binding of IHP can be sensed by the ring current shifted valine E11 methyl signals. As shown in Figure 2, the binding of IHP to oxy Hb induced only a slight broadening of the γ_1-methyl proton resonance. For carbonmonoxy Hb, the γ_1-methyl proton resonance of α and β E11 valine are well resolved in the presence of IHP (5). This implies that binding of IHP does not induce the drastic changes for the heme environmental structure, but it induces only the localized structural changes in the heme environment.

In summary, the present findings show that the binding energy of IHP is enough to change the quaternary structure of oxy and carbonmonoxy Hb, but not sufficient to induce the drastic changes in the heme moiety. In other words, a quaternary structural equilibrium is a general phenomenon in ferrous low spin Hbs and binding of IHP can shift the equilibrium toward the "liganded T state".

REFERENCES

1. Antonini, E., & Brunori, M. (1971) *Hemoglobin and Myoglobin in Their Reaction with Ligands*, North Holland Publishing Co., Amsterdam
2. Schulman, R. G., Ogawa, S., Mayer, A., & Castillo, C. C. (1973) *Ann. N. Y. Acad. Sci.* 22, 9-20.
3. Perutz, M. F., Lander, J. G., Simon, S. R., & Ho, C. (1974) *Biochemistry 13*, 2163-2173.
4. Miura, S., & Ho, C. (1984) *Biochemistry 23*, 2492-2499,
5. Perutz, M. F., Fersht, A., R., Simon., & Roberts, G., C., K. (1974) *Biochemistry 13*, 2174-2186.
6. Perutz, M. F., Kilmartin, J. V., Nagai, K., Szabo, A., & Simon, S. R. (1976) *Biochemistry 15*, 378-387.
7. Fung, L. W. -M. & Ho, C. (1975) *Biochemistry 14*, 2526-2535.
8. Neya, S., & Morishima, I. (1980) *Biochem. Biophys. Res. Commun. 92*, 793-798.

9. Neya, S., & Morishima, I. (1981) J. *Biol. Chem. 256*, 793-798.
10. Neya, S., Hada, H., & Funasaki, N. (1983) *Biochemistry 22*, 258-264.
11. Morishima, I., Hara., M., & Ishimori, K. (1986) *Biochemistry 25*, 7243-7250.
12. Marden, M. C., Kister, B., Bohn, B., & Poyart, C. (1988) *Biochemistry, 27*, 1659-1664.
13. Jones, R. T., Osgood, E. E., Brimhall, B., & Koler, R. D. (1967) *J. Clin. Invest.46*, 1840-1847.
14. Reed, C. S., Hampson, R., Gordon, S., Jones, R. T., Novy, M J., Brimhall, B., Edwards, M. J., & Koler, R. D. (1968) *Blood 31*, 623-632.
15. Weatherall, D. J., Clegg, J. B. Callender, S. T., Wells, R. M. G., Gale, R. E., Huehns, E. R., Perutz, M. F., Viggiano, G., & Ho, C. (1977) *Br. J. Haematol. 35*, 177-191.
16. Kilmartin, J. V. & Rossi-Bernardi. L. (1973) *J. Biol. Chem. 248*, 7039-7043.
17. Russu, I. M., Ho, N. T., & Ho, C. (1987) *Biochim. Biophys. Acta. 914*, 40-48
18. Schneider, R. G., Atkins, R. J., Hostly, T. S., Tomlin, G., Casey, R., Lehmann, H., Lorkin, P. A., & Nagai, K. (1975) *Biochem. Biophys. Acta. 400*, 365-373.
19. Bonaventura, J., & Riggs, A (1968) *J. Biol. Chem. 243*, 980- 991.
20. Ishimori, K., & Morishima, I. (1986) *Biochemistry 25*, 4892- 4898.
21. Viggiano, G., Wiechelman, K. J., & Ho, C. (1978) *Biochemistry 17*, 795-799.
22. Imai, K (1979) *J. Mol. Biol. 133*, 233-247.
23. Brunori, M., Giardina, B., Colosimo, A., Falcioni, G., & Gill, S. (1980) *J. Biol. Chem. 255*, 3841-3843.
24. Takahashi, S., Lin, A. K. -A. C., & Ho, C. (1980) *Biochemistry 19*, 5196-5202.
25. Huang, T. -H. (1979) *Biochemistry 18*, 11467-11474.
26. Fermi, G., & Perutz, M., F. (1977) *J. Mol. Biol. 114*, 421- 431.
27. Linderstrom, T. R., Noren, I. B. E., Charache, S., Lehmann, H., & Ho, C. (1972) *Biochemistry 11*, 1677-1681.
28. Iwaizumi, K., Imai, K., & Tyuma, I. (1979) *J. Biochem. (Tokyo) 86*, 1829-1840.

LEGENDS FOR FIGURES

Figure1.

The proton NMR spectra (300MHz) of native Hb A O_2 with and without IHP, in 0.05 M Bis-Tris at pH 6.2 and 23 °C. The IHP/tetramer ratio was included in the figure. "T" and "R" show the "T" and "R state" marker, respectively.

Figure 2.

The proton NMR spectra (300MHz) of native Hb A O_2 and CO without (A) and with IHP at 23 °C (B), at 5 °C (C) in 0.05 M Bis-Tris at pH 6.2. 2.5 moles of IHP/tetramer was added. "T" and "R" show the "T" and "R state" marker, respectively. "Val E11" shows the resonance of γ_1-methyl group of Val E11 of the α and β subunits.

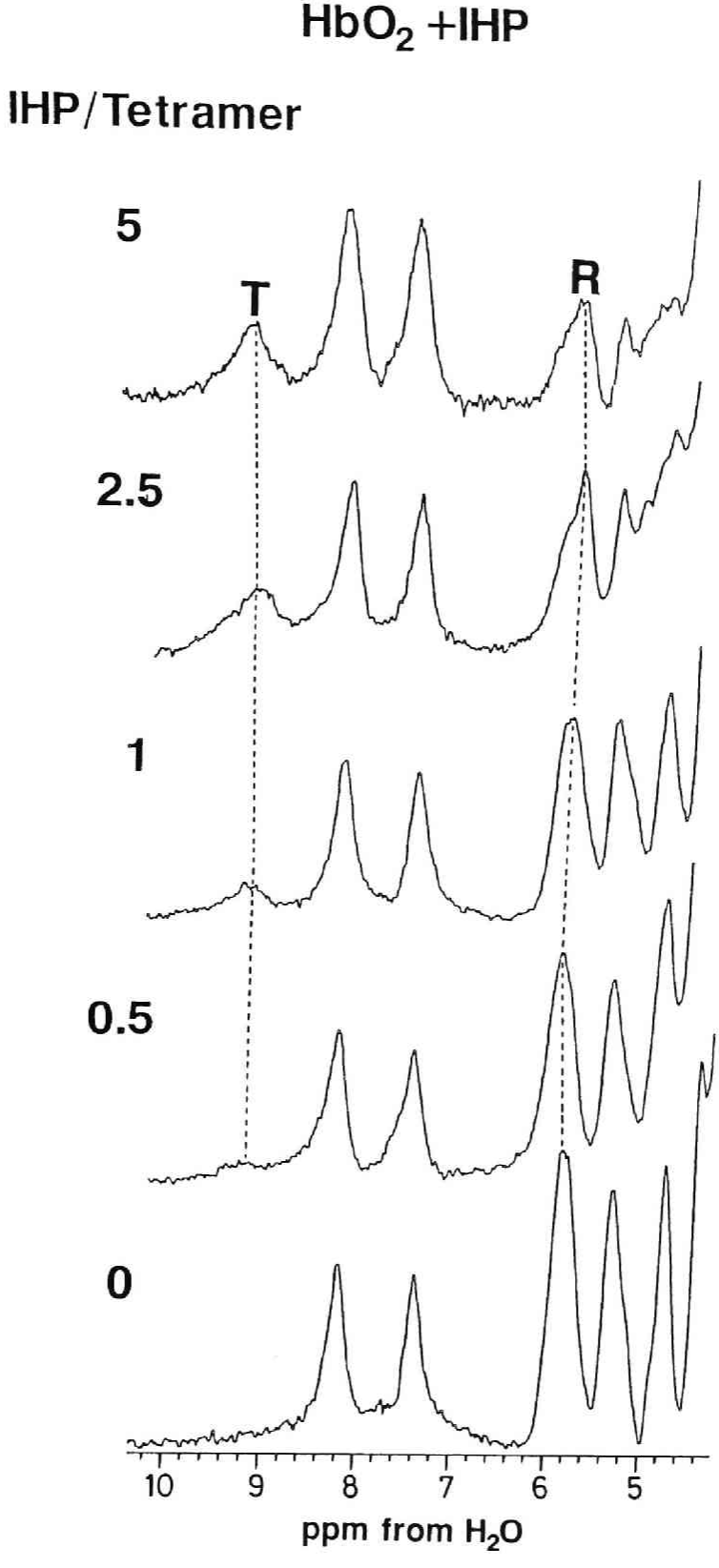

Figure. 1

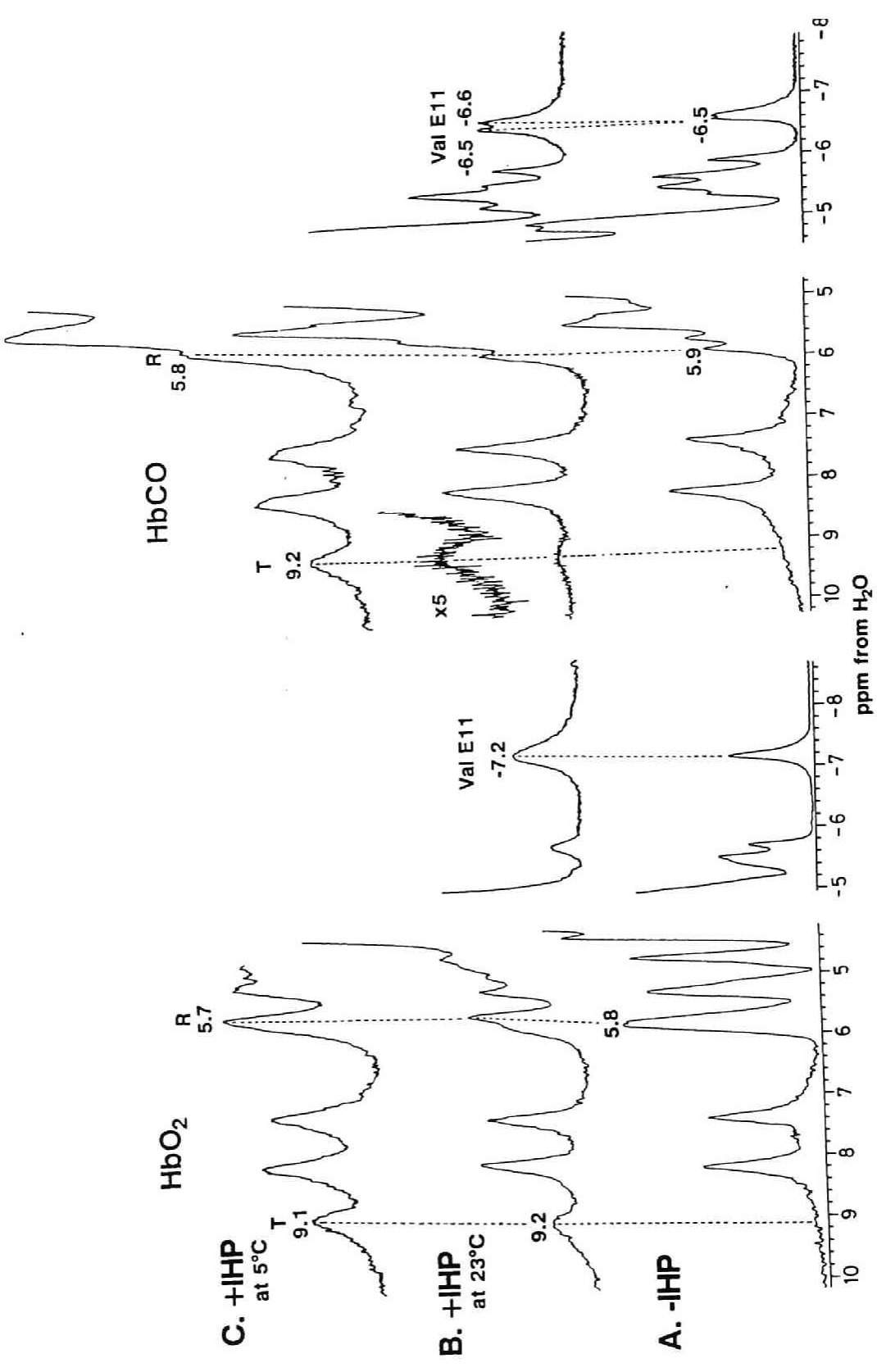
HbO2
HbCO
C. +IHP
at 5°C
B. +IHP
at 23°C
A. -IHP
R
5.7
T
9.1
9.2
5.8
R
5.8
T
9.2
x5
5.9
Val E11
-7.2
Val E11
-6.5 -6.6
-6.5
ppm from H2O

Figure. 2

PART IV.

SITE-DIRECTED MUTAGENESIS OF HUMAN ADULT HEMOGLOBIN

CHAPTER 1.

NMR Study of Human Mutant Hemoglobins Synthesized in *Escherichia coli*.

ABSTRACT: Two artificial human mutant hemoglobins in which a key amino acid residue,α42 (C7) tyrosine (Tyr), was substituted for phenylalanine (Phe) or histidine (His) were synthesized in *Escherichia coli* and their proton NMR spectra were studied with attention to the hyperfine-shifted and hydrogen bonded proton resonances. The hydroxy group of the α42 Tyr is bonded to the carboxylate of the β99 Asp. This hydrogen bond has been considered to be one of the most important hydrogen bonds for the "T-state". However, the native mutation at the 42 (C7) position of the α subunit has not been reported and the role of the tyrosine has not been clear. The site-directed mutagenesis of the α42 Tyr to Phe caused the complete cleavage of this hydrogen bond and revealed that, by the removal of this hydrogen bond, the structure of Hb cannot take the "T-state", but similar to the "R-state", even in the deoxygenated state. Is is rather surprising that the tertiary structure of the β subunit which has no mutation is also similar to the "R-state". On the other hand, the mutation from tyrosine to histidine causes less drastic structural changes and its quaternary and tertiary structure is almost the same as that of native deoxy Hb A. This may be attributable to the formation of a new hydrogen bond between $\alpha_1$42 His and $\beta_2$99 Asp which can compensate the "T-state" marker hydrogen bond between $\alpha_1$42 Tyr and $\beta_2$99 Asp. These observations indicate that the quaternary and tertiary structure of deoxygenated hemoglobin seriously depends on the one specific hydrogen bond in the subunit interfaces.

Expression of cloned genes in appreciate host cell has made it possible to study protein functions by site-directed mutagenesis.[1-5] Studies of hemoglobin (Hb) by this method are of particular interest since it is the only allosteric protein whose structure have been solved to atomic resolution in both the T (tight) and R (relax) states.[6,7] Subunit interaction, binding of various allosteric effectors, and interaction of oxygen with residues in the heme pocket can be studied in detail by introducing various mutations. The effects of such mutations on the electronic state of the heme and mode of ligand binding can be studied spectroscopically.[8] Nagai and co-workers has developed a cleavable fusion protein expression vector to produce α or β-globin in *Escherichia coli* in amounts sufficient for biochemical and X-ray crystallographic studies.[9-11]

In this chapter, we first show some NMR spectra of two mutant Hbs synthesized in *Escherichia coli* to investigate the effect of the hydrogen bond located at the $\alpha_1\beta_2$ subunit interface on the tertiary and quaternary structure of Hb. The hydrogen bonds in subunit interfaces have been considered to be play an important role in maintaining the structure of Hb. Ho and co-worker reported some NMR spectra of native mutant Hbs to assign the resonances of hydrogen bonds and to discuss the relationship of structure and function.[12-13] Of all the hydrogen bonds and salt bridges in the subunit interfaces, the hydrogen bond between $\alpha_1$42 Tyr and $\beta_2$99 Asp has been considered as a key hydrogen bond for the allosteric transition of Hb. Some native mutant Hbs which lack this hydrogen bond such as Hb Yakima (β99 Asp → His)[19], Hb Kempsey (β99 Asp → Asn)[20] and Hb Radcliffe (β99 Asp → Ala)[21] cannot take a "T-state[22]" in the deoxygenated form. Therefore, these mutants exhibit high oxygen affinities and low cooperativities. However, it has not be clear what structural factors of the hydrogen bond induce these functional defects because the point mutation of the α subunit side has not been reported. Thus, we designed new mutant Hbs (α42 Tyr → Phe or His) to get a further insight into the role of this hydrogen bond in the structure of Hb and to discuss the relationship between structure and function of Hb.

In Figure 1, NMR spectra of the oxygenated two mutant Hbs are shown. For native Hb A (Trace C), ring current-shifted proton peak at -7.2 ppm has been assigned to the γ_1-methyl resonance of α and β E11 Val and served as an marker for the tertiary structure around heme vicinity.[15] In downfield region, the peak at 5.9 ppm arises from the hydrogen bond between $\alpha_1$94 Asp and $\beta_2$102 Asn, which has been utilized as an indicator for the "R-state"

quaternary structure.[16] For mutant Hbs (Trace A and B), the corresponding signals were observed at the same position as the native Hb. This indicates that the tertiary and quaternary structures of the oxy form mutants are little perturbed by the amino acid substitution.

Figure 2. illustrates NMR spectra of the two artificial mutant and native deoxy Hbs. The "T-state" marker arising from the hydrogen bond between $\alpha_1$42 Tyr and $\beta_2$99 Asp completely disappeared in mutant A (α42Tyr $\rightarrow$ Phe). The intensity of another "T-state" marker around 6 ppm also reduced concomitant with the amino acid substitution at α42 Tyr. Therefore, the lack of the hydrogen bond between $\alpha_1$42 Tyr and $\beta_2$99 Asp prevents the quaternary structural change from the "R-state" to the "T-state". It should be noticed that the "R-state" marker around 6 ppm also disappeared. This suggests that the mutant A might experience some quaternary structural changes for the deoxygenation, *i.e.* a quaternary transition from the "R-state", but the formation of the normal "T-state" did not occurred.

The mutant A also exhibits the marked spectral differences from that of native Hb A in hyperfine-shifted resonance region (Trace A). The N_1H resonances of its proximal histidine[17] were observed in extremely low field just as the case for the isolated chains.[14] This implies that little strain imposed on the bond between the heme iron and the proximal His of both subunit by deoxygenation.[14] The structural differences between mutant A and native Hb A are also pronounced in the NMR region from 5 to 25 ppm. The hyperfine-shifted resonance pattern of mutant A is similar to that of deoxy des-His(146β)-Arg(141α)-Hb, which is considered to be in the "R-state".[14] It is to be noted that the NMR resonances from the unmodified β subunit are also altered by the amino acid substitution of the α subunit. Therefore, we can conclude that the tertiary structures of *both* subunits of the mutant A are fixed to the "oxy-like" structure. Since the steric hindrance of phenylalanine seems to be almost the same as that of tyrosine, it is unlikely that these alterations come from the steric difference between the two amino acid residues. Above observations indicates the formation of the hydrogen bond between $\alpha_1$42 Tyr and $\beta_2$99 Asp plays a key role not only in forming the "T" quaternary structure but also in increasing the strain between the heme iron and the histidine in *both* subunits, which is characteristic of the deoxy-like tertiary structure.

On the other hand, mutant B (α42Tyr $\rightarrow$ His)exhibits different NMR spectrum from that of mutant A (Figure 2). It is somewhat surprising that,

in spite of the substitution of tyrosine, a small exchangeable proton resonance was observed around 9 ppm where the "T-state" marker would be observed for native deoxy Hb A. Sequence analysis clearly shows that the amino acid residue at the 42 (C7) position of the α subunit is replaced with histidine.[18] This can be interpreted as follows: since histidine has positive charged NH group in its imidazole ring, the NH group is capable of forming a new hydrogen bond to carboxylate ($-COO^-$) of β99 Asp, instead of the hydroxy group of tyrosine.

In hyperfine-shifted portion, the positions of the two histidyl N_1H signals are not perturbed by the amino acid substitution from tyrosine to histidine, except for the slight signal broadening for the N_1H signal of the α subunit. The methyl signal around 18 ppm from the β subunit is also unperturbed, however, the methyl signals from the α subunits are significantly shifted or broadened. Thus, although the substitution of the tyrosine affected localized structural changes in the heme cavity of the α subunit, the tertiary structure of the mutant B, which is manifested by the resonance position of the proximal histidine N_1H and heme methyl group, is almost the same as that of native deoxy Hb A. This suggests that the new hydrogen bond between $\alpha_1$42 His and $\beta_2$99 Asp can fix the α C helix and β G helix to rearrange the tertiary structure of both subunits for the "T-state".

From above discussion, it is clear that the hydrogen bond between $\alpha_1$42 Tyr and $\beta_2$99Asp is essential for the formation of the "T-state" in the deoxygenated state. A complete removal of this hydrogen bond (mutant A; Tyr → Phe) causes a drastic tertiary and quaternary structural changes in the deoxygenated state. The spectrum of this mutant indicates that its tertiary and quaternary structure is not in the "T-state", but similar to the "R-state", even in the deoxy form. On the basis of the oxygen equilibrium curve, mutant A exhibits the extremely high oxygen affinity and hyperbolic curve.[18] This result also shows that the structure of the mutant is fixed to the "R-state" during the oxy- and deoxygenation. On the other hand, for mutant B, the new hydrogen bond between $\alpha_1$42 His and $\beta_2$99 Asp is formed and this bond can be substituted for the "T-state marker" hydrogen bond between $\alpha_1$42 Tyr and $\beta_2$99 Asp. The oxygen equilibrium curve indicates the lower oxygen affinity than mutant A and the significant cooperativity.[18] By this new "T-state" hydrogen bond, the "T-state" in the mutant B is stabilized and its tertiary and quaternary structure can be almost converted to the "T-state" as found for native deoxy Hb A.

In summary, the point mutation of the amino acid residue of the hydrogen

bond located at the subunit interfaces has clearly and directly revealed that the specific hydrogen bond has the critical role in maintaining the structure and the function of Hb. Since it will be more difficult to obtain new native mutant proteins and the mutation is not always satisfied to interests of researchers, the intensive site-directed mutagenesis will need to perform further studies for the purpose of clarifying the relationship between structure and function of proteins.

REFERENCES AND NOTES

(1) Winter, G.; Fersht, A. R.; Willkinson, A. J., Zoller, M.; Smith, M. *Nature (London)* **1982**, *299*, 756-758.

(2) Courtney, M.; Jallet, S.; Tessier, L. -H.; Benavente, A.; Crystal, R. G. *Nature (London)* **1985**, *313*, 149-151.

(3) Rosenberg, S.; Barr, P. J.; Najarian, R. C.; Hallewell, R. A. *Nature (London)* **1984**, *312*, 77-80.

(4) Pielak, G. J.; Mauk, A. G.; Smith, M.; *Nature (London)* **1984**, *313*, 152-154.

(5) Craik, C. S.; Largman, C.; Fletcher, T.; Rocziak, S., Barr, P. J.; Fletterick, R.; Rutter, W. J. *Science* **1985**, *228*, 291-297.

(6) Fermi, G.; Perutz, M. F.; Shaanan, B.; Fourme, R. *J. Mol. Biol.* **1984**, *175*, 159-174.

(7) Shaanan, B. *J. Mol. Biol.* **1983**, *171*, 327-386.

(8) Perutz, M. F.; *Annu. Rev. Biochem.* **1979**, *48*, 327-386.

(9) Nagai, K.; Thogersen, H. C. *Nature (London)* **1984**, *309*, 810-812.

(10) Nagai, K.; Perutz, M. F.; Poyart, C. *Proc. Natl. Acad. Sci. USA.* **1985**, *82*, 7252-7255.

(11) Nagai, K.; Luisi, B.; Shih, D.; Miyazaki, G.; Imai, K.; Poyart, C.; De Young, A.; Kwiatkowsky, L.; Noble, R. W.; Lin, S. -H.; Yu, N. -T. *Nature (London)* **1987** *329*, 858-860.

(12) Fung, L. W. -M.; Ho, C. *Biochemistry* **1975**, *14*, 2526-2535.

(13) Viggiano, G.; Wiechelman, K. J.; Chervenick, P. A.; Ho, C. *Biochemistry* **1978**, *17*, 795-799.

(14) Nagai, K.; La Mar, G. N.; Jue, T.; Bunn, H. F. *Biochemistry* **1982**, *21*, 842-847.

(15) Lindstrom, T. R.; Noren, I. B. E.; Charache, S.; Lehmann, H.; Ho, C. *Biochemistry* **1972**, *11*, 1677-1681.

(16) Takahashi, S.; Lin, A. K. -A. C.; Ho, C. *Biochemistry* **1980**, *19*, 5196-

5202.
(17) La Mar, G. N.; Budd, D. L.; Goff, H. *Biochem. Biophys. Res. Comm.* **1977**, *77*, 104-110.
(18) Imai, K. unpublished data.
(19) Jones, R. T.; Osgood, E. E.; Brimhall, B.; Koler, R. D. *J. Clin. Invest.* **1967**, *46*, 1840-1847.
(20) Reed, C. S.; Hampson, R.; Gordon, S.; Novy, M. J.; Brimhall, B.; Edwards, M. J.; Koler, R. D. *Blood* **1968**, *31*, 623-632.
(21) Weatherall, D. J.; Clegg, J. B.; Callender, S. T.; Wells, R. M. G.; Gale, R. E.; Huehns, E. R.; Perutz, M. F.; Viggiano, G.; Ho, C. *Br. J. Haematol* **1977**, *35*, 177-191.
(22) As discuss in previous papers, more than two quaternary structures may exist in the course of allosteric ligand binding to Hb. One must be careful in using the "T-" and "R-state" terminology. In this paper, the term "T-state" is used to describe the quaternary structure of fully deoxy Hb A, and "R-state" is used to describe the quaternary structure of fully oxy Hb A, respectively.

FIGURE LEGENDS

Figure 1.

The proton NMR spectra (300MHz) of oxygenated mutant A (α42 Tyr → Phe) (A), mutant B (α42 Tyr → His) (B) and native Hb A O_2 (C) in 0.05 M Bis-Tris containing 0.1 M Cl^- at pH 7.4 and 23 °C.

Figure 2.

The proton NMR spectra (300MHz) of deoxygenated mutant A (α42 Tyr → Phe) (A), mutant B (α42 Tyr → His) (B) and native Hb A (C) in 0.05 M Bis-Tris containing 0.1 M Cl^- at pH 7.1 and 23 °C.

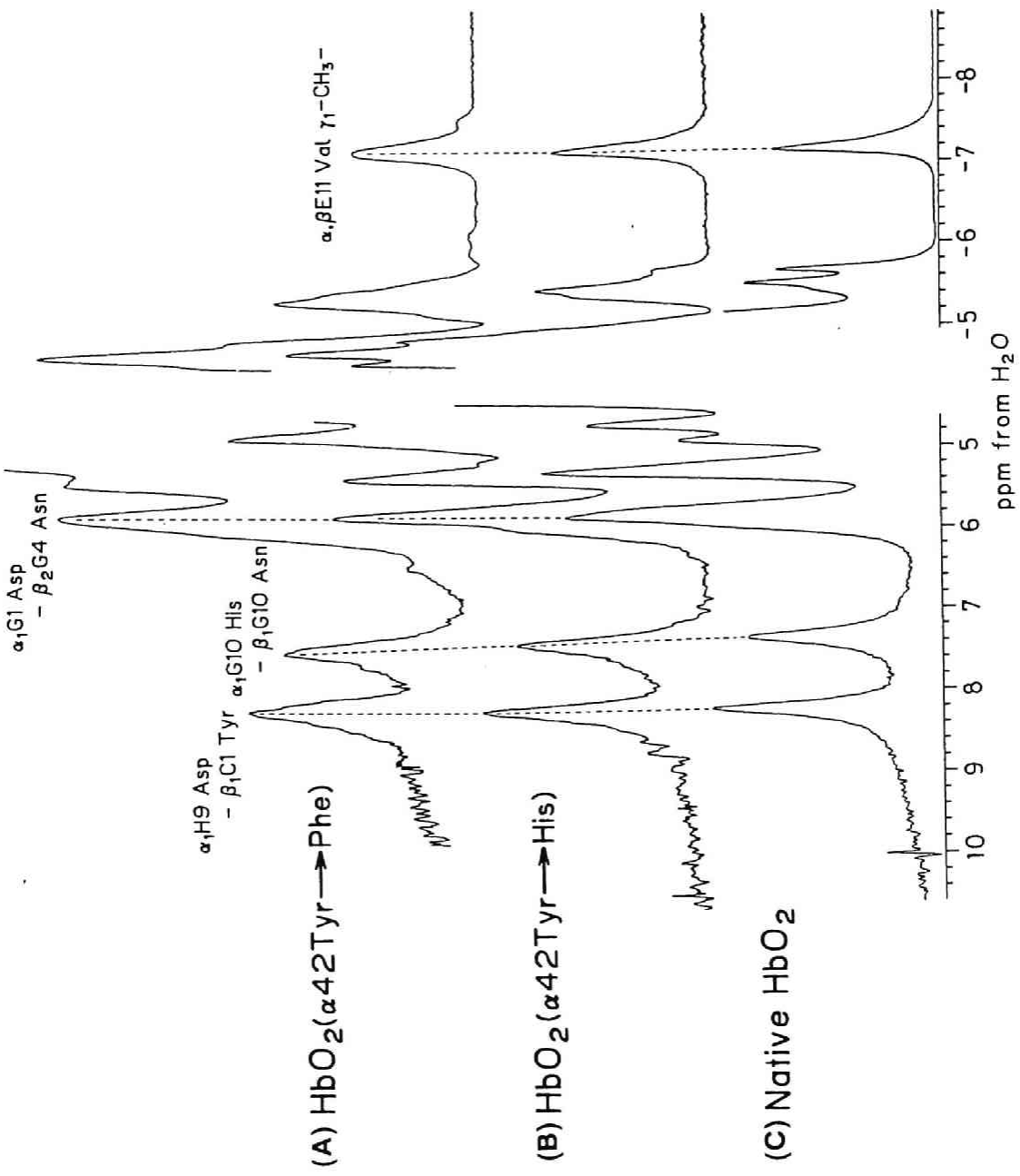
α1G1 Asp
– β2G4 Asn
α1H9 Asp
– β1C1 Tyr
α1G10 His
– β1G10 Asn
α1βE11 Val γ1–CH3–
(A) HbO2(α42Tyr→Phe)
(B) HbO2(α42Tyr→His)
(C) Native HbO2
10
9
8
7
6
5
-5
-6
-7
-8
ppm from H2O

Figure. 1

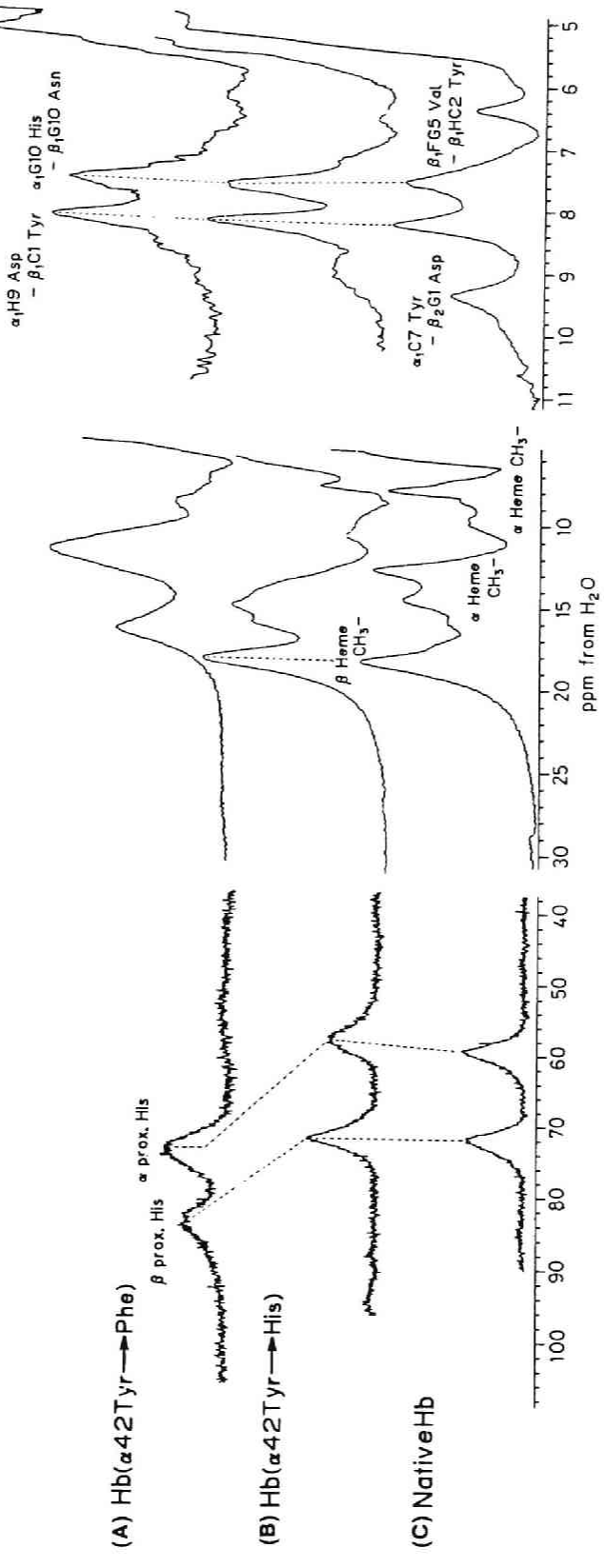
(A) Hb(α42Tyr→Phe)
(B) Hb(α42Tyr→His)
(C) Native Hb
β prox. His
α prox. His
β Heme CH3-
α Heme CH3-
α Heme CH3-
α1H9 Asp - β1C1 Tyr
α1G10 His - β1G10 Asn
α1C7 Tyr - β2G1 Asp
β1FG5 Val - β1HC2 Tyr
ppm from H2O

Figure. 2

PART V.

INTRA- AND INTERMOLECULAR INTERACTION IN HEMOPROTEINS

CHAPTER 1.

NMR Study of Hybrid Hemoglobins Containing Unnatural Heme:

The Effect of Heme Modification on Their Tertiary and Quaternary Structures.

ABSTRACT: The effect of heme modification on the tertiary and quaternary structures of hemoglobins was examined by utilizing the NMR spectra of the reconstituted (mesoHb, deuteroHb) and hybrid heme (meso-proto, deutero-proto) Hbs. The heme peripheral modification resulted in the preferential downfield shift of the proximal histidine N_1H signal for the β subunit, indicating nonequivalence of the structural change induced by the heme modification in the α and β subunits of Hb. In the reconstituted and hybrid heme Hbs, the exchangeable proton resonances due to the *intra*- and *inter*subunit hydrogen bonds, which have been used as the oxy and deoxy quaternary structural probes, were shifted by 0.2 - 0.3 ppm from that of nativeHb upon the β-heme substitution. This suggests that in the fully deoxygenated form, the quaternary structure of the reconstituted Hbs is in an "imperfect" T state in which the hydrogen bonds located at the subunit interface are slightly distorted by the conformational change of the β subunit. Moreover, the two heme orientations are found in the α subunit of deuteroHb, but not in the β subunit of deuteroHb and in both of α and β subunits of mesoHb. The tertiary and quaternary structural changes in the Hb molecule induced by the heme peripheral modification were also discussed in relation to their functional properties.

The cooperative phenomenon, commonly known as the "heme-heme" interaction in hemoglobin (Hb), has been the subject of an intensive research during the past two decades. Despite considerable efforts devoted to the Hb molecule, the detailed molecular mechanism of the cooperative oxygenation of Hb is neither fully understood nor agreed upon by researchers. Comparing the X-ray crystallographic structures of human deoxyHb and oxyhemoglobin-like horse metHb, Perutz (1970) proposed a stereochemical mechanism for the cooperative oxygenation of Hb, in which the correlation between the cooperativity and the R-T quaternary structural transition is emphasized. According to the Perutz's model, the tertiary structural changes take place when a subunit is oxygenated, accompanied by a single concerted quaternary structural R-T transition which is responsible for the cooperativity of the oxygenation process. One of the unsolved problems in the R-T transition mechanism is how the structural change at the heme side is transmitted to the protein and why the changes of tertiary and quaternary structures are induced. Perutz (1970) has suggested the importance of the iron-ligand bond between the proximal histidine F8 imidazole and the heme in controlling the Hb oxygen affinity. Upon oxygenation, the iron atoms in the α and β hemes which are out of the heme plane in deoxyHb move into the centre of the heme plane, thereby "triggering" the tertiary and eventually quaternary structural changes in the Hb molecule.

The heme maintains its relative position in the heme pocket by the coordination and the non-bonding interactions between the heme and the proximal histidine. The characteristic properties of Hb could be also determined by the non-bonding interactions such as van der Waals contacts between the heme and the protein which amount to about 60 within 4 Å of the heme. Some substitutions of amino acid residues in the heme vicinity are known to induce serious functional defects. With the aim to disclose the role of the "non-bonding interactions" in the cooperative oxygenation, a number of investigations of the effect of chemical modification of the heme side chains on the structural and functional properties have been conducted for the reconstituted Hb. Antonini et al.(1959) reported that deuteroHb, which contains deuteroheme (2,4-H) instead of protoheme (2,4-CH_2=CH-), has high oxygen affinity and low cooperativity and that mesoHb containing mesoheme(2,4-CH_3CH_2-) exhibits higher oxygen affinity and lower cooperativity than deuteroHb (Rossi-Fanelli et al.,1959). Recently, a more detailed study of the Hb derivatives reconstituted with the various synthetic hemes was presented by Kawabe et al.(1982). Further, Sugita et al.(1972,

1975; Makino & Sugita,1976) examined functional properties of the Hb derivatives bearing hybrid hemes in the α and β subunits, $\alpha(meso)_2\beta(proto)_2$ and $\alpha(proto)_2\beta(meso)_2$. The most uncompromising problem that we encounter in studying the effect of "non-bonding interactions" on the cooperative phenomenon by utilizing the reconstituted Hbs is the uncertainty of their tertiary and quaternary structures. For example, visible spectra have been examined for the various reconstituted Hb derivatives, but their tertiary and quaternary structural features have not been delineated. The X-ray crystallographic studies for such reconstituted Hbs have not been made due possibly to their unstability. In this sense, the NMR spectral studies are expected to contribute to the structural elucidation of such reconstituted Hbs.

In the present study, we have tried to look at the effect of perturbation of the "non-bonding interactions" exerted by changing the heme peripheral group on the tertiary and quaternary structures of the Hbs by the use of the high resolution proton NMR for deuteroHb, mesoHb, deutero-proto and meso-proto hybrid Hbs. Here we paid much attention to the exchangeable proton resonances due to the *inter-* and *intra*subunit hydrogen bonds, hyperfine shifted resonances for the proximal histidyl N_1H and the ring current-shifted E11 valine methyl signals as well. These resonances are now established to serve as the sensitive probes for tertiary and quaternary structural alterations. The results will be also discussed in relation to the cooperative oxygen affinities for these reconstituted Hbs.

MATERIALS AND METHODS

Human adult Hb was prepared in the usual manner from fresh whole blood obtained from a normal individual. Stripped hemoglobin was obtained by gel filtration on Sephadex G-25 at pH 7.5.(Bermann et al.,1971) Apo Hb was prepared by the treatment of metHb with HCl/MEK (Yonetani,1967) by modifying Teale's method (Teale,1959). Crystalline mesohemin and deuterohemin were dissolved in a minimal volume of 50% pyridine aqueous solution before the recombination experiments. The hematin solution was added dropwise into a stirring solution of apoHb in 10 mM potassium phosphate buffer, pH 7.0. After addition of a small amount of dithionite, the excess hemin, dithionite and pyridine were removed passing through a column of Sephadex G-25 which had previously been equilibrated with 10 mM phosphate buffer, pH 6.5. The reconstituted Hb was purified on a CM-52 column from which the Hb was eluted with 50 mM potassium phosphate

buffer, pH 7.0. All procedures were performed in a cold room (0-5 °C).

The oxygen equilibrium curves of the reconstituted Hbs were determined by the automatic recording method of Imai et al.(1970). The p_{50} and n_{max} values were identical to those previously available (Rossi-Fanelli & Antonini,1959; Rossi-Fanelli et al.,1959; Kawabe et al.,1982).

The isolated α and β chains were prepared by using the method of Gerai et al.(1969). Hybrid Hbs were prepared as reported by Makino & Sugita et al.(1978).

Proton NMR spectra at 300MHz were recorded on a Nicolet NT-300 Spectrometer equipped with a 1280 computer system. Typically, 11-μs (180°) radio frequency pulse and ±36-kHz spectral width were applied to detect the proximal histidine N_1H signal and pyrrole proton for deuteroHb. Conventional WEFT pulse sequence (180°-τ-90° acuire) was used in order to minimize the water signal. A careful setting of τ value (typically 90-100ms) can completely eliminate the H_2O signal under rapid repetition of the sequence; regularly, an interpulse time of about 0.1s was applied. We used the Redfield 2-1-4 pulse sequence with a 28 ~ 29-μs pulse and 8K data points over a 6-kHz spectral width for obtaining proton resonance in the upfield region (ring current-shifted resonances) and in the downfield region (exchangeable proton resonances in the subunits interface). The carrier frequency was in each case placed at 3-kHz upfield and 3.3-kHz downfield from the H_2O resonance. Proton shift were referenced with respect to the water proton signal, which is 4.8ppm downfield from the proton resonance of 4,4-dimethyl-4-silapentane-1-sulfonate (DSS) at 23 °C.

RESULTS

Meso Hemoglobin and Meso-Proto Hybrid Hemoglobins. In Figure 1 are shown the hyperfine shifted proton resonances for deoxy nativeHb (protoHb), mesoHb and their hybrid derivatives. Figure 1D illustrates that deoxy mesoHb in H_2O solution yields two distinct hyperfine shifted proton signals in an extremely low field region at 76.3 ppm and 61.3 ppm. These two peaks were absent under the same pH and buffer conditions in D_2O solution. Similar large downfield paramagnetic shifts have been shown for deoxy nativeHb (Figure 1A) and assigned to the imidazole N_1H proton of the iron-bound proximal histidine F8 (La Mar et al.,1980): these two resonances at 72.1 ppm and 59.5 ppm have been identified as the β and α subunit, respectively (Takahashi et al.,1980). Comparison of the proton NMR spectra between $\alpha^M\beta^P$ ($\alpha(meso)_2\beta(proto)_2$) (Figure 1C) and mesoHb

(Figure 1D) shows that the signal at 76.3 ppm for mesoHb is shifted to 72.0 ppm for $\alpha^M\beta^P$, which is close to the N_1H signal position for the proto β subunits in nativeHb. The signal at 61.5 ppm, which is seen in both mesoHb and $\alpha^M\beta^P$, can be readily assigned to the proximal histidine in the meso α subunit. Therefore, the remaining signal at 76.3 ppm for mesoHb is identified as the N_1H resonance of the meso β subunit. Similar assignment was made by comparing the NMR spectra between $\alpha^P\beta^M(\alpha(\text{proto})_2\beta(\text{meso})_2)$ (Figure 1B) and mesoHb (Figure 1D), as shown in the figure.

Figure 2 illustrates the exchangeable proton resonances for deoxy meso- and meso-proto hybrid Hbs. The peak at 9.4 ppm for deoxy nativeHb($\alpha^P\beta^P$) (Figure 2A) which has been assigned to the *inter*subunit hydrogen bond between α42(C7) tyrosine and β 99(G1) aspartic acid in the $\alpha_1\beta_2$ subunit interface and shown to serve as a deoxy quaternary state marker (T marker) (Fung & Ho,1975), is almost unchanged in its signal position in going from $\alpha^P\beta^P$ to $\alpha^M\beta^P$ (Figure 2B), while it exhibits a 0.2 ppm downfield shift in $\alpha^P\beta^M$ (Figure 2C). A 6.4 ppm resonance (t marker) for nativeHb, which is also characteristic of the deoxy tertiary structure and is assigned to the *intra*subunit hydrogen bond between β98FG5 Val and β145HC2 Tyr (Viggiano et al.,1978), is shifted by 0.1 - 0.2 ppm for the meso- and meso-proto hybrid Hbs. A resonance at 8.3 ppm, which has been assigned to the *inter*subunit hydrogen bond between α126(H8) aspartic acid and β35(C1) tyrosine (Asakura et al.,1976), experiences an upfield shift upon substitution of the β heme, while it is unchanged for the α heme substitution.

In Figure 3 are shown the NMR spectra of meso- and meso-proto hybrid HbO_2 in 50 mM phosphate buffer pH 7.0. For nativeHb, the ring current shifted proton peak at -7.2 ppm which has been assigned (Lindstrom et al.,1972) to the γ_1-methyl resonance of α and β E11 Val is not resolved. For meso Hb (Figure 3D) and their hybrid Hbs (Figure 3B, C), the corresponding signal was observed at the same position as the nativeHb. In the downfield region, a resonance at 8.2 ppm, which was assigned to the proton associated with the hydrogen bond between β135C1 Tyr and α129F9 Asp (Asakura et al.,1976), remains almost unchanged upon the heme substitution. A 5.9 ppm resonance, which has been utilized as an indicator for the oxy-like quaternary structure(Takahashi et al.,1980), is also insensitive to the heme substitution.

Deutero Hemoglobin and Deutero-Proto Hybrid Hemoglobins

Figure 4 illustrates the hyperfine shifted proton spectra of deoxy nativeHb,

deuteroHb and their hybrid Hb derivatives. For deoxy deuteroHb in H_2O (Figure 4D), several resonances appear in the 30 to 75 ppm region. The resonance at 73.2 ppm disappeared and the peak at 60.0 ppm lost its intensity in D_2O. By comparison of the spectra between $\alpha^D\beta^P$ ($\alpha(\text{deutero})_2\beta(\text{proto})_2$) (Figure 4C) and $\alpha^D\beta^D$ (deuteroHb) (Figure 4D), the resonance at 73.2 ppm for deuteroHb in H_2O can be attributed to the N_1H proton of the proximal histidine of the β chain and the 60.0 ppm signal for deoxy deuteroHb to the α subunit.

The remaining signals between 55-35 ppm which are observed for both deutero- and deutero-proto hybrid Hbs are present even in D_2O. On the basis of the relative intensities with respect to the 73.2 ppm peak, these signals are not due to the ring methyl protons of the deuteroporphyrin. Therefore, the signals between 55-35 ppm and the resonance at 60.0 ppm superimposed on the N_1H signal may be assigned to the pyrrole β-protons at 2,4 positions.

In the spectrum of deoxy $\alpha^D\beta^P$, the signals at 54.9, 40.3 and 36.8 ppm may be due to the pyrrole protons at 2,4-positions of the deuteroheme in the α subunit. Since the 59.8 ppm peak has slightly larger intensity than the 72.1 ppm one which has undoubtedly the single proton intensity, the proximal N_1H and 2,4-H peaks for the deutero α subunit appear to be superimposed. It is therefore likely that four one-proton resonances consisting of two sets of 2,4-proton signal are observed in the 35 to 60 ppm region in Figure 4. Jue & La Mar (1984) showed that two sets of resonances found in the spectra of deoxy deuteroHb and deuteroHb$^+CN^-$ arise from the "native" and "disordered" form with the heme rotated 180° about the α-γ-meso axis. However, it seems difficult to determine from the NMR spectra of deoxy deutero-proto hybrid Hb whether deuteroHb has two heme orientations or not. To disclose this problem, we examined the proton NMR spectra of the isolated chains of deoxy deuteroHb (Figure 5) and deuteroHb$^+N_3^-$ (Figure 6). As shown in Figure 5, the NMR spectra for the isolated chains of the deoxy deuteroHb exhibit almost the same spectra as those for deoxy deuteroMb which has previously been shown to have the "heme disorder"(La Mar et al.,1978). This observation implies that the "heme disorder" is found in the isolated chains of deoxy deuteroHb as well as deoxy deuteroMb. However, in the spectrum of deuteroHb$^+N_3^-$ (Figure 6),the resonance from α subunit consists of two sets of signals, whereas β subunit exhibits only one. This may suggest that the orientation of the deuteroheme depends on whether it is embedded in Hb tetramer or in the isolated chains. For the tetrameric

deuteroHb, the heme disorder exists only in the α subunit, not but in the β subunit.

The NMR spectra (Figure 7) of the exchangeable proton resonances for deoxy deutero- and deutero-proto hybrid Hbs in 50 mM Bis-Tris[8] at 23 °C exhibit resonances at about 9.6, 8.3, 7.6 and 6.5 ppm. The substitution of the β heme in nativeHb by the deuteroheme ($\alpha^P\beta^D$) (Figure 7C) results in 0.2 ppm downfield shift of the signal at 9.4 ppm which is characteristic of deoxy quaternary structure in nativeHb, while the α-heme substitution ($\alpha^D\beta^P$) (Figure 7B) experiences only 0.1 ppm upfield shift. A broad resonance at about 6.3 ppm in the spectrum of $\alpha^D\beta^D$ (Figure 7D) and well-resolved signals at about 6.3 ppm for $\alpha^D\beta^P$ and $\alpha^P\beta^D$ could be due to the hydrogen bonded proton in the *intra*subunit of the β chain, by referring the results for the native Hb (Viggiano et al.,1978). This signal is the t state marker which serves as a probe for the deoxygenated tertiary structure.

In the NMR spectra of oxygenated deutero- and deutero-proto hybrid Hbs, the exchangeable proton resonances appear at about 8.2 and 7.4 ppm as shown in Figure 6. The resonance pattern in the 5 to 10 ppm region in Figure 6 is essentially the same as that for nativeHb. Thus, the resonances in this region can be assigned to the *inter*subunit hydrogen bonds for deutero- and deutero-proto hybrid Hbs.

The ValE11 γ_1-methyl protons for deuteroHb exhibit the slightly resolved peaks at -7.2 ppm. This signal splitting may result from the nonequivalence of the heme environment of the α and β subunits, as observed for native HbCO in the presence of IHP (Lindstrom et al.,1972). If this signal splitting is due to two heme orientations in the α subunit as stated above, signal pattern should be much more complicated by the heme disorder for the α subunit and by the α, β nonequivalence. As Figure 8 shows, the resolved two signals exhibit the same intensities, which was more clearly recognized upon the addition of IHP to deuteroHbCO (Morishima & Ishimori, unpublished data). It therefore follows that the Val E11 γ_1-methyl signal in deuteroHb does not sense the heme heterogeneity in the α subunit, but rather responses to the α, β nonequivalence.

All the signal assignments and resonance positions are assembled in Table I, II and III.

DISCUSSION

[8]Abbreviation: Bis-Tris, [bis(2-hydroxyethyl)amino]tris(hydroxymethyl)methane; IHP, inositol hexakis(phosphate).

DISCUSSION

From the present results of the proton NMR spectra of the reconstituted Hbs containing the unnatural heme, it is revealed that the modification of the heme side chains affects the tertiary and quaternary structure of the Hbs.

Tertiary Structure of Reconstituted Hemoglobins. In the deoxy form, the most outstanding feature of the effect of the heme substitution on the proximal histidyl N_1H proton signal in the reconstituted Hbs (Figure 1, Table I) is the preferential downfield shift for the deoxy meso β subunit compared with that for the meso α subunit. This is clearly seen in Figure 1 when the spectrum of the deoxy nativeHb is compared with that of mesoHb. This feature is also found for the hybrid Hbs. As Figure 4 shows, deuteroheme substituted Hbs also experience the similar trend. It thus follows that the modification of the heme side chains in the β subunits exerts a more subtle structural perturbation at the heme proximal side than does the heme side modification in the α subunit. It is also to be noted that the heme substitution in the α and/or β subunit does not appear to affect the heme proximal structure of the complementary subunit. This nonequivalence in the proximal structural changes induced by the heme substitution between the α and β subunits has been also encountered for the Co-substituted Hb and its Co-Fe hybrid Hb derivatives (Inubushi et al.,1983). Substantial difference in the van der Waals contacts in the heme environments between the α and β subunits could be responsible for the present finding.

In the oxygenated form, the Val E11 γ_1-methyl proton signal which serve as a probe for the tertiary structure in the heme distal side exhibits no significant difference between mesoHb, deuteroHb, nativeHb and their hybrid Hbs, except the one for deuteroHb which affords slightly resolved peaks at around -7.2 ppm due to the α, β nonequivalence. This may suggest that the tertiary structure of the oxygenated Hbs is more spacious in the heme vicinity than that of the deoxygenated form, so that the heme substituent hardly exerts the structural perturbation in the heme distal side for the oxygenated Hb.

It is also to be noted that the displacement of the proximal histidine N_1H shift in going from the nativeHb to mesoHb is substantially larger than that in going from nativeHb to deuteroHb. This is somewhat surprising in that a minor chemical modification of the heme vinyl substituents to ethyl groups produces more stereochemical perturbation in the heme proximal side than does the more drastic structural modification at the 2,4-positions for deuteroHb. However, these structural changes seem interesting in relation to

the difference in the functional behaviour of the ferrous forms of these two reconstituted Hbs (Rossi-Fanelli & Antonini,1959; Rossi-Fanelli et al.,1959). MesoHb exhibits pronounced differences in the oxygen-binding properties from nativeHb, while deuteroHb shows the oxygen affinity quite similar to nativeHb. The X-ray structural study of horse metHb reconstituted with deutero- and mesoheme by Seybert & Moffat (1976,1977) showed that numerous small structural changes in the heme environments are seen for met mesohorseHb, while deuterohorseHb experiences only minor and highly localized structural perturbations.

It is quite interesting to find in the present study that the "heme disorder" exists only in the α subunit and a unique heme orientation is maintained in the β subunit for deuteroHb[9]. However, from the X-ray crystallography of aquomet deuterohorseHb (Seybert & Moffat,1976), the heme disorder is not found and deuteroheme combines with the globin with a unique "native" orientation in both α and β subunits. This difference between the results of the X-ray crystallography and that of the present NMR spectra suggests that the conversion from the "disordered" orientation to the "native" orientation could occur with lapse of time or by crystallization of deuteroHb. In fact, the time course spectra of deuteroHbN_3^- showed that the resonances arising from the "disordered" form lose their intensities in time and concomitantly the signals from the "native" orientation form increased (Morishima & Ishimori, unpublished data). Therefore, one should take into account the effect of the heme disorder on the functional properties of deuteroHb. Livingston et al.(1984) reported that the Mb sample containing the "disordered" heme orientation exhibits a higher oxygen affinity. On the other hand, the "heme disorder" is not found for mesoHb, although the heme heterogeneity has been found for meso Mb. It therefore follows that the protein structure of the Hb β subunit is more strictly constructed to accommodate the heme in the native orientation than that of Hb α subunit and that Mb is less strict than Hb for the steric recognition of the heme.

Quaternary Structure of Reconstituted Hemoglobins. As is shown in the NMR spectra of the intersubunit exchangeable proton resonances (Figures.2,3,7, and 8), the quaternary structures of the reconstituted Hbs

---

[9]La Mar et al. (1985) have recently reported that native HbN_3^- experiences ~ 10 % disorder in the β subunit and a single orientation dominates (estimated > 98 %) in the α subunit. The apparent difference in the equilibrium heme disorder between deuteroHb and native Hb could be caused by the change in the steric constraints of the heme periphery, in going from the native to disordered form.

containing the unnatural heme seem similar to those of nativeHb. The resonances at 9.4 and 6.3 ppm in deoxy nativeHb have been shown to serve as the "T marker" signals (Fung & Ho,1975). These signals were also observed in mesoHb, deuteroHb and their hybrid Hbs, although their resonance positions were slightly shifted by 0.2-0.3 ppm from that of nativeHb. This suggests that the heme peripheral modification induces quaternary structural changes in deoxy Hb; that is, these hydrogen bonds are slightly distorted upon the heme substitution. Seybert & Moffat also pointed out on the basis of X-ray crystallography (Seybert & Moffat,1976; 1977) that in the met form of meso- and deuterohorseHbs, the phenolic side chain of α42C7 Tyr moves and some other structural changes occur at the first four residues of the G helix. It has been suggested that the T marker signal at 9.4 ppm in nativeHb arises from the hydrogen bond between α42C7 Tyr - β99G1 Asp which is located at the α_1-β_2 intersubunit and this hydrogen bond plays an important role in the cooperative oxygenation. Some mutant Hbs which lack this hydrogen bond, such as Hb Yakima (β99G1 Asp → His) (Jones et al.,1967), Hb Kempsey (β99G1 Asp → Asn) (Reed et al.,1968; Perutz et al.,1974) and Hb Radcliffe (β99G1 Asp → Ala) (Weatherall et al.,1977), can not take a T state and exhibits the low cooperativity ($n \sim 1.0$). The distortion of the hydrogen bond interferes to form the T state which has low oxygen affinity like deoxy nativeHb. Therefore, it is likely that the deoxy form of the reconstituted Hbs is in an intermediate between the R and T state in nativeHb and it can be concluded that the quaternary structures of the reconstituted Hbs are in an "imperfect" T state even in the fully deoxygenated form.

As shown in Figures.3 and 8, one can find that the difference of the resonance pattern between reconstituted and native Hbs for the oxygenated form is smaller than that for the deoxygenated form. The resonance at 5.7 ppm, which is the R state marker (Fung & Ho,1975), was also observed for reconstituted Hbs. Moreover, the resonances at 8.2 and 7.4 ppm observed for nativeHb are little affected by the heme substitution. These findings imply that the quaternary structure of the reconstituted Hbs in the oxygenated form is more closely similar to that of the nativeHb. Consequently, the structural differences between native and reconstituted Hbs are more distinct in the deoxy state than in the oxy state. We thus conclude that low cooperativity in oxygenation for mesoHb and deuteroHb arises mainly from the distortion of the hydrogen bond in the α_1-β_2 subunit interface, which causes an "imperfect" T state for deoxyHb. The similar

feature has been found in the globin-modified Hbs such as Des-Arg Hb, Des-Arg-Tyr Hb and NES Hb which have low cooperativity and afford the T marker signals with a small shift (0.1-0.2 ppm) (Miura & Ho,1984).

It is also of interest to note that in the deoxygenated form the resonance pattern around 9.4 ppm and 8.3 ppm for $\alpha^{P}\beta^{M}$ is similar to $\alpha^{M}\beta^{M}$ and the one for $\alpha^{M}\beta^{P}$ is rather similar to $\alpha^{P}\beta^{P}$. The same features are also noticed for deutero-proto hybrid Hbs. It is then likely that the quaternary structure of tetrameric deoxy Hb is affected by the structure of the β subunit more effectively than by the α subunit. This phenomenon is also reinterpreted as follows; the tertiary structural change induced by the heme peripheral modification is larger in the β subunit than in the α subunit as shown above. Therefore the structural change in the heme environment of the β subunit is effective enough to slightly distort the hydrogen bond in the *inter*subunit region, whereas that in the α subunit is less effective. It thus follows that the structural change in the heme vicinity induced by the modification of the β heme can propagate to the *inter*subunit region, thereby affecting the quaternary structure of the reconstituted Hbs and such structural change does not occur for the α subunit. As to the functional properties of the hybrid heme Hbs, Sugita et al.(1972) reported the Hill constants (n) for nativeHb ($\alpha^{P}\beta^{P}$) (n = 3.0), $\alpha^{M}\beta^{P}$ (n = 2.6), $\alpha^{P}\beta^{M}$ (n = 1.8) and mesoHb ($\alpha^{M}\beta^{M}$) (n = 1.6). Cooperativity is more effectively influenced by the heme substitution of the β subunit than by that of the α subunit. This appears to parallel with the present results from the NMR studies of the quaternary structures of the hybrid Hbs and that the small difference in the quaternary structure substantially affects the functional properties.

In summary, the perturbation of "non-bonding interactions" between the heme and the globin induces substantial changes of both tertiary and quaternary structures (Figure 9). As to the tertiary structure, the iron-histidine bond is affected in deoxy Hb although in the oxy form no significant structural changes are found by the heme peripheral modification. It has also become clear that the tertiary structural change is different between the α and β subunit in a way that the β subunit is more readily affected by such a perturbation (Figure 9A) and that such structural change in the deoxy β subunit propagates only to the *inter*subunit region and induces slight distortion of the hydrogen bonds (Figure 9C). The quaternary structure of the reconstituted Hbs in the deoxygenated form is in an "imperfect" T state, which is slightly different from the T state of nativeHb. This quaternary structural perturbation arising mainly from the β subunit exerts substantially

large effects on the functional properties such as oxygenation cooperativity. Moreover, the "heme disorder" is confirmed only in the α subunit of deuteroHb. More detailed studies on the "heme disorder" in various Hb derivatives are now under study and will be reported in the forthcoming paper.

REFERENCES

Asakura, T., Adachi, K., Wiley, J. S., Fung, L. W.-M., Ho, C., Kilmartin, J. V., & Perutz, M. F. (1976) *J. Mol. Biol. 104*, 185-195

Bermann, M., Benesch, R., & Benesch, R. E. (1971) *Arch. Biochem. Biophys. 145*, 236-239

Fung, L. W.-M., & Ho, C., (1975) *Biochemistry 14*, 2526-2535

Gerai, G., Parkhurst, L. J., & Gibson, Q. H. (1969) *J. Biol. Chem. 244*, 4664-4667

Imai, K., Morimoto, H., Kotani, M., Watari, H., Hirata, W., & Kuroda, M. (1970) *Biochim. Biophys. Acta. 200*, 189-196

Inubushi, T., Ikeda-Saito, M., & Yonetani, T. (1983) *Biochemistry 22*, 2904-2907.

Jones, R. T., Osgood, E. E., Brimhall, B., & Koler, D. (1967) *J. Clin. Invest. 46*. 1840-1847.

Jue, T. & La Mar, G. N. (1984) *Biochem. Biophys. Res. Commun. 119*, 640-645

Kawabe, K., Imaizumi, K., Yoshida, Z.-I., Imai, K., & Tyuma, I. (1982) *J. Biochem.(Tokyo) 92*, 1713-1722.

LaMar, G. N., Budd, D. L. Viscio, D. B., Smith, K. M., & Langry, K. C. (1978) *Proc. Natl. Acad. Sci. U.S.A. 75*, 5755-5759.

La Mar, G. N., Nagai, K., Jue, T., Budd, D. L., Gersonde, K., Sick. H., Kagimoto, T., Hayashi, A., & Taketa, F. (1980) *Biochem. Biophys. Res. Commun. 96*, 1172-1177

LaMar, G. N., Yamamoto, Y., Jue, T., Smith, K. M., & Pandey, R. K. (1985) *Biochemistry 24*, 3826-3831.

Lindstrom, T. R., Noren, I. B. E., Charache, S., Lehmann, H., & Ho, C., (1972) *Biochemistry 11*, 1677-1681

Livingston, D. J., Davis, N. L., LaMar, G. N., & Brown, W. D. (1984) *J. Am Chem. Soc. 106*, 3025-3026.

Makino, N., & Sugita, Y. (1978) *J. Biol. Chem. 253*, 1174-1178

Miura, S., & Ho, C., (1984) *Biochemistry 23*, 2492-2499

Morishima, I., & Hara, M. (1983) *J. Biol. Chem. 258*, 14428-14432
Perutz, M. F. (1970) *Nature(London) 228*, 726-739
Perutz, M. F., Lander, J. E., Simon,S.R., & Ho, C. (1974) *Biochemistry 13*, 2163-2173
Reed, C. S., Hampson, R., Gordon, S., Jones, R. T., Novy, M. J., Brimhall, B. Edward, M. J., & Kpler, R. D. (1968) *Blood 31*, 623-630
Rossi-Fanelli, A., & Antonini, E. (1959) *Arch. Biochem. Biophys. 80*, 308-317
Rossi-Fanelli, A., Antonini, E., & Caputo, A., (1959) *Arch. Biochem. Biophys. 85*, 37-42
Seybert, D. W., & Moffat, K. (1976) *J. Mol. Biol. 106*, 895-902
Seybert, D. W., & Moffat, K. (1977) *J. Mol. Biol. 113*, 419-430
Sugita, Y., Bannai, S., Yoneyama, Y., & Nakamura, T. (1972) *J. Biol. Chem. 247*, 6092-6095
Sugita, Y. (1975) *J. Biol. Chem. 250*, 1251-1256
Takahashi, S., Lin, A. K.-A. C., & Ho, C. (1980) *Biochemistry 19*. 5196-5202
Teale, F. W. J. (1959) *Biochim. Biophys. Acta. 35*, 543
Viggiano, G., Wiechelman, K. J., Chervenich, P. A., & Ho. C. (1979) *Biochemistry, 17*, 795-799.
Weatherall, D. J., Clegg, J. B., Callender, S. T., Wells, R. M. G., Gale, R. E., Huehus, E. R., Perutz, M. F., Viggiano, G., & Ho, C. (1977) *Brit. J. Haemat. 35*, 177-185
Yonetani, T. (1967) *J. Biol. Chem. 242*, 5008-5013

FIGURE LEGENDS

Figure 1.

Comparison of the paramagnetic proton NMR (300MHz) spectra between nativeHb and mesoHb: (A) deoxy nativeHb, (B) deoxy $\alpha(meso)_2\beta(proto)_2$, (C) deoxy $\alpha(proto)_2\beta(meso)_2$, (D) deoxy mesoHb. All the samples were prepared in 50 mM Bis-Tris buffer at pH 6.5 and 23 °C.

Figure 2.

Comparison of the proton NMR (300MHz) spectra between nativeHb and mesoHb: (A) deoxy nativeHb, (B) deoxy $\alpha(meso)_2\beta(proto)_2$, (C) deoxy $\alpha(proto)_2\beta(meso)_2$, (D) deoxy mesoHb. All the samples were prepared in 50 mM Bis-Tris buffer at pH 6.5 and 23 °C.

Figure 3.

Comparison of the proton NMR (300MHz) spectra between nativeHb and mesoHb: (A) oxy nativeHb, (B) oxy $\alpha(meso)_2\beta(proto)_2$, (C) oxy $\alpha(proto)_2\beta(meso)_2$, (D) oxy mesoHb. All the samples were prepared in 50 mM phosphate buffer at pH 7.0 and 23 °C.

Figure 4.

Comparison of the paramagnetic proton NMR (300MHz) spectra between nativeHb and deuteroHb: (A) deoxy nativeHb, (B) deoxy $\alpha(deutero)_2\beta(proto)_2$, (C) deoxy $\alpha(proto)_2\beta(deutero)_2$, (D) deoxy deuteroHb. All the samples were prepared in 50 mM Bis-Tris buffer at pH 6.5 and 23 °C.

Figure 5.

Downfield hyperfine-shifted portion of the NMR spectra (300MHz) of (A) deuteroMb at 23 °C, (B) deuteroHb β chain at 4 °C and (C) deuteroHb α chain at 23 °C in the deoxy complex form in 50 mM Bis-Tris at pH 6.5.

Figure 6.

Downfield hyperfine-shifted portion of the NMR spectrum (300MHz) of deuteroHb in the met azido complex form, in 50 mM Bis-Tris pH 6.5 and 23 °C. N and D stand for the heme orientation in a native and disordered form, respectively. These assignments were made from the time course

spectral change (see text).

Figure 7.

Comparison of the proton NMR (300MHz) spectra between nativeHb and deuteroHb: (A) deoxy nativeHb, (B) deoxy $\alpha(\text{deutero})_2\beta(\text{proto})_2$, (C) deoxy $\alpha(\text{proto})_2\beta(\text{deutero})_2$, (D) deoxy deuteroHb. All the samples were prepared in 50 mM Bis-Tris buffer at pH 6.5 and 23 °C.

Figure 8.

Comparison of the proton NMR (300MHz) spectra between nativeHb and deuteroHb: (A) oxy nativeHb, (B) oxy $\alpha(\text{deutero})_2\beta(\text{proto})_2$, (C) oxy $\alpha(\text{proto})_2\beta(\text{deutero})_2$, (D) oxy deuteroHb. All the samples were prepared in 50 mM phosphate buffer at pH 7.0 and 23 °C.

Figure 9.

Schematic representations of the present results of the reconstituted Hbs. (A) The heme modification induces the quaternary structural change more effectively in the β subunit than in the α subunit. (B) The quaternary structures of the reconstituted Hbs are closely similar to that of the nativeHb, although their deoxy quaternary structures are in an "imperfect" T state. (C) The heme environmental structural change induced by the modification of the β-heme peripheral substituent propagates to the subunit interface.

Table I: Resonance Positions of the F8 Histidine N_1H for Reconstituted Hemoglobin and Their Assignments

	resonance position(ppm)	
	α subunit	β subunit
MesoHb ($\alpha^M\beta^M$)	61.3	76.3
$\alpha^M\beta^P$	61.5	72.0
$\alpha^P\beta^M$	59.6	76.2
DeuteroHb ($\alpha^D\beta^D$)	60.0	73.2
$\alpha^D\beta^P$	59.8	71.5
$\alpha^P\beta^D$	59.2	73.0
ProtoHb (NativeHb)	59.5	72.1

Table II: Resonance Positions of the Exchangeable Proton of Hydrogen Bonds for Deoxygenated Reconstituted Hemoglobin and Their Assignments

	resonance position (ppm)				
MesoHb	9.6	8.2	7.5	6.3	
$\alpha^M\beta^P$	9.3	8.3	7.5	6.2	
$\alpha^P\beta^M$	9.6	8.1	7.4	6.3	
DeuteroHb	9.6	8.2	7.5	6.6	6.3
$\alpha^D\beta^P$	9.5	8.3	7.6	6.4	6.1
$\alpha^P\beta^D$	9.6	8.2	7.4	6.6	6.4
ProtoHb	9.4	8.3	7.6	6.4	
assignment	α42C7 Tyr -β99G1 Asp	α126H8 Asp -β35C1 Tyr	_____	β98FG5 Val -β145HC2 Tyr	

Table III: Resonance Positions of the Exchangeable Proton of Hydrogen Bonds for Oxygenated Reconstituted Hemoglobin and Their Assignments

	resonance position (ppm)				
MesoHb	8.1	7.4	5.7	-7.2	
$\alpha^{M}\beta^{P}$	8.1	7.3	5.6	-7.2	
$\alpha^{P}\beta^{M}$	8.1	7.3	5.7	-7.2	
DeuteroHb	8.1	7.4	5.8	-7.1	-7.2
$\alpha^{D}\beta^{P}$	8.2	7.4	5.7	-7.2	
$\alpha^{P}\beta^{D}$	8.3	7.5	5.8	-7.2	
ProtoHb	8.2	7.4	5.8	-7.2	
assignment	α126H8 Asp -β35C1 Tyr	_____	α94G1 Asp -β102HC2 Tyr	E11 Val	

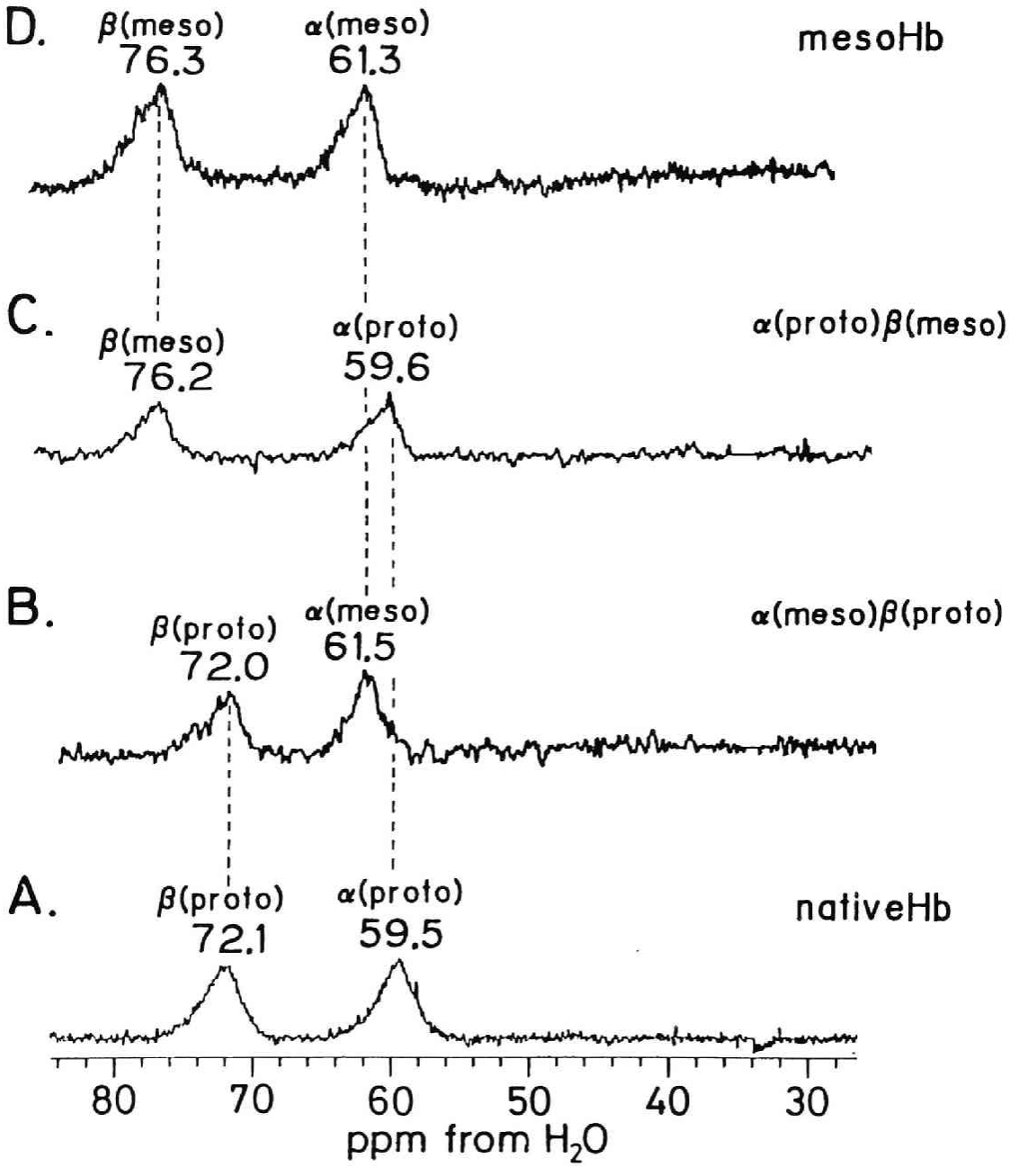
D.
β(meso)
76.3
α(meso)
61.3
mesoHb
C.
β(meso)
76.2
α(proto)
59.6
α(proto)β(meso)
B.
β(proto)
72.0
α(meso)
61.5
α(meso)β(proto)
A.
β(proto)
72.1
α(proto)
59.5
nativeHb
80
70
60
50
40
30
ppm from H2O

Figure. 1

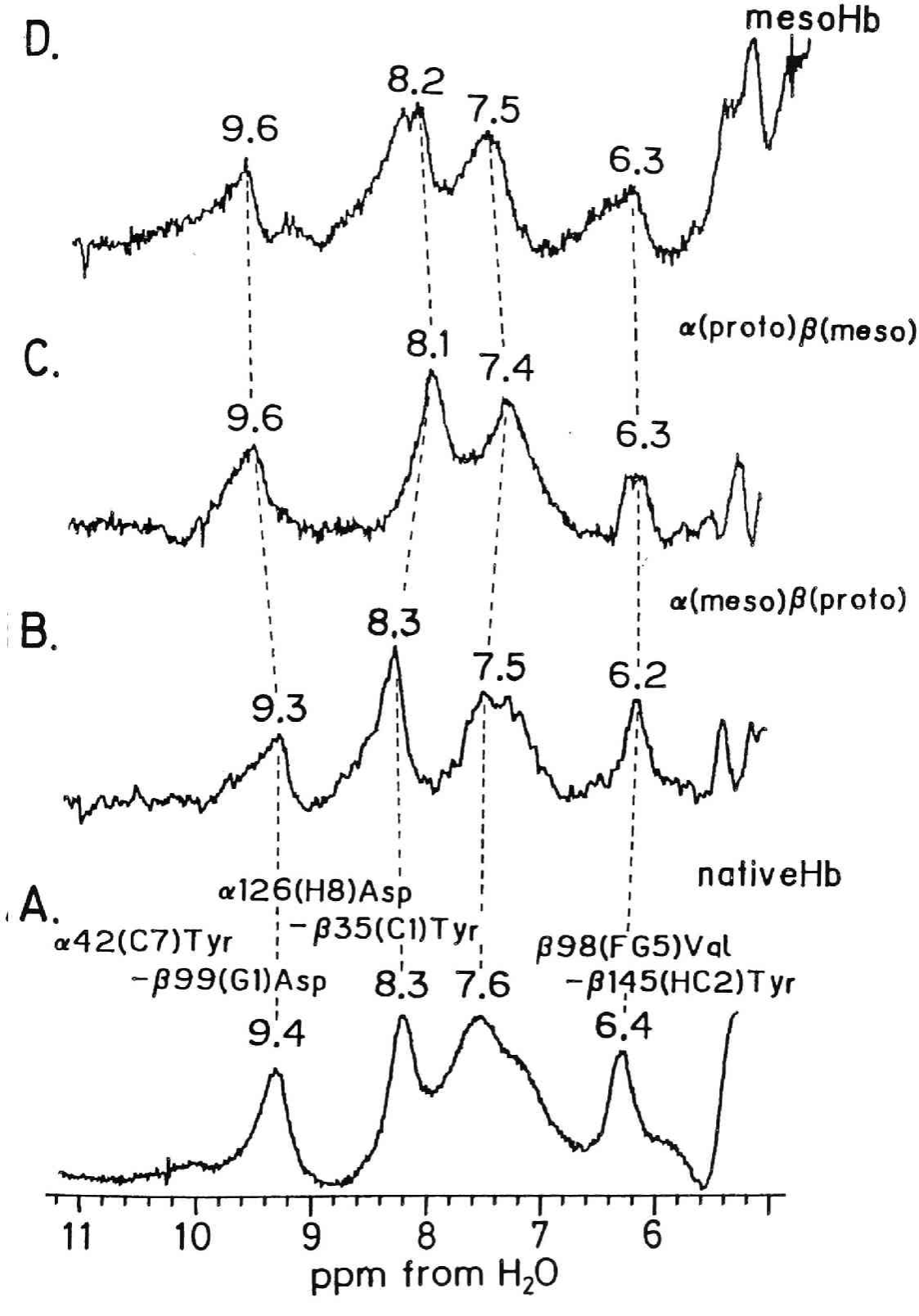
D.
mesoHb
9.6
8.2
7.5
6.3
α(proto)β(meso)
C.
8.1
7.4
9.6
6.3
α(meso)β(proto)
B.
8.3
7.5
6.2
9.3
nativeHb
A.
α126(H8)Asp
−β35(C1)Tyr
α42(C7)Tyr
−β99(G1)Asp
β98(FG5)Val
−β145(HC2)Tyr
8.3
7.6
9.4
6.4
11
10
9
8
7
6
ppm from H2O

Figure. 2

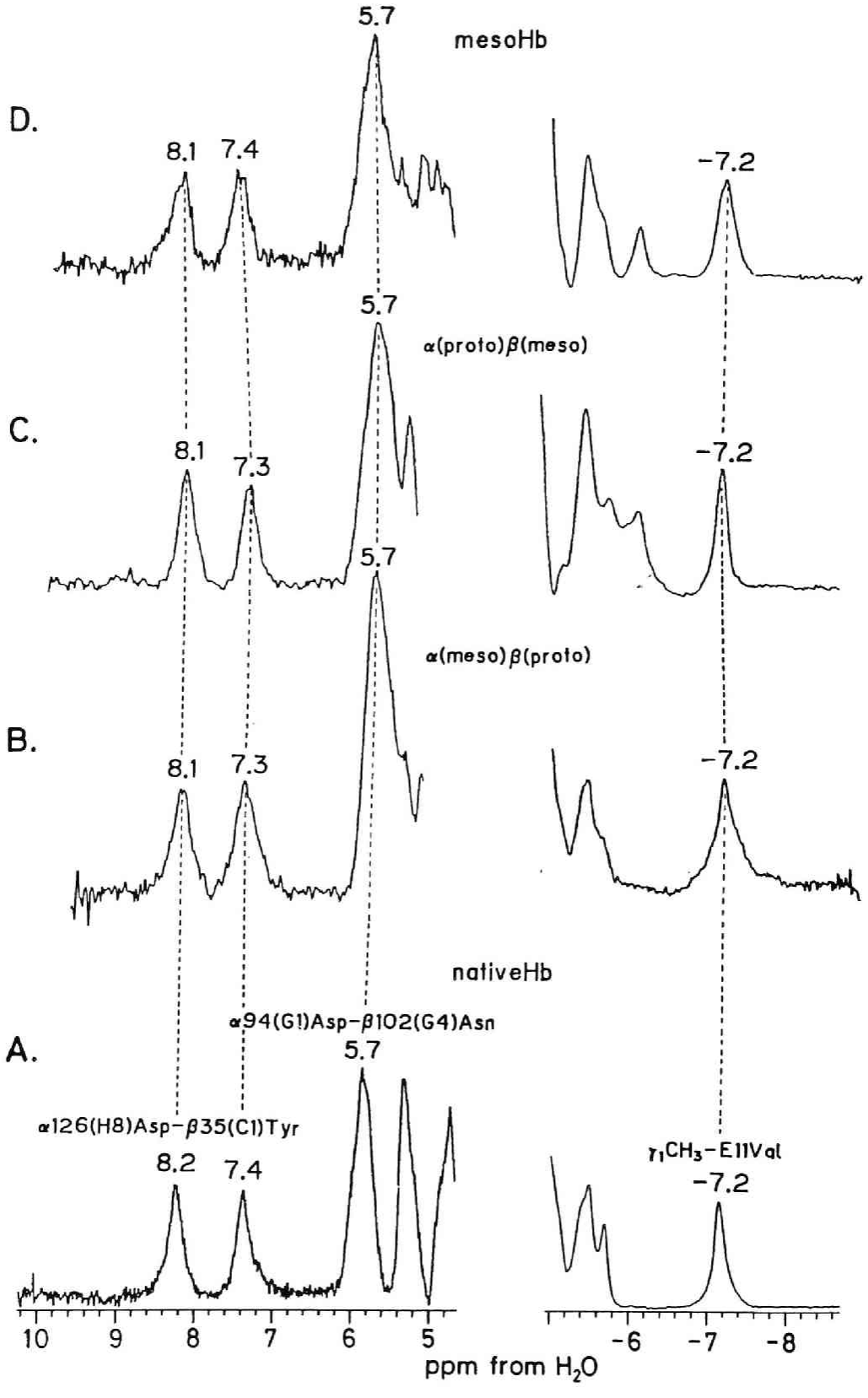
5.7
mesoHb
D.
8.1
7.4
-7.2
5.7
α(proto)β(meso)
C.
8.1
7.3
-7.2
5.7
α(meso)β(proto)
B.
8.1
7.3
-7.2
nativeHb
α94(G1)Asp–β102(G4)Asn
A.
5.7
α126(H8)Asp–β35(C1)Tyr
8.2
7.4
γ1CH3–E11Val
-7.2
10
9
8
7
6
5
-6
-7
-8
ppm from H2O

Figure. 3

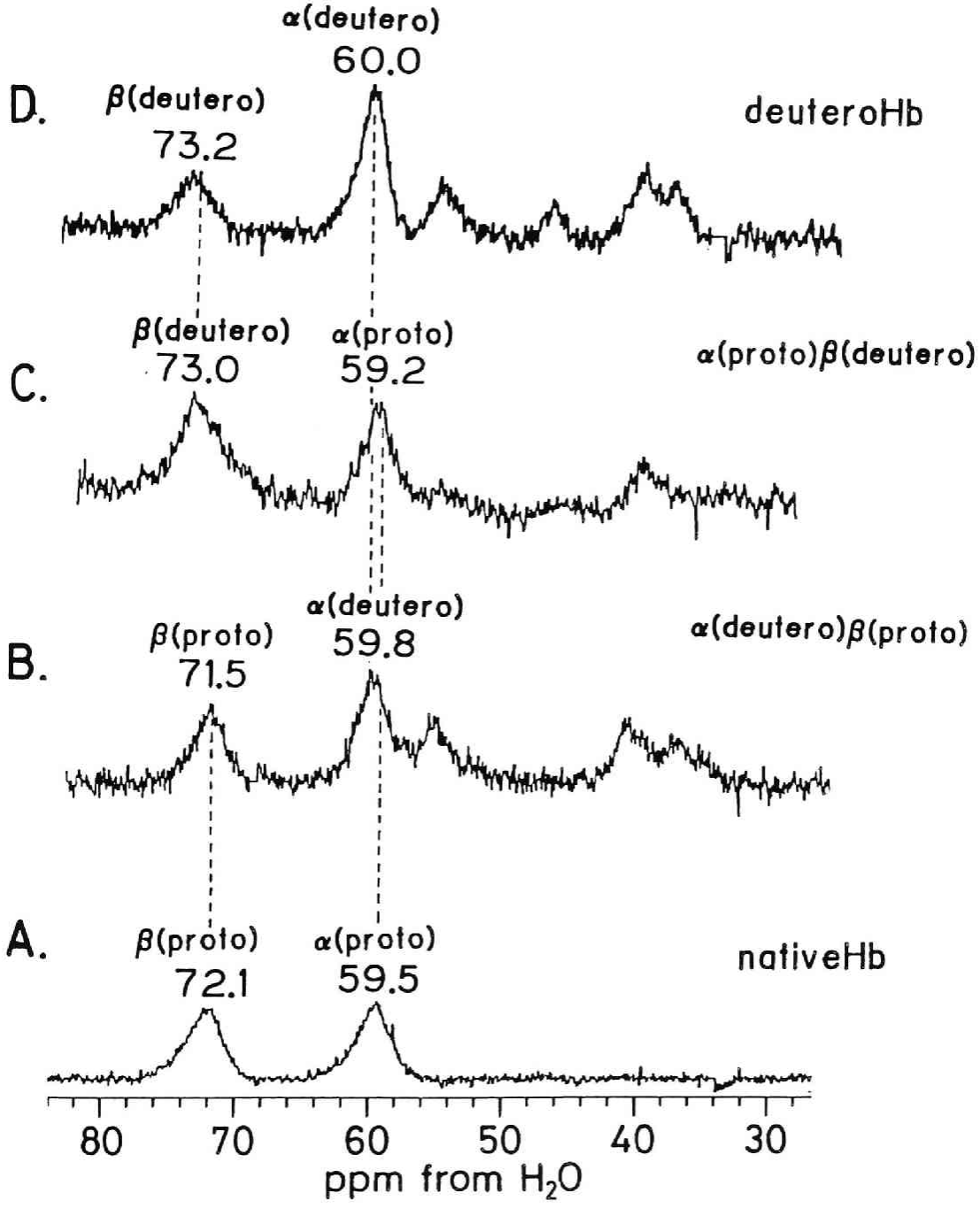
α(deutero)
60.0
D.
β(deutero)
73.2
deuteroHb
β(deutero)
73.0
α(proto)
59.2
C.
α(proto)β(deutero)
α(deutero)
59.8
β(proto)
71.5
B.
α(deutero)β(proto)
β(proto)
72.1
α(proto)
59.5
A.
nativeHb
80
70
60
50
40
30
ppm from H2O

Figure. 4

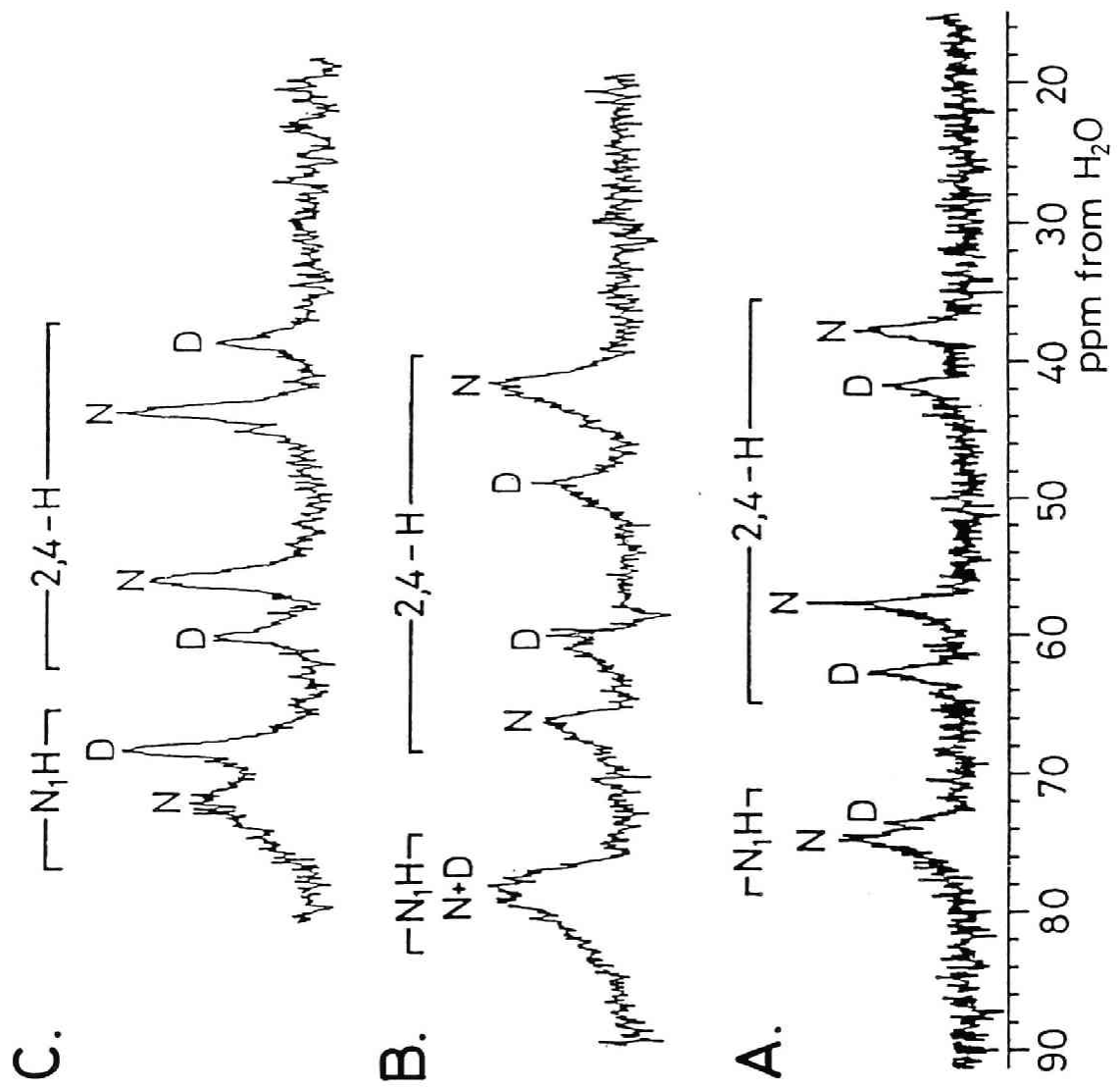
C.
N,H
2,4-H
D
N
D
N
D
B.
N,H
N+D
2,4-H
N
D
N
D
A.
N,H
2,4-H
N
D
N
D
90
80
70
60
50
40
30
20
ppm from H2O

Figure. 5

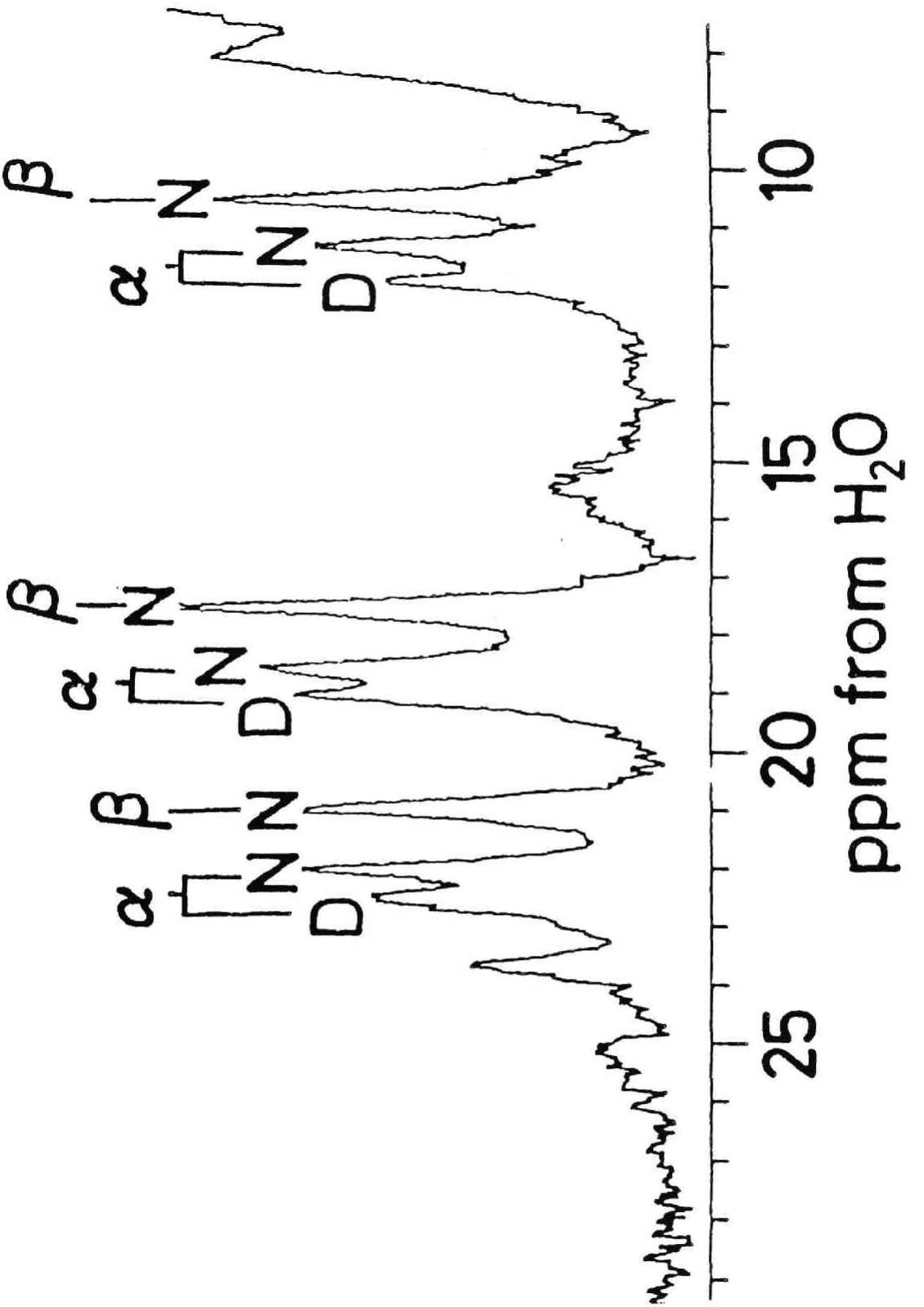

Figure. 6

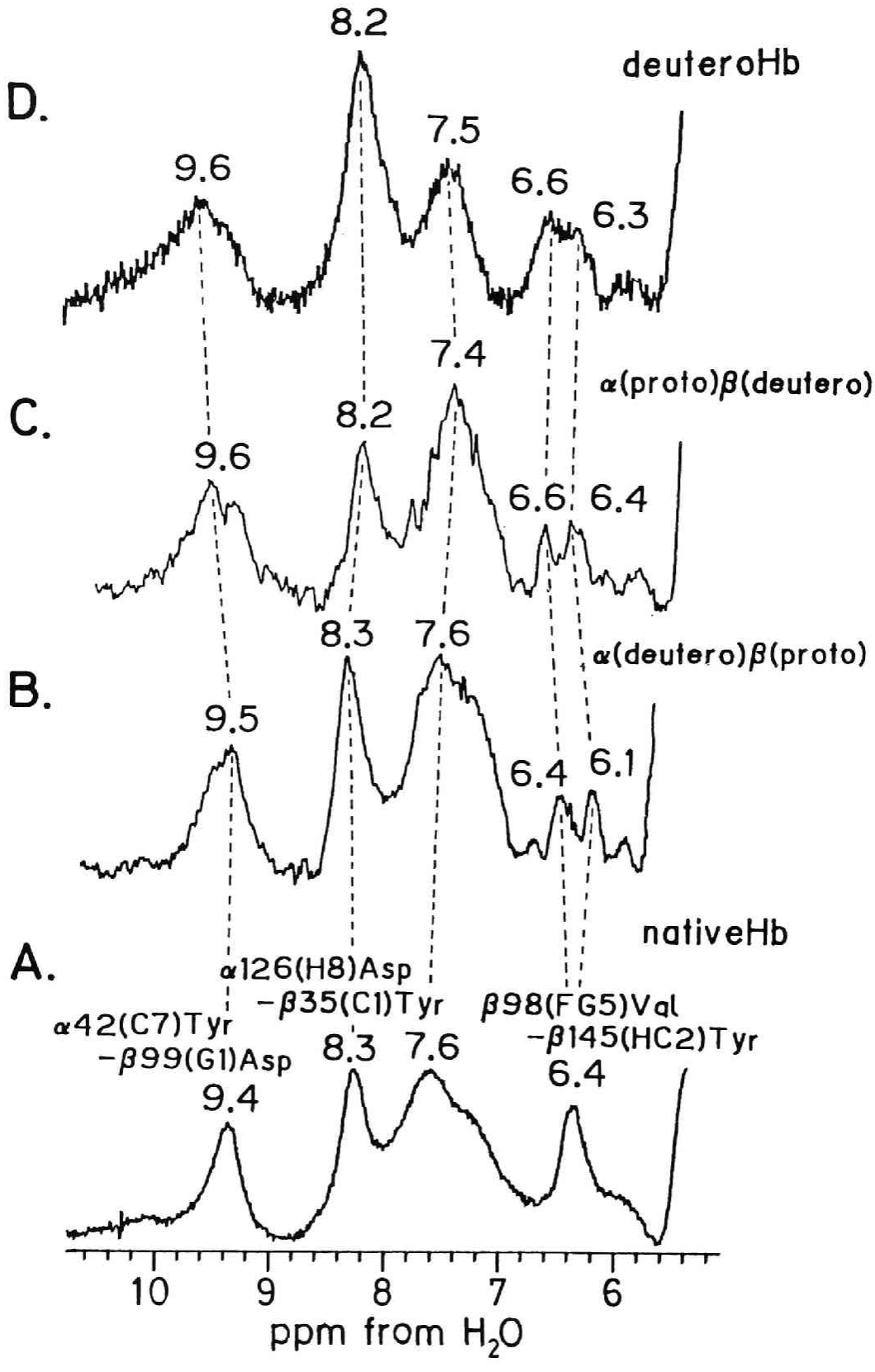
D.
8.2
deuteroHb
9.6
7.5
6.6
6.3
7.4
α(proto)β(deutero)
C.
8.2
9.6
6.6
6.4
8.3
7.6
α(deutero)β(proto)
B.
9.5
6.4
6.1
nativeHb
A.
α126(H8)Asp
−β35(C1)Tyr
β98(FG5)Val
−β145(HC2)Tyr
α42(C7)Tyr
−β99(G1)Asp
8.3
7.6
9.4
6.4
10
9
8
7
6
ppm from H2O

Figure. 7

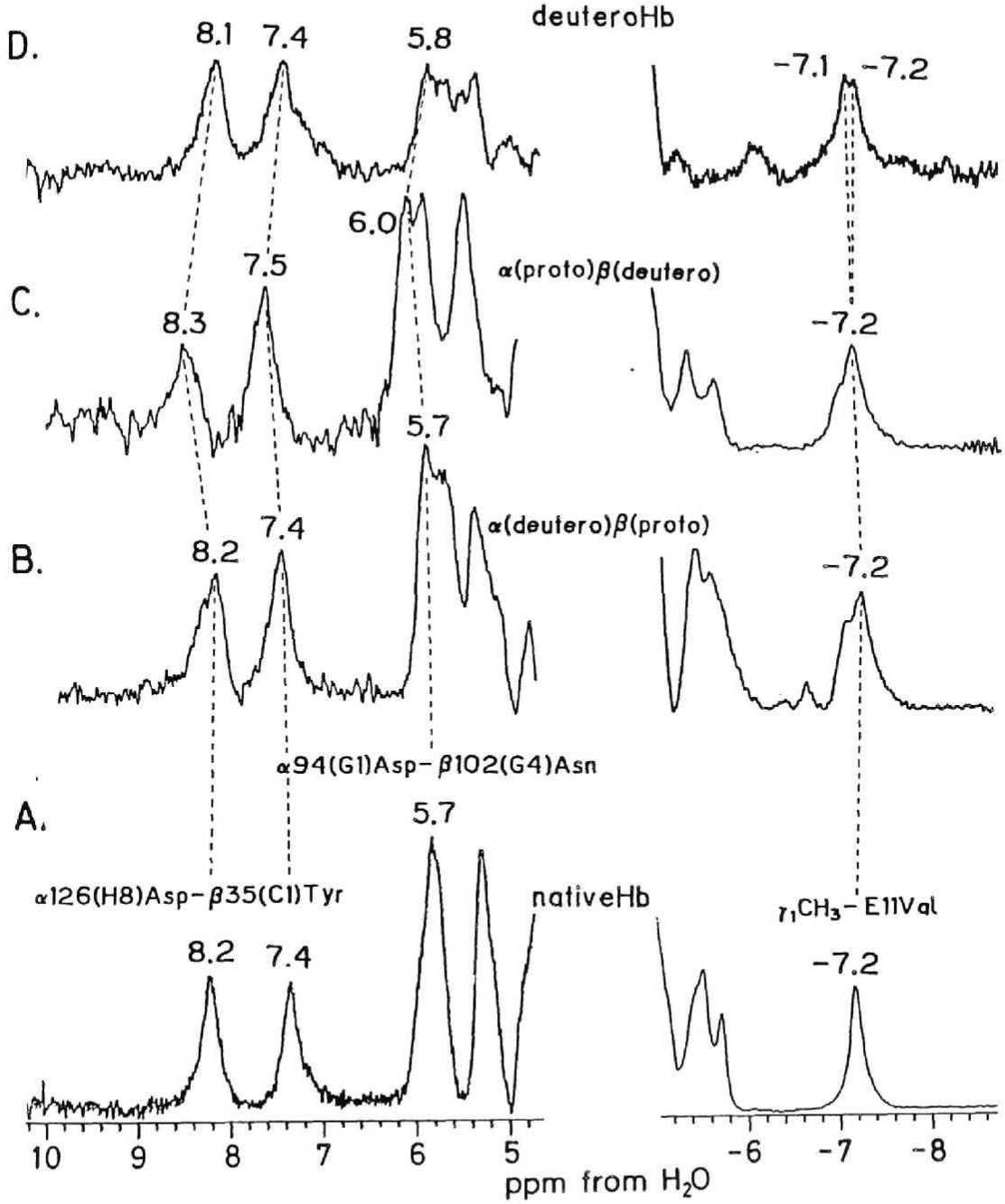
deuteroHb
D.
8.1
7.4
5.8
-7.1
-7.2
6.0
7.5
α(proto)β(deutero)
C.
8.3
-7.2
5.7
7.4
α(deutero)β(proto)
B.
8.2
-7.2
α94(G1)Asp–β102(G4)Asn
A.
5.7
α126(H8)Asp–β35(C1)Tyr
nativeHb
γ1CH3–E11Val
8.2
7.4
-7.2
10
9
8
7
6
5
-6
-7
-8
ppm from H2O

Figure. 8

A. Tertiary Structure

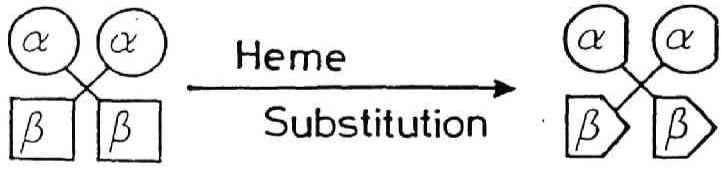

B. Quaternary Structure

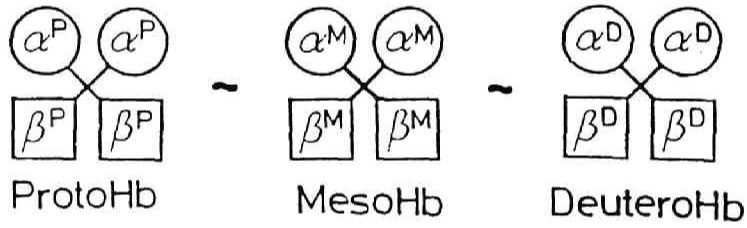

C. Propagation of Confomational Changes

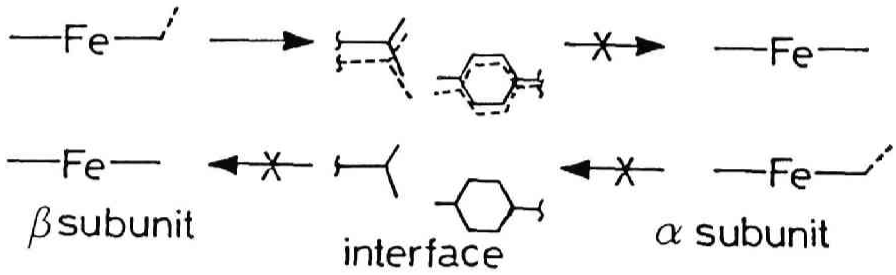

Figure. 9

CHAPTER 2.

Study of the Specific Heme Orientation in Reconstituted Hemoglobins.

ABSTRACT: NMR studies of the recombination reaction of apohemoglobin derivatives with natural and unnatural hemes and of the heme exchange reaction for reconstituted hemoglobin have revealed that the heme is incorporated into the apoprotein with stereospecific heme orientations dependent upon on the heme peripheral 2,4-substituents and the iron axial ligand(s). This determines whether recombination occurs at the α or β subunit, and on whether or not the complementary subunit is occupied by the heme. In the recombination reaction with the azido complex of deuterohemin, the α subunit of the apohemoglobin preferentially combines with the hemin in the "disordered" heme orientation, whereas protohemin is inserted in either of two heme orientations. Mesohemin inserts predominantly in the "native" heme orientation. For the β subunit, specific heme orientation was also encountered, but the specificity was somewhat different from that of the α subunit. It was also shown that the specific heme orientation in both subunits is substantially affected by the heme axial ligands. These findings imply that apohemoglobin senses the steric bulkiness of both the porphyrin 2,4-substituents and of the iron-axial ligands in the heme-apoprotein recombination reaction. To gain an insight into the effect of the protein structure, we also examined the heme reconstitution reaction of semihemoglobin, demonstrating that the heme orientation in the reconstituted semihemoglobin with the azido-deuterohemin complex was in the "native" form. Moreover, when protoheme is added to a solution of the deuteroheme-reconstituted hemoglobin so that the heme exchange reaction takes place, the resulting heme orientation for the α subunit is also quite specific ("native" heme orientation only), which is different from the case of the heme-apoprotein recombination reaction. Therefore, it is concluded that the orientation of the heme inserted into the apoprotein of the hemoglobin subunit depends upon the structure of the complementary subunit. In other words, the subunit structural changes induced by the tertiary structural changes of the complementary subunit through the subunit-subunit interaction subtly affect the stereospecific heme orientation.

The apparently simple and instantaneous (~ 1 ms) reconstitution reaction *in vitro* of heme and apohemoglobin (apoHb)[10] to yield unique holoproteins (Gibson & Antonini, 1960; Rose & Olson, 1983), leads to the view that the last step of the hemoprotein biosynthesis is a rapid folding process which affords the same species as found in single crystals (Gibson & Antonini, 1960; Adams, 1976, 1977). Recent ^{1}H NMR studies have demonstrated that the reconstitution of heme with apo-Mb and -Hb proceeds *via* a random isomeric incorporation, with respect to rotation about the α,γ-meso axis of heme, the result being defined as either the "native" or the "disordered" heme orientation. (Figure 1) (La Mar et al., 1985; Yamamoto & La Mar, 1986). The "disordered" heme orientation goes to the "native" heme orientation within several hours to many days, but a small amount of the "disordered" isomer is present at equilibrium (La Mar et al., 1980, 1983, 1984, 1985; Jue et al., 1983).

We have recently found (Ishimori & Morishima, 1986) that the deuterohemin incorporated into apoHb is disordered only in the α subunit, with the native orientation present in the β subunit. This suggests that interactions between globin and heme could control the heme orientation in each subunit. To gain an insight into how these interactions control the specific heme orientations and to explain the mechanism for stereospecific heme insertion, we have performed ^{1}H NMR studies of the reconstitution reactions of some apoHb derivatives with a variety of hemin-complexes bearing different heme substituents and heme axial ligands.

^{1}H NMR has been shown to be a powerful tool for the investigation of the heme orientation in hemoproteins (La Mar et al., 1985; Yamamoto & La Mar, 1986). The ^{1}H NMR measurements of the hemoproteins were made here as soon as possible after addition of the hemin complex to the apoHb solution to get the ratio of the "native" to "disordered" heme orientations. The results show that apoHb can stereospecifically recognize the heme orientations by the interactions between heme and globin at the time of recombination, and that such a stereospecific recognition in one subunit depends upon the structure of the complementary subunit. It is concluded that the heme orientation is determined by both the steric hindrance exerted by the heme peripheral groups and the axial ligand, as well as by the tertiary

[10]Abbreviation: NMR, nuclear magnetic resonance; Hb A, human adult hemoglobin; met Hb, ferric hemoglobin; Mb, myoglobin; Bis-Tris, [bis(2-hydroxyethyl)amino]tris(hydroxymethyl)methane; ppm, parts per million; MEK, methyl ethyl ketone; WEFT, water-eliminated Fourier transform; semiHb, semihemoglobin; apoHb, apohemoglobin; Tris-HCl, tris(hydroxymethyl)aminomethane hydrochloride.

structure of the complementary subunit.

MATERIALS AND METHODS

Sample Preparation Human adult Hb was prepared in the usual manner from fresh whole blood obtained from a normal individual. Protohemin was obtained by Sigma Chemical Co. (bovine, Type I) and used without further purification. Stripped Hb was obtained by gel filtration with Sephadex G-25 equilibrated with 0.01 M Tris-HCl buffer containing 0.1 M NaCl at pH 7.5 (Bermann et al., 1971). Apohemoglobin was prepared by the treatment of metHb with HCl/MEK (Yonetani, 1967) by modifying Teale's method (Teale, 1959; Ishimori & Morishima, 1986). Reconstituted Hbs were prepared as described in the previous paper (Ishimori & Morishima, 1986). Crystalline deuterohemin, protohemin and mesohemin were dissolved in a minimal volume of 0.1 N NaOD or 50 % aqueous solution of pyridine before the recombination experiments. The hematin solution was diluted with D_2O containing the ligand and was added dropwise into a stirring solution of apoHb in 10 mM potassium phosphate buffer, pH 7.0. The reconstitutions with heme-CO complex were performed as reported by La Mar et al. (1985). Reconstituted Mbs (sperm whale) were prepared in a similar manner as the reconstituted Hbs. After the buffer exchange to 50 mM Bis-Tris pH 7.0 by the ultrafiltration, the reconstituted protein was concentrated to about 1 mM. All the procedures were performed in a cold room (0 ~ 5 °C). SemiHbs were prepared using the method of Cassoly & Banerjee (1971) and reconstituted with hemin in a similar manner as apoHb. For the heme exchange reactions, the appropriate reconstituted holoprotein was diluted to ~ 1 mM in D_2O containing 50 mM Bis-Tris and then a two molar equivalent of protohemin-N_3^- solution in 0.01N NaOD was added.

For NMR measurements, all of the Hb samples, except for met-cyano complex, were converted to the met-azido complex because this complex is the most convenient form of Hb for estimating the relative contents of the heme orientational isomers from its proton NMR spectrum. In addition, conversion from "disordered" to "native" heme orientation isomer is relatively slow in this form (La Mar et al., 1984). This was done for all the ferric reconstituted Hbs, except met-cyano deuteroHb, by adding NaN_3 within 5 min after the recombination. The heme orientation for met-cyano deuteroHb was determined by on the basis of the β-pyrrole proton resonances. Reconstituted HbCO was converted to the met-azido complex by adding ferricyanide and sodium azide.

NMR Measurements Proton NMR spectra at 300 MHz were recorded on a Nicolet NT-300 Spectrometer equipped with a 1280 computer system. Typically, 13μs (180°) radio-frequency pulse and a ±12kHz spectral width were used to detect the heme methyl signal for reconstituted hemoglobins (5 ~ 30 ppm from H_2O). Conventional WEFT pulse sequence (180°-τ-90° acuire) was used in order to minimize the water signal. A careful setting of τ value (typically 90 100ms) can completely eliminate the H_2O signal under rapid repetition of the sequence. Usually, an interpulse time of about 0.1 s was used (Inubushi et al., 1983). Proton shift were referenced with respect to the water proton signal, which was 4.8 ppm downfield from the proton resonance of 4,4-dimethyl-4-silapentane-1-sulfonate (DSS) at 23 °C.

RESULTS AND DISCUSSION

Heme Peripheral Effect on the Heme Orientation Figure 2 shows the hyperfine-shifted portion ^1H NMR spectra of sperm whale deuterohemin-met MbN_3^- which was obtained by the reconstitution reaction of apoHb with twice a stoichiometric amount of deuterohemin-azido complex. The spectrum recorded immediately after reconstitution (Figure 2A) consists of two sets of heme methyl resonances. By referring to the previously reported spectra for the reconstituted met-azido protoMb, met-cyano protoMb (Mayer et al., 1974; La Mar et al., 1981, 1983) and met-cyano deuteroMb (La Mar et al., 1978) and the time dependences of these spectra, the heme methyl peaks M_1, M_2 and M_3 can be assigned to the "native" heme orientation isomer of deuteroMb. The peaks M'_1, M'_2, M'_3 and M'_4, which decreased in their intensities with time (Figure 2B), can readily be assigned to the heme "disordered" form. Traces C and D in Figure 2 illustrate the spectra for met-azido deuteroHb obtained 15 min and 2 days after reconstitution, respectively. Our previous report (Ishimori & Morishima, 1986) has shown that the methyl resonances labeled α_n and α'_n (n = 1,2,3) are attributed to the α and β subunit, respectively. In addition to the six peaks in the NMR spectrum taken immediately after the reconstitution (Figure 2, trace C), we find three additional peaks labeled α_1, α_2 and α_3 which have larger intensities than the three methyl peaks α'_1, α'_2 and α'_3 in a trace D. Intensities of the peaks α_n (n = 1,2,3) increase in time at the expense of the peaks α'_n (n = 1,2,3), whereas the peaks β_1, β_2 and β_3 exhibit no significant time dependent changes. It is therefore likely that the species affording the peaks α'_n (n = 1,2,3) is metastable and converts slowly to the form that generates the peaks α_n (n = 1,2,3). This indicates that the protein

conformation formed initially is not stable and that two forms of the protein conformation are present 2 days after the reconstitution. The presence of these two sets of peaks appears similar to that found for freshly reconstituted deuteroMb as shown in Figure 2A. On the basis of the time dependent spectral changes for reconstituted deuteroMb and Hb, it is concluded that the metastable component giving the peaks α_n (n = 1,2,3) bears the "disordered" heme orientation, whereas the resonances α_n and β_n (n = 1,2,3) arise from the "native" heme orientation. Therefore, upon incorporation of deuterohemin-N_3^-, the apoHb α subunit prefers the "disordered" heme orientation, while the β subunit prefers the "native" orientation.

Jue and La Mar (1984) reported that the heme disorder exists in both α and β subunits of deoxygenated and met-cyano deuteroHbs. We previously found (Ishimori & Morishima, 1986) that the "reversed" heme reorientation reaction occurs from the "native" to "disordered" form when the ferric-azido deuteroHb is reduced to the ferrous deoxygenated form. Therefore, the "disordered" form which Jue and La Mar (1984) observed for the deuteroHb β subunit appears to originate from the "native" form by the "reversed" reorientation conversion.

Figure 3 shows the ^1H NMR spectra of the azido complexes of reconstituted proto Mb (A), proto Hb (B), meso Mb (C) and meso Hb (D). In trace A, the three methyl signals M_1, M_2 and M_3 are assigned to the "native" heme orientation and the two methyl signals M'_1 and M'_2 are assigned to the "disordered" form, as judged from the time course of the NMR spectra. For the reconstituted protoHb, the preferential azide binding to the β subunit of met-azido Hb A (Gibson et al., 1969) and the time course spectra (La Mar et al., 1985) have led to the assignments of the α_1, α_2, α_3 and β_1, β_2, β_3 methyl resonances to the "native" heme orientation for the α and β subunits (Neya & Morishima, 1981) and the α'_1, α'_2, α'_3 and β'_1, β'_2, β'_3 resonances to the "disordered" one for the α and β subunits, respectively (Yamamoto & La Mar, 1986). The use of the methyl-deuterated heme for the reconstituted Hb and Mb allowed La Mar et al. (1983, 1985) to assign individual methyl resonances for protoMb as M_1(5-CH_3), M_2(1-CH_3) and M_3(8-CH_3), and those for protoHb as α_1, β_1(5-CH_3), α_2, β_2(1-CH_3) and α_3, β_3(8-CH_3). The spectrum for the reconstituted mesoMb (trace C) also exhibits two sets of heme methyl resonances arising from the two heme orientations, the signals M_1, M_2 and M_3 from the "native" heme orientation and the peaks M'_1 and M'_2 from the "disordered" one. On the other hand, as shown in a trace D, mesoHb consists of only one component. Signal α_1 has been assigned to

the α subunit and the peak $\alpha_2+\beta_1$ to the combined signals arising from the α and β subunits (Neya & Funasaki 1986). These results indicate that both Mb and Hb reconstituted with protohemin and the reconstituted mesoMb contain two heme orientation isomers, whereas the reconstituted mesoHb fevers only one heme orientation. The relative proportions of the two orientation isomers in Hb and Mb reconstituted with met-azido hemin complex are assembled in Table I.

The present results of the proton NMR spectra of reconstituted Hbs have revealed that the heme orientation depends on the heme peripheral 2,4-substituents (Figures 2, 3 and Table I). Since the apoHb α subunit combines with the deuterohemin-N_3^- preferentially in the "disordered" heme orientation, the apoHb α subunit can sense the difference in the steric bulkiness between heme methyl groups at the 1,3- position and protons at the 2,4- position when heme is embedded in the heme crevice. The preferential "native" heme orientation for mesoHb suggests that apoHb can also distinguish stereochemically between the methyl and the ethyl groups at the heme periphery. However, as apoHb initially accommodates protohemin-N_3^- in two orientations equally, apoHb cannot stereochemically distinguish between the vinyl and the methyl groups. It is therefore likely that apoHb recognizes the heme peripheral substituents at the early stage of the incorporation reaction, thereby determining the specific heme orientation taken up.

These findings allow us to propose a mechanism for the stereospecific heme incorporation into the apoHb α subunit as schematically shown in Figure 4. When the heme is incorporated into the heme cavity, it is proposed that the apoHb α subunit and hemin form an intermediate complex (I,I') in which apoHb recognizes the relative steric bulkiness of the substituents at the heme positions 1, 2, 3 and 4. The sites 1, 2, 3 and 4 in Figure 4 are defined as follows. For native Hb, the vinyl groups at the 2,4-position of protohemin are located at sites 2 and 4, while the methyl groups at the 1,3-position are at sites 1 and 3. This heme orientation is referred to as the "native" heme orientation. In the intermediate complex, the apoHb α subunit orients the hemin in a position where the bulkier groups occupy sites 2 and 4 as shown in the figure. Since deuterohemin (1,3-CH_3-, 2,4-H-) bears bulky groups at the 1 and 3 position, the heme orientation has to be "disordered" by a 180°rotation about the a,r-meso axis (I). On the other hand mesohemin (1,3-CH_3-, 2,4-CH_3CH_2-), with much bulkier groups at the 2,4-position, is embedded in the "native" orientation (I').

After the recombination reaction is completed, slow change of the heme orientation is observed for deuteroHb and protoHb, implying that the heme orientation selected during complex (I) formation becomes meta-stable in complex (II). It is of interest that this second step occurs for deuteroHb and in the "disordered" protoHb α subunit, in which the heme sites 1 and 3 are occupied by the proton and the vinyl group, respectively. The sites 1 and 3 for mesoHb and the "native" protoHb α subunit which did not exhibit a heme orientational conversion are occupied by the methyl group. It is therefore tempting to suggest that after the intermediate complex is converted to the stable complex (II, II'), the sites which recognize the methyl groups may be formed on the protein at sites 1 and 3. For the deuteroHb α subunit in which apoHb initially combines with the "disordered" deuterohemin, with the sites 1 and 3 occupied by the protons, the "disordered" form is slowly converted to the more stable complex (III) with the "native" heme orientation, in which the sites 1 and 3 are occupied by the methyl groups. On the other hand, the α subunit of apoHb initially combines with the mesohemin in the "native" heme orientation, with the sites 1 and 3 already occupied by the methyl groups, and therefore does not experience further conversion of heme orientation. As for protohemin-N_3^-, which reacts with apoHb to afford two heme orientation isomers, the "disordered" heme orientation is slowly converted to the "native" heme orientation at the second stage. This implies that the heme orientation may be determined at two independent stages (stage I and II in Figure 4).

As for the apoHb β subunit, the mechanism could be somewhat different than for the α subunit. Deuterohemin-N_3^- is initially inserted to apoHb β subunit in one orientation so that the protein structure senses the relative steric difference between proton and methyl at the heme periphery, as found for apoHb α subunit. However, the deuteroHb β subunit prefers the "native" heme orientation, in contrast to the "disordered" heme orientation for the α subunit. Mesohemin-N_3^- fevers the "native" heme orientation in mesoHb β subunit, as also found in the α subunit. It is suggested that at the first step of the determination process for the heme orientation in the apo β subunit, its protein conformation does not orient the heme in favour of less bulky groups located at the sites 1 and 3, as found for α subunit. Rather, it favors the heme oriented in such a way that methyl groups occupy the sites 1 and 3, as shown in Figure 4. That is, protein recognizes the methyl group at the sites 1 and 3 immediately after apoHb combines with heme. Non-stereospecific heme orientation in the β subunit for the reconstitution reaction with

protohemin-N_3^- implies that at the first stage the β subunit cannot recognize the difference between the vinyl and the methyl groups. Since the "disordered" form is converted to the "native" form in the reconstituted protoHb, the protein may recognize the difference between the vinyl and the methyl groups in the β subunit at the second stage. Therefore, the heme orientation is determined at two stages for both apo α and β subunits.

Heme Ligand Effect on the Heme Orientation In order to look at the effect of the heme axial ligand on the heme orientations the recombination reaction of apoHb, with the hemin complexes coordinated with a variety of axial ligands, was followed by NMR. Figure 5 compares the NMR spectra of deuteroHbN_3^-, which is formed either by reconstitution with deuterohemin-N_3^-(A) or by reconstitution with deuterohemin-pyridine followed by subsequent addition of NaN_3^- (B). The deuterohemin-pyridine complex incorporates into apoHb to afford two orientation isomers for the α subunit as seen by the signals α_1, α_2, α_3 arising from the "native" heme orientation and the α'_1, α'_2, α'_3 peaks from the "disordered" one, but one heme orientation conformer for the β subunit (the signals β_1, β_2, β_3 due to the "native" orientation). This heme orientation behaviour for the α subunit differs from the case in which azido-hemin is directly incorporated into apoHb. Mesohemin-pyridine incorporates into the α and β subunits in two heme orientations (Table II-A and II-B), while the azido-complex is inserted in a different way. It follows that the heme orientation depends not only on the heme substituents but also on the heme axial ligand.

Figure 5, Table II-A and Table II- B show that the stereospecific recognition of the heme orientation as illustrated in Figure 4 is substantially influenced by the heme axial ligand. When bis pyridine- or bis cyano-complexes of hemin are inserted into apoHb, nearly equal percentages of the two heme orientations are seen. In the case where the reconstitution reaction is performed between deuterohemin-pyridine and the β subunit, the percentages are different. This may suggest that at the first stage of recombination of recombination there is no specific recognition by apoprotein of the heme orientation when the axial ligand is rather bulky and/or when hemin is bis-coordinated. Non-bonded interactions between globin and the iron-bonded ligand(s) may be more important than the globin-heme peripheral group interactions, leading to non-stereospecific recognition of the heme orientation irrespective of the 2,4-substituent.

Effect of Apoprotein Structure on the Heme Orientation In an effort to determine the effect of the apoprotein structure on the heme orientation we

examined the reconstitution by utilizing semiHbs which contained heme in only one subunit. In Figure 6B is shown the NMR spectrum taken immediately after addition of the deuterohemin-N_3^- to semiHb β which contained protoheme only in the β subunit. Figure 6A illustrates the NMR spectrum of nativeHbN_3^-. As a reference, the spectrum of deuteroHbN_3^-, which was reconstituted with deuterohemin-pyridine followed by addition of N_3^-, is shown in Figure 6C. Upon addition of deuterohemin-N_3^- to semiHb β the new peaks grow up at 18.5 (D_2) and 11.5 (D_3) ppm, due to deuteroHb α subunit in the "native" heme orientation. The resonance P_1+D_1, which has an intensity two times as large as the resonances D_2 or P_2, is presumably originates from the methyl signals (β_1 and α_1) arising from proto- and deuteroheme, respectively. In other words, the resonance P_1+D_1 does not resolved into α_1 and β_1 in this case.

To gain further insight into the effect of heme incorporation on heme orientation in the complementary subunit, a heme exchange reaction was performed. In Figure 7, the time dependent spectral changes for deuteroHbN_3^-, after protohemin-N_3^- is added, are illustrated. Figures 7A, 7B and 7C, respectively, show the spectra before, 1 hour after and 12 hours after the addition of protohemin-N_3^-. The resonances at 22.5, 22.0, 18.9, 18.7, 11.9 and 11.3 ppm, assignable to the deuteroHb α subunit, decrease in their relative intensities with time, and the new peaks are observed at 23.0 and 9.7 ppm. The resonance positions of these new peaks coincide with those for the "native" heme orientation isomer in protoHb α subunit. However, the resonances due to the deuteroHb β subunit exhibit no significant changes. The results of the reconstitution reactions of semiHbs with some hemin derivatives are compiled in Table III.

As shown in Table III, the order of the specificity of the heme orientation is as follows; α subunit for the heme exchange reaction > β subunit in semiHb α > α subunit in semiHb β > β subunit in apoHb > α subunit in apoHb > apoMb.

It has been revealed that apoMb is monomeric, while semiHb β and apoHb are dimeric, and semiHb α is tetrameric (Cassoly & Banerjee, 1971; Winterhalter et al., 1968). The specificity of the heme orientation mentioned above appears to parallel the extent of the protein aggregation (semi Hb α > semi Hb β, apo Hb > apo Mb). This implies that a subunit-subunit interaction in Hb renders the heme orientation stereospecific. The NMR resonances of the hydrogen bonded protons (α126H8 Asp - β35C1 Tyr and α103G10 His - β108G10 Asn) (Russu et al., 1987) which are located at

the $\alpha_1\beta_1$ intersubunit interface are observed in apoHb, semiHb α and semiHb β (Ishimori & Morishima, unpublished data). This suggests that these Hbs containing heme-free subunits maintain their quaternary structures by intersubunit hydrogen bonds. Quaternary structure could affect the tertiary structure of an apo subunit so that recognition of the heme orientation is highly stereospecific.

It is noted that heme is more stereospecifically inserted into the apo subunit of semiHb derivatives having the heme embedded in the complementary subunit than into apoHb with all subunits free of heme. As shown in Table III, apoHb exhibits the lowest specificity. SemiHbs exhibit a higher specificity. The highest specificity of the heme orientation is exhibited in the heme exchange reaction where the heme is inserted into one subunit of the Hb molecule with the other three subunits occupied by heme. As heme incorporation stabilizes the tertiary structure of the apoprotein conformation, it could give rise to the same effects on the stereospecific heme orientation as those exerted by aggregation of the subunit. From the above discussion, it is suggested that the heme orientation could be determined by the protein conformational flexibility, which is modulated by the formation of the intersubunit hydrogen bonds and/or by the incorporation of the heme.

The effect of the apoprotein structure on the heme orientation is also noticed for α and β subunits of apoHb and semiHb. Table III shows that the β subunit exhibits higher specificity in the heme orientation than the α subunit. It is likely that this difference between the α and β subunit arises from the relative differences in their heme environmental structures. We previously reported (Ishimori & Morishima, 1986) that the modification of the heme side chains in the β subunit exerts a more subtle structural alteration than does heme side modification in the α subunit. These nonequivalent structural changes induced by the heme substitution between the α and β subunits have also been encountered for metal-substituted Hb and its hybrid Hb derivatives (Inubushi et al., 1983; Shibayama et al., 1987; Ishimori & Morishima, 1987). This nonequivalence may arise from the substantial difference in van der Waals contacts in heme environments between the α and β subunits; the van der Waals contacts in the β subunit are more substantial than in the α subunit. The stronger interactions between heme and globin in the β subunit bring about more stereospecific recognition of the heme orientation in the β subunit than in the α subunit.

In summary, in the present NMR study we have found factors which

control the heme orientation at reconstitution, leading to a proposal of a mechanism for the determining process of heme orientation (Figure 4). ApoHb senses the steric difference of both the porphyrin 2,4-substituents and the iron-axial ligand in the heme-apoprotein recombination reaction; the process determining heme orientation consists of the two stages. Furthermore, subunit structural changes propagated from the complementary subunit through subunit-subunit interactions are quite sensitively sensed by the stereospecific heme orientation, suggesting that the intersubunit interactions play an important role in the stereospecific recognition of the heme into apoproteins.

REFERENCES

Adams, P. (1976) *Biochem. J. 159*, 371-376.

Adams, P. (1977) *Biochem. J. 163*, 153-158.

Bermann, M., Benesch, R., & Benesch, R. E. (1971) *Arch. Biochem. Biophys. 145*, 236-239.

Cassoly, R., & Banerjee, R. (1971) *Eur. J. Biochem. 19*, 514-522.

Fermi, G. (1975) *J. Mol. Biol. 97*, 237-256.

Gibson, Q. H., & Antonini, E. (1960) *Biochem. J. 77*, 328-341.

Gibson, Q. H., Parlchurst, L. J., & Geraci, C. (1969) *J. Biol. Chem. 244*,4668-4676.

Inubushi, T., Ikeda-Saito, M., & Yonetani, T. (1983) *Biochemistry 22*, 2904-2907.

Ishimori, K., & Morishima, I. (1986) *Biochemistry 25*, 4892-4898.

Ishimori, K., & Morishima, I. (1987) *Biochemistry 27*, 4060-4066.

Jue, T., Krishnamoorthi, R., & La Mar, G. N. (1983) *J. Am. Chem. Soc. 105*, 5701-5702.

Jue, T., & La Mar, G. N. (1984) *Biochem. Biophys. Res. Comm. 119*, 640-645.

La Mar G. N., Budd, D. L., Viscio, D. B., Smith, K. M., & Langry, K. C. (1978) *Proc. Natl. Acad. Sci. U. S. A. 75*, 5755-5759.

La Mar G. N., Smith, K. M., Gersonde, K., Sick, H., & Overkamp, M. (1980) *J. Biol. Chem. 255*, 66-70.

La Mar, G. N., Burns, P. D., Jackson, T. J., Smith, K. M., Langry, K. C., & Strittmatter, P. (1981) *J. Biol. Chem. 256*, 6075-6079.

La Mar, G. N., Davis, N. L., Parish, D. W., & Smith, K. M. (1983) *J. Mol. Biol. 168*, 887-896.

La Mar, G. N., Toi, H., & Krishnamoorthi, R. (1984) *J. Am. Chem. Soc. 106*, 6395-6401.

La Mar, G. N., Yamamoto, Y., Jue, T., Smith, K. M., and Pandey, R, K. (1985) *Biochemistry 24*, 3826-3831.

Mayer A., Ogawa, S., Shulman, R. G., Yamane, T., Cavaleiro, J. A. S., Rocha Gonsalves, A. M., Kenner, G. W., & Smith K. M. (1974) *J. Mol. Biol. 86*, 749-756.

Neya, S., & Morishima, I. (1981) *J. Biol. Chem. 256*, 793-798.

Neya, S., & Funasaki, N. (1986) *Biochemistry 25*, 1221-1226.

Perutz, M. F. (1970) *Nature(London) 228*, 726-739.

Rose, M. Y., & Olson, J. S. (1983) *J. Biol. Chem. 258*, 4298-4303.

Russu, I. M., Ho, N. T., & Ho. C. (1987) *Biochim. Biophys. Acta. 914*, 40-48.

Shibayama, N., Inubushi, T., Morimoto, H., & Yonetani, T. (1987) *Biochemistry 26*, 2194-2201.

Teale, F., W., J. (1959) *Biochim. Biophys. Acta. 35*, 543.

Winterhalter, K. H., Amiconi, G., & Antonini, E. (1968) *Biochemistry 7*, 2228-2232.

Yamamoto, Y., & La Mar, G. N. (1986) *Biochemistry 25*, 5288-5297.

Yonetani, T. (1967) *J. Biol. Chem. 242*, 5008-5013.

FIGURE LEGENDS

Figure 1.

Two possible orientations of the heme relative to the proximal histidyl imidazole plane. (A) The form which is determined by the X-ray crystallography of Hb A (Fermi, 1975) and (B) the heme rotated 180° about the α,γ-meso axis of the form (A). The shaded rectangle indicates the orientation of the proximal histidyl imidazole plane.

Figure 2.

Downfield hyperfine-shifted portions of the 300MHz ^{1}H-NMR spectra of reconstituted deutero Mb and Hb as the met-azido complex in 50 mM Bis-Tris pH 7.0 at 23 °C. Reconstituted deuteroMb, (A) 15 min and (B) 2 days after reconstitution. Reconstituted deuteroHb, (C) 15 min and (D) 2 days after reconstitution.

Figure 3.

Downfield hyperfine-shifted portions of the 300MHz ^{1}H-NMR spectra of reconstituted proto Mb, Hb, meso Mb and Hb as the met-azido complex taken 30 min after the reconstitution in 50 mM Bis-Tris pH 7.0 at 23 °C. (A) Reconstituted protoMb. (B) Reconstituted protoHb. (C) Reconstituted mesoMb. (D) Reconstituted mesoHb.

Figure 4.

Schematic representations of the mechanism of the specific heme orientation (see text).

Figure 5.

Downfield hyperfine-shifted portions of the 300MHz ^{1}H-NMR spectra of reconstituted deuteroHb as the met-azido complex taken 30 min after the reconstitution in 50 mM Bis-Tris pH 7.0 at 23 °C. (A) Reconstituted with deuterohemin-pyridine. (B) Reconstituted with deuterohemin-N_3^-.

Figure 6.

Downfield hyperfine-shifted portions of the 300MHz ^{1}H-NMR spectra of nativeHb, semiHb and reconstituted deutero Hb as the met-azido complex in 50 mM Bis-Tris pH 7.0 at 23 °C. (A) Native Hb. (B) SemiHb β taken 30 min after addition of deuterohemin-N_3^- (C) deuteroHb reconstituted with deuterohemin-pyridine complex.

Figure 7.

The heme exchange reaction as followed by the 300MHz ^{1}H-NMR spectra of the met-azido complex of deuteroHb in 50 mM Bis-Tris pH 7.0 at 23 °C. (A) In the absence of protohemin-N_3^-. (B) 1 hour after addition of protohemin-N_3^-. (C) 12 hours after addition of protohemin-N_3^-.

Table I The proportions of the "native" orientation relative to the "disordered" orientation in the reconstitution reaction between hemin-azide complex and apoMb, apoHb in 50 mM Bis-Tris pH 7.0 at 23 °C.

	myoglobin	hemoglobin-α	hemoglobin-β
deuterohemin	7:3	0:10	10:0
protohemin	5:5	5:5	6:4
mesohemin	6:4	10:0	10:0

Table II-A The proportions of the "native" orientation relative to the "disordered" orientation in the reconstitution reaction between α subunit of apoHb and some hemin derivatives coordinated with a variety of axial ligands in 50 mM Bis-Tris pH 7.0 at 23 °C.

axial ligand	H_2O	CO	N_3^-	CN^-	pyridine
deuterohemin	0:10	0:10	0:10	4:6	5:5
protohemin	5:5	5:5	5:5	---[a]	6:4
mesohemin	10:0	10:0	10:0	---[a]	4:6

[a]Not determined.

Table II-B The proportions of the "native" orientation relative to the "disordered" orientation in the reconstitution reaction between β subunit of apoHb and some hemin derivatives coordinated with a variety of axial ligands in 50 mM Bis-Tris pH 7.0 at 23 °C.

axial ligand	H_2O	CO	N_3^-	CN^-	pyridine
deuterohemin	10:0	10:0	10:0	5:5	10:0
protohemin	5:5	5:5	6:4	---[a]	5:5
mesohemin	10:0	10:0	10:0	---[a]	5:5

[a]Not determined.

Table III The proportions of the "native" orientation relative to the "disordered" orientation in the reconstitution reaction between hemin-azide complex and SemiHbs and in the heme exchange reaction in 50 mM Bis-Tris pH 7.0 at 23 °C.

hemin	deuterohemin		protohemin		mesohemin	
subunit	α	β	α	β	α	β
ApoHb	0:10	10:0	5:5	6:4	10:0	10:0
SemiHb α	---	10:0	---	10:0	---	10:0
SemiHb β	10:0	---	6:4	---	10:0	---
Heme Exchange[a]			10:0	N.R.[b]		

[a]Exchange from deuteroheme to protoheme in deuteroHbN3- [b]No reaction.

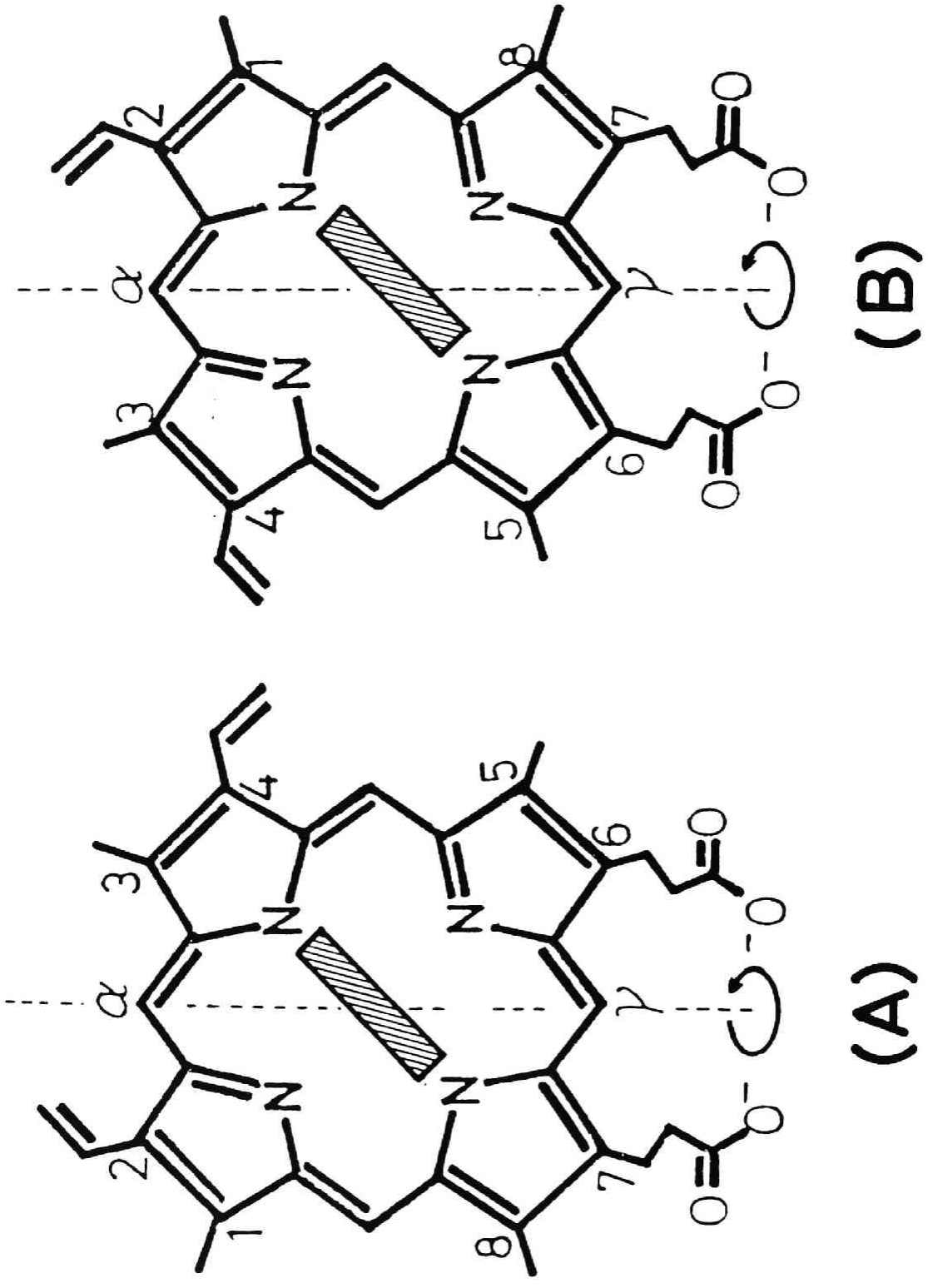

Figure. 1

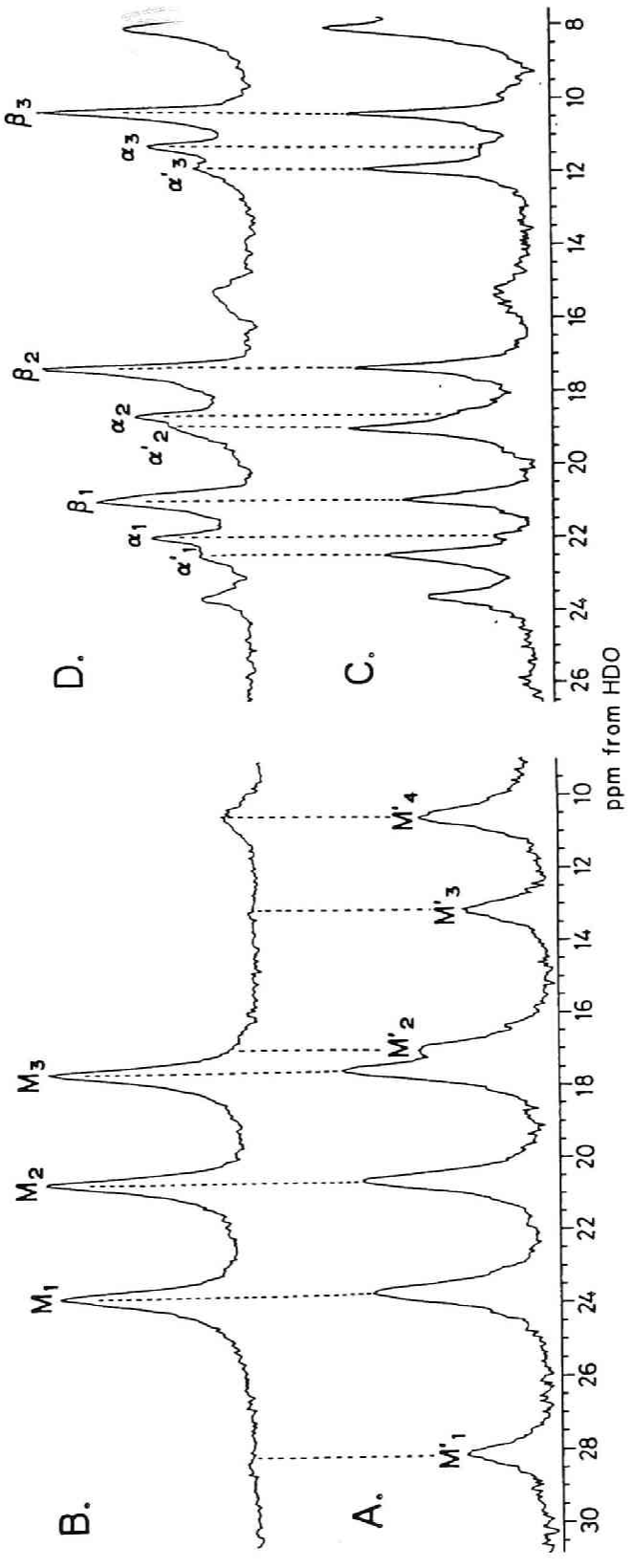

Figure. 2

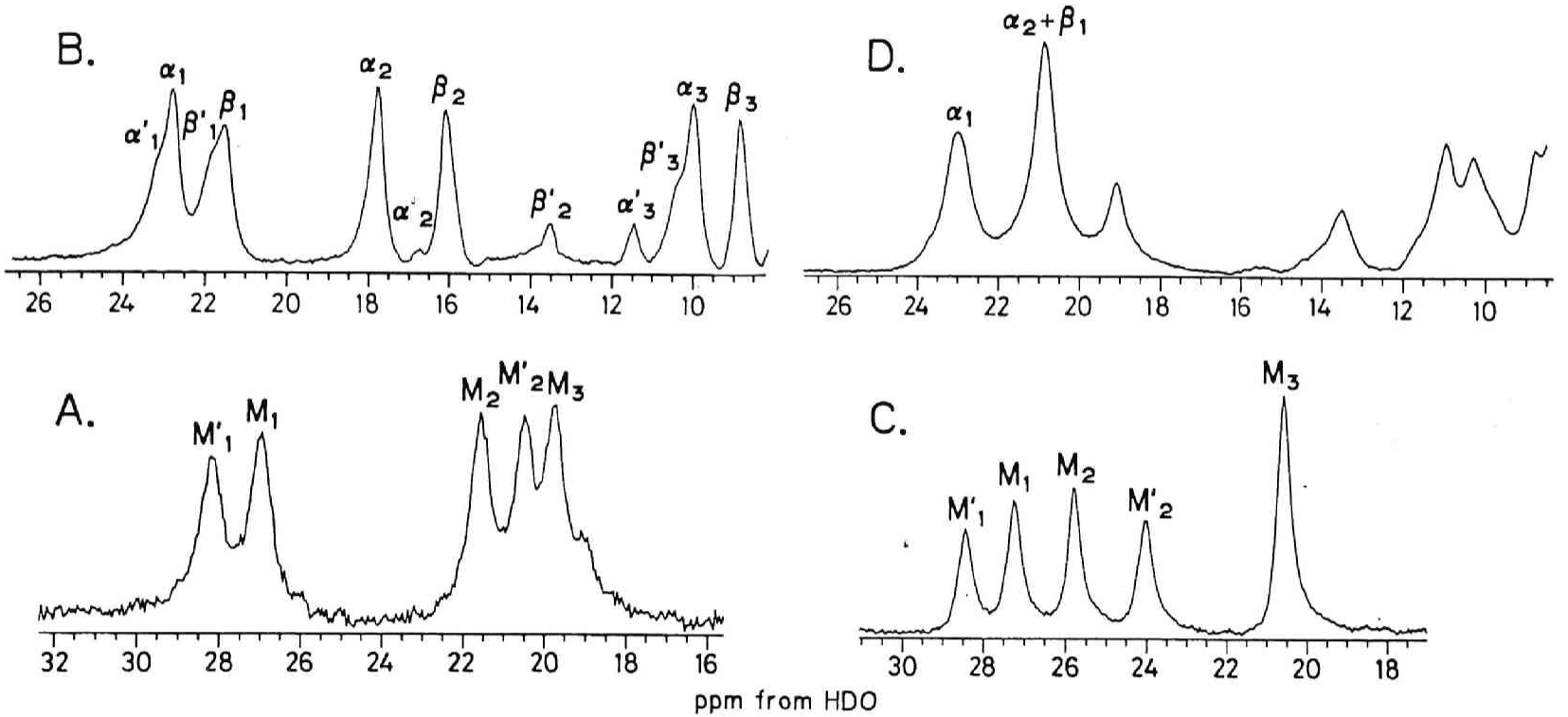
B.
α1
α'1
β'1
β1
α2
β2
α'2
β'2
α'3
β'3
α3
β3
26 24 22 20 18 16 14 12 10
D.
α2+β1
α1
26 24 22 20 18 16 14 12 10
A.
M'1
M1
M2
M'2
M3
32 30 28 26 24 22 20 18 16
C.
M'1
M1
M2
M'2
M3
30 28 26 24 22 20 18
ppm from HDO

Figure. 3

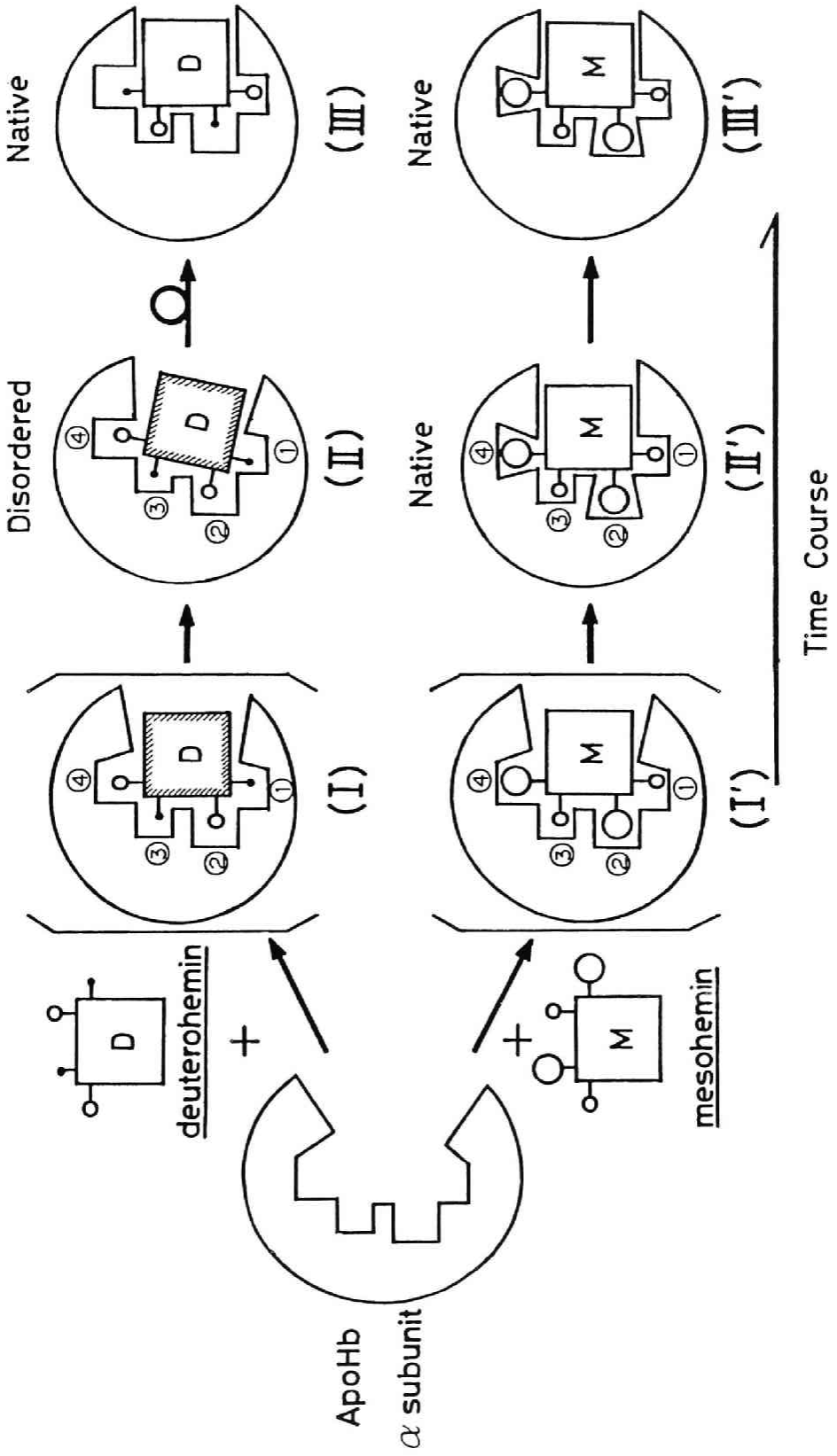
Native
Disordered
Native
Native
(III)
(II)
(I)
(I')
(II')
(III')
Time Course
D
M
deuterohemin
mesohemin
ApoHb
α subunit
q
1
2
3
4

Figure. 4

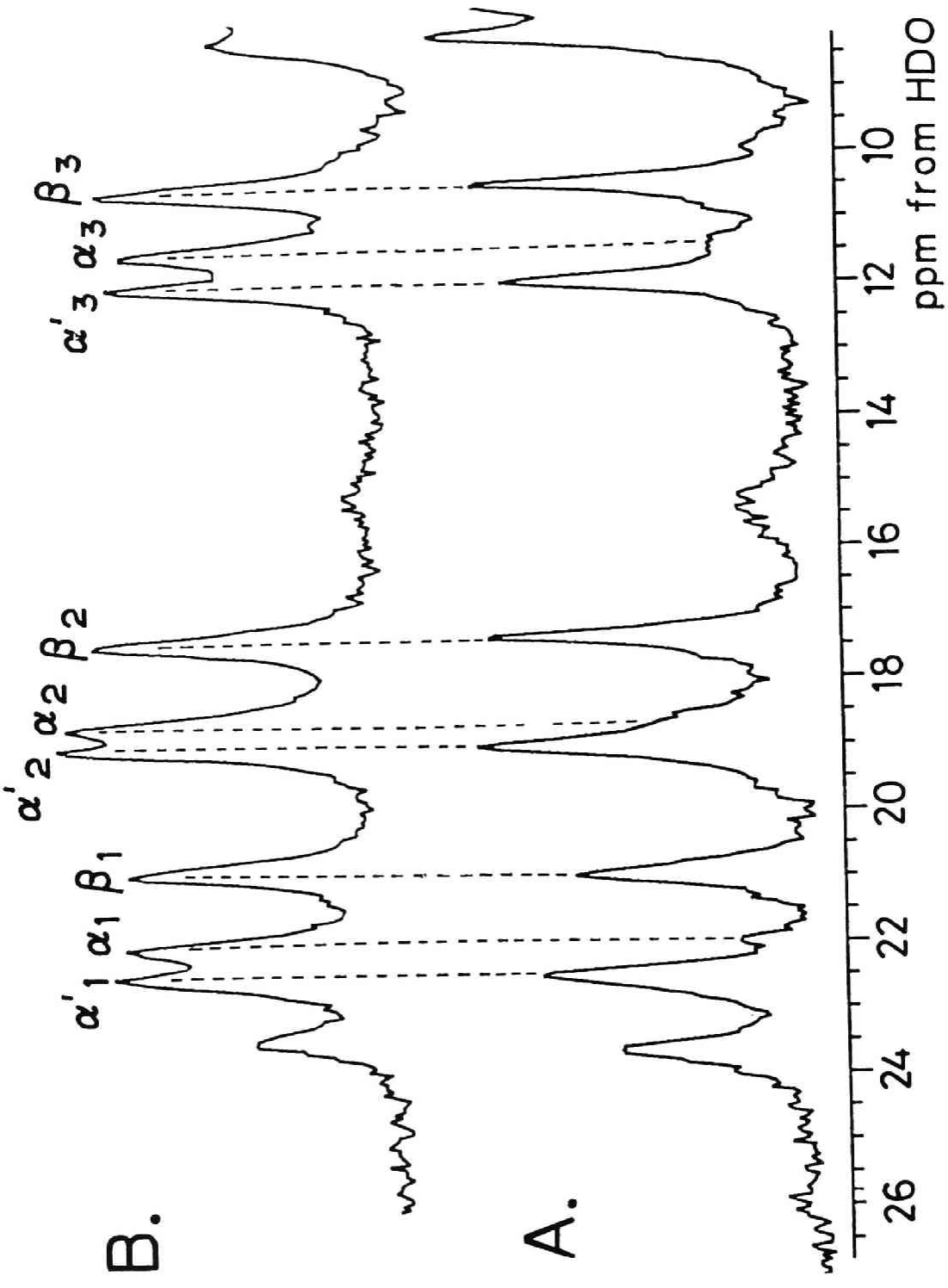

Figure. 5

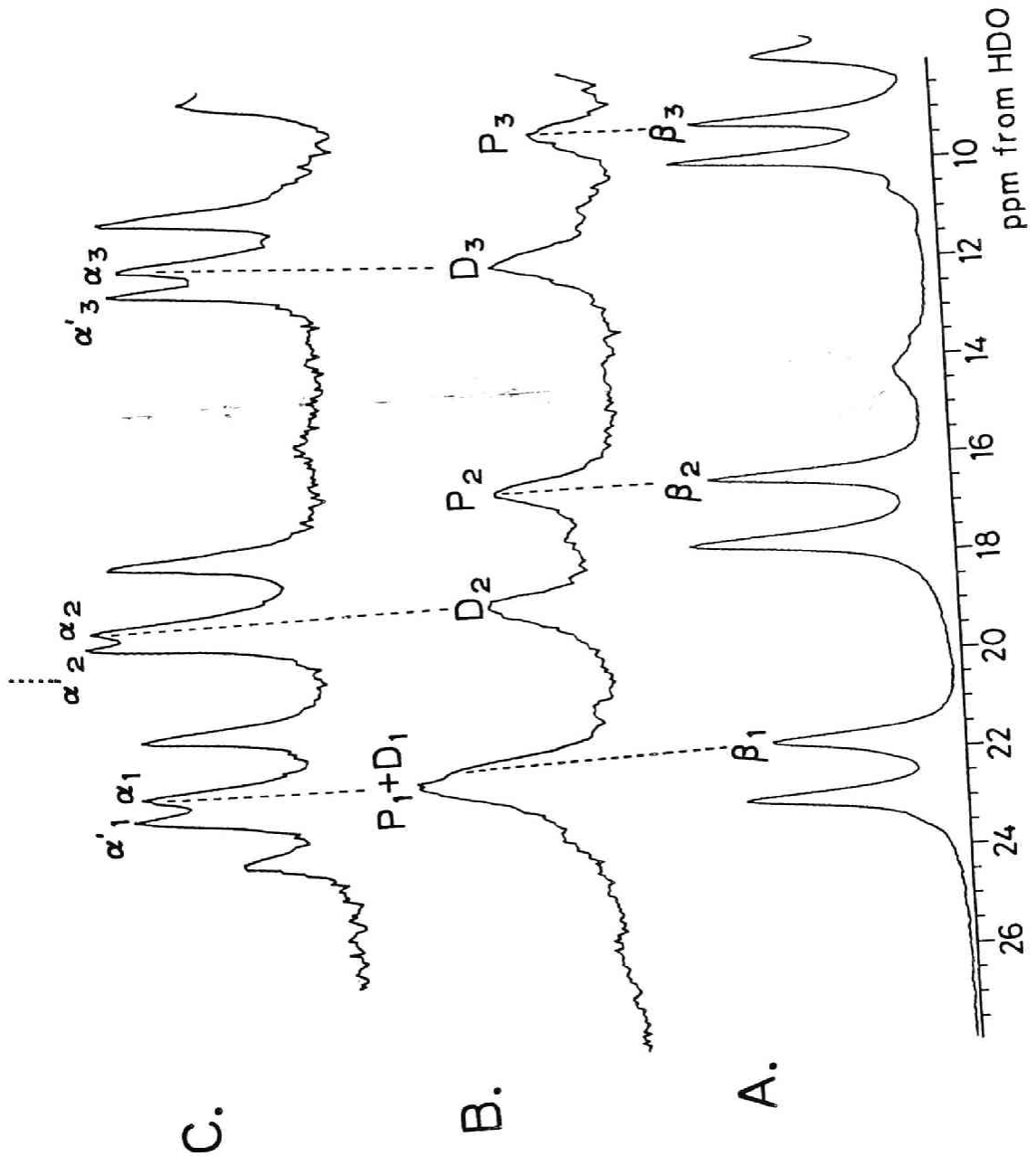
C.
B.
A.
α'1 α1
α'2 α2
α'3 α3
P1+D1
D2
P2
D3
P3
β1
β2
β3
ppm from HDO
10
12
14
16
18
20
22
24
26

Figure. 6

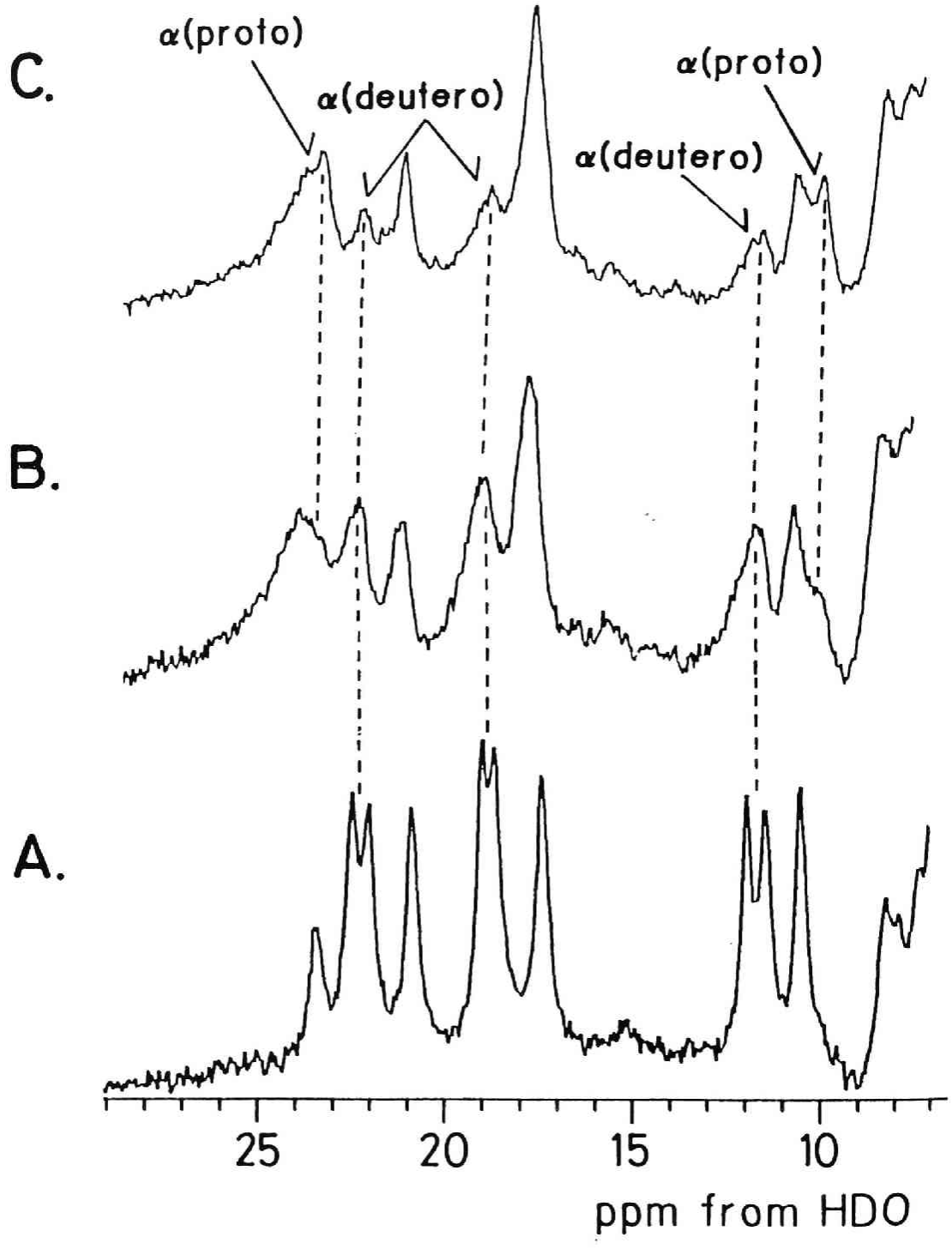

Figure. 7

CHAPTER 3.

NMR Study of Heme Exchange Reaction of Native Myoglobin and Hemoglobin.

ABSTRACT: A proton nuclear magnetic resonance study of the heme exchange reactions of native myoglobin and hemoglobin with the various hemes reveals that the heme displacement reaction is induced in native hemoproteins as has been found in the reconstituted hemoproteins containing unnatural hemes. It was found that protoheme was excluded from the native hemoprotein by the presence of modified heme to yield less stable reconstituted hemoprotein reconstituted hemoprotein. This reaction seems to be promoted by the conformational fluctuation arising from the thermal motion of the protein molecule and implies that the conformational fluctuation in native hemoprotein is large enough to dissociate the heme from the hydrophobic heme crevice. This heme exchange reaction rate was different in myoglobin and the hemoglobin subunits. This indicates that the conformational fluctuation is significantly different in these proteins probably due to difference in the *intra*molecular interactions, although these proteins have almost similar three dimensional structures as visualized by the X-ray diffraction study. From above results, we suggest that one feature of the conformational fluctuation in native hemoprotein.

In the presence of protohemin, an unnatural heme located in a reconstituted hemoprotein is excluded from heme pocket and is replaced with protohemin, to yield a more stable complex containing protoheme (Rossi-Fanelli & Antonini, 1960; LaMar et al., 1984). These observations have been considered to arise from the unstable structure of the reconstituted hemoprotein and the low binding affinity of the modified heme. However, LaMar and co-workers (LaMar et al., 1985; Yamamoto & LaMar, 1986) reported that fleshly prepared Hb A pocess a structural heterogenity, an equilibrium heme rotational disorder as found for reconstituted hemoproteins. This indicates that the two heme orientational reaction, *i.e.* one is the native heme orientation to the disordered one and the other is the disordered orientation to the native one, proceed under the physiological conditions. Since the heme reorientation reaction requires the cleavage of the bond between the heme iron and proximal histidine, the possibility of the has become increasingly more evident in recent years that proteins are not rigid systems and conformational fluctuations frequently play a major role in their biological activities (Karplus & McCanmon, 1981; Westhof et al., 1984; Tainer et al., 1984). Recent comparative X-ray (Frauenfelder et al., 1979), visible (Doster et al., 1982), Mossbauer (Levy & Rifkind, 1985), and Raman (Ondrias et al., 1983) measurements try to establish the relationships of the cryogenetic conformational fluctuations to functional proteins at physiological temperature. However, only few papers reported details of the conformational fluctuation of the hemoprotein molecule under physiological conditions. The NMR[11] study of these dynamic processes at room temperature offers experimental advantages in term of investigating the dynamic structure of the protein under physiological conditions, and expecting to reveal the relationships between the conformational fluctuation and the interactions of the protein system.

To gain an insight into the conformational fluctuation of native hemoprotein, we performed here ^{1}H NMR studies of the heme exchange reactions of native Mb and Hb. Mb and Hb are globular proteins which non-covalently enfold protoheme IX (Fermi et al., 1984; Dickerson & Geis, 1983). Although the heme maintains its relative position in the heme pocket by the iron-histidyl bond and hydrophobic interactions between heme periphery and amino acid residues inside the heme crevice, the heme

[11]Abbreviations; NMR, nuclear magnetic resonance; Hb A, human adult hemoglobin; Mb, myoglobin; Bis-Tris, [bis(2-hydroxyethyl)imino(hydroxymethyl)methane]; ppm, parts per million

reorientation or exchange reactions were observed for the reconstituted protein (LaMar et al., 1984; Ishimori & Morishima, 1988a). This indicates that the cleavage of the bond between the heme iron and the histidine and the displacement of the heme from the heme cavity can be caused under certain conditions. Recently, LaMar and co-worker reported an equilibrium heme disorder in native hemoprotein (LaMar et al., 1985; Yamamoto & LaMar, 1986) and pointed out a possibility of a large conformational fluctuation in native hemoproteins. Moreover, the appreciable flexibility at the entrance to the heme pocket is required to permit access of ligands to the binding site of native hemoprotein (Case & Karplus, 1979). It is, therefore, likely that a large conformational fluctuation is not only characteristic of the reconstituted protein which has less stable structure, but also a general property for the native hemoprotein. Further, previous paper (Ishimori & Morishima, 1988a) reported the specific heme orientation at the reconstitution of various hemes with globin and suggested that the interactions which determine the heme orientation are related to the fluctuation of the protein. Therefore, in this chapter, we demonstrate that the heme exchange reaction occurs in even native hemoproteins and discuss the conformational fluctuation and the relationship between the conformational fluctuation and interactions in native hemoprotein.

MATERIALS AND METHODS

Sample Preparation. Human adult hemoglobin was prepared in the usual manner from fresh whole blood from a normal individual. After injection of CO gas, the hemolysate was passed through Sephadex G-25 equilibrated with 0.1M Tris-HCl buffer containing 0.1 M NaCl at pH 7.5 (Bermann et al., 1971). Then the elution was passed through Sephadex G-25 equilibrated with 10 mM phosphate buffer pH 6.5 and applied to CM-52 (Whatman) equilibrated with the same buffer. After the washing by 10 mM phosphate buffer pH 6.5, the HbCO were eluted with 0.1M phosphate buffer pH 7.0. The purified HbCO were concentrated to ~ 2 mM by the ultrafiltration and buffer was exchanged to 50 mM Bis-Tris pD 6.5. Sperm whale Mb was purchased from Sigma as a lyophilized, salt-free powder. 50 mg of Mb was dissolved in 0.1 M Tris-HCl pH 7.0 (1 ml,4 °C) to yield met-aquo Mb. The purification of MbH_2O were same manner as HbCO. MbN_3^- was prepared from their met-aquo complexes by the addition of small amount of sodium azide.

Crystalline hemin which is twice as much molar as the protein was

dissolved in a minimal volume of 0.1 N NaOD before experiments. The hemin solution was diluted by D_2O containing small amount of sodium azide and added dropwise into a stirring solution of the protein solution. The sample solution was left to get time evolution spectra at 23 °C.

NMR Measurements. Proton NMR spectra at 300MHz were recorded on a Nicolet NT-300 spectrometer equipped with a 1280 computer system. Hyperfine shifted NMR spectra were obtained by a 4K data transform of ± 12-kHz spectral width and 5.5-μs 90° pulse after the strong solvent resonance in H_2O solution was suppressed by 500-μs low power pulse. Proton shifts were referenced with respect to the water proton signal, which was 4.8 ppm downfield from the proton resonance of 4,4-dimethyl-4-silapentane-1-sulfonate (DSS) at 23 °C.

RESULTS

Heme Exchange Reaction in Native MbN_3^-. The time evolution of the heme hyperfine-shifted methyl proton resonances resulting from the heme exchange reaction of native MbN_3^- with twice a stoichiometric amount of deuterohemin-N_3^- (2,4-H-) and mesohemin-N_3^- (2,4-CH_3CH_2-), to yield the respective metazido complexes are illustrated in Figure 1 and 2, respectively. In each case, as previously reported (LaMar et al., 1983), the signals at 27.0, 21.4 and 19.6 ppm are assigned to the methyl groups for native MbN_3^-. The new peaks appeared in time at 23.8, 20.5 and 17.6 ppm are identified as the methyl signals of deuteroMb-N_3^- (LaMar et al., 1981). Therefore, these time evolution spectra indicate that the heme exchange from protoheme to deuteroheme is induced for the native Mb in the presence of excess deuterohemin, although the heme exchange rate is very slow and almost 80% of the protein still exists as native Mb at equilibrium (30 days after addition of deuterohemin, result not shown). In Figure 2, mesohemin also reacts with native Mb to form mesoMbN_3^- (the signals at 25.8 and 20.5 ppm arise from mesoMb). Although mesohemin has more bulky substituents at the 2,4-position of the porphyrin, its heme exchange reaction rate is almost the same as that of deuterohemin.

In order to look for the heme exchange reaction between native hemoprotein and native hemin (protohemin), we followed the time dependent spectral changes of the native Mb after addition of [*methyl*-1,3-^{2}H]protohemin by utilizing ^{2}H NMR (Figure 3). The two new signals at 21.2 and 7.6 ppm appeared in time and can be readily assigned to the deuterated methyl groups arising from MbN_3^- reconstituted with [*methyl*-

1,3-^{2}H]protohemin. Comparison with the proton NMR spectrum of native MbN_3^- show that the signal at 21.2 ppm is identified as the 1-methyl group of the porphyrin and the signal at 7.6 ppm as the 3-position. This observation indicates that the proto Mb containing [*methyl*-1,3-^{2}H]protohemin is formed by the heme exchange reaction between native protohemin and [*methyl*-1,3-^{2}H]protohemin.

Heme Exchange Reaction in Native HbCO. As the metazido derivative of Hb is less stable than that of Mb, an attempt to look for the heme exchange reaction in nativeHbN_3^- has not be successful yet. Thus, native HbCO as the most stable complex of Hb, was examined to see heme exchange reaction. Figure 4 shows the time course spectra of HbCO in the presence of deuterohemin-N_3^-. Since HbCO is diamagnetic, the paramagnetic resonances found in Figure 4 arise from met-azido native Hb formed by auto-oxidation of HbCO and/or metazido deuteroHb by the heme exchange reaction. By comparing the comparison with the spectra of deuteroHbN_3^- with that of nativeHbN_3^-, the assignments of the paramagnetic resonances are determined as indicated in the figure. The intensities of the signals at 21.8 and 17.4 ppm are larger than other methyl resonances because the methyl signals of deuteroheme are overlapped on those of protoheme. Figure 4 also indicates that the heme exchange reaction occurred in both α and β subunits for nativeHb, although the rate of the reaction is somewhat different between two subunits. It is of interest to see that the exchange rate for the α subunit is almost the same as that for Mb, whereas the exchange rate for the β subunit is slower than that for Hb α subunit and Mb.

Figure 5 illustrates the heme exchange reaction of nativeHbN_3^- with mesohemin-N_3^-. The comparison with the spectrum of meso HbN_3^- has allowed us to assign of the signal at 21.0 ppm to the α and β subunits of mesoHb (Neya & Funasaki, 1986; Ishimori & Morishima, 1988a) and the peak at 23.4 ppm to the α subunit of mesoHb and nativeHb. The heme exchange reaction for mesoHb is slightly slower than deuteroHb and even after 9 days the almost of protein remained as native Hb.

Unfortunately, in native Hb, an attempt to look for the heme exchange from native heme to deuterated protoheme as found for native Mb was not successful probably due to its large molecular weight. To make sure that the heme exchange reaction occurred between native Hb and protohemin, the time course spectral changes of native HbCO in the presence of ferric protohemin-N_3^- was examined. Figure 6 shows the time course spectra 30 min (A) and 3 days (B) after addition of protohemin-N_3^-. Traces 6C and 6D

illustrated the spectra without protohemin 30 min (C) and 3 days (D) after addition of sodium azide. As clearly shown in the Figure 6, in the two spectra obtained 3 days after addition of sodium azide and/or protohemin-N_3^-, there is a remarkable difference in the relative intensities between the methyl signals for the α and β subunits. Figure 6B, which is the case of excess protohemin, shows that the methyl signals for the α subunit exhibited much larger intensities than those for the β subunit, whereas in the absence of protohemin (Figure 6D) the methyl signals formed by the auto-oxidation for the α and β subunit exhibit the comparable intensities. Therefore, such a marked different intensities arise from the difference of the heme exchange rate from the diamagnetic CO-protoheme complex to the paramagnetic azido-protoheme complex between the two subunits. Therefore, we conclude that the heme exchange rate from protohemin in the heme cavity to protohemin in bulk for the α subunit is faster than that for the β subunit.

DISCUSSION

The present NMR study has revealed that the protoheme embedded in the heme cavity is displaced by the other protoheme or modified heme in native hemoprotein as found for some Mbs and Hbs reconstituted with the modified heme (LaMar et al., 1984; Rossi-Fanelli & Antonini, 1960; Ishimori & Morishima, 1988a). For the reconstituted hemoproteins, the heme exchange reaction from the modified heme to protoheme seems to make the protein structure thermodynamically more stable. However, it is somewhat surprising that the protoheme is replaced by the modified heme to yield less stable reconstituted hemoprotein under normal conditions. Our present results show that the protoheme can be replaced from the heme crevice by the structural fluctuation induced by the normal thermal motion of the protein molecule. This implies that the heme displacement reaction arises not only from the structural unstability of the reconstituted protein or the low binding affinity of the modified heme to apoprotein as mentioned previously (Rossi-Fanelli & Antonini, 1960; LaMar et al., 1984), but also arises from the intrinsic property of native hemoproteins. In other words, the finding of the heme exchange reaction in native hemoproteins implies that the energy of the conformational fluctuation is large enough to compensate for the hydrophobic interactions and the coordination of the proximal histidine which maintain the protoheme in the heme crevice.

In order to gain further insight into details of the conformational fluctuation of native hemoproteins, the schematic representations of the

conformational fluctuation is illustrated in Figure 7. The states A and A' represent the native and the reconstituted (disordered) hemoprotein, respectively, which have similar structures to those obtained by the X-ray diffraction study. In the state B, the heme crevice is opened out and the iron-histidyl bond is weakened so that the heme can rotate about α,γ-meso axis but it is maintained with its position in the heme crevice by the hydrophobic interactions between the heme substituents and amino acid residues inside the heme crevice, forming some sort of a protein "cage" (LaMar et al, 1984). The state C has an apo-protein like structure which has no heme in the heme pocket, thereby the heme being extracted from the holoprotein against the hydrophobic interaction.

The intermediate complexes B and C have been considered to exist only in reconstituted hemoproteins (Rossi-Fanelli & Antonini, 1960; Jue et al., 1983; La Mar et al., 1978, 1984). Recently, LaMar and co-worker (LaMar et al., 1985; Yamamoto & LaMar, 1986) reported unambiguous assignment of ^{1}H NMR resonances of native hemoproteins demonstrates 2 ~ 10 % equilibrium heme disorder in native Mb, the α and β subunits of Hb. They suggested that the two heme rotational reactions, from the disordered form to the native form (A'-B-A) and from the native to the disordered (A-B-A'), simultaneously proceed and reach to an equilibrium state in native hemoprotein under the normal conditions. This implies that the large conformational fluctuation so as to rotate the heme is induced in the native hemoproteins. On the other hand, there has been no evidence for the existence of the state C in native hemoprotein, because LaMar et al (1984) concluded that the reorientation occurs by an *intra*molecular mechanism (A'-B-A), not an *intra*molecular mechanism (A'-C-A). However, present results clearly indicate the dissociation of the heme from the heme cavity and implies that the state C is generated by the conformational fluctuation in native Hb and Mb. Therefore, one can see that native hemoprotein attains equilibrium among three states A, B and C in the solution at room temperature. In other words, the apoprotein like meta-stable conformation (C) exists constantly in native hemoproteins and the thermal motion of the protein molecule promotes the large conformational fluctuation which induced the interconversion from the stable stage (A) to meta-stable state (B and C). It is, thus, likely that the native proteins may function under such a large conformational fluctuation.

It is also of interest that the relative rates of the heme exchange reaction depends on the structure of protein, not the structure of the heme; the slower

rate is observed for Hb β subunit and the faster rate for Mb and Hb α subunit. This suggests that the rate determining step of the reaction is the dissociation of protoheme from the heme cavity, but not the combination of heme to apoprotein. Since the dissociation rate of the protoheme seems to depend on the magnitude of the conformational fluctuation, the larger fluctuation is induced for the α subunits of Hb and Mb, the smaller is for the β subunit. Such a difference in the fluctuation in Mb and Hb subunits is probably due to the difference of the *intra*subunit interaction, that is, substantial difference in the van der Waals contacts in the heme environments. On the basis of NMR spectra of the hybrid heme Hbs, our previous report (Ishimori & Morishima, 1986) concluded that the modification of the heme side chains in the β subunit exerts a more subtle structural perturbation at the heme moiety than does the heme side modification in the α subunit and suggest that the interaction between the heme and amino acid residue inside the heme cavity exerts more effectively in the β subunit than in the α subunit. Such a nonequivalence induced by the intrasubunit interaction between the α and β subunits was also encountered for the metal-substituted Hbs (Inubushi et al., 1983; Shibayama et al., 1987; Ishimori & Morishima, 1988b). Moreover, the heme orientation immediately after the reconstitution of apoprotein with various hemes also indicates the nonequivalent behaviour among the hemoproteins (Ishimori & Morishima, 1988a). In the previous paper, we reported that the specificity of the heme orientation exerts more strictly in the β subunit than in the α subunit and apoMb had no heme orientational specificity. These observations indicate that the strong interaction between heme and amino acid residues in the β heme cavity make the fluctuation of the subunit small and heme exchange in the β subunit requires more energy. Therefore, the *intra*subunit interaction seriously affects the conformational fluctuation of the hemoproteins and the difference in the *intra*subunit interaction causes the various characteristic dynamic properties for hemoproteins.

In summary, the present NMR study elucidated that the conformational fluctuation in the native Hb and Mb is large enough to induce the heme displacement reaction and that the conformational fluctuation depends on the *intra*molecular interactions of hemoprotein, suggesting one feature of the fluctuation in native hemoprotein under physiological condition. Therefore, it become clear that the structure obtained by the X-ray diffraction study is not sufficient to investigate the different dynamic properties among Mb and Hb subunits and that the conformational fluctuation must be considered to

understand the functions of the proteins.

REFERENCES

Baldwin, J., & Chotia, C. (1979) *J. Mol. Biol. 129*, 175-200.

Bermann, M., Benesch, R., & Benesch, R. E. (1971) *Arch. Biochem. Biophys. 145*, 236-239.

Case, D., & Karplus, M. (1979) *J. Mol. Biol. 132*, 343-368.

Dickerson,R. E., & Geis, I (1983) *Hemoglobin: Structure, Function, Elution and Pathology,* Benjamin/Cummings, Menlo Park, CA.

Doster, W., Beece, D., Bowne, S. F., Di Iorio, E. E., Eisenstein, L., Frauenfelder, H., Reinisch, L., Shyamsunder, E., Winterhalter, K. H., & Yue, T. K. (1982) *Biochemistry 21*, 4831-4839.

Fermi, G. (1975) *J. Mol. Biol. 97*, 237-256.

Fermi, G., Perutz, M. F., Shaatian, B., & Fourme, R. (1984) *J Mol. Biol. 175*, 159-174.

Frauenfelder, H., Petsko, G. A., & Tsernoglou, D. (1979) *Nature (London) 280*, 558-563.

Gibson, Q. H., & Antonini, E. (1960) *Biochem. J. 77*, 328-341.

Inubushi, T., Ikeda-Saito, M., & Yonetani, T. (1983) *Biochemistry 22*, 2904-2907.

Ishimori, K, & Morishima, I. (1986) *Biochemistry 25*, 4892-4898.

Ishimori, K, & Morishima, I. (1988a) *Biochemistry 27*, 4747-4753.

Ishimori, K, & Morishima, I. (1988b) *Biochemistry 27*, 4066-4066.

Jue, T., Krishnamoorthi, R., & LaMar, G. N. (1983) *J. Am. Chem. Soc. 105*, 5701-5703.

Karplus, M. S., & McCanmon, J. A. (1981) *CRC Crit. Rev. Biochem. 9*, 273-349.

LaMar, G. N., Budd, D. L., Viscio, D. B., Smith, K. M., & Langry, K. C. (1978) *Proc. Natl. Acad. Sci. U. S. A. 75*, 5755- 5759.

LaMar, G. N., Burns, P. D., Jackson, T. J., Smith, K. M., Langry, K. C., & Strittmatter, P. (1981) *J. Biol. Chem. 256*, 6075-6079.

LaMar, G. N., Krishnamoorthi, R., Smith, K. M., Gersonde, K., & Sick, H. (1983) *Biochemistry 22*, 6239-6246.

LaMar,G. N., Toi, H., & Krishnamoorthi, R. (1984) *J. Am. Chem. Soc. 106*, 6395-6401.

LaMar, G. N., Yamamoto, Y., Jue. T., Smith. K. M., & Pandey, R. K. (1985) *Biochemistry 24*, 3826-3831.

Levy, A., & Rifkind, J. M. (1985) *Biochemistry 24*, 6050-6054.
Neya, S., & Funasaki, N. (1986) *Biochemistry 25*, 1221-1226.
Ondrias, M. R., Friedman, J. M., & Rousseau, D. L. (1983) *Science (Washington, D.C.) 220*, 615-617.
Perutz (1970) *Nature (London) 228*, 726-739.
Rose, M. Y., & Olson, J. S. (1983) *J. Biol. Chem. 258*, 4298-4303.
Rossi-Fanelli, A., & Antonini, E. (1960) *J. Biol. Chem. 235*, PC4.
Tainer, J. A., Getzoff, E. D., Alexander, H., Houghton, R. A., Olson, A. J., Lerner, R. A., & Hendrickson, W. A. (1984) *Nature (London) 312*, 127-134.
Yamamoto, Y. & LaMar, G. N. (1986) *Biochemistry 25*, 5288-5297.
Westhof, E., Allschuh, D., Moras, D., Bloomer, A. C., Mondragon, A., Klug, A., & Van Regenmortel, M. H. V. (1984) *Nature (London) 311*, 123-126.

FIGURE LEGENDS

Figure 1.

Downfield hyperfine-shifted portion of the 300MHz ^{1}H NMR spectra of native Mb as the met-azido complex with and without met-azido deuterohemin at pH 7.0 and 23 °C. (A) Without met-azido deuterohemin. (B) 3 days, (C) 8 days, (D) 16 days after the addition of met-azido deuterohemin.

Figure 2.

Downfield hyperfine-shifted portion of the 300MHz ^{1}H NMR spectra of native Mb as the met-azido complex with and without met-azido mesohemin at pH 7.0 and 23 °C. (A) Without met-azido mesohemin. (B) 3 days, (C) 8 days, (D) 16 days after the addition of met-azido mesohemin.

Figure 3.

Downfield hyperfine-shifted portion of the 46.1 MHz ^{2}H NMR spectra of native Hb as the met-azido complex with met-azido [*methyl*-1,3-^{2}H]protohemin at pH 7.0 and 23 °C. (A) 4 hours (B) 4 days, (C) 7 days, (D) 15 days after the addition of met-azido [*methyl*-1,3-^{2}H]protohemin.

Figure 4.

Downfield hyperfine-shifted portion of the 300MHz ^{1}H NMR spectra of native Hb as the met-azido and CO complex with and without met-azido deuterohemin at pH 7.0 and 23 °C. (A) Without met-azido deuterohemin. (B) 1 days, (C) 2 days after the addition of met-azido deuterohemin. (D) 8 days after the addition of met-azido deuterohemin with ferricyanide.

Figure 5.

Downfield hyperfine-shifted portion of the 300MHz ^{1}H NMR spectra of native Hb as the met-azido and CO complex with and without met-azido mesohemin at pH 7.0 and 23 °C. (A) Without met-azido mesohemin. (B) 1 days, (C) 2 days after the addition of azido mesohemin. (D) 8 days after the addition of met-azido mesohemin with ferricyanide.

Figure 6.

Downfield hyperfine-shifted portion of the 300MHz ^{1}H NMR spectra of native Hb as the met-azido and CO complex with and without met-azido

protohemin at pH 7.0 and 23 °C. (A) 30 minutes, (B) 3 days after the addition of met-azido protohemin. Without protoheme (C) 30 minutes, (D) 3 days after the addition of sodium azide.

Figure 7.

Schematic representations of the conformational fluctuation of the protein (see text).

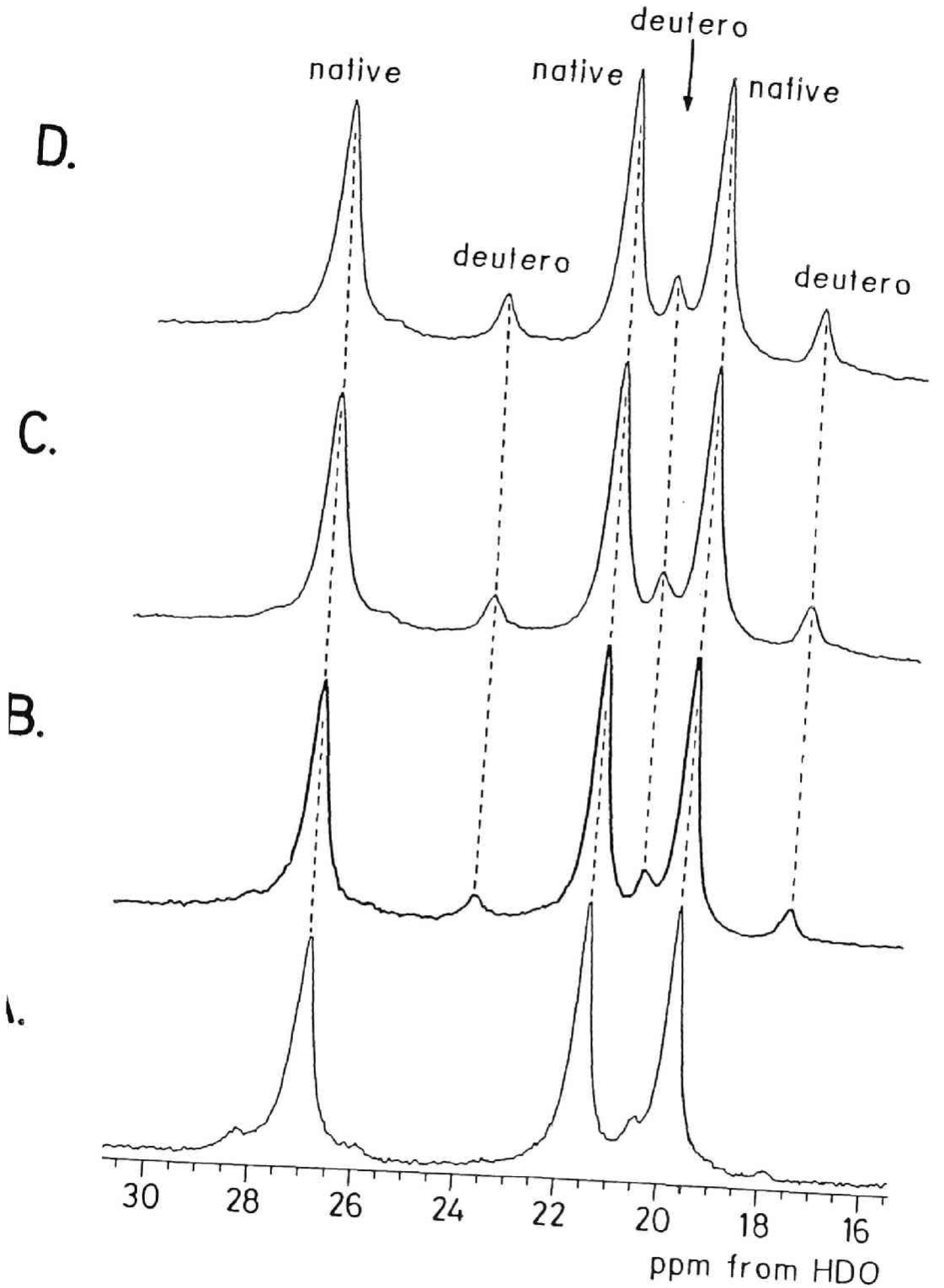
deutero
native
native
native
D.
deutero
deutero
C.
B.
30
28
26
24
22
20
18
16
ppm from HDO

Figure. 1

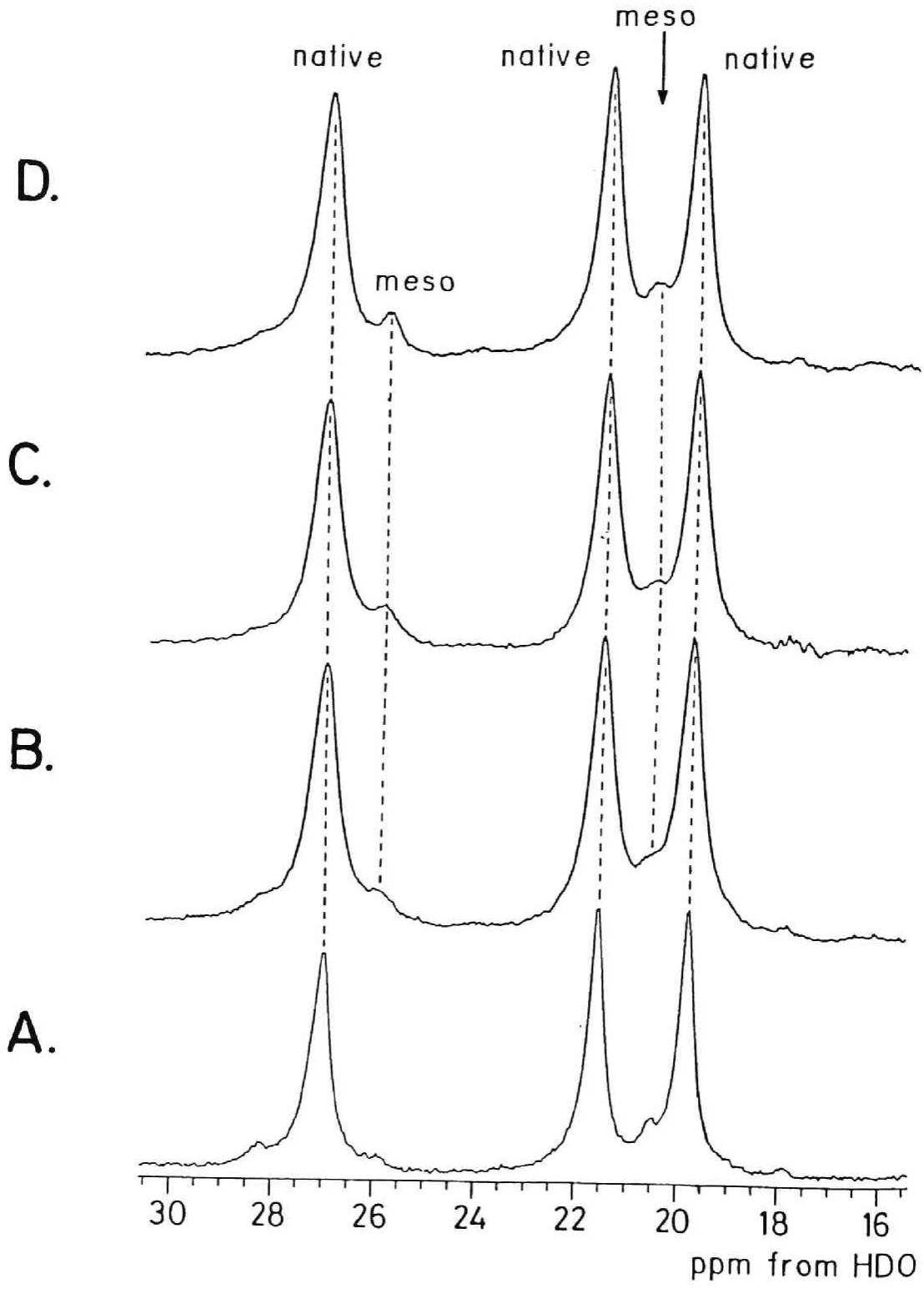
meso
native
native
native
D.
meso
C.
B.
A.
30
28
26
24
22
20
18
16
ppm from HDO

Figure. 2

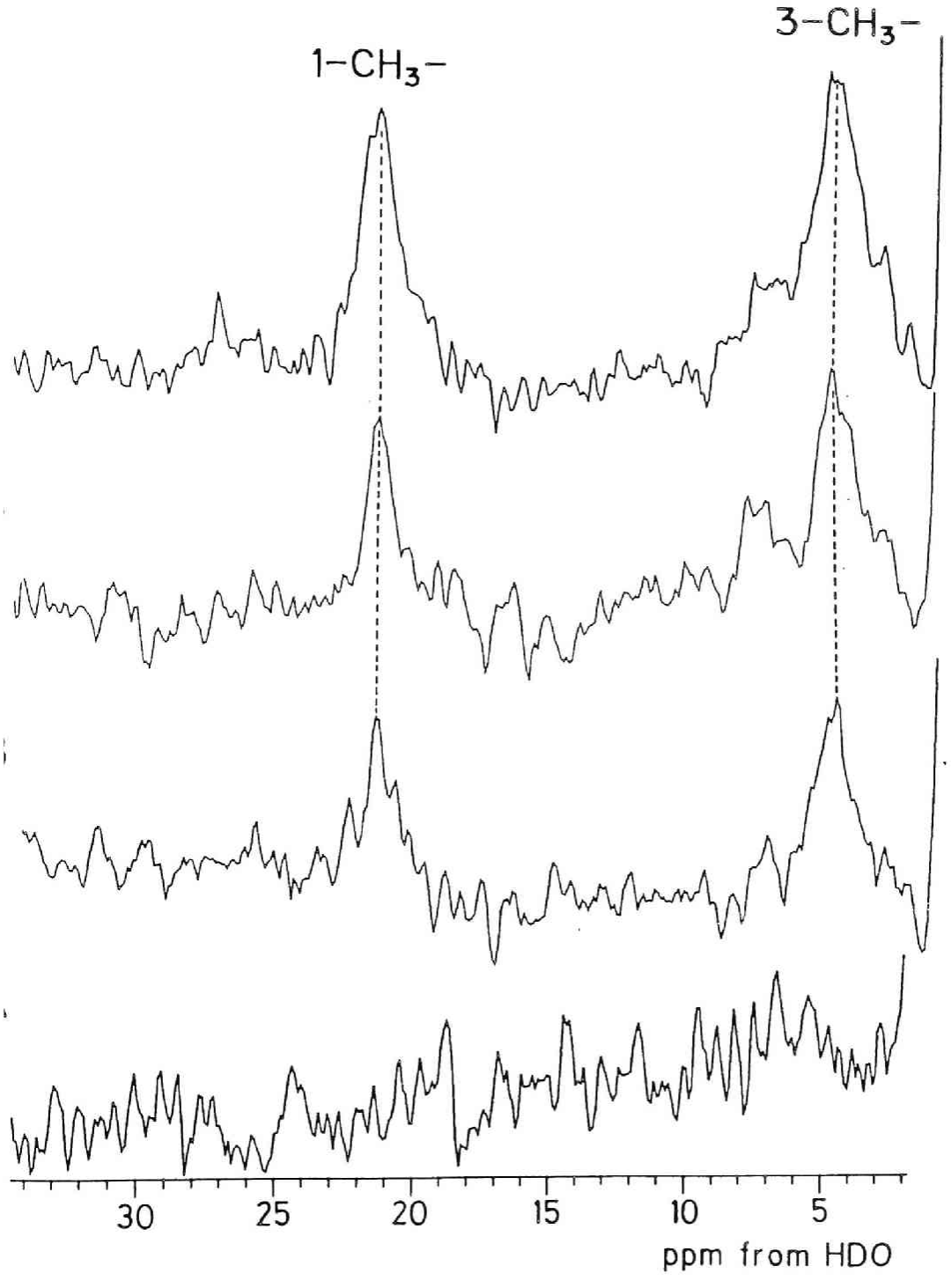

Figure. 3

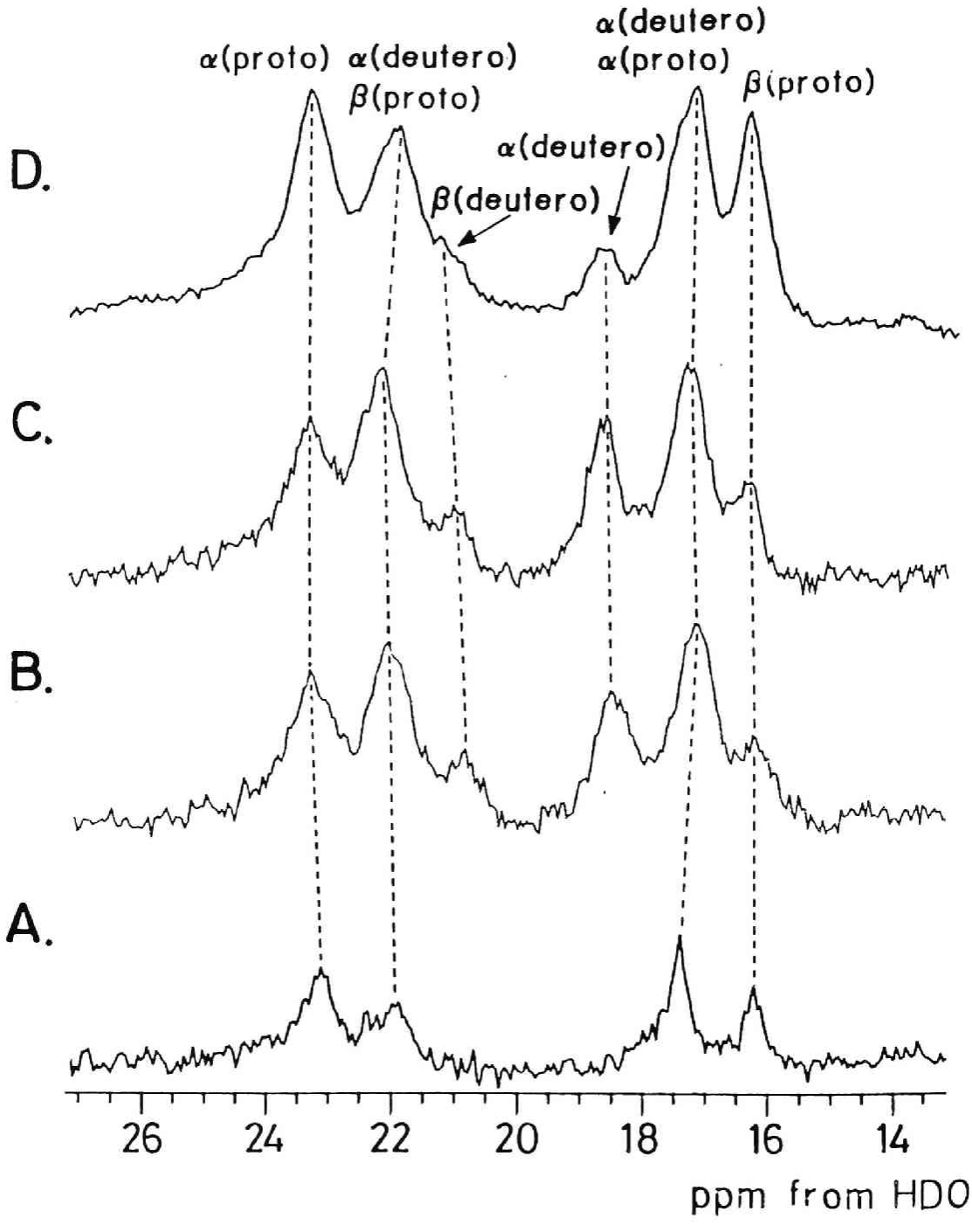
α(proto)
α(deutero)
β(proto)
α(deutero)
α(proto)
β(proto)
α(deutero)
β(deutero)
D.
C.
B.
A.
26
24
22
20
18
16
14
ppm from HDO

Figure. 4

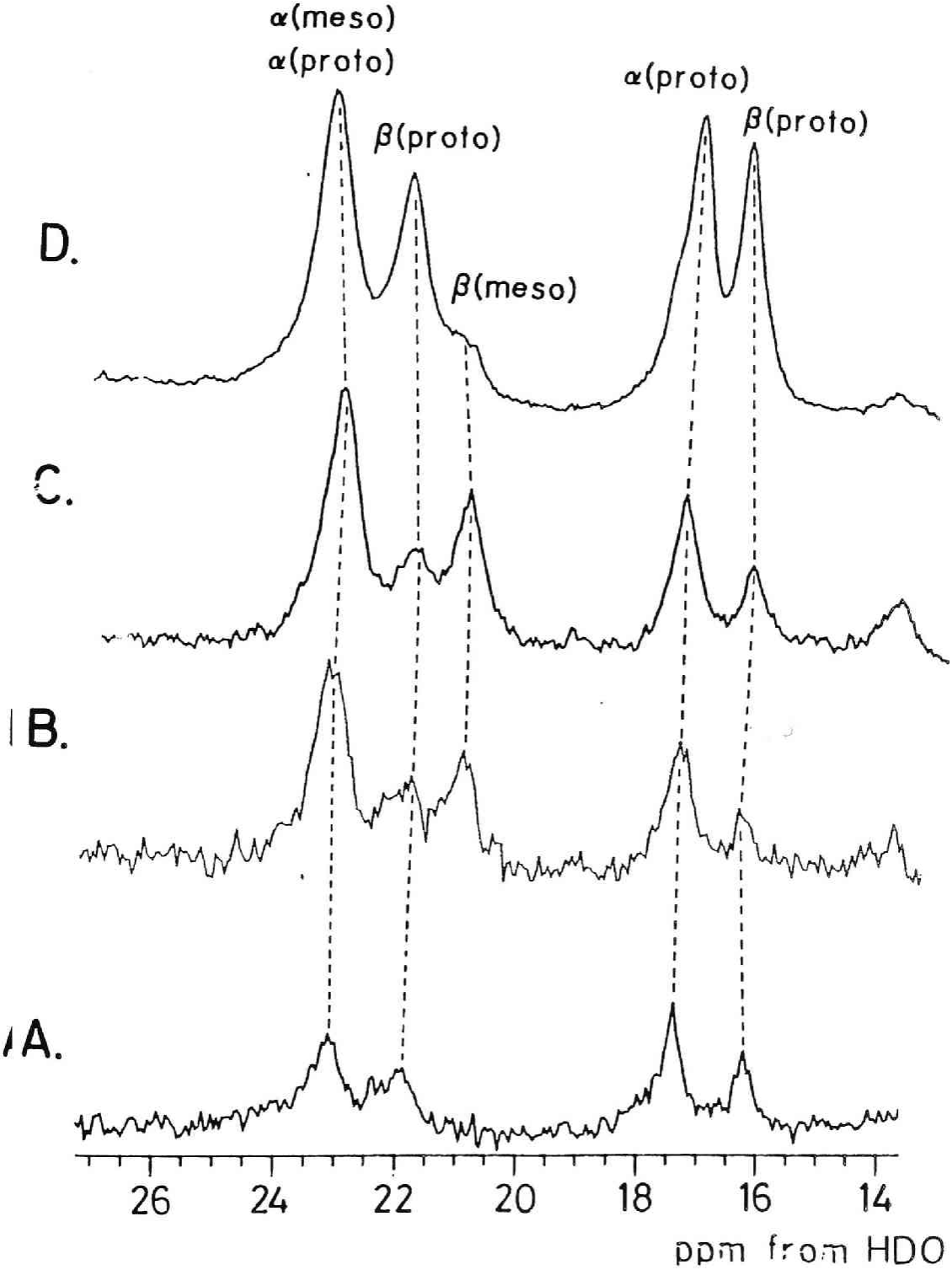
α(meso)
α(proto)
β(proto)
β(meso)
α(proto)
β(proto)
D.
C.
B.
A.
26
24
22
20
18
16
14
ppm from HDO

Figure. 5

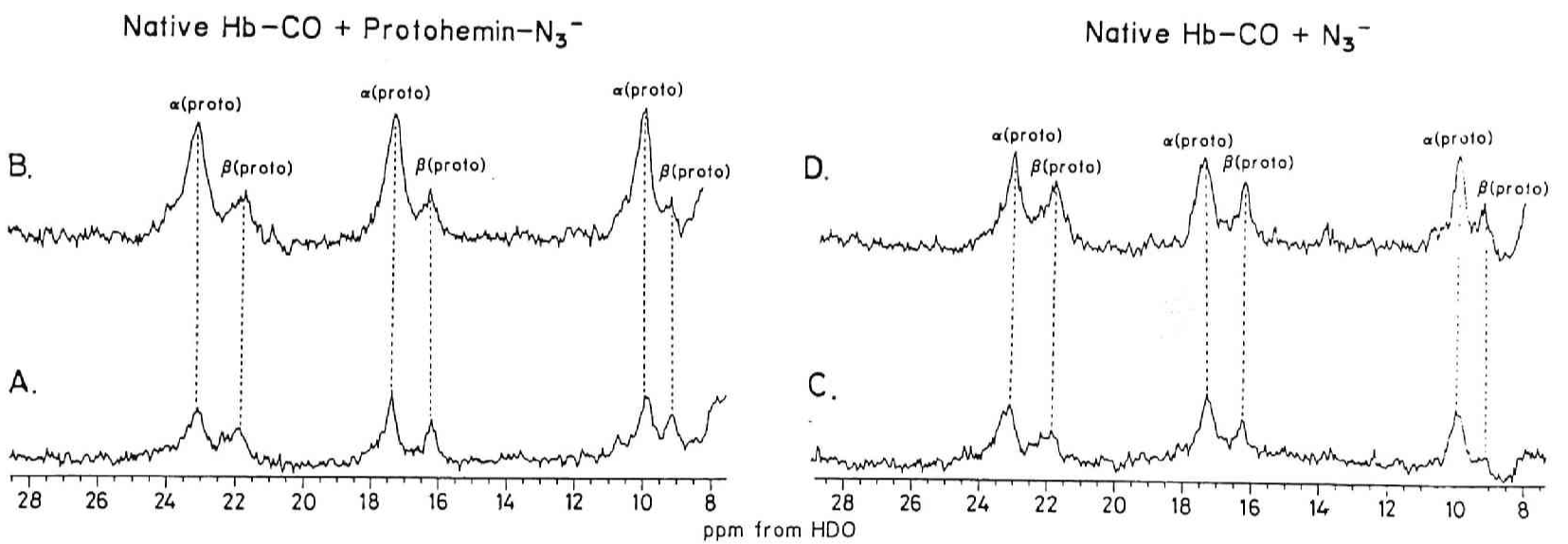
Native Hb−CO + Protohemin−N3−
Native Hb−CO + N3−
α(proto)
β(proto)
B.
A.
D.
C.
28
26
24
22
20
18
16
14
12
10
8
ppm from HDO

Figure. 6

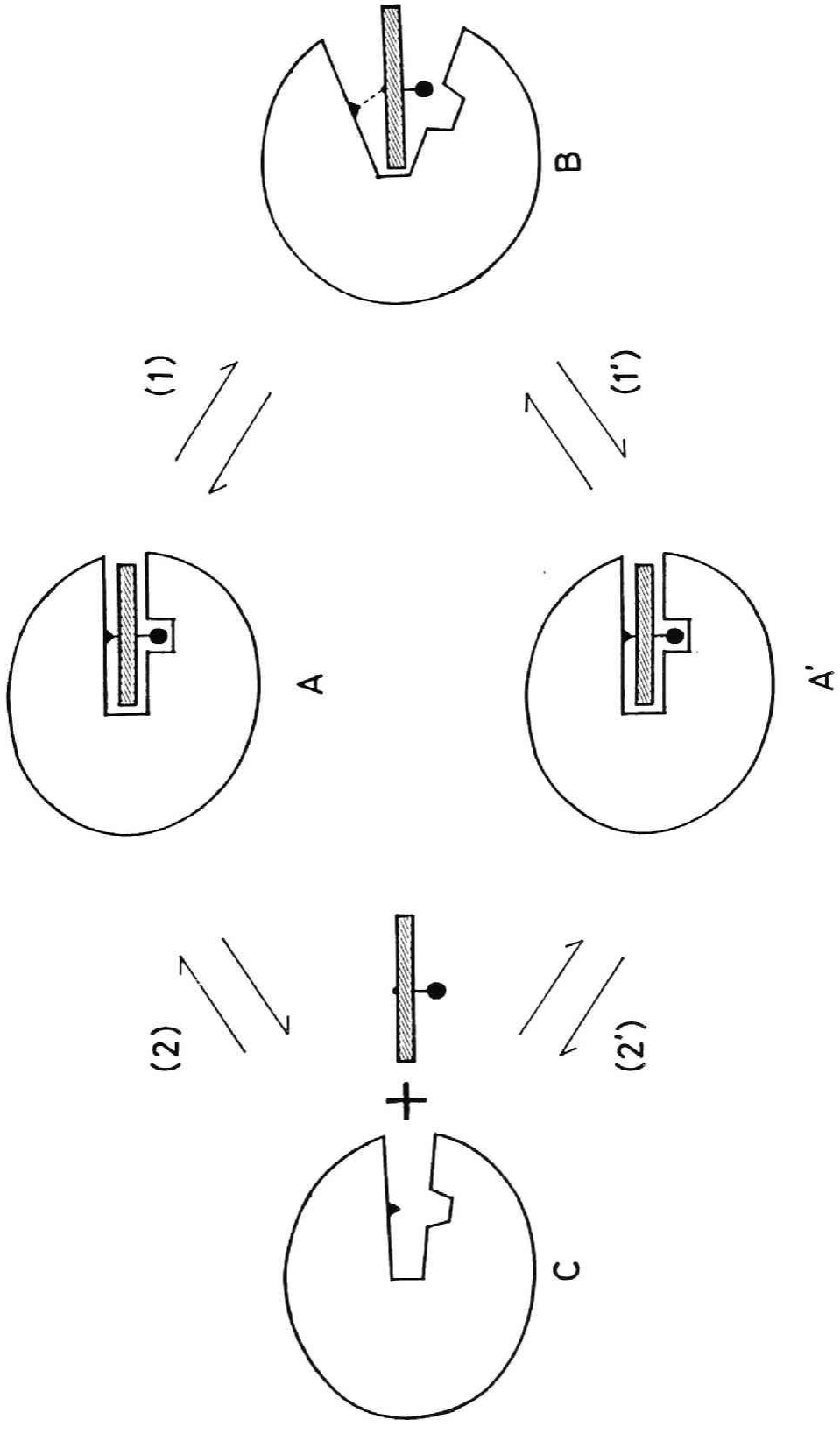

Figure. 7

CHAPTER 4.

Spin-State Equilibrium of the α and β Subunits in Some Hybrid Hemoglobins:

NMR and Low Temperature Absorption Spectra Investigation.

ABSTRACT: To get a insight for the effect of the subunit-subunit interaction on the spin-equilibrium, we examined here the spin-equilibrium in two hybrid hemoglobins containing one met (azidomet- and isocyanate met-) subunit and one carboxy subunit. From analysis of the temperature-dependent visible spectral changes and shifts of the heme methyl resonances, the thermal spin-state equilibria of the α and β subunits in the hybrids were independently analysed. The thermodynamic values of the spin-equilibrium of the isocyanate met α and β subunits in the isocyanate-carboxy hybrid hemoglobins were comparable with those of the intact tetramer, suggesting that the spin-equilibrium properties are almost independent of the spin-state of the partner subunit in isocyanate met hemoglobin. However, a comparison of the thermodynamic values of the azidomet-carboxy hybrids and the intact tetramer revealed that the values of the α subunit are almost identified to those of the intact azidomet tetramer, while the β subunit in the hybrid hemoglobin exhibited the smaller negative values of entropy and enthalpy between the low and high spin state. This shows that the spin-equilibrium of the β subunits affected by the spin-state changes of the complementary subunit, that is, from the spin-equilibrated azido heme to the pure low spin carboxy heme through the subunit-subunit interaction.

During the past a few decades experimental evidence from different sources has indicated that the subunit-subunit interaction has a key role of the cooperative phenomenon of hemoglobin (Hb[12]). [for example, see Monad et al.(1965) and Koshland et al. (1966)] The X-ray structural analyses of Hb crystals carried out by Perutz and his colleagues clearly show many interaction between the subunits of Hb such as hydrogen bonds, salt bridges and van der Waals contacts (Perutz, 1970; Perutz & Ten Eyck,1971; Fermi, 1975). These interaction is believed to be important for the structure-function relationship of Hb and many spectroscopic studies such as NMR (Miura & Ho, 1982,1984, Nagai et al., 1982; Ishimori & Morishima, 1986,1988), ESR (Miura & Morimoto, 1980) or resonance Raman (Nagai & Kitagawa, 1980) have tried to elucidate the mechanism of the subunit-subunit interaction. The changes of the spin-state by the subunit-subunit interaction, which has been paid considerable attention because changes of the spin-state involved in ligand binding to deoxyhemoglobin, however, only few paper have investigated the subunit-subunit interaction in terms of the changes of the spin-state (Henry et al., 1985; Neya and Funasaki, 1986).

In order to examine the effect of the subunit-subunit interaction on the spin-state, the spin-equilibrium Hbs can be utilized as one of the most suitable model. The spin-equilibrium is observed in the case for the binding of some ligands to heme iron (Iizuka & Yonetani, 1970), some of them have been extensively characterized with Mössbauer (Winter et al., 1972), infrared (McCoy & Caughey, 1970; Alben & Fager, 1972), resonance Raman (Scholler & Hoffman, 1979; Cho, et al., 1981), ESR (Scholler & Hoffman, 1979), visible absorption (Neya et al., 1983) and NMR (Iizuka & Morishima, 1974; Morishima et al., 1978; Neya & Morishima, 1980 Neya & Funasaki, 1986) spectroscopies and magnetic susceptibility measurements (Beetlestone & George, 1964; Iizuka & Kotani, 1969; Philo & Dreyer, 1985; Messana et al., 1978). Although these previous studies revealed the detailed magnetic properties of the intact or the reconstituted Hbs containing four ferric hemes, the effect of the subunit-subunit interaction on the spin-equilibrium is not clear.

In this chapter, we examined the spin-equilibrium for two different valency hybrid Hbs containing one spin-equilibrium subunit and compared with their thermodynamic values of the intact spin-equilibrated tetramer to discuss the effect of the spin-state changes in one subunit on the spin-

[12]Abbreviations used: Hb, hemoglobin; NMR, nuclear magnetic resonance; ESR, electron spin resonance; Bis-Tris; [bis(2-hydroxyethyl)imino]tris(hydroxymethyl)methane

equilibrium in another subunit through the subunit-subunit interaction.

MATERIALS AND METHODS

Sample Preparation. Human adult hemoglobin was prepared from whole blood as reported previously (Morishima & Hara, 1983). The isolated α and β chains were prepared by the method of Ikeda-Saito et al. (1981).

The isocyanate-carboxy hybrid Hbs were prepared by addition of potassium isocyanate to aquomet-carboxy hybrids. The aquomet-carboxy hybrids and ruthenium-iron hybrid Hbs were obtained as the previous reports (Morishima et al., 1986; Ishimori & Morishima, 1988).

Measurement of Low Temperature Absorption Spectra. Visible and ultraviolet absorption spectra were recorded on a Shimadzu MPS-2000 spectrophotometer quipped with a nitrogen Dewar. Sample temperature was controlled to ±0.1 °C with a heater and monitored with a thermocouple detector.

Measurement of NMR Spectra. Proton NMR spectra at 300 MHz were recorded on a Nicolet NT-300 spectrometer equipped with a 1280 computer system. Probe temperature was determined by the temperature control unit of the spectrometer, accurate to ±0.5 °C. The volume of the NMR sample was 0.3 mL, and heme concentration was about 2 mM. Proton shifts (± 0.01 ppm) were referenced with respect to the proton resonance of 4,4-demethyl-4-silapentane-1-sulfonate (DSS).

Data Analysis. Computer-assisted data analysis was carried out on a NEC PC-9800 microcomputer as reported previously (Neya & Funasaki, 1986).

RESULTS

Low Temperature Absorption Spectra of the Isocyanate Isolated Chains and Isocyanate-Carboxy Valency Hybrid Hemoglobins. Figure 1 illustrates the temperature-dependent visible spectra of the isolated α and β chains. For the α chain (A), the raising temperature led to the increase of the peak at 625 nm which is assignable to the "high spin band" and concomitantly reduced the intensities of the peaks at 537 and 560 nm arising from the "low spin" component. Three isosbestic points at 466, 516 and 470 nm were found in the visible region. These spectral changes are closely similar to those reported for isocyanate met tetramer (Iizuka & Yonetani, 1970). The spectral changes for the β chain (B) is somewhat different from that of the α

chain (A) as shown in Figure 1. Although the "high spin" peak at 625 nm increased its peak intensity, its spectral changes are smaller than those of the α chain or the intact tetramer. The isosbestic points (465, 520 and 475 nm) are almost the same as found for the α subunit and the intact tetramer.

In Figure 2, the temperature-dependent visible spectra of isocyanate-carboxy valency hybrids, $\alpha(Fe^{III}\text{-}OCN^-)_2\beta(Fe^{II}\text{-}CO)_2$ (A) and $\alpha(Fe^{II}\text{-}CO)_2\beta(Fe^{III}\text{-}OCN^-)_2$ (B), are shown. The spectral feature of the α-isocyanate met hybrid exhibited three peaks at 536, 570 and 626 nm and its temperature-dependence spectra has no isosbestic points. With raising temperature, the absorption increased in all visible range. Since the increase of the "high spin band" absorption was observed, the "low spin band" should lose its peak intensity. However, the absorption from 500 to 580 nm, in which the "low spin band" appears, also increased, not decreased. This observation implies that the absorption changes in the carboxy subunits were induced by raising temperature. For the β isocyanate hybrid, its temperature-dependent absorption spectra were almost identical to that of its counterpart hybrid, but some significant differences were detected. These spectra have the peaks at 536, 570 and 626 nm and a comparison of the visible spectra of the two hybrids indicates that the peaks at 536 and 570 nm of the β isocyanate met hybrid, $\alpha(Fe^{II}\text{-}CO)_2\beta(Fe^{III}\text{-}OCN^-)_2$, were sharper than those of the complementary hybrid $\alpha(Fe^{III}\text{-}OCN^-)_2\beta(Fe^{II}\text{-}CO)_2$. The "high spin" peak around 625 nm was sharper in $\alpha(Fe^{III}\text{-}OCN^-)_2\beta(Fe^{II}\text{-}CO)_2$ than in $\alpha(Fe^{II}\text{-}CO)_2\beta(Fe^{III}\text{-}OCN^-)_2$, corresponding to the difference between the isolated α and β chains.

Analysis of the Absorption Spectra. The absorbance of Hb in the spin-equilibrium is presented as a weighted average:

$$A = (1-\alpha)A_L + \alpha A_H$$

where A_L and A_H are absorbance of the pure low and high spin conformer, respectively, and α is the high spin conformer fraction. The best values of A_L and A_H are defined as those that give a linear van't Hoff equation. The estimation of these values are performed as described previously (Neya et al., 1983; Neya & Funasaki, 1986). The ΔH and ΔS associated with the spin equilibrium of the isocyanate met hemoglobin derivatives are calculated from a van't Hoff Hoff equation:

$$\ln\frac{A_L - A}{A - A_H} = -\frac{\Delta H}{R}\frac{1}{T} + \frac{\Delta S}{R}$$

The estimated ΔH and ΔS are summarized in Table I.

Temperature-Dependent NMR Spectra of Ruthenium(II)-Iron(III) Metal Hybrid Hemoglobin. In order to get further insight of the spin-equilibrium in the hybrid Hbs containing one ferric subunit, we tried to measure the temperature dependence absorption spectra of azidomet-carboxy hybrid Hbs. Unfortunately, azidomet-carboxy hybrid Hbs gradually oxidized to the azidomet Hb due to the oxidation by azido ion. Therefore, we could not get the reliable data from the temperature dependent absorption spectra of azidomet-carboxy hybrid Hbs. To avoid the oxidation of the carboxy-heme, ruthenium(II)-carbonmonoxyporphyrin which was served as a model for the stable carboxy-heme (Ishimori & Morishima, 1988) could be utilized. However, ruthenium(II)-iron(III) hybrid Hbs were less stable than the intact tetramer, it is difficult to measure their absorption spectra above room temperature because of the formation of some precipitate. Thus, we decided to investigate the temperature-dependent NMR measurement of ruthenium(II)-iron(III) hybrids, which was expected to the precise examination. Figure 3 shows some proton NMR spectra of ruthenium(II)-iron(III) azidomethemoglobins, $\alpha(Fe^{III}\text{-}OCN^-)_2\beta(Ru^{II}\text{-}CO)_2$ (A) and $\alpha(Ru^{II}\text{-}CO)_2\beta(Fe^{III}\text{-}OCN^-)_2$ (B) , recorded in the 5 - 50 °C. The chemical shifts of the heme methyl protons are temperature-dependent; some of peaks show upfield shift and others down field shift with increasing temperature. Figure 4 illustrates the temperature dependence of the heme methyl shifts. It is to be noted that all the heme methyl shifts exhibit deviation from Curie law, which predicts linear temperature dependence of the hyperfine-shifted resonance shift on the reciprocal of absolute temperature (Wüthrich, 1970), as found for native azido Hb. In addition, the α_3-heme and β_3-heme methyl peaks in Figure 4 show slopes opposite in sign to those expected from the Curie law. These deviations from the Curie law are indicative of thermal spin-state equilibrium between the high- and low-spin states (Iizuka & Morishima, 1974; Morishima et al., 1978; La Mar et al., 1983). The analysis of the heme methyl shifts were carried out by use of the following equation (Neya & Funasaki, 1986):

$$\ln\frac{H \quad T(\delta - 3.6)}{T(\delta - 3.6) \quad - L} = -\frac{\Delta H}{R}\frac{1}{T} + \frac{\Delta S}{R}$$

where L and H are temperature dependence of the spin equilibrium constant, δ is the observed methyl shift and T is absolute temperature. In Tables II and III are summarized the parameters obtained from the analysis.

DISCUSSION

Spin-State Equilibrium in the Isolated Isocyanate α and β Subunits and Isocyanate-Carboxy Valency Hybrid Hemoglobins. Present results show that the isocyanate met α and β subunits as the isolated chain and in the isocyanate met-carboxy valency hybrid Hbs are in the spin-equilibrium state between the "high spin" and the "low spin". As shown in Table I, the ΔH values for the isolated α and β subunits (- 760 and - 700 cal/mol, respectively) were essentially similar to that of intact isocyanate met tetramer (- 710 cal/mol) (Iizuka & Yonetani, 1970), although the ΔH for the isolated α subunit exhibited slightly larger negative value. Therefore, the spin-equilibrium in the α and β isocyanate met subunit is not affected by the combination of another spin-equilibrium subunit. In other words, the spin-equilibrium by binding of isocyanate ion is one of the inherent properties of the isolated subunits.

The substitution from isocyanate heme to carboxy heme in one subunit allows independent examination of the spin equilibria of the α and β subunits in tetramer. It is to be noted that the two isocyanate met-carboxy hybrid Hbs (- 650 cal/mol for $\alpha(Fe^{III}\text{-}OCN^-)_2\beta(Fe^{II}\text{-}CO)_2$ and - 700 cal/mol for $\alpha(Fe^{II}\text{-}CO)_2\beta(Fe^{III}\text{-}OCN^-)_2$) also give almost the similar values of ΔH to that of the tetramer. ΔH of α-isocyanate met hybrid was slightly smaller negative value. Such a comparison of the ΔH values of isocyanate met-carboxy hybrid Hbs and intact Hb indicates that the spin-equilibrium in the isocyanate met β subunit is independent of the spin state of the partner α subunit and the isocyanate met α subunit is slightly affected by the spin state of the β subunit, however, the deviations of its thermodynamic values in the isolated chain and the hybrid from the intact one are relatively small. Therefore, these observations imply that the spin-equilibrium in one isocyanate subunits cannot be drastically perturbed by the changes of the spin state in the complementary subunit. The spin-equilibrium arising from isocyanate bound heme is not regulated by the binding of the other spin-equilibrium subunits and the changes of the spin state in the other subunit.

Although previous papers has revealed that the nonequivalence between the α and β subunits encountered for many physicochemical and physiological properties, it is interesting that the difference of the spin-equilibrium properties in two isocyanate met subunit is rather small. This similarity was observed for the intact azido Hb (Neya & Funasaki, 1986). Above discussion indicates that the spin-equilibrium properties of isocyanate heme is almost independent of the structure of globin. Therefore, one can

conclude that the nature of the spin-equilibrium in isocyanate Hb is primary determined by the heme itself and the structural difference of the heme vicinity has little effect on the spin-equilibrium as suggested for azidohemoprotein (Neya & Funasaki, 1986). It is likely that the thermodynamic parameters of isocyanate met hemoprotein can be also thought to arise from the intrinsic values of the prosthetic group.

Spin-State Equilibrium in Ruthenium(II)-Iron(III) Azidomethemoglobin. Proton NMR spectra observation of ruthenium(II)-iron(III) azidomet Hbs allows independent examination of the spin equilibria of the α and β subunits in the hybrid tetramer. The thermodynamic values of the α subunit in the hybrid, ΔH = - 5000 cal/mol and ΔS = 11.5 eu, compare well with the spin equilibrium parameters obtained from the α subunit of the intact tetramer (ΔH = - 4980 cal/mol and ΔS = -13.3 eu) and the bulk paramagnetic susceptibility (Iizuka & Kotani, 1969), infrared (Alben & Fager, 1972), and visible absorption (Neya et al., 1983) measurements. The free-energy change, ΔG, were determined to be -1600 cal/mol for the α-azidomet hybrid and -1100 cal/mol for the α subunit of the intact tetramer (Neya & Funasaki, 1986). These value indicate that the low spin state is more stable in the hybrid than in the intact tetramer. The compensation temperature of the α-azidomet hybrid is higher than that of the intact tetramer, also suggesting the stabilization of the low spin state in the α subunit. Thus, although a drastic change in the spin-equilibrium of the α subunit did not occur, the substitution from the spin-equilibrated heme (azidomet heme) to the pure low spin heme (carboxy heme) induced the stabilization of the low spin state in the α subunit.

On the other hand, the β subunit in the hybrid Hb exhibited smaller negative thermodynamic values (about 60 %) than those of intact Hb. The drastic change of ΔH and ΔS of the β subunit in the hybrid implies that the spin state of the β subunit is affected by spin-state of the partner α subunit. The compensation temperature,T_c, was estimated to 405 K for the β subunit in the intact tetramer (Neya and Funasaki, 1986) and 500 K for that in the β-azidomet hybrid Hb, implying that in the azidomet-carboxy hybrids the low spin state is more stable than in the intact tetramer. However, the free-energy change accompanying the transition between the high and low spin, ΔG_{HS}, was determined to be -1400 cal/mol for the β subunit of the intact tetramer and -1200 cal/mol for the β-azidomet hybrid. The decrease of ΔG_{HS} value shows that the energy difference between the high and low spin state is smaller in the hybrid than in the intact tetramer and indicates the

stabilization of the high spin state. Such discrepant results suggest that the significant changes of the mechanism of the spin-equilibrium are induced. The changes of the spin-equilibrium in the β-azidomet hybrid Hb indicate two conformational alterations from the intact tetramer. One is a change of van der Waals contact between heme and globin. Otsuka (1970) found that the low spin fraction is reduced by increase of the van der Waals contact. It is likely that by the substitution from azido heme to carboxy heme of the α subunit, the van der Waals contact between heme and amino acid residue in the β subunit were changed by subunit-subunit interaction. Second point is a deviation of the bond between heme iron and proximal histidine. Neya et al. reported (1985) that the spin-equilibrium mechanism of hemin-azido-imidazole systems inside and out side of the heme pocket are essentially identical and the position of spin equilibrium was primarily determined by the ligand field strength of the axial base trans to the azide by use of the model complex. In view of the model complex study and the present spin equilibrium analysis of the β subunit in the hybrid and intact tetramer, it is likely that the substitution of the azido heme to carboxy heme in the α subunit induces some structural changes around heme vicinity such as changes of van der Waals contacts and the bond strain of Fe-N_ε(His F8) in the β subunit through subunit-subunit interaction, however, the detailed structural changes requires more investigation.

It is interesting that the effect of the heme substitution on the spin-equilibrium was preferentially enhanced in the case of the azidomet-carboxy hybrids, not in isocyanate met-carboxy hybrids. Although the detailed mechanism to regulate the spin-equilibrium has been unclear yet, this observation suggests that the spin-equilibrium mechanism of the hemoproteins is depends on their spin-equilibrated ligand. The changes of the interaction from the globin, which arise from another subunit through the subunit-subunit interaction, also has a effect on the mechanism of the spin-state under certain ligand binding condition.

REFERENCES

Alben, J. C., & Fager, L. Y. (1972) *Biochemistry 11*, 842-847.

Beetlestone, J., & Geroge, P. (1964) *Biochemistry 3*, 707-714.

Fermi, G. (1975) *J. Mol. Biol. 97*, 237.

Henry, E. R., Rousseeau, D. L., Hopfield, J. J., Noble, R. W., & Simon, S. R. (1985)*Biochemistry 24*, 5907-5918.

Iizuka, T., & Kotani, M. (1969) *Biochim. Biophys. Acta 371* , 1-13.

Iizuka, T., & Yonetani, T. (1970) *Adv. Biophys. 1*, 157.
Iizuka, T.,& Morishima, I. (1974) *Biochim. Biophysi. Acta 371*, 1-13.
Ishimori, K., & Morishima, I. (1986) *Biochemistry 25*, 4892-4898.
Ishimori, K., & Morishima, I. (1988) *Biochemistry 27*, 4060-4066.
La Mar, G. N., Krishnamoorthi, R., Smith, K. M., Gersonde, K., & Sick, H. (1983) *Biochemistry 22*, 6239-6246.
Messana, C., Cerdonio, M., Shenkin, P., Noble, R. W., Fermi, G. F., Perutz, R. N., & Perutz, M. F. (1978) *Biochemistry 17*, 3652-3662.
McCoy, S., & Caughey, W. S. (1970) *Biochemistry 9*, 2387-2393.
Miura, S., & Morimoto, H. (1980) *J. Mol. Biol. 143*, 213-221.
Miura, S., & Ho, C. (1982) *Biochemistry 21*, 6280-6287.
Miura, S., & Ho, C. (1984) *Biochemistry* 23, 2492-2499.
Morishima, I., Neya, S., Inubushi, T., Yonezawa, T., & Iizuka, T. (1978) *Biochim. Biophys. Acta 534*, 307-316.
Morishima, I., & Hara, M. (1983) *J. Biol. Chem. 258*, 14428-14432.
Nagai, K., & Kitagawa, T. (1980) *Proc. Natl. Acad. Sci. U.S.A. 77*, 2033-2037.
Nagai, K., La Mar, G. N., Jue, T., & Binn, H. F. (1982) *Biochemistry 21*, 842-847.
Neya, S., Hada, S., & Funasaki, N. (1983) *Biochemistry 22*, 3686-3691.
Neya, S., Hada, S., Funasaki, N., Umemura, J., & Takenaka, T. (1985) *Biochim. Biophys. Acta 827*, 157-163.
Neya, S., & Funasaki, N. (1986) *Biochemistry 25*, 1221-1226.
Neya, S., & Morishima, I. (1980) *Biochemistry 19*, 258-265.
Otsuka, J. (1970) *Biochim. Biophys. Acta 214*, 233-235.
Perutz, M. F. (1970) *Nature (London) 228*, 726.
Perutz, M. F., & Ten Eyck, L. F. (1971) *Cold Spring Harbor Symp. Quant. Biol. 36*, 295.
Philo, J. S., & Dreyer, U. (1985) *Biochemistry 24*, 2985-2992.
Scholler, D. M., & Hoffman, B. M. (1979) *J. Am. Chem. Soc. 101*,1665-1662.
Scholler, D. M., Wang, N. -Y. R., & Hoffamn, B. M. (1979) *Methods Enzymol. 52*, 487-493.
Winter, M. R. C., Johnson, C. E., Lang, G., & Williams, R. J. P. (1972) *Biochim. Biophys. Acta 263*, 515-534.
Wüthrich, K. (1970) in *Structure and Bonding* (Hemmerich, R., Jorgensen, C. K., Neilands, J. B., Nyholm, S. R. S., Reinen, D., Williams, R. J. P., Eds.) Vol. 8, pp53-121, Springer-Verlag, West Berlin.

FIGURE LEGENDS

Figure 1.

Thermal spectra of azidomet subunit, (A) $\alpha(Fe^{III}\text{-}OCN^-)$ and (B) $\beta(Fe^{III}\text{-}OCN^-)$, in 0.1 M NaN_3 plus 50 mM Bis-Tris pH 6.5. Spectra were recorded in a 117.0 - 179.0 K for $\alpha(Fe^{III}\text{-}OCN^-)$ and 134.5 - 186.9 K for $\beta(Fe^{III}\text{-}OCN^-)$.

Figure 2.

Thermal spectra of azidomet-carboxy valency hybrid Hbs, (A) $\alpha(Fe^{III}\text{-}OCN^-)_2\beta(Fe^{II}\text{-}CO)_2$ and (B) $\alpha(Fe^{II}\text{-}CO)_2\beta(Fe^{III}\text{-}OCN^-)_2$, in 0.1 M NaN_3 plus 50 mM Bis-Tris pH 6.5. Spectra were recorded in a 104.5 - 203.7 K for $\alpha(Fe^{III}\text{-}OCN^-)_2\beta(Fe^{II}\text{-}CO)_2$ and 103.2 - 195.2 for $\alpha(Fe^{II}\text{-}CO)_2\beta(Fe^{III}\text{-}OCN^-)_2$.

Figure 3.

Proton NMR spectra of ruthenium(II)-iron(III) azidohemoglobin containing (A) α azidomet subunit or (B) β azidomet subunit in 50 mM Bis-Tris, pD 7.0 in the presence of 0.1 M NaN_3 at the indicated temperatures.

Figure 4.

Temperature dependence of the α-(●) and β-heme (▲) methyl shifts of ruthenium(II)-iron(III) azidohemoglobins in 50 mM bis-tris pD 7.0 in the presence of 0.1M NaN_3. The solid curves represent the least-squares fit calculated with the parameters in Tables I and II.

Table I.

Thermodynamic Values of the Spin Equilibrium of Human Isocyanate-subunit in Isocyanate-Carboxy Hybrid Hemoglobins

hemoglobin	subunit	ΔH (cal/mol)	ΔS (eu)
$\alpha(Fe^{III}\text{-}OCN^-)$	α	- 760 ± 50	0
$\beta(Fe^{III}\text{-}OCN^-)$	β	- 700 ± 50	0
$\alpha(Fe^{III}\text{-}OCN^-)_2\beta(Fe^{II}\text{-}CO)_2$	α	- 650 ± 50	0
$\alpha(Fe^{II}\text{-}CO)_2\beta(Fe^{III}\text{-}OCN^-)_2$	β	- 700 ± 50	0
$\alpha(Fe^{III}\text{-}OCN^-)_2\beta(Fe^{III}\text{-}OCN^-)_2$[a]	—	- 710	0.014

[a]Iizuka & Yonetani, (1970)

Table II: Thermodynamic Values of the Spin Equilibrium of Human Azidomet subunit in Ruthenium(II) - Iron(III) Hybrid Hemoglobins

hemoglobin	subunit	ΔH (cal/mol)	ΔS (eu)	T_c[b]	low spin fraction at 20°C
$\alpha(Fe^{III}\text{-}N_3^-)_2\beta(Ru^{II}\text{-}CO)_2$	α	- 5000 ± 350	- 11.5 ± 0.9	435 ± 65	0.94 ± 0.08
$\alpha(Ru^{II}\text{-}CO)_2\beta(Fe^{III}\text{-}N_3^-)_2$	β	- 2900 ± 200	- 5.8 ± 0.5	500 ± 85	0.89 ± 0.08
$\alpha(Fe^{III}\text{-}N_3^-)_2\beta(Fe^{III}\text{-}N_3^-)_2$[a]	α	- 4980 ± 200	- 13.4 ± 0.7	374 ± 35	0.86 ± 0.08
$\alpha(Fe^{III}\text{-}N_3^-)_2\beta(Fe^{III}\text{-}N_3^-)_2$[a]	β	- 5060 ± 210	- 12.5 ± 0.6	405 ± 36	0.90 ± 0.05

[a]Neya & Funasaki (1986)

[b]Compensation temperature where the high- and low-spin fractions are the same.

Table III: *H* and *L* Values in ppm·K Used for the Chemical Shift Calculation of the Heme Methyl Protons

hemoglobin	methyl peak	*H*	*L*		*H*	*L*
$\alpha(Fe^{III}\text{-}N_3^-)_2\beta(Ru^{II}\text{-}CO)_2$	α_1	14950	6850			
	α_2	14850	5150			
	α_3	15000	1950			
	α_4	14900	1950			
$\alpha(Ru^{II}\text{-}CO)_2\beta(Fe^{III}\text{-}N_3^-)_2$				β_1	10250	5550
				β_2	14950	4600
				β_3	14750	1700
$\alpha(Fe^{III}\text{-}N_3^-)_2\beta(Fe^{III}\text{-}N_3^-)_2$[a]	α_1	10650	6600	β_1	9400	6550
	α_2	8150	5000	β_2	7300	4950
	α_3	10450	2000	β_3	9200	2400

[a]Neya & Funasaki (1986)

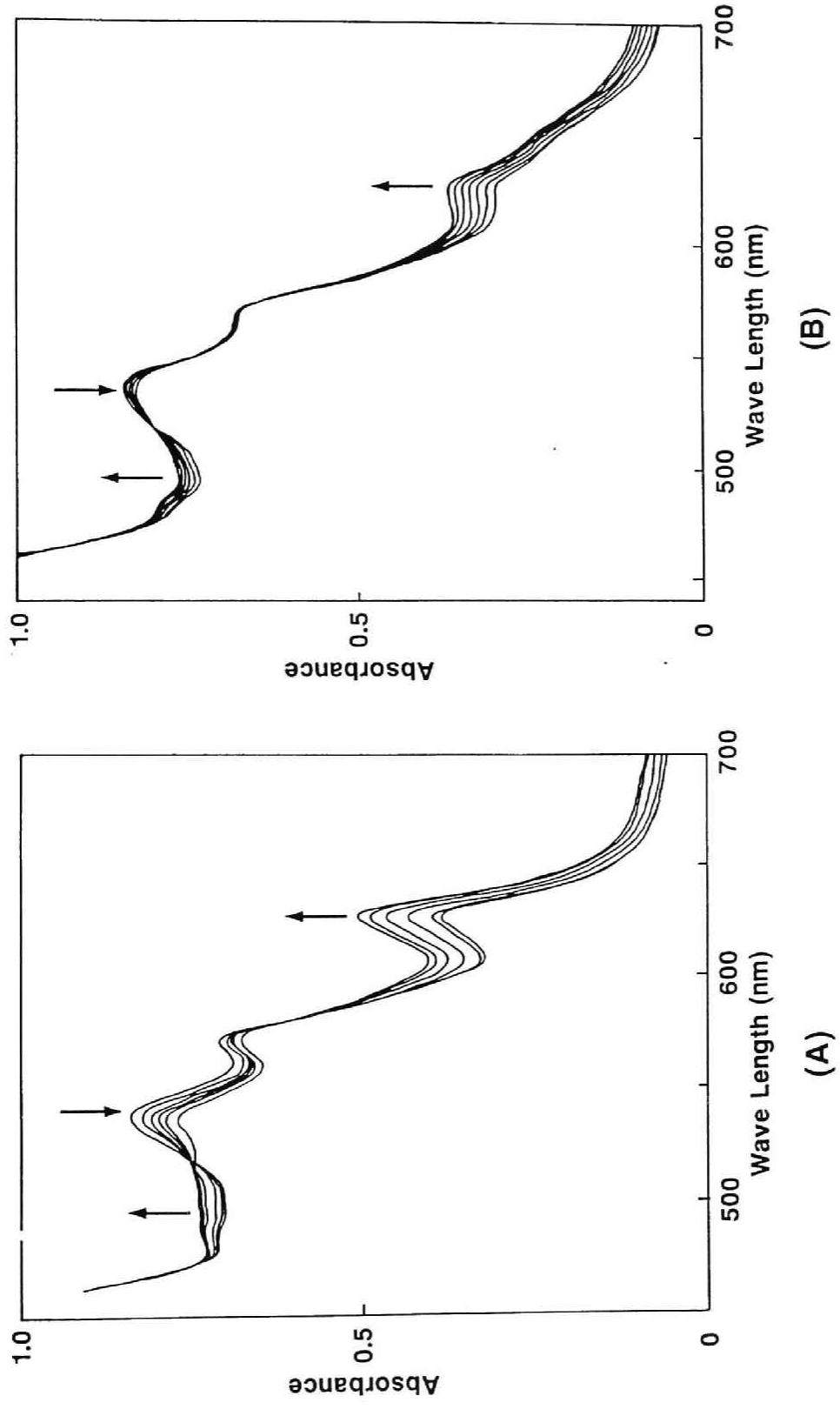
Absorbance
1.0
0.5
0
500
600
700
Wave Length (nm)
(B)
Absorbance
1.0
0.5
0
500
600
700
Wave Length (nm)
(A)

Figure. 1

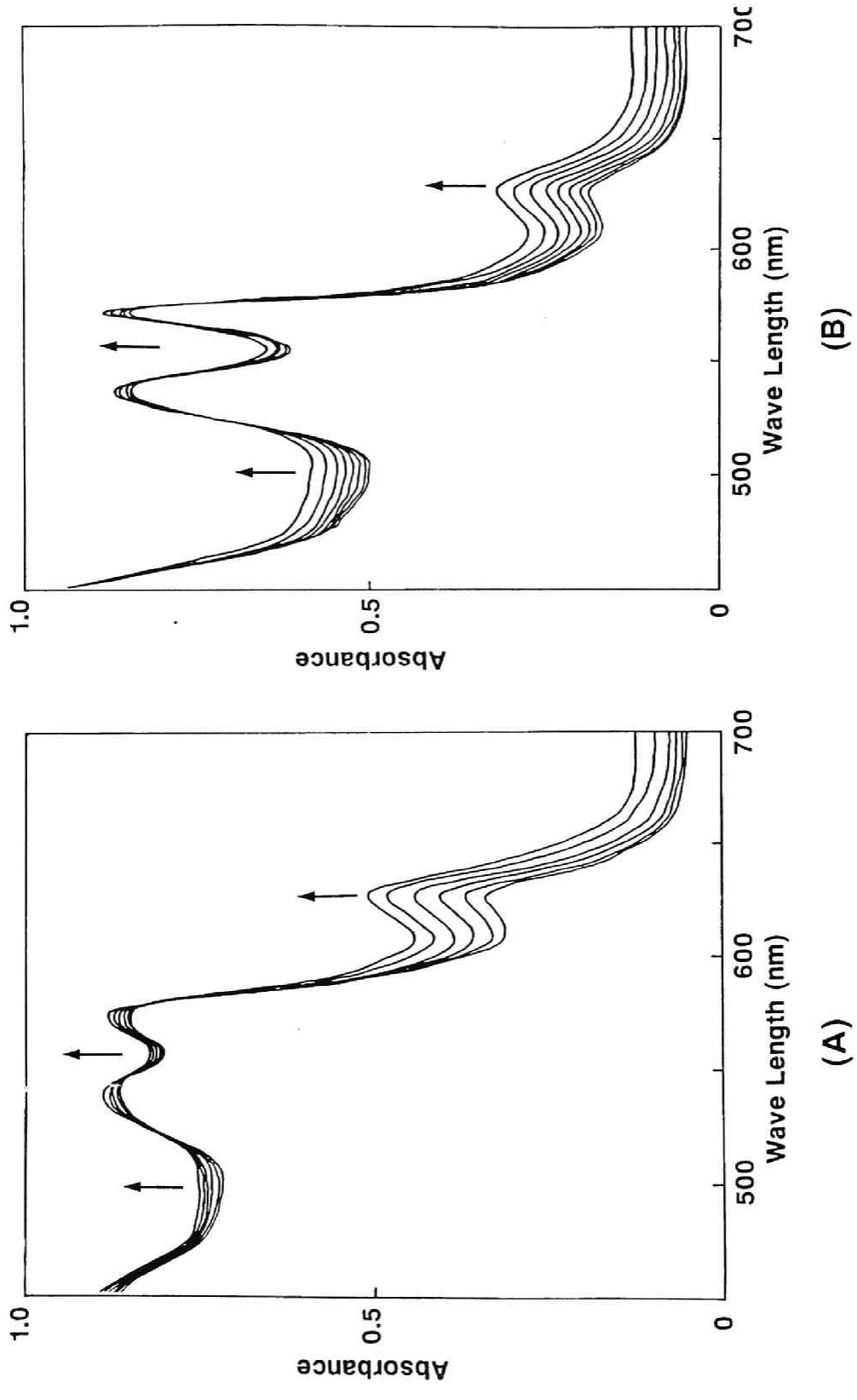
Absorbance
1.0
0.5
0
500
600
700
Wave Length (nm)
(A)
Absorbance
1.0
0.5
0
500
600
700
Wave Length (nm)
(B)

Figure. 2

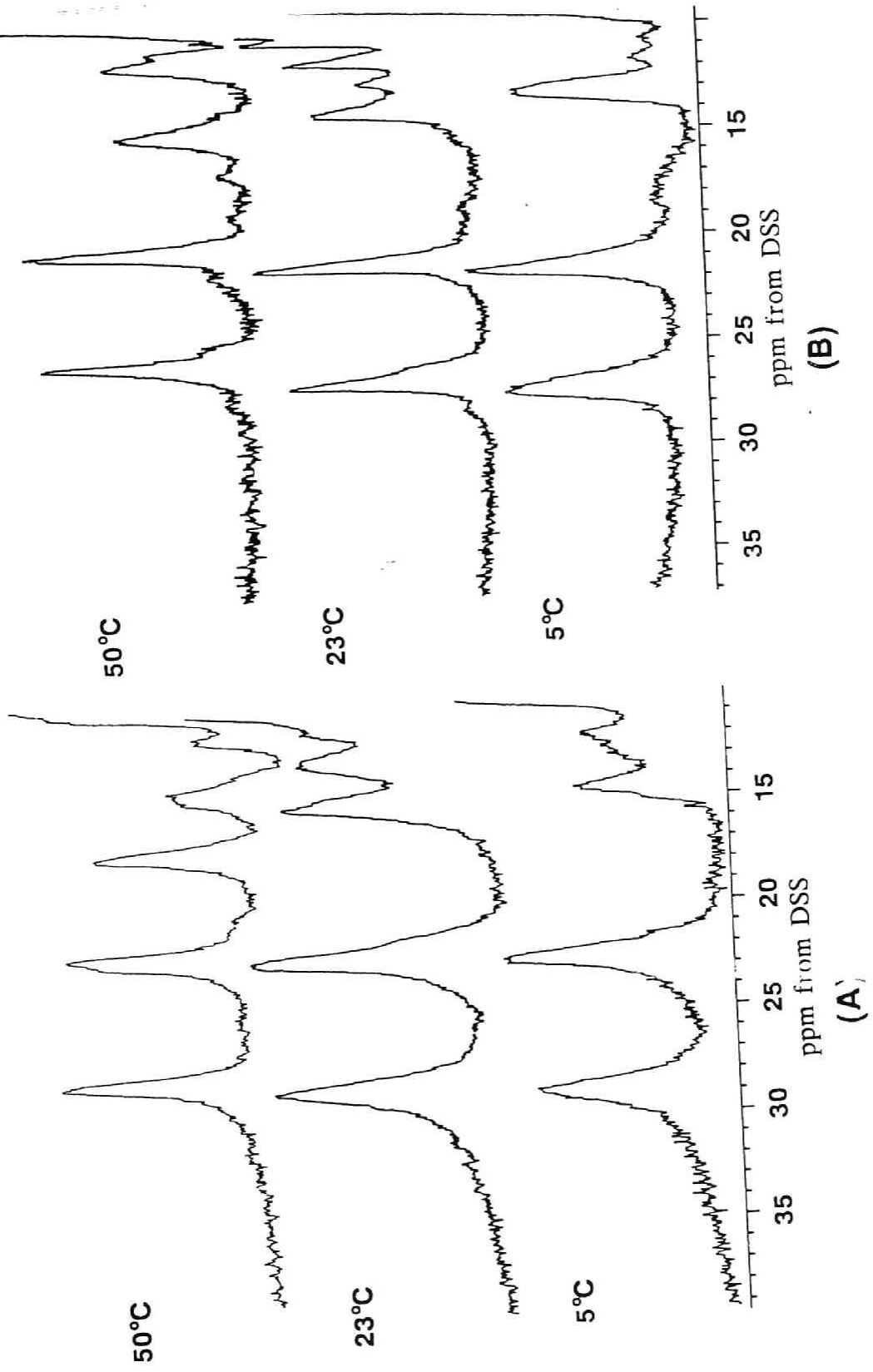
50°C
23°C
5°C
35
30
25
20
15
ppm from DSS
(A)
50°C
23°C
5°C
35
30
25
20
15
ppm from DSS
(B)

Figure. 3

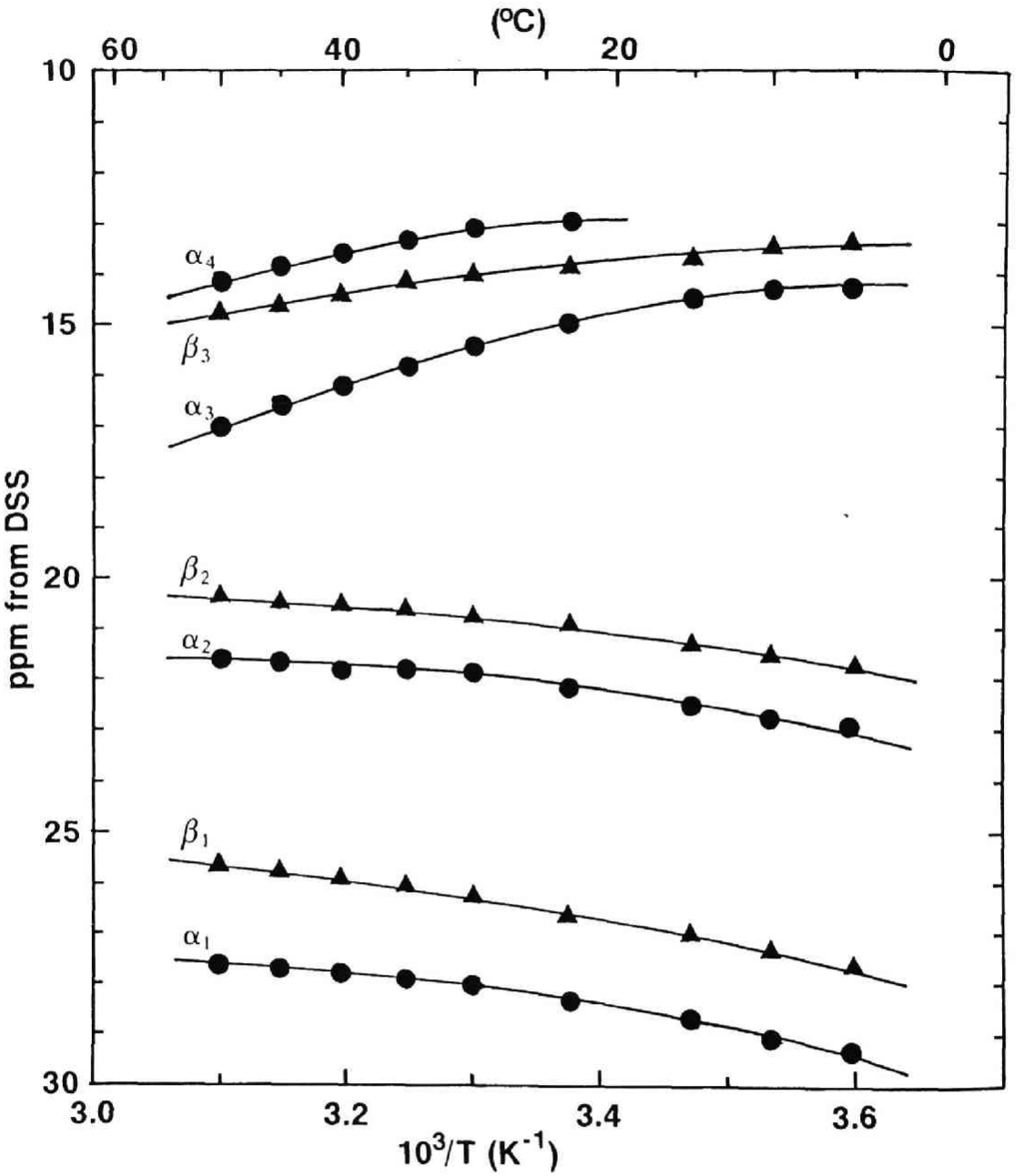
(°C)
60
40
20
0
10
15
20
25
30
ppm from DSS
α_4
β_3
α_3
β_2
α_2
β_1
α_1
3.0
3.2
3.4
3.6
$10^3/T\ (K^{-1})$

Figure. 4

PART VI.

SINGLET OXYGEN PRODUCTION IN HEMOPROTEIN

CHAPTER 1.

Singlet Oxygen Production of Porphyrin-Substituted Myoglobin and Hemoglobin.

ABSTRACT: The time course of the singlet molecular oxygen production by porphyrin substituted hemoglobin and myoglobin was investigated by ESR spectroscopy. After a lag phase (20-60 min), the porphyrin substituted hemoproteins produced singlet oxygen more effectively by light irradiation than free porphyrin in aqueous solution. During the lag phase, absorption spectral changes were detected, suggesting the modification of amino acid residues and heme by photooxidation at the initial illumination. Since the incorporation of porphyrin into apoprotein allows porphyrin to be located in the hydrophobic environment and isolated each other without any interaction, it is likely that the photoexited energy of the porphyrin can transfer to the oxygen molecular more effectively, resulting high yield of singlet oxygen production.

In erythropoietic protoporphyria (EPP[13]), which is one of the hereditary diseases, the iron-free derivative of heme, protoporphyrin IX, is incorporated into globins instead of a normal protoheme (iron-porphyrin complex) in the red cell because of the lack of one enzyme in heme synthesis system (1). Since porphyrin is a potent photosensitizing agent that act *via* the formation of singlet molecular oxygen (2-5), the photo-hypersensitivity such as the cutaneous photosensitivity (1), the rupture of the erythrocyte membrane (5) or lysosomal damage (6) is induced. De Paolis et al. reported that the photohemolysis by the lipid-oxidation was induced when porphyrin dissociated from the globin was intercalated into the erythrocyte membrane in the presence of oxygen molecular and light irradiation (5), however, the production mechanism of singlet oxygen has not been fully understood yet. Although the patient's erythrocyte contains porphyrin Hb, it is unclear whether the porphyrin incorporated into the heme pocket can produce singlet oxygen by irradiation of light or not. With an aim to shed light on the mechanism of singlet oxygen generation in the red cell, we prepare the porphyrin substituted hemoproteins, porphyrin Mb (7) and porphyrin Hb (8), and examined the effect of incorporating porphyrin into the heme cavity on the efficiency of the singlet oxygen production by utilizing of ESR radical trap measurement.

MATERIALS AND METHODS

Sample Preparation. Hemolysate was prepared in the usual manner from fresh whole blood obtained from the local blood bank. Mb (horse heart, type III) was purchased from Sigma Co. Ltd. Apo-protein was prepared as described in our previous paper (9). Purification of the porphyrin-substituted hemoproteins were the same as that of the reconstituted hemoprotein (10).

ESR Spectra Measurements. ESR spectra were measured at room temperature using a JES-FE-3XG spectrometer with 100-kHz field modulation. The relative yield of singlet oxygen was measured using 2,2,6,6,-tetramethyl-4-piperidone as singlet oxygen trap, according to the modified Lion's method (11). Typical samples (50 μl) contained 0.1 M Tris-HCl (pH 8.0), 50 μM hemoprotein and 50 mM 2,2,6,6-tetramethyl-4-piperidone. The light illumination was performed as described in the

[13]The Abbreviations used are: EPP, erythropoietic protoporphyria; Mb, myoglobin; Hb, hemoglobin; ESR, electron spin resonance; Tris, tris(hydroxymethyl)aminomethane; 4-oxo-TEMPO, 2,2,6,6,tetramethyl-4-piperidone-*N*-oxyl

previous paper (12,13).

RESULTS AND DISCUSSION

Figure 1 illustrates the time dependent ESR spectra indicating the triplet signals of the nitroxide radical (4-oxo-TEMPO) produced from 2,2,6,6-tetramethyl-4-piperidone by trapping singlet oxygen generated during the illumination of porphyrin Mb. These ESR spectra clearly show that the signal intensities of the nitroxide radical increased with time. Since previous paper confirmed that such trap reagent preferentially reacts on singlet oxygen (11), we can estimated the yield of singlet oxygen on the basis of the signal heights. In order to get the concentration of singlet oxygen, 50 μM 4-oxo-TEMPO solution was used as reference of the radical concentration.

The plots of the yield of singlet oxygen production by porphyrin Mb, porphyrin Hb and free porphyrin in aqueous solution against the illumination time are shown in Figure 2. The most outstanding feature in this figure is a characteristic lag phase for the porphyrin-substituted hemoproteins. The concentration of the radical produced by free porphyrin in the aqueous solution increased almost linearly with the duration of illumination, whereas singlet oxygen production by porphyrin-substituted hemoprotein suppressed at the initial stage of the illumination. The period of the lag phase was different between porphyrin Mb and Hb. Porphyrin Hb exhibited longer and more distinct lag time (~ 60 min) than porphyrin Mb (~ 20 min). These lag phases can be interpreted as following; singlet oxygen at the initial stage of the illumination reacts on the amino acid residues inside of the heme cavity and it cannot reach to the trap reagent in the solution. In fact, the previous studies pointed out the photooxidation of some amino acid residues by the illumination of light (7,14).

It is also to be noted that a large absorption spectral changes, that is, the decrease of the Soret peak intensity and appearance of a new peak around 665 nm, was observed in the illumination time as shown in Figures 2 and 3. Moreover, the spectral changes were enhanced during the lag phase. Since it is unlikely that the modification of the amino acid residues induced such a large spectral changes, the modification of the porphyrin itself is also to be considered. Cox and Whitten (15) reported that protoporphyrin was photooxidized to yield a mixture of photoprotoporphyrin derivatives in the presence of oxygen. The broad peak around 665 nm as shown in Figure 3 also suggests that the porphyrin was converted to chlorin derivatives (16),

such as photoprotoporphyrin, however, the detailed structure of the modified porphyrin was not clear. Further investigations now go on.

Another characteristic point of the singlet oxygen production by the porphyrin-substituted hemoproteins is their high efficiency. After the lag phase, porphyrin Mb produced singlet oxygen for ~ 0.10 μM per minutes and porphyrin Hb for ~ 0.09 μM, while the generation rate of the nitroxide radical produced by free porphyrin was only ~ 0.014 μM per minutes under the same condition. This observation implies that the porphyrin globin is one of the effective singlet oxygen generation system. The porphyrin incorporated into heme pocket seems to have two advantages for the production of the singlet oxygen. One is the hydrophobic environment inside the heme cavity. In order to maintain the protoheme in the heme cavity, the hydrophobic interactions are exerted between the side chains of protoheme (methyl and vinyl groups) and amino acid residues inside the heme cavity. Since the hydrophobic environment enable the life-time of singlet oxygen to be prolonged, these interactions not only fix the porphyrin, which has no coordination site for the amino acid residue, in the heme pocket, but also induce the prolongation of the life-time of singlet oxygen (17). Second point, which seems to be more effective to produce singlet oxygen, is the isolation of a porphyrin from the other porphyrins. Free porphyrin in aqueous solution often aggregates or forms the stacking for one another. In such case, when one porphyrin was excited by the irradiation of light, the photoexcited energy is scattered through many interactions such as energy transfer to other porphyrins. On the other hand, porphyrin incorporated into the heme pocket is isolated from other porphyrins by "the protein matrix". Therefore, the interactions which scatter the photoexcited energy do not work in porphyrin-substituted hemoprotein and the energy is effectively transferred from photoexcited porphyrin to triplet oxygen molecule to generate singlet oxygen.

In conclusion, present study revealed that the porphyrin-globins (porphyrin Mb and porphyrin Hb) are the effective singlet oxygen generation system and at the initial period of the illumination, they have a lag time probably due to the modification of their amino acid residues and porphyrin itself.

REFERENCES

1. Magnus, J. A., Jarrett, A., Prankert, T. A. J., & Rimington, C. (1961)

Lancet. 2, 448-451.
2. Goldstein, B. D., & Harber, L. C. (1972) *J. Clin. Invest. 51*, 892-901.
3. Dalton, J., McAuliffe, C. A., & Slater, D. H. (1972), *Nature (London) 235*, 338.
4. Mathews-Roth, M. M. (1984) *Photochem. Photobiol. 40*, 63-67.
5. De Paolis, A., Chandra, S., Charalambides, A. A., Bonnett, R., & Magnus, I. A. (1985) *Biochem. J. 226*, 757-766.
6. Slater, T. F., & Riley, P. A. (1966) *Nature (London) 209*, 151-154.
7. Mauk, M. R., & Girotti, A. W. (1973) *Biochemistry 12*, 3187-3193.
8. Ainsworth, S., & Treffery, A. (1974) *Biochem. J. 137*, 331-337.
9. Ishimori, K., & Morishima, I. (1988) *Biochemistry 27*, 4060-4066.
10. Ishimori, K., & Morishima, I. (1986) *Biochemistry 25*, 4892-4898.
11. Lion, J., Gandin, E., & Van de Vorst, A. (1980) *Photochem. Photobiol. 31*, 305-309.
12. Kawanishi, S., Inoue, S., Sano, S. & Aiba, H. (1986) *J. Biol. Chem. 261*, 6090-6095.
13. Inoue, S., & Kawanishi, S. (1987) *Canc. Res. 47*, 6522-6527.
14. Mauk, M. R., & Girotti, A. W. (1974) *Biochemistry 13*, 1757-1763.
15. Cox, G. S., & Whitten, D. G. (1982) *J. Am. Chem. Soc. 104*, 516-521.
16. Cubeddu, R., Keir, W. F., Ramponi, R., & Truscott, T. G. (1987) *Photochem Photobiol. 46*, 633-638.
17. Rodjers, M. A. J. (1983) *J. Am. Chem. Soc. 105*, 6021.

FIGURE LEGENDS

Figure 1.

ESR spectra of nitroxide generated during illumination of the porphyrin Mb solution. The illumination times are indicated the left side of each spectrum.

Figure 2.

The time course for the yield of singlet oxygen produced by the photoexcited porphyrin derivatives. Porphyrin Mb (○), porphyrin Hb (△) and free porphyrin (□). Open symbols denote the concentration of nitroxide radical and filled ones indicates the absorption at the Soret peak.

Figure 3.

Absorption spectra of porphyrin-substituted Mb before and after illumination.

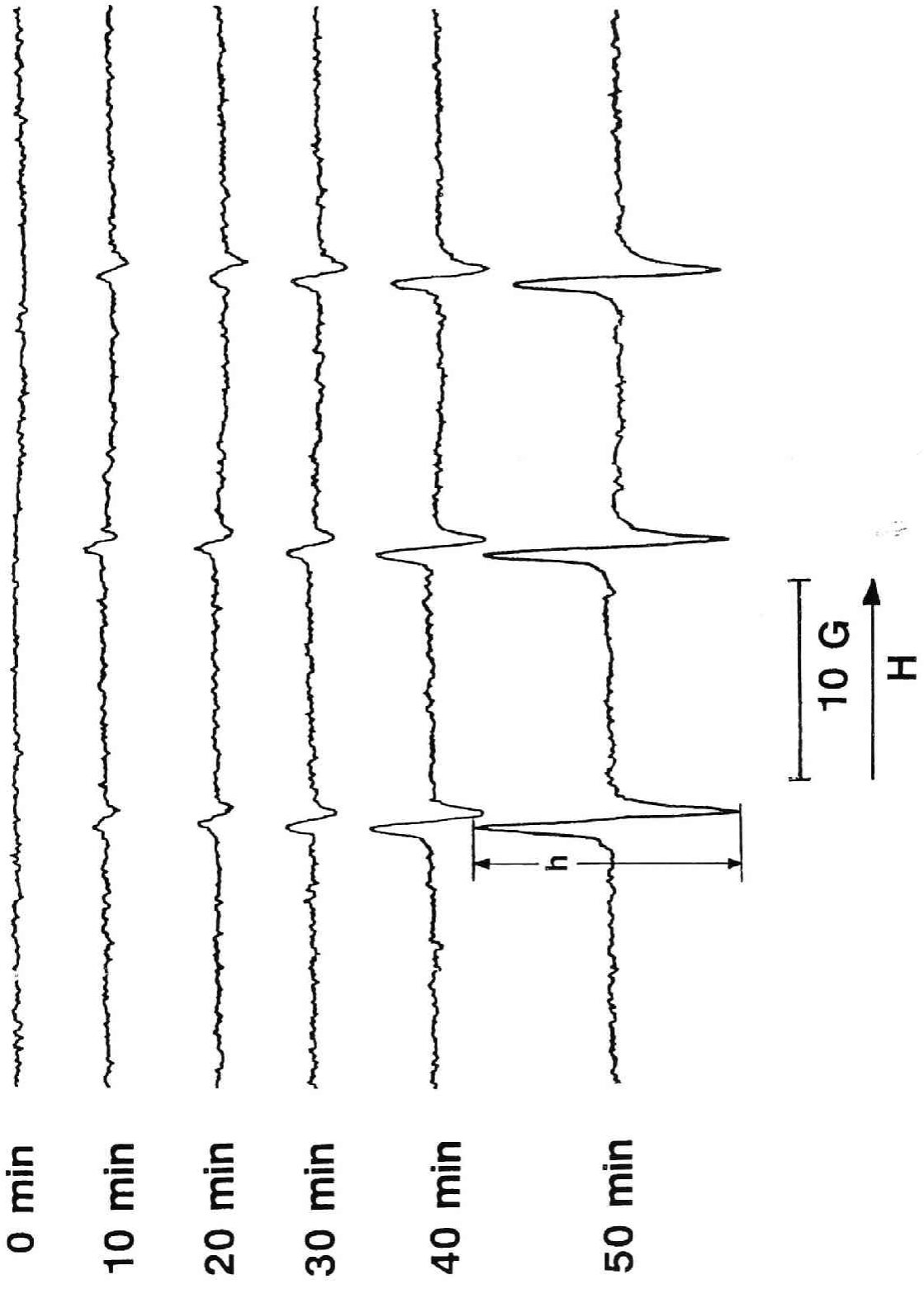

Figure. 1

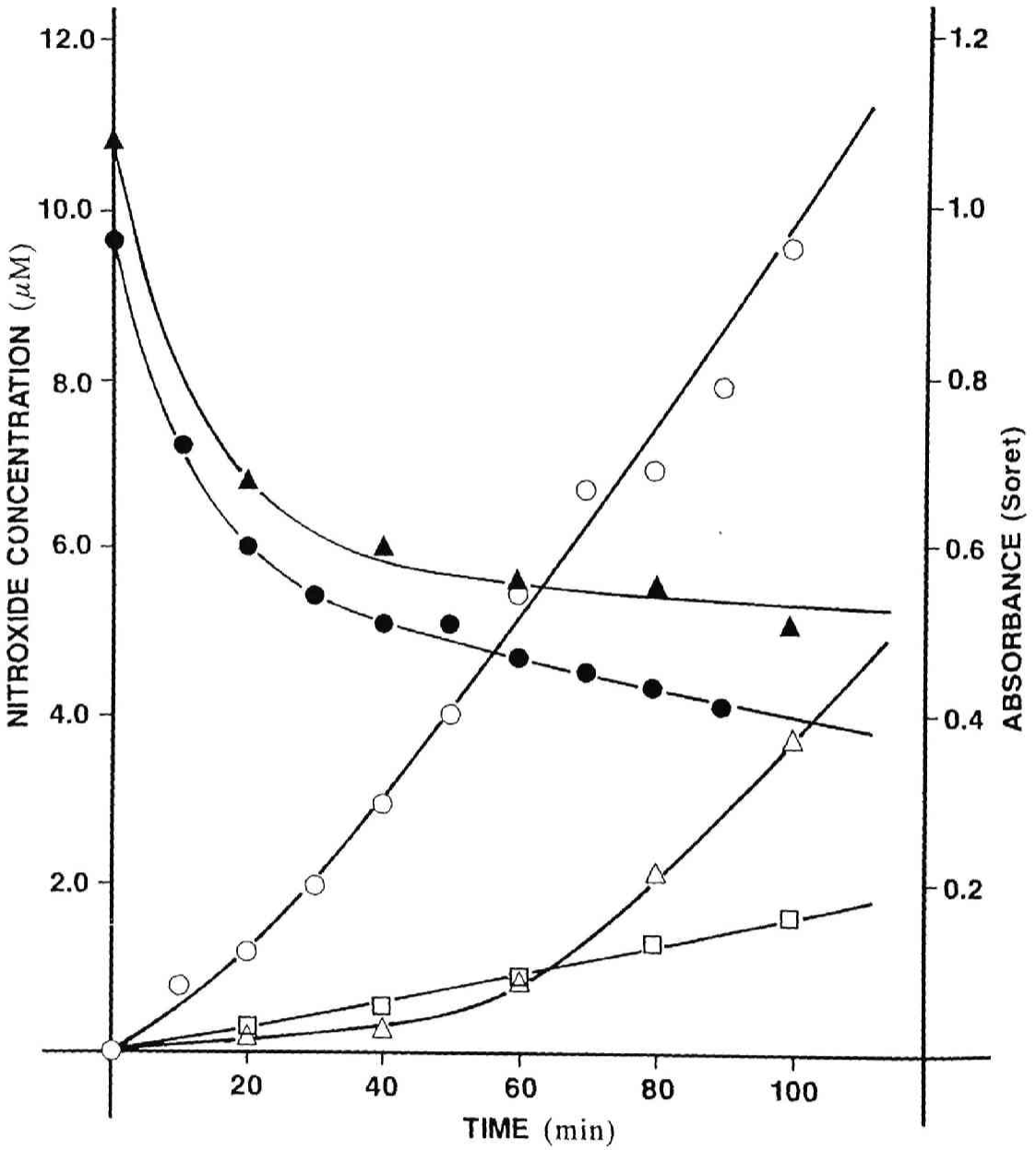
12.0
10.0
8.0
6.0
4.0
2.0
NITROXIDE CONCENTRATION (μM)
1.2
1.0
0.8
0.6
0.4
0.2
ABSORBANCE (Soret)
20
40
60
80
100
TIME (min)

Figure. 2

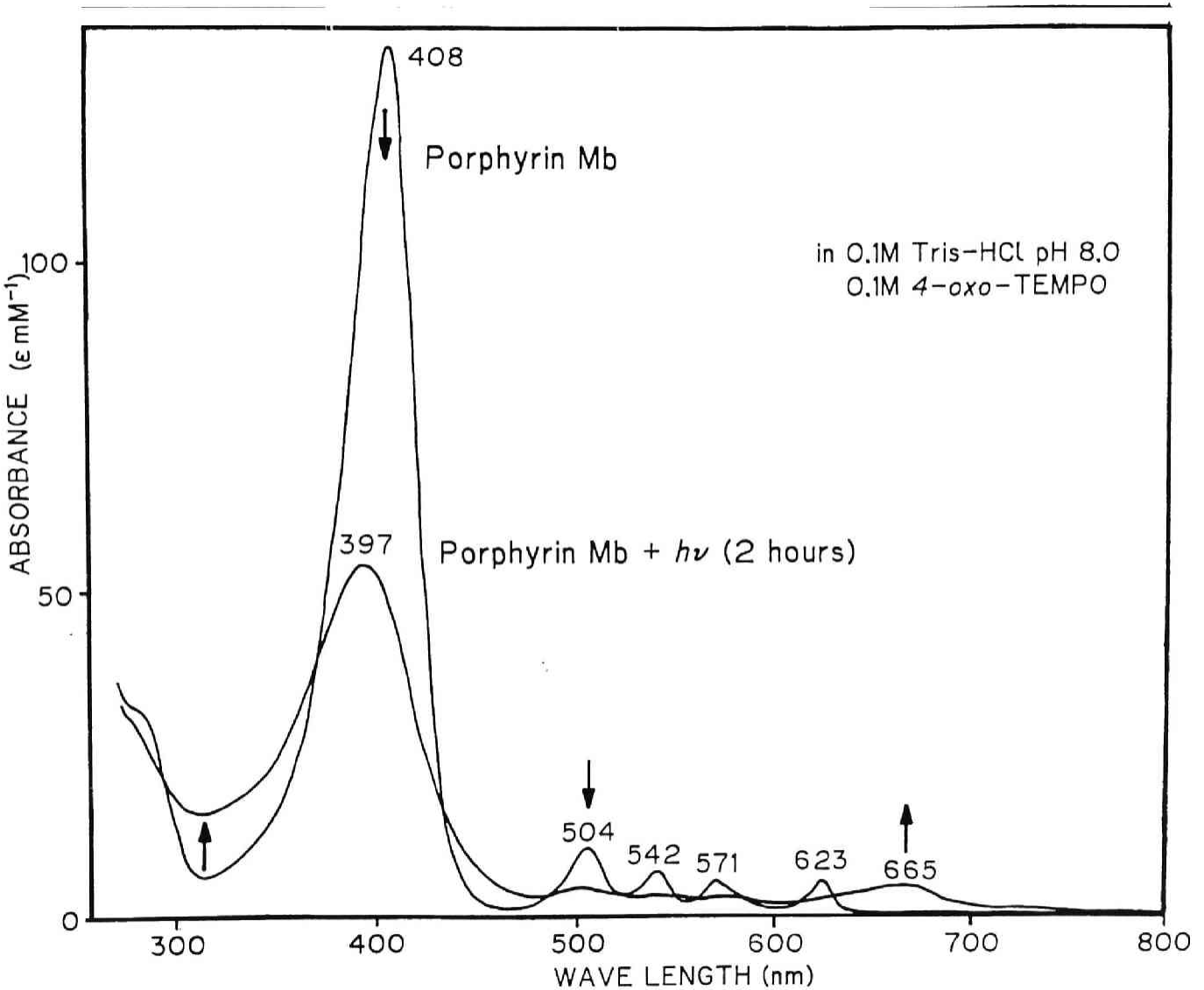
408
Porphyrin Mb
in 0.1M Tris-HCl pH 8.0
0.1M 4-oxo-TEMPO
ABSORBANCE (ε mM⁻¹)
100
50
0
397
Porphyrin Mb + hν (2 hours)
504
542
571
623
665
300
400
500
600
700
800
WAVE LENGTH (nm)

Figure. 3

PART VII.

SUMMARY AND GENERAL CONCLUSION

As discussed in the present thesis, oxygen binding hemoprotein has a number of characteristic and unique properties in their function and structure. In order to establish the relationship between the molecular structure and function in oxygen binding hemoprotein, the detailed and extensive investigations in the fields of physico-chemistry, biochemistry, physiology and biology have been carried out and will be required from now on. In this thesis, the author aimed at the comprehensive study of the molecular mechanism of oxygen binding hemoprotein on the basis of structural studies by physicochemical approaches and functional studies by physiological approaches. Present thesis also showed that the site-directed mutagenesis can be used as a new and potential approach to investigate oxygen binding hemoproteins and provide many novel knowledges which have never been accessible by other means.

In Part II, III and IV, with an aim to shed light on the molecular mechanism of the cooperative oxygen binding in native human hemoglobin, two different strategies were selected. The first one is the modification of its oxygen binding site, heme, and the second one is the modification of globin by the substitution of the specific amino acid residue. As the first approach, the author prepared ruthenium(II)-iron(II) metal hybrid hemoglobins which can serve as an unique model for the intermediate species of oxygenation step in hemoglobin and their structural and functional studies were performed. The physicochemical measurements including nuclear magnetic resonance, absorption spectrum, resonance Raman spectrum and kinetics study revealed the detailed structure of the half-liganded ruthenium(II)-iron(II) hybrid hemoglobins and a mechanism of propagation of conformational changes from the liganded subunit to the un-liganded subunit was proposed. On the basis of these structural investigations, it is concluded that the ligation of one subunit induces the different conformational changes and the structural changes accompanied by the oxygen binding are not concerted in different parts of hemoglobin. At the binding of two ligands, the break of the salt bridge at the $\alpha_1\beta_2$ interface precedes other structural transitions and then the changes of the bonds between the heme iron proximal histidine binding are induced. The rerrangement of the hydrogen bonds located at the $\alpha_1\beta_2$ interface could occur when the third oxygen molecule is bound to the heme. At the same time, the physiological studies of the ruthenium(II)-iron(II) hybrid hemoglobins disclosed their functional properties such as oxygen affinity, cooperativity constant and oxygen binding parameters. These physiological

studies not only revealed that the ruthenium-iron hybrid hemoglobins imitate the intermediate species in the oxygenation step of native hemoglobin, but also suggested a mechanism of the structural regulation of the cooperative function. The changes of the function and structure do not occur all at once by binding of some oxygen molecule as expected in the simple "Two State Model". The present thesis has shown that the functional and structural properties gradually change from the "T" state (low oxygen affinity form) to the "R" state (high affinity form). Such a molecular flexibility of hemoglobin was encountered in the IHP (inositol hexakisphosphate, an allosteric effector to lower the oxygen affinity of hemoglobin) effect on the structure as discussed in Part IV. The "Two State Model" based on the extensive X-ray structural studies states that the quaternary structure of hemoglobin is governed by the movement of the heme iron. The quaternary "T state" corresponds to the "in plane" heme structure and the "R-state" to the "out of plane" structure. However, the author showed that the low spin hemoglobin derivatives in which heme iron is fixed on the porphyrin plane undergo the quaternary structural changes by binding of IHP and their quaternary structure can be converted into the "T-like state" in the presence of IHP. These observations imply that the quaternary structure is tuned not only by the change of the iron-histidyl bond, but also by the binding of the allosteric effectors, suggesting that hemoglobin has a regulation device which can fit its structure and function depending on the different environmental conditions.

The amino acid substitution at the specific site by the site-directed mutagenesis was also useful technique to investigate the mechanism of the cooperativity. In Part III, the author focused on the effect of the hydrogen bond network at the $\alpha_1\beta_2$ interface on the structure and function of hemoglobin. The point mutation at α42 tyrosine to phenylalanine not only broke the hydrogen bond linked to β99 asparatic acid of another subunit, but also induced drastic changes in the structure and function. The mutant hemoglobin (α42 Tyr $\rightarrow$ Phe) cannot take the typical "T state" as found for native deoxy hemoglobin even in the deoxygenated state. It is therefore likely that its structural and functional properties almost coincide to those of the "R state" hemoglobin such as native oxyhemoglobin. Another mutant hemoglobin (α42 Tyr $\rightarrow$ His) exhibited minor functional and structural defects compared with the phenylalanine-substituted mutant because the histidyl NH proton can be hydrogen bonded to the carboxylate of the β99 asparatic acid. These results clearly show that the hydroxy group of α42

tyrosine has a key role to stabilize the low affinity form in the deoxygenated hemoglobin. As mentioned in this thesis, the detailed investigation of the site-specific amino acid substituted hemoglobins will be further required to establish a function - structure relationship in the molecular level.

Hemoglobin also have numerous interactions in intra- and intermolecule through van der Waals contacts, hydrogen bonds and salt bridges. In Part V are studied some interactions between heme and globin or subunit and subunit by using of spectroscopic methods. As clarified in the reconstitution reaction of hemoglobin (Chapter 2), apohemoglobin, which has no hemes in its heme cavity, could combine some heme in the specific heme orientation, implying that apohemoglobin can distinguish the steric hindrance of the porphyrin at the binding of the heme. This recognition could be mediated through relatively weak interactions such as van der Waals contacts between heme and globin. And it is to be noted that such a recognition of steric hindrance of porphyrin depends on the structure of globin. The orientation of heme in semihemoglobin which contains hemes in one subunit is different from that of apohemoglobin. Therefore, this recognition property through van der Waals contacts can be thought to be partially responsible for the substrate specificity regulated by the structure of protein.

Since hemoglobin is an oligomeric hemoprotein, many interactions intersubunit serve to maintain the structure and function. In Chapter 1 and 4 of Part V, the effects of this intersubunit interactions on the structure and spin state are examined. The extensive studies carried out here have revealed that the small changes of the structure and the spin-state in one subunit can be propagated to another subunit through the network of the hydrogen bonds and the salt bridges in the subunit interface.

It is also interesting that such interactions in protein are exerted in the dynamic state where the thermal fluctuation continuously occurs. As shown in Chapter 3 of Part V, native hemoprotein containing native protoheme can be converted into the reconstituted hemoprotein containing modified heme in the presence of excess amount of modified hemin. This observation implies that hemoprotein exhibits large fluctuation by which some hemes are taken out from the heme cavity to a bulk solution. Although this phenomenon might be characteristic of hemoprotein, it is rather surprising that such large fluctuation is induced under physiological condition.

In aspect of chemistry, it seems useful to apply the protein to chemical reaction. As one example, the singlet oxygen production of porphyrin-

substituted hemoprotein by irradiation of light was investigated in Part VI. Singlet oxygen was poorly generated in porphyrin aqueous solution. However, irradiation of light to porphyrin-substituted hemoprotein which contains porphyrin instead of native heme caused effective production of singlet oxygen. The efficiency for the porphyrin hemoprotein system was almost seven times as much as for the system of free porphyrin in aqueous solution. This indicates that the heme cavity can serve as the effective reaction site for the energy transfer from photoexcited porphyrin to oxygen molecule and the possibility to apply hemoprotein to chemical reaction was suggested.

In the present thesis, the author intended to clarify the structural regulation of function in oxygen binding hemoprotein. At the same time, he also tried to apply hemoprotein to chemical reactions. At the present time, it is premature to say that we can fully understand the molecular mechanism of the structural regulation of function of oxygen binding hemoproteins. The stabilization mechanism of reversible binding of oxygen molecule has not yet been clear and few detailed investigations have been carried out with attention hydrogen bonds and salt bridges at the intersubunit region. However, it can be also said that the time will come soon when the essential mechanism is fully disclosed by the further studies of hemoproteins using new techniques such as the site-directed mutagenesis. These fundamental studies will also allow us to design and make new functional molecules we have never obtained before. The author hopes that the present conclusions and suggestions in this thesis will contribute to these important area in the protein chemistry.